"VARIABLE STRUCTURE TECHNIQUES IN CONTROL SYSTEM DESIGN"

by

J. TRISTAN DAVID

Thesis submitted to the Heriot-Watt University, Edinburgh for the degree of Doctor of Philosophy.

Department of Electrical and Electronic Engineering.

June 1980.

CONTENTS

ACKNOWLEDGEMENTS

The work reported in this Thesis was undertaken in the Department of Electrical and Electronic Engineering at Heriot-Watt University, Edinburgh and was supported by the South of Scotland Electricity Board.

I wish to express my deep gratitude to Dr. G.T. Russell for his guidance and encouragement and my appreciation for the splendid work done by Mrs. F. Samson and Mrs. H. Vaughan in typing the manuscript.

Finally a very special acknowledgement goes to my wife, Mary, for her patience and support during the past few years.

ABSTRACT

During the last twenty years, control theorists belonging almost exclusively to the USSR, have laid down the foundations of variable-structure systems (commonly abbreviated to VSS). As the name implies, such systems are allowed to change their structure through time in accordance with some preassigned algorithm. The theory has demonstrated that some significant advantages could be gained by adopting that approach in the design of automatic control systems, amongst which are good transient responses and insensitivity to parametric variations and to external disturbances. The VS controller is slightly more complex than a fixed structure design based on standard methods such as state feedback or frequency response techniques, but is a great deal less complex than some adaptive designs. It also lends itself to a straightforward microcomputer implementation.

While the theoretical aspect of VSS has been well explored, its general applicability to engineering problems is yet to be established. There are still unanswered questions as to the suitability of the method for practical systems, which invariably contain a certain amount of noise, uncertainties and nonlinearities. The work described in this thesis concentrates on that particular aspect and is, in brief, an investigation of VSS as an engineering design procedure. The theory of VSS is reviewed and the principles are then applied to a number of engineering examples. The performance of the systems are assessed from digital simulation runs, hybrid computation and the microcomputer control of a DC motor.

CHAPTER ONE

INTRODUCTION

One of the areas of control theory which has been developing rapidly over the last two decades is that of Variable Structure Systems (VSS). The theory which has been the subject of extensive research in the USSR, provides a new approach to the control problem of linear time-varying plants through the enforcement of an invariant motion known as a sliding regime. The formation of such a regime is achieved by constraining the state point of the system to move on a predetermined hyperplane (or hyperplanes) in space thus giving a response which is insensitive to parameter variations and disturbances [1.1].

Research in VSS has so far been largely theoretical and has dealt specifically with the mathematical conditions leading to a stable sliding regime. The practical realisation of sliding in linear time-varying systems has barely been reported in the literature [1.2], [1.3] and has been confined to second-order examples. As with any new theory, a credibility gap exists between the theory and application of VSS which can only be bridged with a detailed investigation of test cases. The objective of this thesis is to elaborate on that particular aspect to allow an engineering assessment of the theory.

The control of linear time-varying plants is first reviewed and the underlying reasons for studying VSS amongst other possible theories are explained.

1.1 Linear Time-Varying Systems

In designing automatic control systems for time-varying plants, the control engineer very often starts by assuming that the plant is time-invariant and linear around some nominal operating point. A host of design techniques based on frequency and state-space methods is then available to him for the design of a conventional linear fixed structure controller. A detailed presentation of these methods can be found in [1.4] for the single-input plant and in [1.5] for the multi-input plant. These methods ensure through feedback principles that the performance of the basic closed-loop system will not degrade appreciably with parameter variations and disturbances. The usefulness of these techniques, however, becomes restrictive for plants with significant parameter variations, which for example can manifest themselves in systems operating over wide ranges. If linear system theory is adopted in such cases, the designs are inevitably compromised to maintain adequate stability margins under all operating conditions and normally result in conservative transient responses.

It is possible in certain cases to introduce high-gain feedback coefficients in the controller to improve its robustness to parameter variations while maintaining an overall satisfactory transient response [1.6]. The method, however, is not always favoured as the high gains in the system may cause certain signals to saturate resulting in unpredictable nonlinear performance. Improperly located high gains can also excessively amplify any noise which may be present in the system, also causing unsatisfactory performance.

Faced with these circumstances, the designer is compelled to investigate other methods which promise a more satisfactory performance under all known operating conditions. One area of control theory which can provide good solutions to that class of problems is that of preprogrammed adaptive control, which has been applied in such areas as the aerospace industry for missile guidance [1.7]. The basis of the method is to preprogram time variations of controller parameters or to schedule controllers to achieve instantaneous optimum control at all times. The structure of the system is in essence a variable one but it differs from VSS described herein in that no sliding regime is enforced. Further, the decision to switch from one controller to another is normally dependent on the direct measurement of only one or two time-varying elements of the plant such as airspeed in helicopter control [1.8]. The design methodology suggests that adaptation is performed at discrete time intervals, but this is not always the case. The automatic gain control (AGC) of radio receivers is an analogue example of the theory in which the variation in the output signal is used to regulate the amplifier's forward gain.

The above method assumes that the time-varying property of the plant is known beforehand or that it can be measured on-line in a relatively short period. But when preprogrammed adjustments cannot be made because of a lack of knowledge relating the system performance to a time-varying environment, the need for an adaptive system based on real time identification and control is of apparent necessity. This classification of adaptive systems is not radically different from the preprogrammed adaptive system, but is a great deal more complex to analyse and implement. The

generally agreed definition here of the adaptive system is the control of uncertain systems with a controller structure that includes a subsystem for the on-line estimation of unknown parameter values or system structure and a subsystem for the generation of suitable control inputs based on estimated parameter values or system structure. One of the first examples in that class was reported by Draper and Li [1.9]. They considered a control system which could optimise the performance of an internal combustion engine in spite of uncertainties in the shape of the performance characteristics.

The parameters of the plant are sometimes identified using a model and this leads to the idea proposed by Narendra [1.10], Caroll [1.11] and their co-workers, of an adaptive observer and controller for the joint problem of state-parameter estimation and control in slowly time-varying systems. The principles, based on Lyapunov's stability theorem, have a strong appeal in that they guarantee convergence in the state and parameter spaces. They still have some unsolved difficulties with regard to stability and disturbances [1.12]. The end product of the adaptive control system for the linear time-varying plant is generally then a complex nonlinear controller.

The controller design must in the end be dependent on the particular application and the design specification. But when there is uncertainty about the design philosophy because (i) a full adaptive system is too sophisticated, (ii) a pre-programmed adaptive controller is unable to cope with the bounded but random nature of the parameter variations and (iii) a fixed linear controller can result in a conservative performance, then

an acceptable solution can be found in variable structure theory. This point will be demonstrated later by some examples.

The interest in VSS was first brought about with the work of Scott [1.13] who investigated the problem of controlling a two-integrator phase-lock loop along a given trajectory through the switching of feedback gains. The interest was deepened with the publication of Itkis book in 1976 [1.1] giving an account of its theoretical developments.

The theory offers the possibility of analysing and designing controllers for plants with bounded time-varying parameters and subject to external disturbances, without any significant sacrifice in the transient performance and without any reliance on identification or complex adaptive control procedures. Further, the decision type structure of the VS controller makes it attractive for implementation as a micro-computer program. These promising features of VSS provided the motivation for further research into its theory and its engineering applicability.

1.2 Work Organisation

The contents of subsequent chapters are outlined below.

Chapter two introduces the theory of VSS through a second order example. Phase plane methods are used to explain the formation of a sliding regime and its invariancy property to parameter variations.

Chapter three generalises the concepts of chapter two to higher order plants. The plant is assumed to be linear and time-varying, and, that the error and its derivatives are available to the control function. These assumptions imply that the plant exists either in phase-variable form or that its output is differentiable to the nth order where n is the order of the plant. The conditions for hitting, sliding and stability in a given hyperplane are discussed. The application of VSS to plants with more general structures and with zeros in their transfer function together with the tracking of inputs is then investigated.

Chapters four and five deal with specific applications which highlight the interesting properties of VSS. In chapter four, a coiler drive system is considered in detail and it is shown how a time-varying parameter eventually leads to instability. An alternative design based on variable structures is then presented which guarantees stability and good response over the system's operating range.

In chapter five, the state-variable feedback design of a ship's autopilot is discussed. The design objectives in this example are to minimise (i) the effects of parameter variations and (ii) the rudder activity which occurs as a result of sea disturbances. High gain values are introduced in the state-feedback controller to compensate for the parametric variations but with a deteriorating effect on the rudder activity. A VS autopilot with reduced gains is then designed and is shown to improve the performance of the ship with respect to the two design goals.

The above case-studies clarify the mechanism of control in VSS. The VS controller behaves in a similar manner as an integral controller in that it synthesises an average level at the plant's input which is sufficient for maintaining its output at the desired level and for compensating external disturbances and parametric variations. This mean level is derived through the switching of the derivatives and/or the state variables. It is shown that in a type 0 system such as the coiler-drive, the VS control law must include the switching of the reference input to enforce a sliding regime whereas in a type 1 system such as the ship, this is not necessarily the case.

Having established the basic properties of VSS, chapter six proceeds to consider the effects of noisy measurements in the above designs. Real plants are characterised by imperfections which arise from noise, delays and nonlinearities. An ideal sliding regime cannot be formed under these conditions but can be approximated by a high frequency switching regime referred to as a quasi-sliding regime. It is shown that noise causes drift and that smoothing improves the performance considerably.

Chapter seven considers a VSS under more realistic conditions. The exact digital simulation used in the previous chapters is replaced by a microcomputer control analogue system to investigate the VS control of a third order system. In spite of the inherent problems of drift, noise, mains interference, delays due to program execution time and conversion times, and inaccuracies due to finite word lengths, the controller behaves in close accordance with the analysis and is able to compensate for a variety of disturbances introduced at different points in the plant.

It is shown for example that a sinusoidal input disturbance of arbitrary frequency can be completely eliminated from the plant's output; it is impossible to obtain such a performance using linear techniques.

Chapter eight extends the experimental work to the VS speed control of a DC motor using the microcomputer as the controller. The application combines all the factors detrimental to a good VS solution. It is shown that starting from an ill-defined model of the plant and using a VS controller based on differentiation, a satisfactory speed performance can be achieved.

Chapter nine concludes the investigation. The main contribution and salient points are summarised, and the areas which merit further investigation are discussed.

CHAPTER TWO

A SECOND-ORDER VARIABLE STRUCTURE CONTROL SYSTEM

As already pointed out in Chapter One, variable structure systems possess some interesting and desirable properties which result from the formation of a sliding regime; the phenomenon is well-known in switching systems and has been discussed by several authors, [2.1] and [2.2]. The motion occurs when the system is constrained to move on a given hyperplane in space. In theory, this trajectory is realised by allowing the structure of the system to change during the transient response, the times at which these changes occur being determined by the current value of the error and its derivatives. Once in a sliding plane, the motion is effectively invariant to plant parameters and external disturbances and can be regarded as equivalent to the motion of a certain new system with a fixed structure differing from any of the structures on which the original VSS design was based.

The transient response of the system can thus be split into two independent stages: a brief motion starting from any initial conditions in space to the beginning of the sliding regime (referred to as "hitting"), characteristic of which is a rapid rate of decrease in the value of the absolute error, and an unlimited period of motion in the sliding regime, characterised by rapidly damped oscillations. A second order example is considered in the next section to clarify that type of transient behaviour.

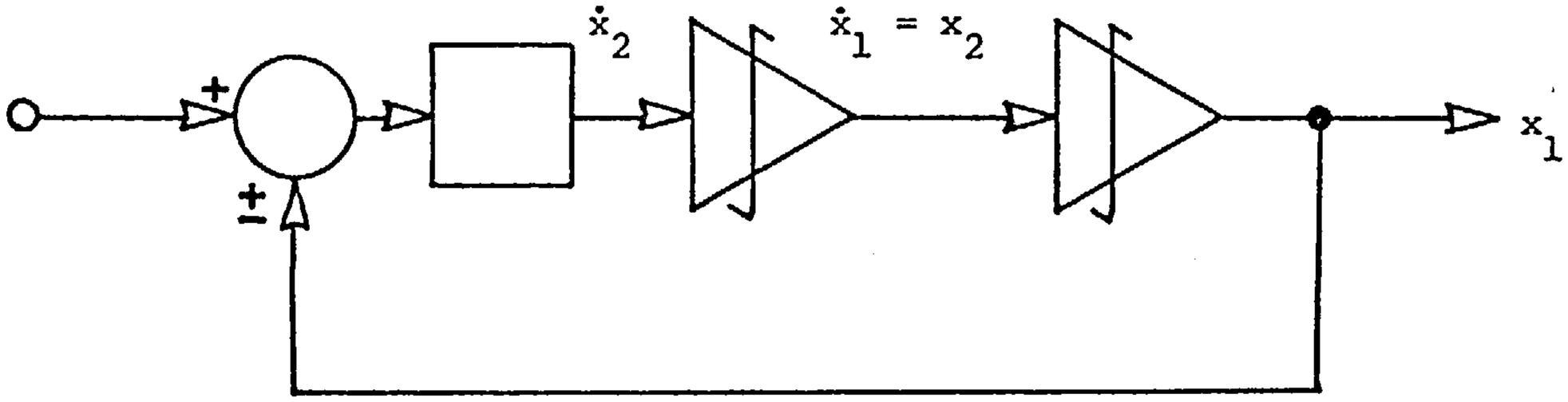

(a)

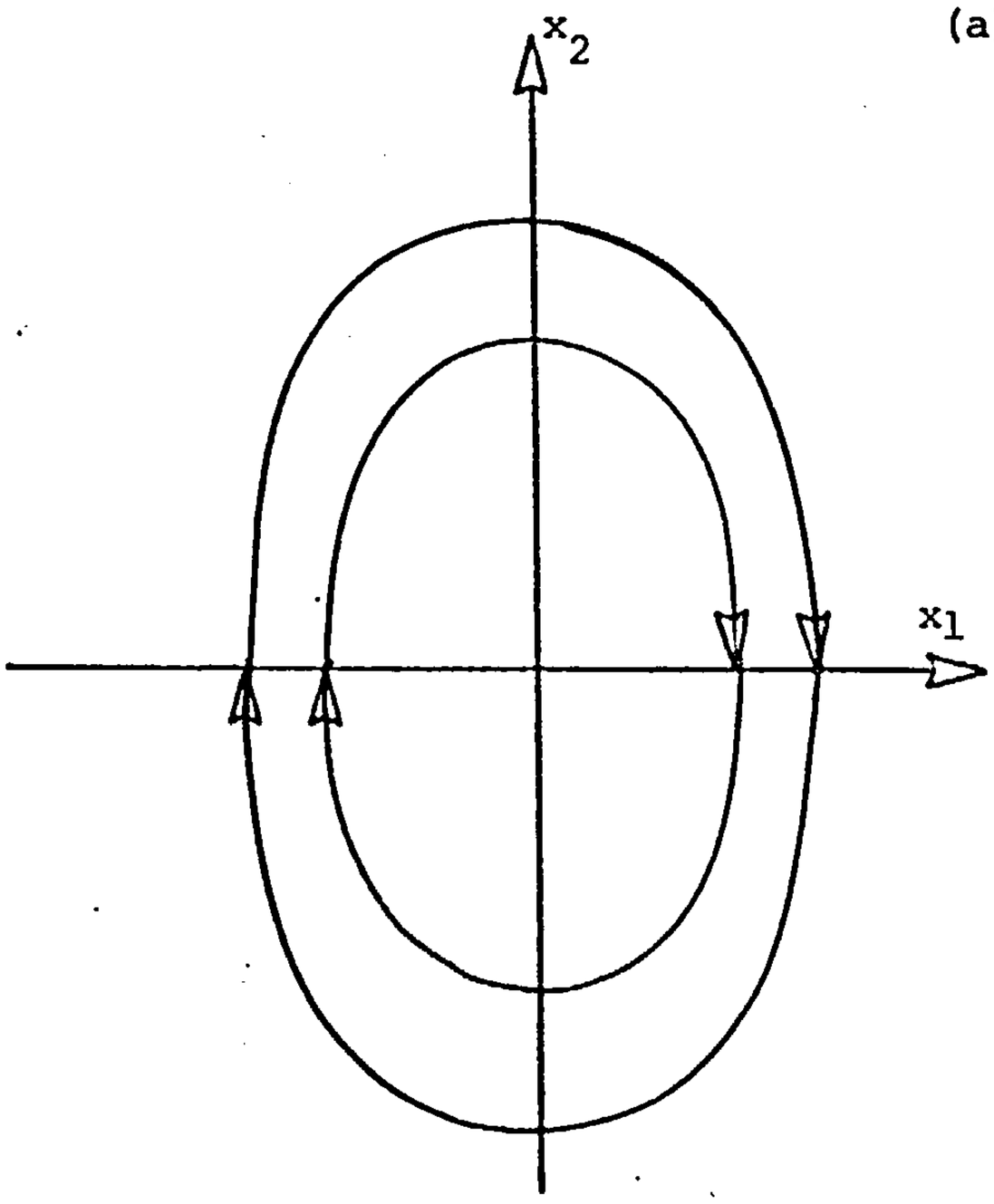

(b)

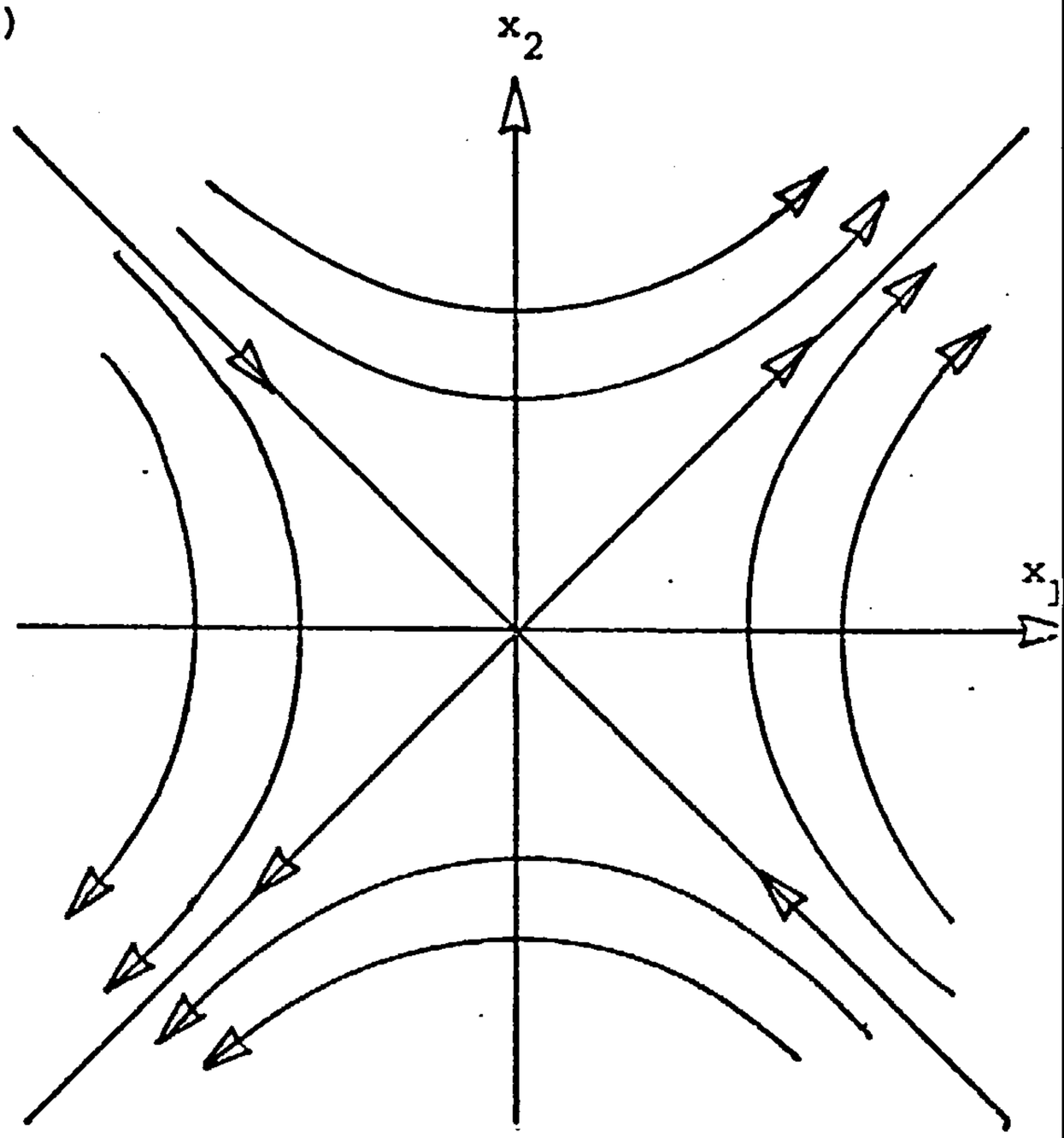

(c)

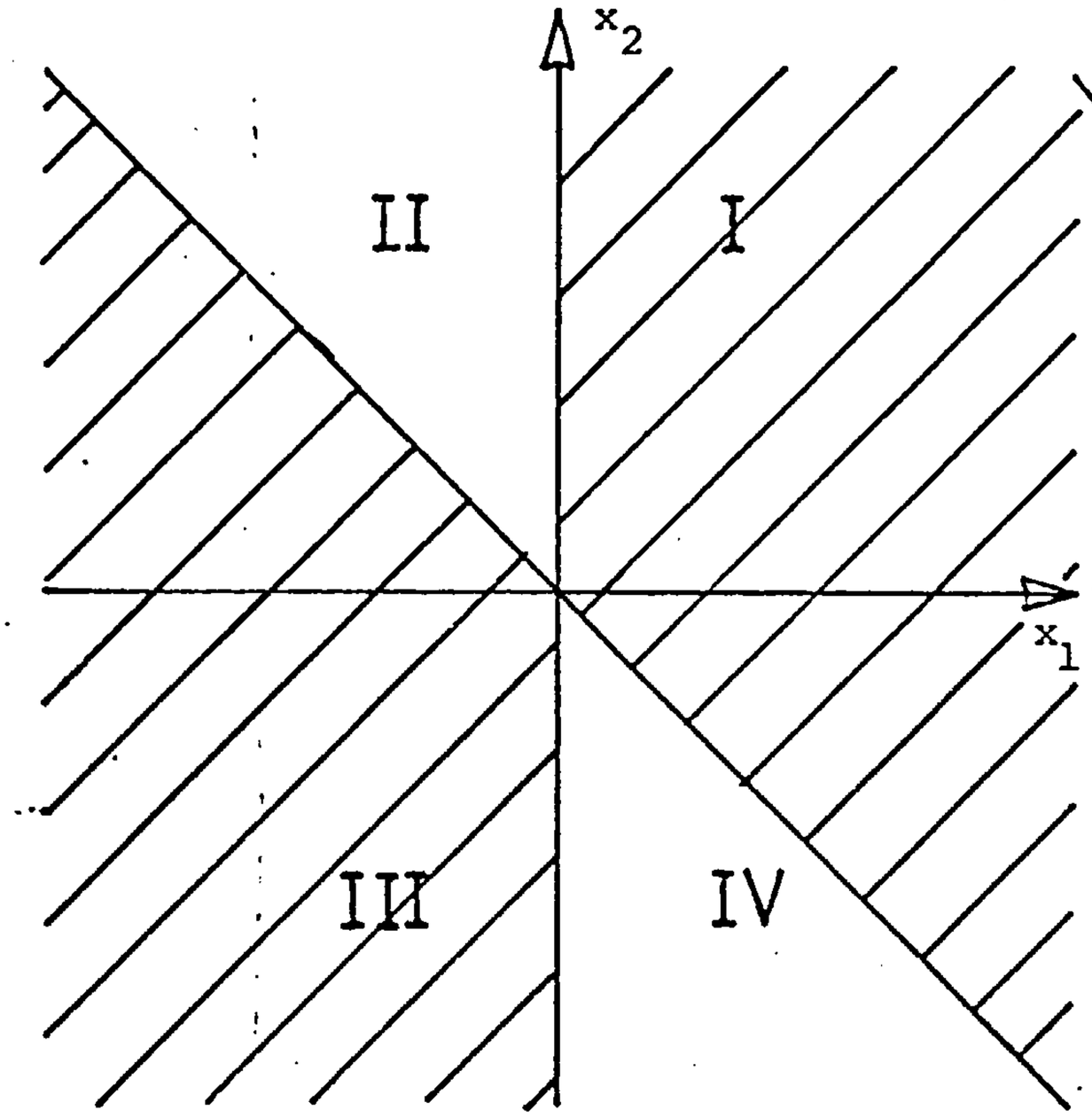

(d)

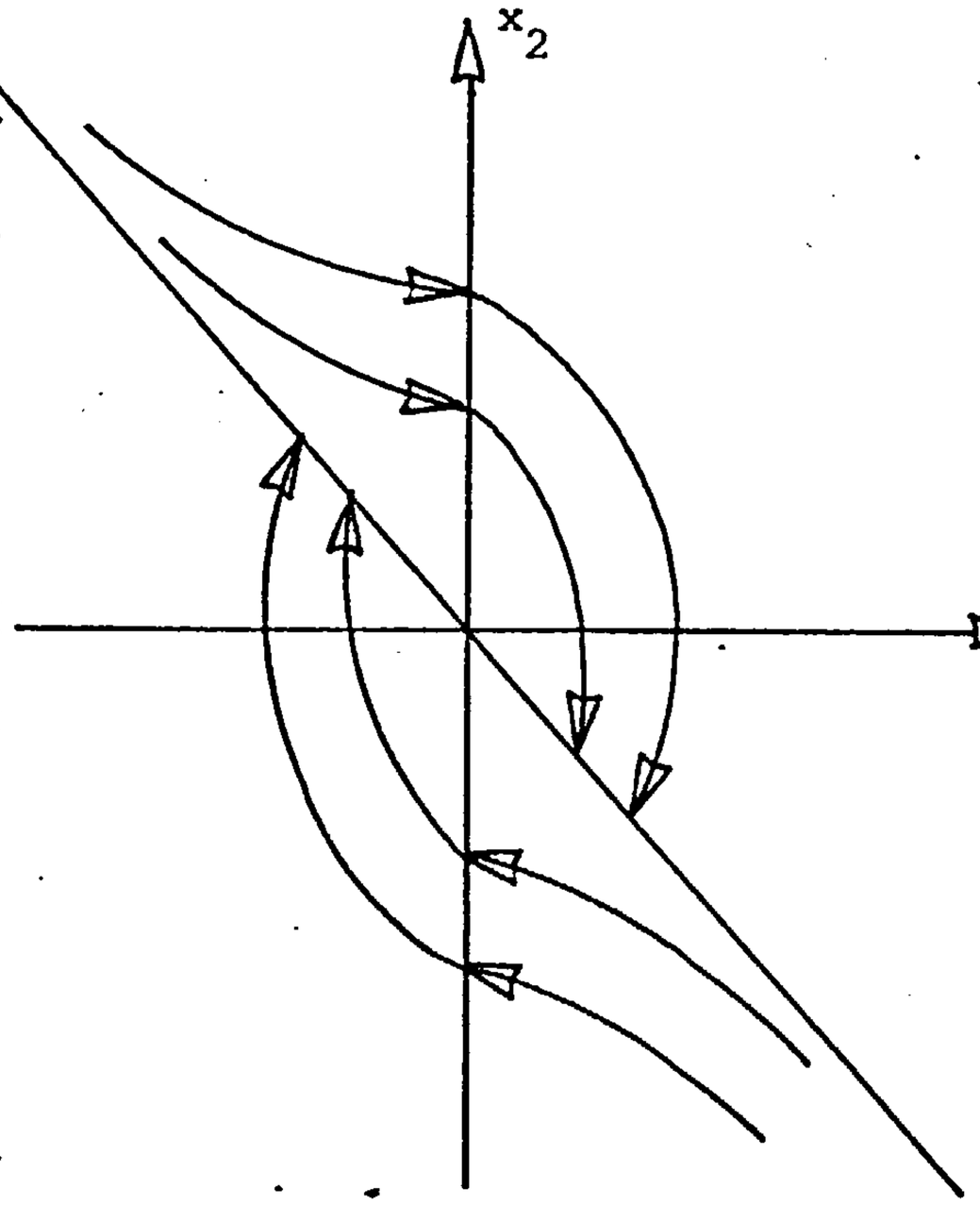

(e)

Figure (2.1) Second-Order System with Positive and Negative Feedback

2.1 A Second-Order Plant

The system under consideration consists of two integrators connected in series and is the type of plant which is encountered in phase-lock loops, see fig. (2.1a). With negative feedback, the resulting control system is conservative and its free motion is described by a second-order system of differential equations.

$$\left.\begin{aligned} \dot{x}_1 &= x_2 \\ \dot{x}_2 &= -a_1 x_1 \end{aligned}\right\} \qquad (2.1)$$

where x_1 is the output signal and x_2 its derivative. The characteristic equation is given by

$$s^2 + a_1 = 0 \qquad (2.2)$$

If $a_1 > 0$ the phase trajectories of the system are elliptic as shown in fig. (2.1b).

With positive feedback and with $a_1 > 0$, the system's equations are

$$\left.\begin{aligned} \dot{x}_1 &= x_2 \\ \dot{x}_2 &= +a_1 x_1 \end{aligned}\right\} \qquad (2.3)$$

and the characteristic equation is given by

$$s^2 - a_1 = 0 \qquad (2.4)$$

The phase trajectories in this instance are hyperbolic, see fig. (2.1c), and the system is unstable for all initial conditions except for those lying on the asymptote $x_2 + \sqrt{a_1}\, x_1 = 0$. From stability considerations, both systems (2.1) and (2.3) are unacceptable. However, certain parts of the phase trajectories are satisfactory which when suitably combined can produce a stable system. Let the phase

space be divided into four regions by the straight lines $x_1 = 0$ and $x_2 + \sqrt{a_1}\, x_1 = 0$, with the latter line representing a stable eigenvector of system (2.3), see fig. (2.1d). If the feedback sign is switched such that the system is elliptic in regions I and III and hyperbolic in regions II and IV, then the composite trajectories are as shown in fig. (2.1e). The system is now stable with an aperiodic transient response.

For the system under consideration, the asymptote $\sigma = x_2 + \sqrt{a_1}\, x_1 = 0$ and the ordinate axis $x_1 = 0$ act as switching boundaries for the structure. In general, a switching boundary need not be an asymptote and could be a straight line of the form,

$$\sigma = cx_1 + x_2 \quad (0 < c < \infty) \tag{2.5}$$

passing through the origin. Two cases then arise:

(i) $c > \sqrt{a_1}$, and

(ii) $0 < c < \sqrt{a_1}$.

In case (i), the phase trajectories are as in fig. (2.1e) with elliptic arcs in regions I and III, and with hyperbolic arcs which deviate away from the asymptote in regions II and IV.

In case (ii), i.e. for $0 < c < \sqrt{a_1}$, the phase trajectories are elliptic and hyperbolic as in case (i) but have opposite directions in the neighbourhood of the switching line $\sigma = 0$, fig. (2.2). Starting from any initial condition in region I, the phase point moves along an elliptic trajectory and crosses the line $\sigma = 0$ into region IV at some finite time. The system switches to a hyperbolic one and the phase trajectories are such that the phase point is pushed back into region I. The system switches instantly back to an elliptic structure and the phase point is again forced back into region IV with the

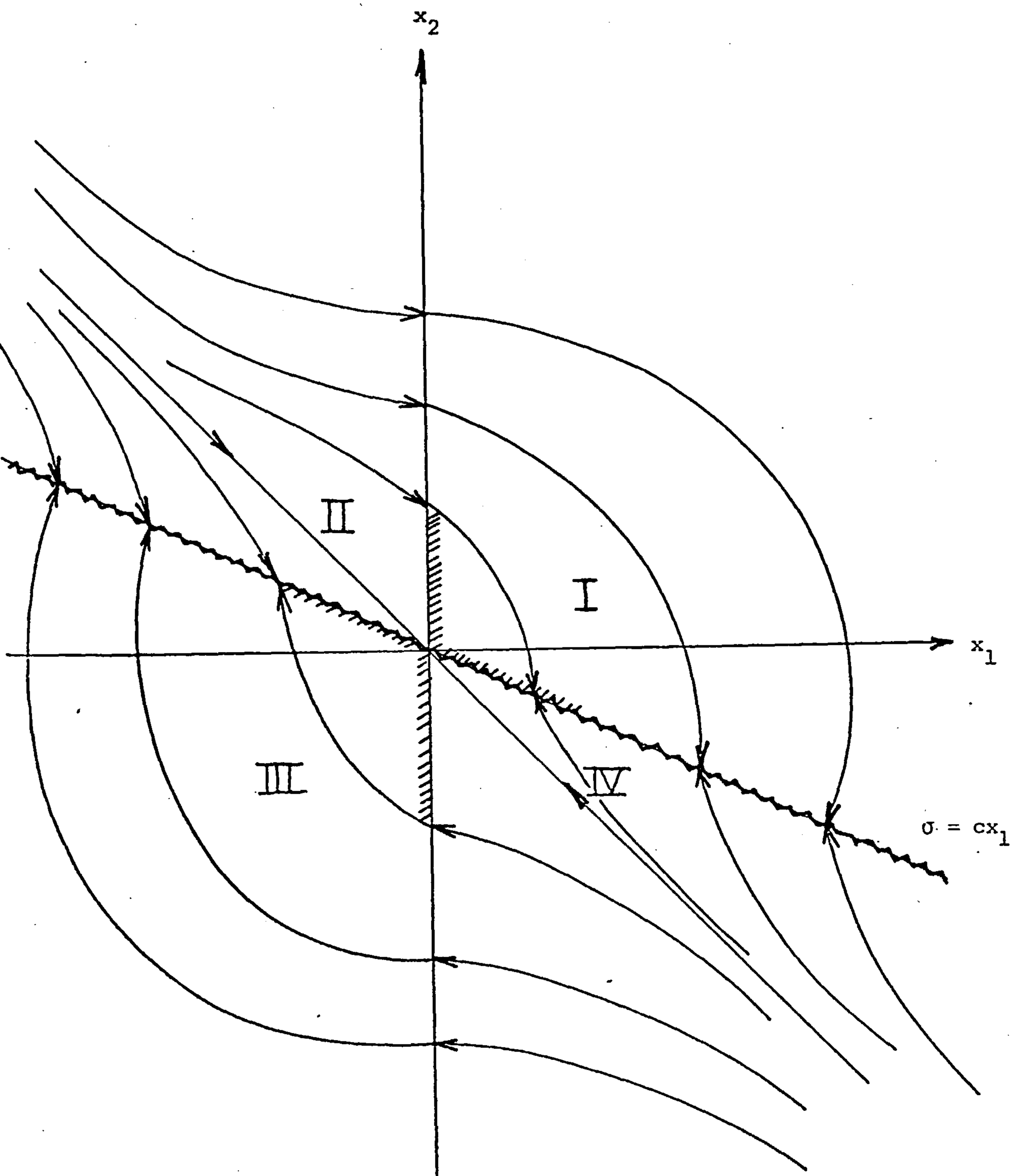

Figure 2.2: Sliding Regime in a Second-Order Plant

process repeating itself. The phase point is thus constrained to move on the switching boundary in a special regime known as a sliding regime, [2.1] [2.2].

From a rigorous mathematical standpoint, the motion of the system is undefined and requires further clarification. This may be accomplished by idealising the motion of a real VSS. In a real VSS, a small delay t exists in the system's switching circuits, and instead of switching over from elliptic to hyperbolic at time t_1, the structure changes at time $t_1 + t$. In the interim, the phase point has penetrated into region IV along an elliptic trajectory. At time $t_1 + t$, the phase point approaches the line $\sigma = 0$ along an arc of a hyperbola. At some time $t_2 > t_1 + t$ it crosses the boundary, but the structure does not switch over until time $t_2 + t$, when the phase point continuing to move along a hyperbolic trajectory has already trespassed into region 1. At time $t_2 + t$, the structure changes and the phase point again returns to region IV and so on, thus performing small oscillations around the switching line. Fig. (2.2) indicates that while oscillating in this way, the phase point moves on the average towards the origin. As $t \to 0$, the amplitude of the oscillations is reduced while the frequency increases, and in the limit the phase point will oscillate with infinitesimal amplitude and infinitely high frequency. The motion of the system can then be described by the differential equation,

$$cx_1 + \frac{dx_1}{dt} = 0 \qquad (2.6)$$

and is the definition of an ideal sliding regime.

2.2 Properties of the Sliding Regime

Equation (2.6) reveals that the sliding motion is dependent only on the fixed parameter c and does not involve the plant parameter a_1 explicitly. If a_1 assumes values in the range,

$$0 < a_{1min} \leq a_1 \leq a_{1max} \tag{2.7}$$

and if

$$0 < c < \sqrt{a_{1min}} \tag{2.8}$$

then the phase trajectories will be as shown in fig. (2.2) for all variations of a_1. A change in a_1 defined by,

$$-\infty \leq \frac{da_1}{dt} \leq \infty \tag{2.9}$$

corresponds simply to a jump from one trajectory to another in the same sector. Consequently the sliding regime will only be affected to the extent that its initial formation is either brought forward or delayed.

An external disturbance f(t) acting on the system in the following way,

$$\left.\begin{aligned} \dot{x}_1 &= x_2 \\ \dot{x}_2 &= \pm a_1 x_1 - f(t) \end{aligned}\right\} \tag{2.10}$$

will have a similar effect on the sliding motion provided that it does not alter the directions of the trajectories. In general, the disturbance f(t) will only distort the shapes of the phase trajectories but not their directions.

Invariancy conditions to parametric and external disturbances are discussed more fully later.

It is immediately evident that certain criteria must be fulfilled before a sliding motion can be realised. Firstly, starting from any initial condition in space, the phase point must be able to reach the sliding surface; this condition has been described in the literature as the 'hitting condition'. Secondly the phase trajectories on each side of the hypersurface must point towards it to ensure the existence of a sliding mode, and, thirdly, motion in the sliding surface must be stable. These topics are discussed in detail in the following chapter for an n^{th} order system along with several other important ones such as the tracking of input signals, the effect of zeros in the transfer function and sliding in state-space systems.

CHAPTER THREE

VARIABLE STRUCTURE CONTROLLERS FOR SINGLE-INPUT SYSTEMS

The criteria of hitting, existence of sliding modes and stability of the sliding motion have formed the basis of the research in VSS. One of the most eminent early researchers in the field was S.V. Emelyanov [3.12, 3.13, 3.14]. His pioneering work along with the contribution of other Russian scientists have led to the formulation of a number of theorems for the fulfilment of these criteria in linear time-invariant and time-varying systems.

The purpose of this chapter is to review the theory of VSS based on sliding modes for an nth order system with a single input. Some fundamental areas of control systems theory and design are studied in the light of the new theory and are categorised under the following headings:

i) time-invariant plant in phase-variable form.

ii) time-varying plant in phase-variable form.

iii) state-space systems.

iv) effects of zeros in VSS.

v) tracking of inputs.

The theorems dealing with the conditions for the formulation of a sliding motion in these systems are presented and their implications are discussed. The first theorem enunciated in VS theory was related to plants represented in phase-variable form and it is thus convenient to start the study at that point. The following sections are in the main a summary of the work of S.V. Emelyanov and his co-researchers which is reported in [1.1] and [3.1].

3.1 VSS for Phase Variable Plants

The realisation of a VSS controller for an n^{th} order linear plant, as originally conceived, relied on the availability of the first n derivatives. In many practical systems, such as speed control in motor systems or heading control of ships, the derivatives can be measured directly as the phase-variable form is inherent of the system's structure. For other systems with general plant matrices, the phase-canonical form is derived through a transformation [3.2] or differentiation. Assuming that the full state vector can be represented and measured in phase variable form, then the analysis of the VSS proceeds as follows.

3.1.1 Time-Invariant Plant

In this section, the following system is considered:

$$\left.\begin{aligned} \dot{x}_i &= x_{i+1} \qquad i = 1, \ldots, n-1 \\ \dot{x}_n &= -\sum_{i=1}^{n} a_i x_i + u \end{aligned}\right\} \tag{3.1}$$

where x_i are the state variables, u is the driving input and a_i are the plant's parameters, assumed constant. In the frequency domain, equation (3.1) can be represented by the transfer function,

$$G(s) = \frac{x_1(s)}{u(s)} = \frac{1}{s^n + a_n s^{n-1} + \ldots + a_2 s + a_1} \tag{3.2}$$

where 's' is the Laplace operator. A sliding hyperplane S can be formed by a linear combination of the elements of the state vector $\underline{x}$ and is given by

$$\sigma = \sum_{i=1}^{n} c_i x_i \qquad c_i = \text{constant}, \; c_n = 1 \tag{3.3}$$

A sufficient condition for sliding to occur on the above hyperplane is given by

$$\lim_{\sigma \to +0} \dot{\sigma} < 0 < \lim_{\sigma \to -0} \dot{\sigma} \tag{3.4}$$

The above inequality indicates that if the phase point is above the hyperplane, then its velocity must be negative in order to drive it towards S, and vice-versa if it is below S. In deriving the sliding equations, the inequalities of (3.4) are usually replaced by the following equations which were proposed by Wonham and Johnson [3.3].

$$\sigma = 0 \quad \text{and} \quad \dot{\sigma} = 0 \tag{3.5}$$

In physical terms, the above equality replaces the fast oscillations of the phase point about S (Fig. 2.2) by the slow average component of the motion in S. Hence during the sliding regime, the phase point (or representative point RP) simply moves on $\sigma = 0$, never leaving it; this is formally represented by the vanishing of the function σ and its derivative.

Solving equation (3.3) when $\sigma = 0$ for the variable x_n and substituting into equation (3.1) gives the equations of the sliding mode, i.e.

$$\left.\begin{aligned} \dot{x}_i &= x_{i+1} \qquad i = 1, \ldots, n-2 \\ \dot{x}_{n-1} &= -\sum_{i=1}^{n-1} c_i x_i \end{aligned}\right\} \tag{3.6}$$

Equation (3.6) is only dependent on the parameters c_i and is thus invariant to the parameters a_i. It is of (n-1)th order as a consequence of the linear dependence of x_n on the remaining states.

The solution of equation (3.5) is linked to the type of control exerted. Control laws based on linear combinations of the vector $\underline{x}$ are discussed below together with the criteria for reaching the hyperplane and stability in the sliding mode for the linear time-invariant system.

Case (i)

The problem of regulating the output x_1 around zero is first considered. The following control law, proposed by Emelyanov, equates the control function u to a piecewise linear function of x_1 with discontinuous coefficients.

$$u = - b\ \psi_1 x_1$$

$$\psi_1 = \begin{cases} \alpha_1 & \text{if } x_1\sigma > 0 \\ \beta_1 & \text{if } x_1\sigma < 0 \end{cases}$$

$$\text{where} \quad \sigma = \sum_{i=1}^{n-1} c_i x_i + x_n \qquad (3.7)$$

$$c_i = \text{constant} > 0 \quad i = 1, 2, \ldots, n-1$$

$$c_n = 1$$

The conditions $x_1\sigma > 0$ and $x_1\sigma < 0$ identify four sub-spaces in the phase-space as shown in fig. (3.1), with the hyperplane S projected in the plane $x_1 - x_2$. The fundamental difference between VSS and optimal relay systems [3.4] in which the control u assumes one of two possible values can now be appreciated. In this particular VSS, u is zero when x_1 is zero whereas in a practical relay system, the control is unable to settle at zero and is permanently switching between the

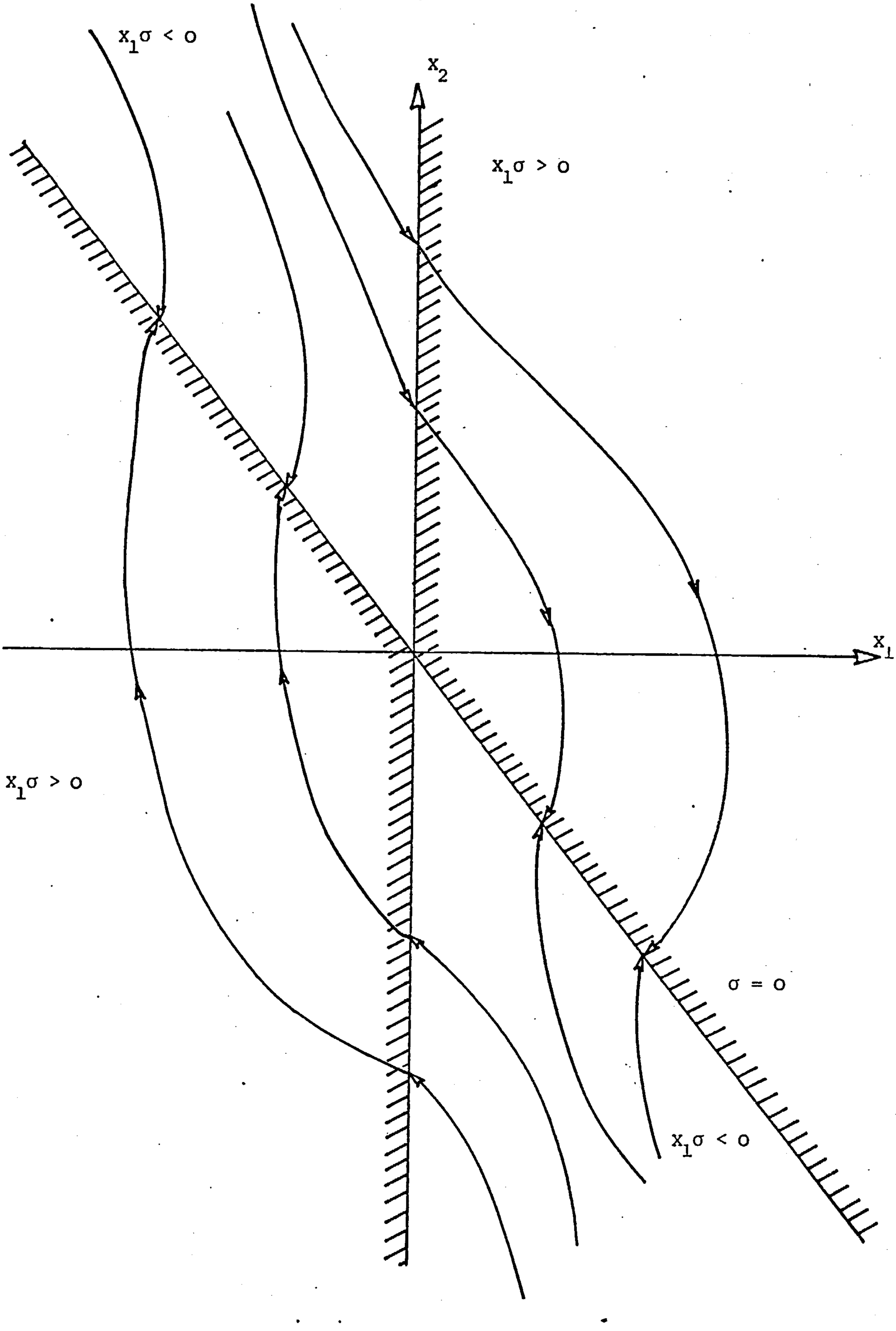

Figure 3.1 Trajectories at Switching Boundaries

two extreme values.

Replacing u in equation (3.1) gives,

$$\left.\begin{aligned} \dot{x}_i &= x_{i+1} \qquad i = 1, 2, \ldots, (n-1) \\ \dot{x}_n &= -\sum_{i=1}^{n} a_1 x_1 - b\,\psi_1 x_1 \end{aligned}\right\} \tag{3.8}$$

The regions of interest in fig. (3.1) are defined by the hyperplanes $x_1 = 0$ and $\sigma = 0$. It is readily seen that the RP pierces the hyperplane $x_1 = 0$, because the sign of the rate of change of x_1, i.e. x_2, on each side of the boundary is unaffected. The boundary conditions can be formulated as follows:

$$\left.\begin{aligned} &\lim_{x_1 \to +0} \dot{x}_1 > 0 < \lim_{x_1 \to -0} \dot{x}_1 \qquad \text{if } x_2 > 0 \\ &\lim_{x_1 \to +0} \dot{x}_1 < 0 > \lim_{x_1 \to -0} \dot{x}_1 \qquad \text{if } x_2 < 0 \end{aligned}\right\} \tag{3.9}$$

and,

These inequalities do not fulfil the sliding regime conditions given in (3.4), hence the direction of the trajectory remains unchanged across the boundary $x_1 = 0$.

However, when $\underline{x}(t)$ crosses the hyperplane $\sigma = 0$, the rate of change of σ, i.e. $\dot{\sigma}$, is controllable through x_1 and it is thus possible to reverse the trajectory to form a sliding regime. The derivative of σ along the trajectories of system (3.7) and (3.8) is given by:

$$\left.\begin{aligned}\dot{\sigma} &= \sum_{i=1}^{n-1} c_i \dot{x}_i + \dot{x}_n \\ &= \sum_{i=1}^{n-1} c_i x_{i+1} - \sum_{i=1}^{n} a_i x_i - b\,\psi_1 x_1\end{aligned}\right\} \qquad (3.10)$$

By equation (3.5), $\sigma = 0$ in a sliding mode, i.e.

$$x_n = -\sum_{i=1}^{n-1} c_i x_i \qquad (3.11)$$

Hence,

$$\dot{\sigma} = \sum_{i=2}^{n-1} (c_{i-1} - a_i + c_i a_n - c_i c_{n-1}) x_i + (c_1 a_n - a_1 - c_1 c_{n-1} - b\,\psi_1) x_1 \qquad (3.12)$$

To guarantee the second condition in equation (3.5) of $\dot{\sigma} = 0$ implies that the first term in (3.12) must vanish, i.e.

$$\frac{c_{i-1} - a_i}{c_i} = c_{n-1} - a_n \qquad i = 2, \ldots, n-1 \qquad (3.13)$$

Equation (3.12) is reduced to,

$$\dot{\sigma} = (-a_1 + c_1 a_n - c_1 c_{n-1} - b\,\psi_1) x_1 \qquad (3.14)$$

Equation (3.14) must also disappear. A straight application of the condition $\dot{\sigma} = 0$ only indicates that,

$$\theta_1 = \frac{1}{b}(-a_1 + c_1 a_n - c_1 c_{n-1}) \qquad (3.15)$$

where θ_1 is the mean value of ψ_1. If instead, the following equivalent inequality of (3.4) is applied, i.e.

$$\lim_{\sigma \to 0} \sigma\dot{\sigma} \lesssim 0 \qquad (3.16)$$

then the following condition for the existence of a sliding regime is obtained from (3.14),

$$\sigma\dot{\sigma} = (-a_1 + c_1 a_n - c_1 c_{n-1} - b\,\psi_1) x_1 \sigma \lesseqgtr 0 \qquad (3.17)$$

and if,

$$\left.\begin{aligned} x_1\sigma > 0 \quad \text{then } \psi_1 = \alpha_1 \gtrless \frac{1}{b}(-a_1 + c_1 a_n - c_1 c_{n-1}) \\ \text{and if} \\ x_1\sigma < 0 \quad \text{then } \psi_1 = \beta_1 \lesseqgtr \frac{1}{b}(-a_1 + c_1 a_n - c_1 c_{n-1}) \end{aligned}\right\} \qquad (3.18)$$

It is interesting to consider the physical meaning of the control function u. In a sliding mode, the control function u may be regarded as consisting of a low frequency or average component corresponding to conditions (3.5) and (3.15). Deviations from the hyperplane cause the gains α_1 or β_1 to be switched thus adding a high frequency component to the control function u, which is associated to conditions (3.4) and (3.18). It is intuitive that the behaviour of the system primarily depends on the average rather than on the high frequency components, and this average value of the control is often known as the "equivalent control", [3.5].

The stability of motion in the sliding mode is dependent on the roots of the equivalent reduced system (equation 3.6). If the coefficients c_i (i=1, ..., n-1) satisfy the Routh-Hurwitz criterion, then the sliding motion is stable. But the coefficients c_i are already subjected to certain restrictions (3.13) and these may contradict the Routh-Hurwitz conditions. In fact, there may exist plant parameters a_1, ..., a_n for which there are no coefficients c_1, ..., c_{n-1} such that the motion in the sliding regime is stable.

The following theorem gives a general criterion relating the stability of the sliding regime to the plant parameters [1.1].

Theorem 3.1: The motion in the sliding regime on the hypersurface $\sigma = 0$ is stable if and only if all the roots of the characteristic equation of the system described by equations (3.1) and (3.7) with $\psi_1 = \frac{1}{b}(- a_1 + c_1 a_n - c_1 c_{n-1})$ have negative real parts except for the nth root which may be arbitrary.

The proof of Theorem 3.1 is given in Appendix A. Since the main objective is the interpretation, evaluation and application of VSS theory and its theorems, proofs are outlined in the appendices.

The above theorem indirectly points to two important properties of VSS. Firstly in the sliding regime, the mean value of the controller gain, i.e. $\psi_1 = \theta_1 = \frac{1}{b}(- a_1 + c_1 a_n - c_1 c_{n-1})$ is a useful fact in the assignment of the closed loop eigenvalues and in the selection of the coefficients of the hyperplane. Secondly the nth root λ_n does not affect the stability of the sliding motion; it is shown in Appendix A that this condition is a result of x_n being linearly dependent on $x_i (i = 1, \ldots, n-1)$ in that mode.

The conditions for the existence of a sliding regime and for stability of the sliding motion for the system described by equation (3.8) have been established. Finally it is necessary to guarantee that the sliding plane is reached from all initial states. The reaching or hitting conditions of the hyperplane S are formulated in the following theorem:

Theorem 3.2: If the plane $\sigma = 0$ is a sliding plane and if the sliding mode is asymptotically stable, then the state $\underline{x}$ will reach $\sigma = 0$ with $c_i > 0$ provided that all real eigenvalues of system (3.8) with $\psi_1 = \alpha_1$ be non-negative.

The proof of Theorem 3.2 is given in Appendix B.

Theorem 3.2 is of considerable interest as it allows the closed loop system to have complex eigenvalues with positive real parts. The selected hyperplane can thus be reached in spite of wide variations in the pole locations and therefore precise identification of the plant's parameters is not required.

Case (ii)

The driving function u is chosen in this instance as a piecewise linear function of a subset of the vector $\underline{x}$ with discontinuous coefficients, i.e.

$$\left.\begin{aligned} u &= -\sum_{i=1}^{k} \psi_i x_i \qquad 1 \leq k \leq n-1 \\ \psi_i &= \begin{cases} \alpha_i & \text{if } x_i\sigma > 0 \\ \beta_i & \text{if } x_i\sigma < 0 \end{cases} \\ \text{where: } \sigma &= \sum_{i=1}^{n-1} c_i x_i + x_n \end{aligned}\right\} \qquad (3.19)$$

Using the above control law and following the procedure of Case (i), necessary and sufficient conditions for a sliding plane to exist are given by,

$$\left.\begin{aligned} &\alpha_i \geq c_{i-1} - a_i - c_i c_{n-1} + c_i a_n \\ &\beta_i \leq c_{i-1} - a_i - c_i c_{n-1} + c_i a_n \\ &\text{for} \quad i = 1, \ldots, k \qquad c_o = 0 \\ &\text{and} \quad c_{i-1} - a_n = c_i (c_{n-1} - a_n) \\ &\text{for} \quad i = k+1, \ldots, n-1 \end{aligned}\right\} \qquad (3.20)$$

The condition for stability in the sliding plane is an extension of theorem 3.1 and is as follows:

Theorem 3.3: If $\lambda_1, \lambda_2, \ldots, \lambda_n$ are the eigenvalues of the system described by equations (3.1) and (3.19) with

$$u = - \sum_{i=1}^{k} \theta_i x_i$$

where $\theta_i = c_{i-1} - a_i - c_i c_{n-1} + c_i a_n$

then the sliding mode is asymptotically stable if Re $\lambda_i < 0$ for $i = 1, \ldots, n-1$.

The eigenvalue λ_n again does not affect the stability of the sliding mode. The proof of the theorem is omitted here but is similar to that of Theorem 3.1. The stability of the sliding motion is dependent on the average gains θ_i of the controller which can be selected through the pole-assignment procedure described in Appendix C.

The hitting conditions are expressed in the following reformulation of Theorem (3.2), [3.7],

Theorem 3.4: If the plane $\sigma = 0$ is a sliding plane and if the sliding motion is asymptotically stable, then the state $\underline{x}$ will reach the plane $\sigma = 0$ with $c_i > 0$ provided that all the real eigenvalues of (3.1) and (3.19) with $\psi_i = \alpha_i$ be non-negative.

Again the sliding plane can be reached for virtually any pole positions with $\psi_i = \alpha_i$. As pointed out in the proof of Theorem 3.2, this restriction does not apply with $\psi_i = \beta_i$, since the RP will eventually cross the hypersurface for any positive real roots, thus fulfilling the hitting conditions.

Finally it is to be noted in equation (3.20) that if $k = (n-1)$, then the equality constraints of the type $c_{i-1} - a_i = c_i(c_{n-1} - a_n)$ are eliminated thus allowing a wider choice of the parameter c_i.

3.1.2 Time-Varying Plant

Since the main advantage of a sliding system is its independence to parametric variations, it is important to establish the conditions of existence, reachability and stability for the sliding plane in linear time-varying systems. The plant considered is described by the following set of differential equations in phase-variable form,

$$\left.\begin{aligned} \dot{x}_i &= x_{i+1} \qquad i = 1, \ldots, n-1 \\ \dot{x}_n &= -\sum_{i=1}^{n} a_i(t)\, x_i - b(t) \sum_{i=1}^{k} \psi_i x_i \end{aligned}\right\} \tag{3.21}$$

where $a_{imin} \lesssim a_i(t) \lesssim a_{imax}$ $(i = 1, \ldots, n)$ are the bounded piece-

wise-continuous parameters of the plant and the gain b(t) is also bounded and piecewise-continuous, $b_{min} \leq b(t) \leq b_{max}$. The parameters are assumed to be inaccessible for measurement. The control law is defined by,

$$\left.\begin{aligned} \psi_i &= \begin{cases} \alpha_i & \text{if } x_i\sigma > 0 \quad i = 1, \ldots, k \\ \beta_i & \text{if } x_i\sigma < 0 \end{cases} \\ \text{where} \quad \sigma &= \sum_{i=1}^{n-1} c_i x_i + x_n \\ c_i &= \text{const} > 0 \quad i = 1, \ldots, n-1 \end{aligned}\right\} \qquad (3.22)$$

The necessary and sufficient conditions for the existence of a sliding regime for the system (3.21) and (3.22) are given by,

$$\left.\begin{aligned} \alpha_i &\geq \sup \frac{1}{b(t)} \left[c_{i-1} - a_i(t) + c_i a_n(t) - c_i c_{n-1}\right] \\ \beta_i &\leq \inf \frac{1}{b(t)} \left[c_{i-1} - a_i(t) + c_i a_n(t) - c_i c_{n-1}\right] \\ &\text{for} \quad i = 1, \ldots, k \\ c_{i-1} &- a_i(t) = c_i(c_{n-1} - a_n(t)) \\ &\text{for} \quad i = k+1, \ldots, n-1 \\ &\text{and } \inf a_n(t) \geq c_{n-1} \end{aligned}\right\} \qquad (3.23)$$

The proof of equation (3.23) is given in Appendix D. It is interesting to note that the rates of change of $a_i(t)$ $i = 1, \ldots, k$ do not affect the sliding conditions.

The sliding motion is stable if the coefficients c_i $(i=1, \ldots, n-1)$ satisfy the Routh-Hurwitz conditions. Theorems (3.1) and (3.3) have related the coefficients c_i to the plant's parameters for the time-

invariant case, and have shown that the control can settle at a constant mean level as defined by equation (3.15). But in a time-varying system, the control switches around a mean level (according to equation (3.23)) and forces the trajectory to lie on the sliding hyperplane. It is not possible in this instance to relate the average gain θ_i to a_i and c_i as in Theorem 3.3.

The hitting conditions for the time-varying system have been derived for the cases when $k = n-1$ and $1 \leq k \leq n-2$ where 'k' is defined in equation (3.21). The latter case is the more interesting one as it is preferable to minimise the number of feedback sensors from a cost point of view. A sufficient condition for hitting to take place in the time-varying system of (3.21) is given in the following theorem.

Theorem 3.5: If conditions expressed in (3.23) hold, then the hyperplane $\sigma = 0$ will be hit from any initial position in the phase plane, or else $\lim_{t \to \infty} x_i(t) = 0 \quad (i = 1, \ldots, k)$.

The proof of Theorem 3.5 is given in Appendix E.

It is not possible to determine the Laplace Transform of equation (3.21) but if the parameters $a_i(t)$ and $b(t)$ change in discrete steps, then the characteristic equation can be written as,

$$s^n + a_n s^{n-1} + \ldots + a_{k+1} s^k + (a_k + b\psi_k) s^{k-1} + \ldots + (a_1 + b\psi_1) = 0 \qquad (3.24)$$

Theorem 3.5 implies that a_{imin} $(i = k+1, \ldots, n)$ must all be positive and that $a_i + b\psi_i$ $(i = 1, \ldots, k)$ must also be positive when $\psi_i = \alpha_i$. The theorem then unlike its counterpart for the time-invariant case is not specific in the pole locations with $\psi_i = \alpha_i$.

3.1.3 Comments on the Control Method

In the last two sections, attention has been focused on the theorems in VSS theory which define the existence, stability and hitting of a sliding plane for plants with constant and time-varying parameters. The theory has a very appealing feature in that it can be interpreted as a two-level type of control system. In the time-invariant case, the first level of control consists in determining a continuous state feedback vector of the form $u = \sum_{i=1}^{k} \theta_i x_i$ which positions (n-1) eigenvalues as close as possible to some desired locations (Theorem 3.3). The second level of control takes the form of equation (3.19) which assures the existence of the sliding plane. A similar interpretation applies to the time-varying case if the state-feedback design is worked around some nominal plant parameter values and the values of α_i, β_i in (3.23) are chosen to take care of all parameter variations through the enforcement of a sliding regime. This feature of VSS is highlighted later in the design of a ship's autopilot.

The theory of VSS as presented to this point has certain drawbacks which restricts its field of application (i) the plant is in phase-variable form, (ii) all the states are required in synthesising the switching surface, although not all the states are required in composing the control function. Restriction (i) may or may not be a problem if the system,

$$\dot{\underline{x}} = \underline{A}\underline{x} + \underline{b}u \tag{3.25}$$

can be transformed to the equivalent phase-variable form, [3.2]

$$\dot{\underline{y}} = \hat{\underline{A}}\underline{y} + \hat{\underline{b}}u \tag{3.26}$$

where,

$$\hat{\underline{A}} = \begin{bmatrix} 0 & 1 & 0 & \dots & 0 \\ 0 & 0 & 1 & \dots & 0 \\ \vdots & \vdots & \vdots & & \vdots \\ 0 & 0 & 0 & \dots & 1 \\ a_1 & a_2 & a_3 & \dots & a_n \end{bmatrix} \qquad \hat{\underline{b}} = \begin{bmatrix} 0 \\ 0 \\ \vdots \\ 1 \end{bmatrix} \tag{3.27}$$

A sliding motion can then be organised in the system based on the state vector $\underline{y}$. In the time-invariant case, i.e. $\underline{A}$ and $\underline{b}$ are constants, the invariant motion of system (3.26) will produce an equivalent invariant motion in system (3.25) since $\underline{y}$ and $\underline{x}$ are linearly related. When $\underline{A}$ and $\underline{b}$ are time-varying, Silverman [3.2] has shown that under certain conditions, the transformation from (3.25) to (3.26) still applies. But $\underline{y}$ and $\underline{x}$ are now related by a time-varying matrix; thus sliding in system (3.26) does not necessarily imply sliding in system (3.25). It can be inferred from the above argument that other conditions must be fulfilled to achieve a sliding motion in a time-varying system. This point is discussed further in the next section.

Restriction (ii) appears to be a severe one and raises some very important questions. Since all the states are required in the switching function, it implies that the structure of the plant is well-defined which is rarely the case in practical examples. The question arises then about the possibility of synthesising the switching function using only the variables associated with the dominant time constants of the plant and the robustness of the VSS to such plant uncertainty. Would a system based on linear principles yield a better solution under these circumstances? Other questions concerning noisy states and nonlinearities such as

saturation, also arise which make it difficult to give a direct quantitative comparison of VSS and linear system design or any other design technique. Consequently, comparison of different methods is avoided. Instead, in the examples studied in subsequent chapters, attention is primarily focused on the areas of the designs which can be improved by VSS. It is felt that this approach will be considerably more beneficial to the designer who can decide then which method to adopt for his particular application.

3.2 Sliding in State-Space Systems

To achieve the invariance conditions of a sliding motion, it was shown that it is necessary to obtain instantaneous values of the coordinate as well as its derivatives to the nth order which restricts the application of the technique to plants in phase-variable form. Drazenovic [3.8] has shown that VSS can be extended to encompass systems with more general structures, and using a state-space representation of linear systems has proved that a sliding motion can be realised using the state-variables. The work is of considerable practical interest and is discussed below.

3.2.1 Sliding Equations

The following single input system described by a set of first order differential equations is considered,

$$\dot{\underline{x}} = \underline{\underline{A}}\underline{x} + \underline{b}u \qquad (3.28)$$

where $\underline{x}$ is the n x 1 state vector, $\underline{b}$ is the n x 1 input coupling vector, $\underline{\underline{A}}$ is the n x n plant matrix and u is the scalar input.

The switching hypersurface is defined by a linear combination of the states,

$$\sigma = \underline{c}^T \underline{x} = 0 \tag{3.29}$$

where $\underline{c}^T$ is a constant 1 x n row vector. In an ideal sliding mode, the phase point does not leave the hypersurface, hence the phase velocity is given by,

$$\dot{\sigma} = \underline{c}^T \dot{\underline{x}} = 0 \tag{3.30}$$

Substituting $\dot{\underline{x}}$ in equation (3.28) gives,

$$\underline{c}^T \underline{\underline{A}} \underline{x} + \underline{c}^T \underline{b}\, u_s = 0 \tag{3.31}$$

where u_s is the average value of the control input in the sliding mode, and is determinable uniquely from equation (3.31),

$$u_s = -(\underline{c}^T \underline{b})^{-1}\ \underline{c}^T \underline{\underline{A}} \underline{x} \tag{3.32}$$

and substituting this value of u_s in (3.28) gives the sliding mode equations,

$$\left.\begin{aligned} \dot{\underline{x}} &= [\underline{\underline{I}} - \underline{b}(\underline{c}^T \underline{b})^{-1}\ \underline{c}^T]\ [\underline{\underline{A}} \underline{x}] \\ \underline{c}^T \underline{x} &= 0 \end{aligned}\right\} \tag{3.33}$$

Comparing equation (3.6) with equation (3.33), it can be seen that the latter is not completely independent of the plant's parameters. If the control is a linear combination of k state variables (where $1 \leq k \leq n-1$) with switchable coefficients, then

$$u = -\sum_{i=1}^{k} \psi_i x_i \tag{3.34}$$

where

$$\left.\begin{aligned} \psi_i &= \alpha_i \quad \text{if } x_i \sigma > 0 \\ &= \beta_i \quad \text{if } x_i \sigma < 0 \end{aligned}\right\} \tag{3.35}$$

Using the procedure described in Appendix D, it can be shown that a sliding regime exists on the hyperplane $\sigma = 0$ if,

$$\left.\begin{aligned} \alpha_i &> \frac{1}{\underline{c}^T\underline{b}} [\underline{c}^T\underline{a}_i - \underline{c}_i(\underline{c}^T\underline{a}_n)] \\ \beta_i &< \frac{1}{\underline{c}^T\underline{b}} [\underline{c}^T\underline{a}_i - \underline{c}_i(\underline{c}^T\underline{a}_n)] \end{aligned} \right\} \quad i = 1, \ldots, k \qquad (3.36)$$

and

$$\underline{c}^T\underline{a}_i = \underline{c}_i(\underline{c}^T\underline{a}_n) \qquad i = k+1, \ldots, n-1$$

where $\underline{a}_i$ are the column vectors of the plant matrix $\underline{A}$. The equality constraint of (3.36) vanishes when $k = n-1$. Assuming that $k = n-1$ and that $\underline{A}$ is a time varying matrix with step-wise changes in its elements, then if conditions expressed in (3.36) are fulfilled for all values of a_{ij}, a sliding regime will exist on the defined hyperplane. As indicated in equation (3.33), the sliding equations will differ for different $\underline{A}$ matrices; the transient behaviour of the sliding motion changes accordingly. Fig. (3.2) illustrates the trajectories in a third order system. The conditions for complete invariance to parametric and external disturbances are discussed in the next section.

The control law described by equations (3.34) and (3.35) can be expressed differently. Since,

$$\dot{\sigma} = \underline{c}^T\underline{A}\underline{x} + \underline{c}^T\underline{b}u \qquad (3.37)$$

hence

$$\sigma\dot{\sigma} = [\underline{c}^T\underline{A}\underline{x} + \underline{c}^T\underline{b}u]\ \sigma \lesssim 0 \qquad (3.38)$$

$$\left.\begin{aligned} u &> -\ (\underline{c}^T\underline{b})^{-1}\ \underline{c}^T\underline{A}\underline{x} \qquad \text{if } \sigma \to -0 \\ \text{and} \quad u &< -\ (\underline{c}^T\underline{b})^{-1}\ \underline{c}^T\underline{A}\underline{x} \qquad \text{if } \sigma \to +0 \end{aligned} \right\} \qquad (3.39)$$

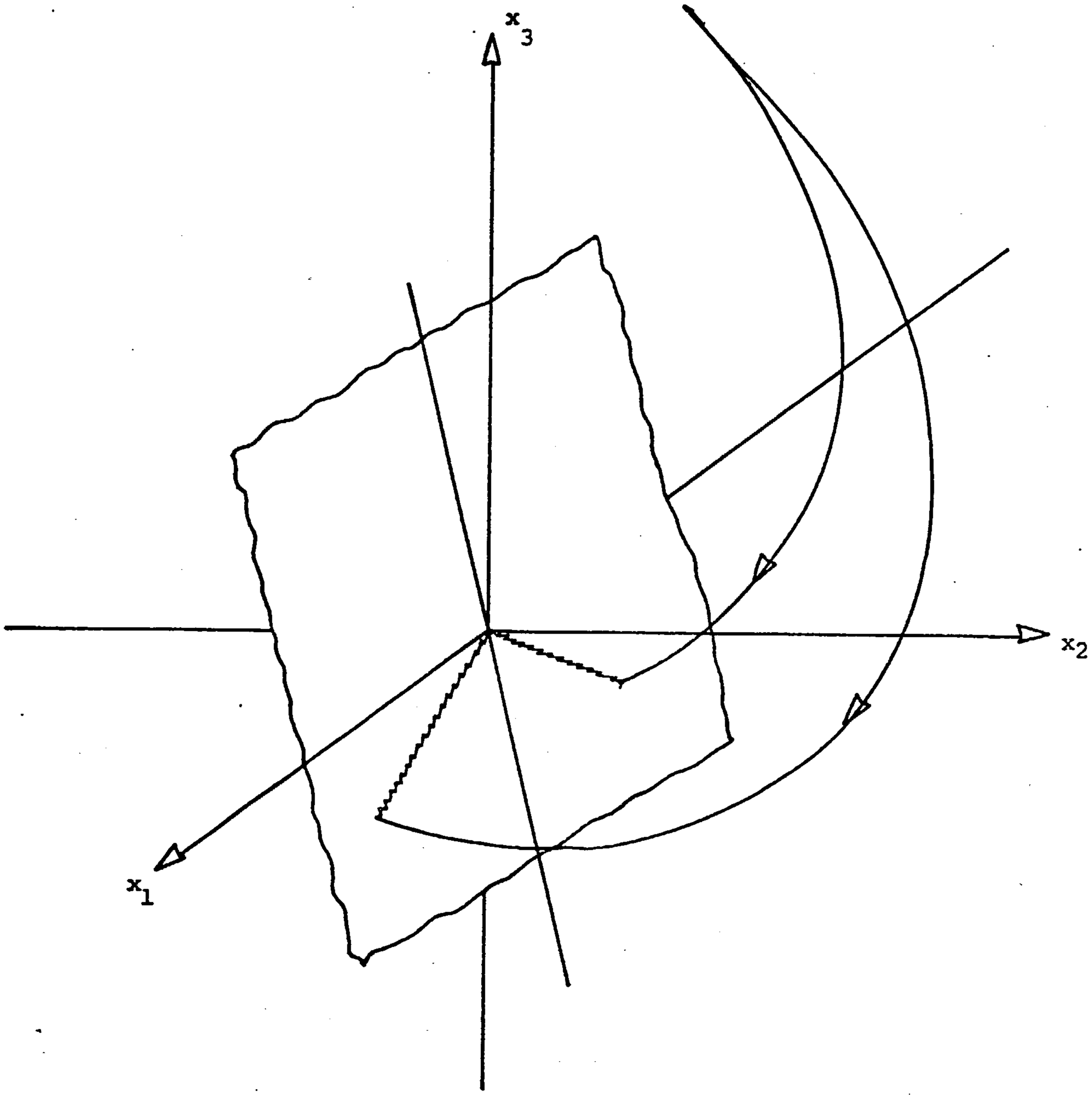

Figure 3.2 Sliding Trajectories for Different Plant Matrices

provided that $\underline{c}^T\underline{b} > 0$. The inequalities of (3.39) can be simplified further if $\underline{c}^T$ is chosen as the eigenvector row of $\underline{A}$ corresponding to eigenvalue λ, i.e.

$$\underline{c}^T\underline{A}\underline{x} = \lambda\ \underline{c}^T\underline{x} = \lambda\sigma \tag{3.40}$$

The control law of (3.39) can thus be written as,

$$u = - K|x_k|\text{sign}\ \sigma \tag{3.41}$$

where 'K' is an arbitrary positive number, x_k is an arbitrary state variable and λ is assumed negative. The $\underline{c}^T$ vector must be such that the sliding equations described by (3.33) are stable.

An alternative way of selecting the $\underline{c}^T$ vector is through the pole assignment procedure of Appendix C and starts with the determination of a continuous control $u = - \sum_{i=1}^{k} \theta_i x_i$ which places (n-1) eigenvalues as close as possible to some desired locations, where θ_i is the average gain defined by,

$$\theta_i = \frac{1}{\underline{c}^T\underline{b}} [\underline{c}^T\underline{a}_i - \underline{c}_i(\underline{c}^T\underline{a}_n)] \tag{3.42}$$

solutions for $\underline{c}^T$ can be estimated using equation (3.42) and the stability of the sliding motion can then be checked. Design values for $\underline{c}^T$ and θ_i which result in satisfactory responses are unlikely to be derived in the first instance and several computations may be required. A software control design package of the type described by Melsa in [3.9] is consequently invaluable in the design stage.

Unfortunately, the hitting conditions for state-space systems have not been clearly formulated in the literature. They are loosely described in [3.8] by the following statement:

"In general, it might be said that the suggested form of 'u' provides the fall on to the switching surface S, if the linear system obtained by a substitution of variable coefficients for the constant ones, is stable. An opposite statement may not be correct".

No proof is given in the reference for the above statement but it is intuitive that systems with stable trajectories will eventually hit the hyperplane. The statement is imprecise on unstable systems as it indicates that the fall (or hitting) does not necessarily imply a stable system. The presence of complex roots with positive real parts thus may or may not give rise to trajectories which intercept the switching hyperplane; the verification of hitting in such systems can be resolved using simulation.

3.2.2 Invariance Conditions

Even though sliding occurs in the system of (3.28), invariance to external and parametric disturbances is not necessarily guaranteed. External disturbances are included in the analysis by modifying the state-space equations of (3.28) to,

$$\underline{\dot{x}} = \underline{A}\underline{x} + \underline{b}\underline{u} + \underline{d}f \tag{3.43}$$

where $\underline{d}$ is a n x 1 vector coupling the disturbance f to the system. The sliding mode equations of (3.33) thus become,

$$\left.\begin{aligned} \underline{\dot{x}} &= [\underline{I} - \underline{b}(\underline{c}^T\underline{b})^{-1}\underline{c}^T][\underline{A}\underline{x} + \underline{d}f] \\ \underline{\sigma} &= \underline{c}^T\underline{x} = 0 \end{aligned}\right\} \tag{3.44}$$

The disturbance f disappears from the sliding equations if,

$$[\underline{I} - \underline{b}(\underline{c}^T\underline{b})^{-1}\underline{c}^T]\,\underline{d}f = 0 \tag{3.45}$$

It is shown in Appendix F that equation (3.45) can be satisfied for all possible values of f if,

$$\text{rank } [\underline{b}\underline{d}] = \text{rank } [\underline{b}] \tag{3.46}$$

i.e. the vector $\underline{d}$ is a linear combination of vector $\underline{b}$. In practical terms, condition (3.46) demands that the points where the disturbances and controls enter into the system are the same.

The conditions for parametric invariance can be derived in a similar manner if the plant matrix $\underline{A}$ is represented by,

$$\underline{A} = \underline{A}_v + \underline{A}_c \tag{3.47}$$

where $\underline{A}_v$ contains the variable elements and $\underline{A}_c$ the constant ones. The sliding mode equations become,

$$\left.\begin{aligned} \dot{\underline{x}} &= [\underline{I} - \underline{b}(\underline{c}^T\underline{b})^{-1}\underline{c}^T][\underline{A}_c\underline{x} + \underline{A}_v\underline{x}] \\ \underline{c}^T\underline{x} &= 0 \end{aligned}\right\} \tag{3.48}$$

Again the parameters included in the matrix $\underline{A}_v$ will disappear from the sliding mode equations if the following is fulfilled,

$$[\underline{I} - \underline{b}(\underline{c}^T\underline{b})^{-1}\underline{c}^T]\ \underline{A}_v\underline{x} = 0 \tag{3.49}$$

Equation (3.49) will be fulfilled if,

$$\text{rank } [\underline{b}\ \underline{A}_v] = \text{rank } [\underline{b}] \tag{3.50}$$

The above condition is obtained using the procedure of Appendix F and has the same practical significance as condition (3.46).

Fig. (3.3) illustrates the invariance conditions in a third order system; the matrix $\underline{A}_v$ only affects the initial conditions of the sliding mode but has no influence on the sliding trajectory.

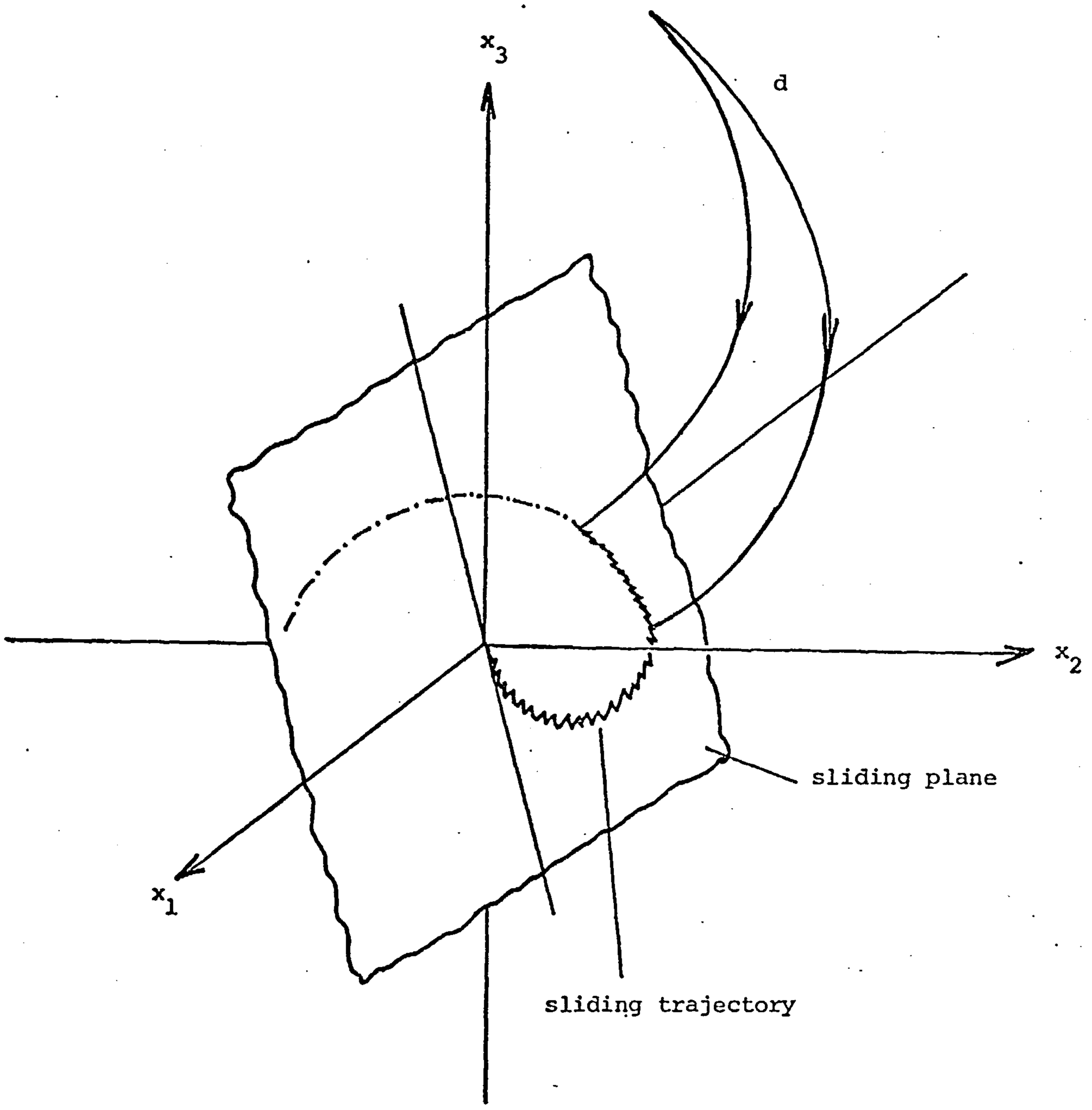

Fig. 3.3 Invariance Conditions in Sliding Systems

Conditions (3.46) and (3.50) are automatically met in systems (3.8) and (3.21) since all the rows of the matrix $\underline{A}_v$ and vectors $\underline{b}$ and $\underline{d}$ are zero except for the last one.

3.3 Zeros in VSS

Zeros in VSS may or may not present difficulties and this depends largely upon the form of the model used in the design stage. If the problem is formulated in a state-space framework, as it is often the case in the aerospace industry, the zeros usually arise as a result of feedforward loops within the plant. Fig. (3.4) shows how a zero could occur; its transfer function is given by

$$G(s) = \frac{y(s)}{u(s)} = \frac{bs + ab + 1}{(s + a)(s + c)} \qquad (3.51)$$

A typical example is that of the model of the longitudinal motion of a helicopter. Wright has derived the linearised equations for a particular helicopter in [1.8] and has shown that they can be represented in state-space form as follows:

$$\dot{\underline{x}} = \begin{bmatrix} 1.0 & 0.0 & 0.0 & -0.69 \\ 2.73 & -32.2 & -0.0284 & 0.0 \\ 1.0 & 0.0 & 0.0 & 0.0 \\ -0.61 & 0.0 & 0.00609 & 0.0 \end{bmatrix} \underline{x} + \begin{bmatrix} 0.0 \\ 32.2 \\ 0.0 \\ -6.65 \end{bmatrix} u \qquad (3.52)$$

where, x_1 = downward air-speed

x_2 = forward air-speed

x_3 = pitch angle

x_4 = pitch rate

and

u = cyclic pitch on rotor.

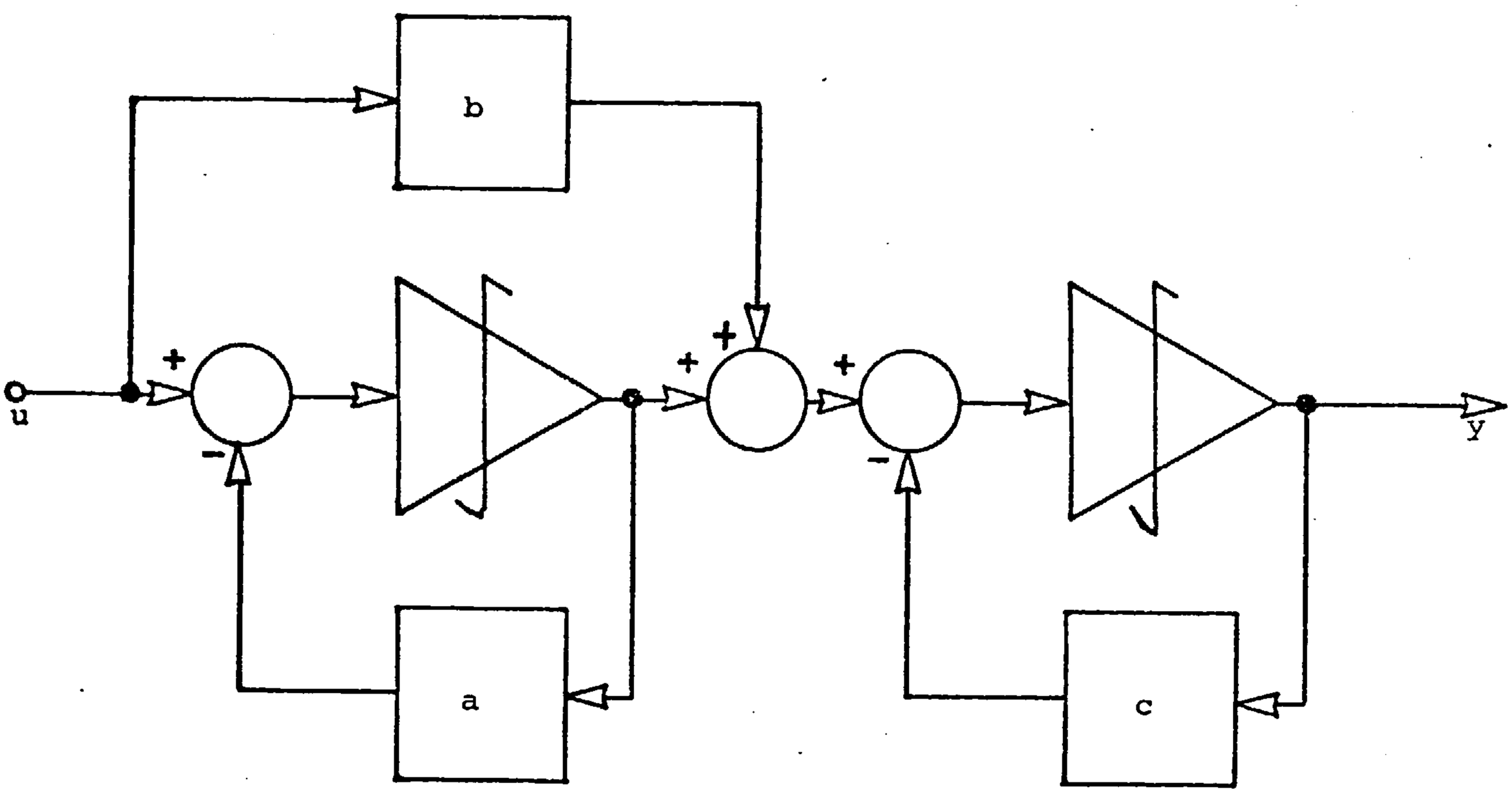

Figure 3.4 Zero Formation

Inspection of equation (3.52) reveals several feedforward paths which lead to the formation of zeros. If the states are available, then a sliding regime can be organised in the system. Further if condition (3.50) is observed, then the motion can be made invariant to parameter changes in rows two and four. Wright has also shown that the elements b_{11} and b_{31} of the $\underline{b}$ vector can assume non-zero values at different air speeds. Under these circumstances, condition (3.50) is met for all the rows of the plant matrix $\underline{A}$ and complete invariance to parameter variations can be achieved. The range of values which the input coupling vector $\underline{b}$ can assume is consequently an important input to the VS design.

Very often the available model is described from an input-output basis by a transfer function. A system with zeros is thus described by,

$$G(s) = \frac{b_m s^{m-1} + \ldots + b_2 s + b_1}{s^n + a_n s^{n-1} + \ldots + a_2 s + a_1} \qquad (3.53)$$

If the internal structure of the plant is unknown, then the VS control of system (3.53) presents some difficulties. In [1.1], Itkis assumes that equation (3.53) can be represented in canonical form by,

$$\left.\begin{aligned} \dot{x}_i &= x_{i+1} \qquad i = 1, \ldots, n-1 \\ \dot{x}_n &= -\sum_{i=1}^{n} a_i x_1 - \sum_{i=1}^{m} b_i u^{i-1} \end{aligned}\right\} \qquad (3.54)$$

where u^1 is the first derivative of u^o (=u) etc.(Fig. 3.5). The control of (3.54) by VSS involves certain difficulties due to the fact that the control u is discontinuous, hence its derivatives $u^{(i-1)}$ have

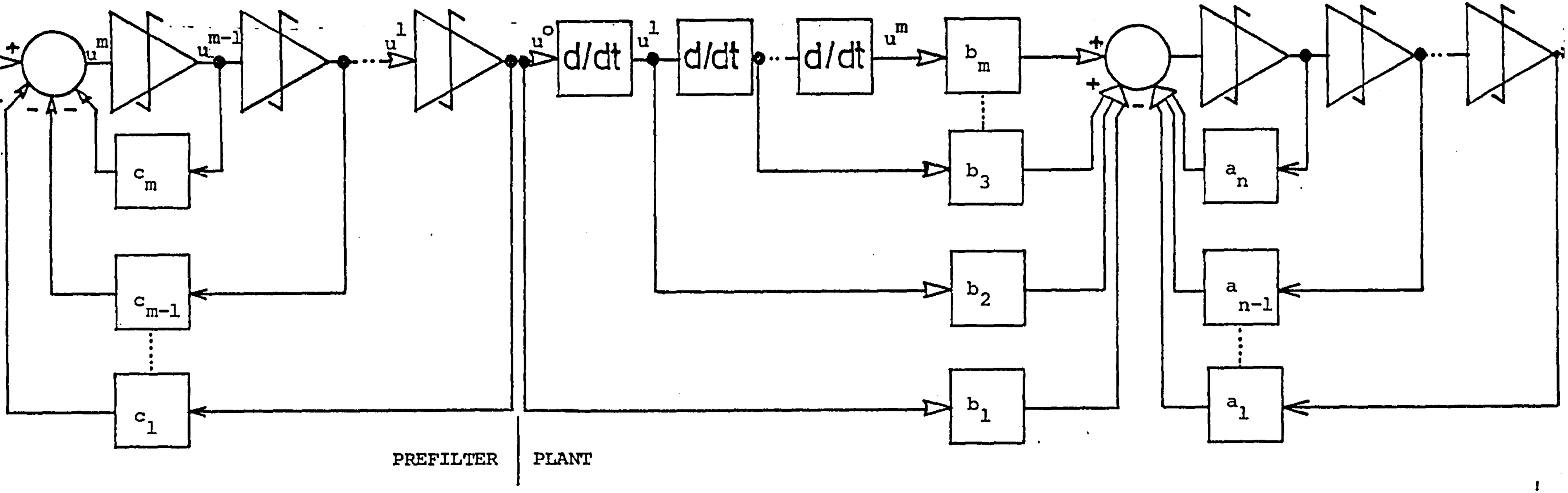

Figure 3.5 VS Control of System with Zeros

infinite discontinuities. As a result the function $x_n(t)$ has finite discontinuities and the phase trajectory is no longer continuous. Itkis suggests that if the signal u(t) is passed through an (m-1)th order pre-filter, where (m-1) is the order of the numerator of the plant's transfer function, then it will be converted into a function with (m-2) continuous derivatives and whose (m-1)th derivative is discontinuous. The signal u(t) when differentiated (m-1) times within the plant may then produce a sliding regime in the system.

From a linear point of view, equation (3.54) is a valid representation of (3.53) and can also be shown to be similar to (3.28) under certain conditions. However, in designing the VS controller, the internal structure of the plant cannot be ignored because if the filter method proposed by Itkis is adopted for the state-space system of (3.28), then the control function after (m-1) integrations cannot produce a sliding regime in (3.28) as it is no longer discontinuous on the switching surface. It is important then to preserve the structure of the plant when designing VS controllers and as such systems which are described in state-space form are better suited as VSS.

3.4 Tracking of Inputs

In the discussion, it has been assumed that the zero state is the equilibrium state of the system. But in practice the desired equilibrium state (known as the set point) is usually a point in space different from the origin and which may be constant over long periods and shifted from time to time. In dealing with these problems, it is customary to shift the coordinates of the plant. In the time-invariant case, for example, if the state equations are,

$$\dot{\underline{x}} = \underline{\underline{A}}\underline{x} + \underline{b}u \qquad (3.55)$$

and the desired set point is given by $\underline{x}_o$, then the new input u_o must be related to $\underline{x}_o$ by,

$$o = \underline{\underline{A}}\underline{x}_o + \underline{b}u_o \tag{3.56}$$

Whether or not the system can be maintained at the given set point depends on whether equation (3.56) can be solved for u_o. If the solution exists, then the following definitions of the shifted input and the shifted state,

$$\left.\begin{aligned} u'(t) &= u(t) - u_o \\ \underline{x}'(t) &= \underline{x}(t) - \underline{x}_o \end{aligned}\right\} \tag{3.57}$$

can be substituted in equation (3.55) and shown to satisfy the following equivalent equation,

$$\dot{\underline{x}}' = \underline{\underline{A}}\underline{x}' + \underline{b}u' \tag{3.58}$$

In simple examples where one is interested in regulating only one of the state variables around a changing set point, the solution is usually found by incorporating an integrator in the loop. When several variables have to be set, the problem is more complex and the reader is referred to [3.10], [3.11] for a treatment of regulator and tracking systems.

In the control problems considered in subsequent chapters, the prime interest is tracking step and ramp inputs and, the extent to which VS theory can solve these is briefly reviewed in the next section.

3.4.1 Regulation and Tracking in VSS

The problem of regulation and tracking in VSS have been studied by several authors. In some early papers [3.12], [3.13], Emelyanov and Fedotova have considered the tracking of input signals of the form $g(t) = \alpha t^n$ in second-order systems. In a following paper [3.14], Emelyanov and Utkin have generalised the tracking of $g(t)$ to an nth order system where $g(t)$ can be an exponential, a sinusoid or polynomial. The method consists essentially in deriving an error vector of the form,

$$\underline{\varepsilon} = [\varepsilon_1, \varepsilon_2, \ldots, \varepsilon_n]^T \tag{3.60}$$

where ε_1 is the error between the reference and the plant's output and ε_2, to ε_n are its second to nth derivatives respectively. The control function to steer the phase point on to the sliding surface $\sigma = \underline{c}^T\varepsilon$ is found using the procedures of sections 3.1.1 and 3.1.2. The technique is of course unrealistic in applications where the plant's order is higher than two or three.

Unfortunately there is no formal mathematical presentation of tracking in VSS which is acceptable from an engineering standpoint. For instance, a VS theory dealing with tracking of set points in state space systems would be desirable. However, some insight can be gained into the problem by studying the work of Lindorff [3.15], [3.16] and Monopoli [3.17] on model tracking systems using relay controllers and linear switching functions. Using a state-space approach, Lindorff has shown that the error vector between the plant's and the model's state variables can be reduced through a sliding regime approach. The essence of the method consists in defining a Lyapunov function of the form,

$$V = \frac{1}{2}\,\sigma^2(e) \tag{3.61}$$

to be positive definite, where $\sigma(e)$ represents the switching plane as a linear function of the error variables between the plant and model states. It is defined by,

$$\sigma(e) = \underline{c}^T\underline{e} \tag{3.62}$$

If a control law can be found such that the time derivative of V,

$$\dot{V} = \sigma\dot{\sigma} \tag{3.63}$$

is negative definite, then at some time $\underline{e}$ lies on the hyperplane and is confined to it, (note the different approach in deriving the existence of a sliding regime). The conditions which assure not only stability but also that the $\lim_{t \to \infty} \underline{e}(t) \to 0$ must then be derived.

Stability is guaranteed by demanding that the sliding equations meet the Routh-Hurwitz conditions. For example if system (3.55) is considered and, $\underline{e}$ is given by

$$\underline{e} = \underline{x} - \underline{x}_r \tag{3.64}$$

where $\underline{x}_r$ is a reference vector (in the model tracking system $\underline{x}_r$ would be generated by the model and would be a function of time), then

$$\left.\begin{aligned} \dot{\underline{e}} &= \underline{\underline{A}}\underline{x} + \underline{b}u = \underline{\underline{A}}\underline{e} - \underline{\underline{A}}\underline{x}_r + \underline{b}u \\ \text{and} \quad \sigma &= \underline{c}^T\underline{e} = 0 \end{aligned}\right\} \tag{3.65}$$

for the sliding equations where 'u' is a discontinuous function of $\underline{e}$. The conditions for global asymtotic stability of (3.65) are not known. This gap in the theory is not unsurmountable and using simulation techniques, one can investigate the merits of the method in particular examples.

3.5 General Comments

Chapter three has been mainly concerned with summarising the contribution made by VS theory in some fundamental areas of control systems. The conditions dealing with the hitting, existence of sliding and stability are well-established for time-invariant and time-varying plants in phase-variable form. With a more general plant matrix, a sliding regime can be organised but invariancy to parameters and disturbances can only be fulfilled under certain rank conditions. The hitting criterion in such systems also appear to be more restrictive. The suggested design method for the tracking of set-points in plants described by a transfer function is satisfactory only in cases where a low-order differentiation is possible, and the regulation of an arbitrary state in a plant described by a set of ordinary differential equations presents as many theoretical difficulties as with a linear approach.

In spite of these problems, VS theory is still an attractive proposition from an engineering viewpoint owing to its invariancy properties. In the following chapters these properties are explored further through the detailed design of VS controllers for two test cases which possess the right characteristics for variable structure solutions. In chapter four, the analysis and design of a VSS for a slowly time-varying coiler-drive is considered and it is shown that zero steady-state error can be achieved in a type 0 plant without integration. In chapter five, the analysis and design of a VS autopilot is considered and it is shown that zero steady-state error can also be achieved in a type 1 plant subject to external disturbances, where a type 2 loop would normally be required.

Further, the purposes of studying these two specific design cases are (i) to expose the problems associated in applying new theory to practical examples, and (ii) to assess the performance of the new solutions to such uncertainties as random noise, etc.

CHAPTER FOUR

ANALYSIS AND DESIGN OF A VSS FOR A SLOWLY TIME-VARYING TYPE 0 PLANT

The outstanding property of VSS is its invariancy to parameter variations. This property is investigated further by analysing and designing a VS controller for a slowly time-varying type 0 plant. The results obtained indicate that the VS controller shares a common property with an integral type controller in being capable of providing at the plant's input, a mean control level through a switching action, thereby maintaining a zero steady-state error in the plant's output. But, in addition, the VS controller also guarantees the long term stability of the system in the particular application under study.

4.1 Control Problems of Coiler-Drive Systems

The case study is that of designing a controller for a coiler-drive system. The example is eminently suitable as a VS application as it contains some parameters which vary slowly over a wide range and can lead to instability of the closed-loop system in a linear design. This problem can be remedied by incorporating a suitable phase advance network in the controller but since the objectives here are to acquire experience with VS theory and assess its potential, alternative solutions are not considered.

As it is often the case when applying theory, the coiler-drive system does not fit neatly into a VS formulation and solution. Nonlinear loops involving multipliers and dividers exist within the system which complicate the VS design. The complexities are

avoided by regarding the system as linear but with bounded, time-varying parameters. The rates of change of the parameters are assumed to have a negligible effect. This assumption is subsequently validated by simulation.

Other problems arise in the design procedure regarding

i) The choice of controller gains and of the coefficients of the switching plane

ii) the effect of a forced motion on the sliding, hitting and stability conditions.

In the theory it is suggested that high values of gains should be selected for a fast transition from the initial conditions to the switching surface and that the coefficients of the latter should be such as to provide a good and stable sliding transient. It is, however, extremely difficult to relate these controller parameters to transient performance in a quantitative way, hence simulation is used extensively in selecting appropriate values. Item (ii) above presents the greatest obstacle in the application of VS theory in this particular system. It is shown that sliding cannot be enforced solely by the switching of the error vector $\underline{e}$ as proposed in section (3.4.1) and that the input reference (or disturbance) V_R must be included in the switching control, fig. (4.1). A consequence of this is that the hitting conditions expressed in Theorem (3.5) for a time-varying system are not applicable. Some broad conditions for hitting to occur can however be formulated by considering some trajectories of $\underline{e}$

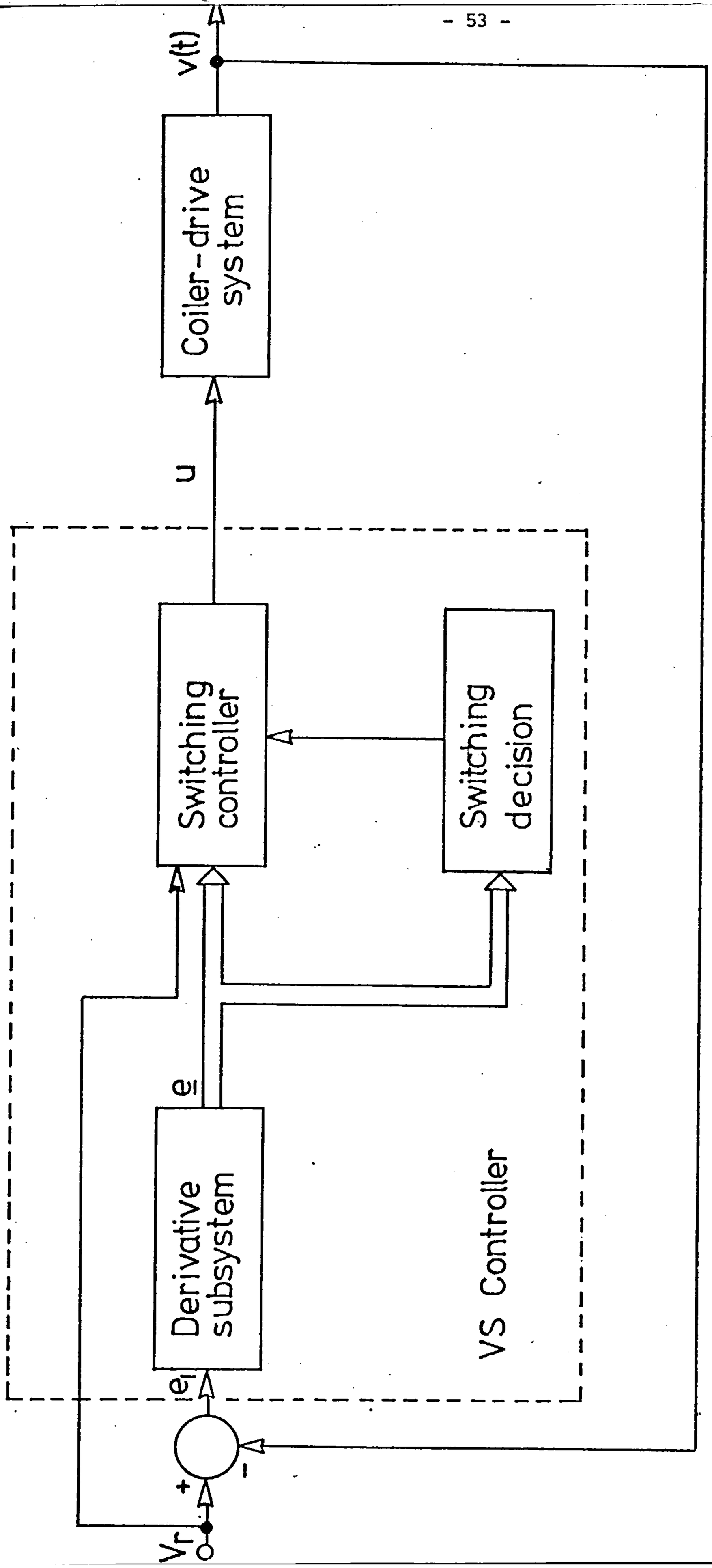

Figure 4.1 Structure of VS Controller

from a sample of initial conditions and verified by simulation.

With these problems overcome, it is shown that the coiler-drive system can be forced in the initial part of its transient into a sliding motion, which then leads to a stable equilibrium point that can be maintained over the desired operating range by the VS controller.

4.2 Analysis of the Coiler-Drive with a Linear Controller

A coiler-drive system is a process for winding material at a constant linear speed on a rotating drum. The plant, consists of a drum which is coupled to the shaft of a dc motor via a gearbox. A tachometer measures the rotational speed of the drum which is compared to a reference. The error signal produced is amplified and used in controlling the armature voltage. Design difficulties arise primarily because the loop gain of the system is time-varying as a result of an increase in radius and inertia of the drum as more material is wound on.

Neglecting saturation and other nonlinear effects within the motor, the relationship between the armature voltage V_a, the armature current I_a and the back emf of the motor is given as,

$$V_a = I_a R_a + L_a \frac{dI_a}{dt} + E_a \tag{4.1}$$

where R_a and L_a are the resistance and the inductance of the motor respectively. The back emf E_a is related to the motor speed $\dot{\theta}_m$ and the field current I_f by,

$$E_a = k_1 I_f \dot{\theta}_m \tag{4.2}$$

where k_1 is a constant of appropriate dimension.

The motor torque T_m is related to the armature and field current by,

$$T_m = k_2 I_a I_f \tag{4.3}$$

where k_2 is a constant, and the accelerating torque which is the difference between the motor torque T_m and the load torque T_ℓ is related to the rate of change of angular momentum by,

$$T_m - T_\ell = \frac{d}{dt}[J_m \dot{\theta}_m] \tag{4.4}$$

where J_m is the inertia of the motor. A block diagram of the motor described by equations (4.1) to (4.4) is shown in fig. (4.2).

The motor speed is stepped down through an N to 1 gearbox to produce a coiling drum speed $\dot{\theta}_\ell$. If the material wound on the drum is considered to have a thickness 'a' and the drum has a radius R, then the radius r(t) at any time t can be given by,

$$r(t) = R + \frac{a}{2\pi N} \int_0^t \dot{\theta}_m(t)\,dt \tag{4.5}$$

where $\dot{\theta}_m$ is specified in radians per second.

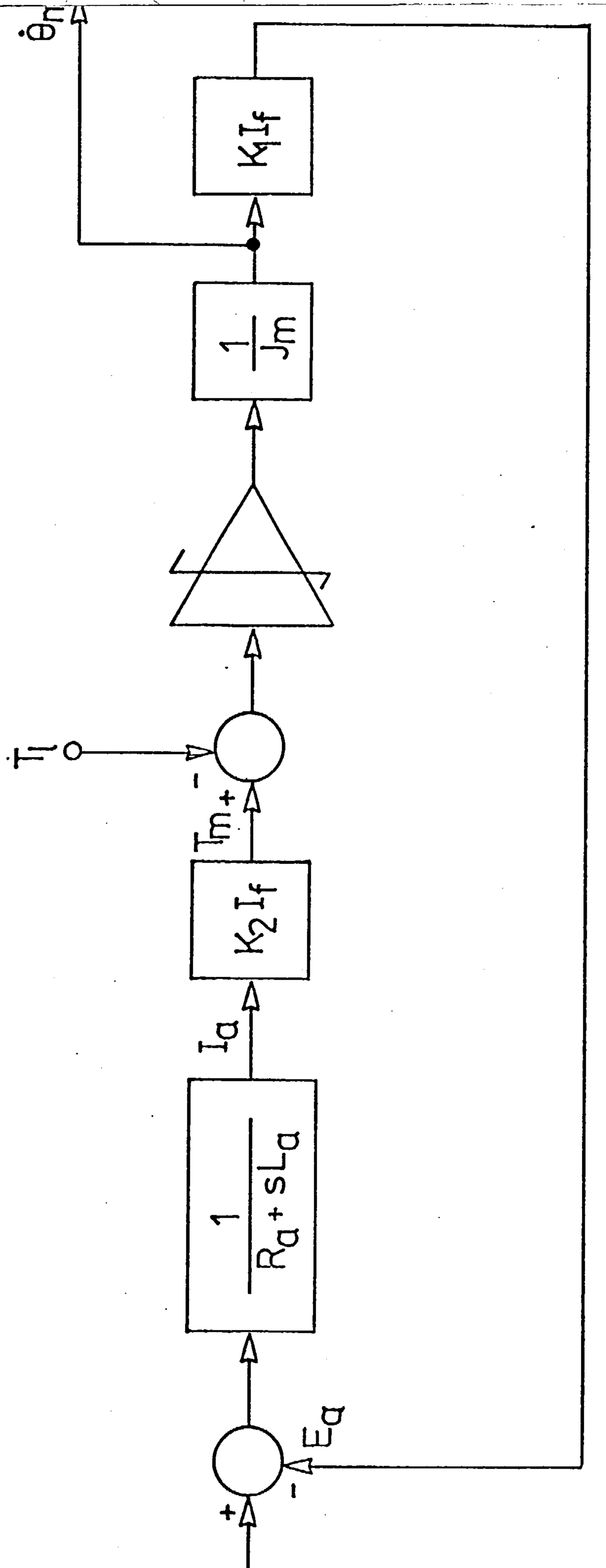

Figure 4.2 Block Diagram of Motor

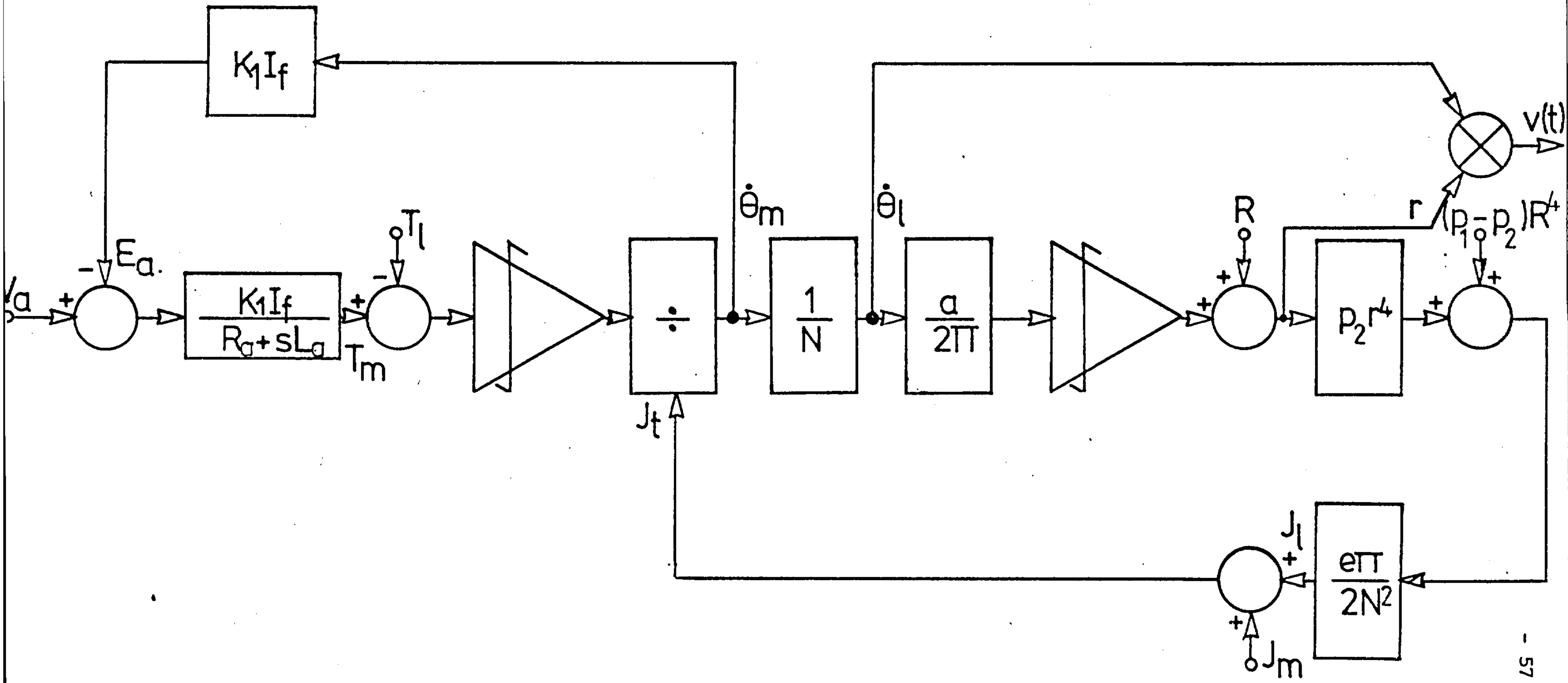

Figure 4.3 Coiler Drive - Open Loop System

Thus the linear velocity is,

$$V(t) = r(t)\dot{\theta}_{\ell}(t) \tag{4.6}$$

As the inertia of an annulus with mass M and, internal and external radii r_1 and r_2 respectively is given as,

$$J = \frac{M}{2}(r_1^2 + r_2^2) \tag{4.7}$$

hence the inertia of the coiled mass is,

$$J_1 = \frac{\pi e}{2}\rho_2[r^4(t) - R^4] \tag{4.8}$$

and the inertia of the steel drum is,

$$J_2 = \rho_1 \frac{e\pi}{2} R^4 \tag{4.9}$$

where

ρ_1 = density of steel (Kg/m^3)

ρ_2 = density of material (Kg/m^3)

e = length of drum (m)

The total inertia of the load is consequently given by,

$$J_3 = J_1 + J_2 \tag{4.10}$$

which when referred to the motor side of the gearbox is related by,

$$J_{\ell} = \frac{J_3}{N^2} \tag{4.11}$$

i.e. $$J_{\ell} = \frac{e\pi}{2N^2}[R^4(\rho_1 - \rho_2) + \rho_2 r^4(t)] \tag{4.12}$$

A block diagram of the complete open-loop coiler drive system relating the input armature voltage to the output speed is shown

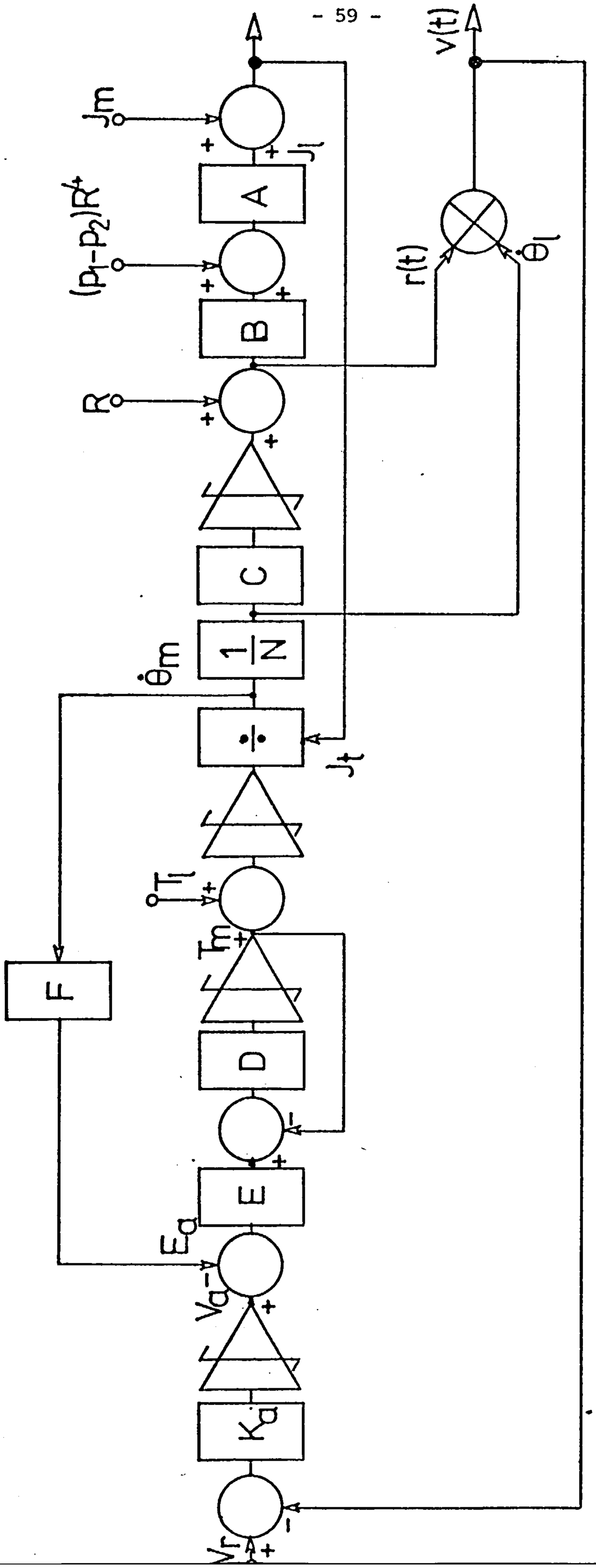

Figure 4.4 Coiler Drive - Closed Loop System

```
TITLE   COILER DRIVE SYSTEM
PARAMETER VREF =1. 27, KA=350. 0, K2=0. 3183, IF=4. 0, RA=0. 05, LA=0. 005,...
K1=0. 3183, JM=0. 5, N=10. 0, R=0. 075, RAU1=7840. 0, RAU2=1120. 0,...
THICK=0. 01, LENGTH=1. 0
DYNAMIC
*
*    INTEGRAL CONTROLLER
*
E1=VREF-VELO
E2=INTGRL(0. 0, E1)
VA=350. 0*E2
*
*    MOTOR SUBSYSTEM
*
E=(K2*IF)/RA
D=RA/LA
F=K1*IF
TL=0. 0
TMDOT=(E*(VA-EA)-TM)*D
TM=INTGRL(TMO, TMDOT)
ACTORQ=TM-TL
TEMP1=INTGRL(ACO, ACTORQ)
MOTVEL=TEMP1/JT
EA=MOTVEL*F
*
*     LOAD SUBSYSTEM
*
JT=JM+JL
LDAVEL=MOTVEL/N
C=THICK/(2. 0*3. 141592)
RADOT=C*LDAVEL
RAD=INTGRL(RO, RADOT)
TOTRAD=R+RAD
VELO=LDAVEL*TOTRAD
TEMP2=(RAU1-RAU2)*(R**4)
TEMP3=RAU2*(TOTRAD**4)
TEMP4=TEMP2+TEMP3
TEMP5=(LENGTH*3. 141592)/(2. 0*N*N)
JL=TEMP4*TEMP5
METHOD TRAPZ
TIMER FINTIM=200. 0, DELT=0. 002, OUTDEL=4. 0
PRTPLOT VREF, E1, E2, SIGMA, VELO, VA
PRTPLOT MOTVEL, LDAVEL, TOTRAD, JL, JT
PRTPLOT EA, VX, VY, VXVY
END
STOP
```

FIG. 4. 5 CSMP PROGRAM - INTEGRAL CONTROL OF COILER DRIVE SYSTEM

in fig. (4.3). The total load as seen by the motor is,

$$J_t = J_m + J_\ell \qquad (4.13)$$

where J_m is the motor inertia.

In order to produce a zero steady error, a basic integral was proposed by Cole [4.1], giving the overall closed-loop system of fig. (4.4). The actual values of the parameters A,B,C ... F for a specific system are given in Appendix G. The controller gain k_a in fig. (4.4) was set at 350.0, the reference speed demand was 1.27 m/sec and the characteristics of the wound material were as follows;

i) Thickness of material $a = 0.01$ m

ii) Width of material $e = 1.0$ m

iii) Density of film $\rho_2 = 1120$ Kg/m^3

Using the above values, the coiler drive system was simulated using IBM's CSMP (Continuous System Modelling Program). A copy of the program is shown in fig. (4.5) to illustrate the ease with which simulation problems can be programmed.

The transient response of the system is shown in fig. (4.6). The drum responds very quickly to the initial step demand and settles at the reference value. But as the radius of the drum increases, fig. (4.7), the loop gain increases correspondingly; the inertia J_t also increases, but since the loop gain is inversely proportional to J_t, its effect is a stabilising one. However, the combined result of these two parameters is to de-stabilise the closed-loop system. After approximately fifty seconds, instability sets in. Fig. (4.8) which shows the driving function

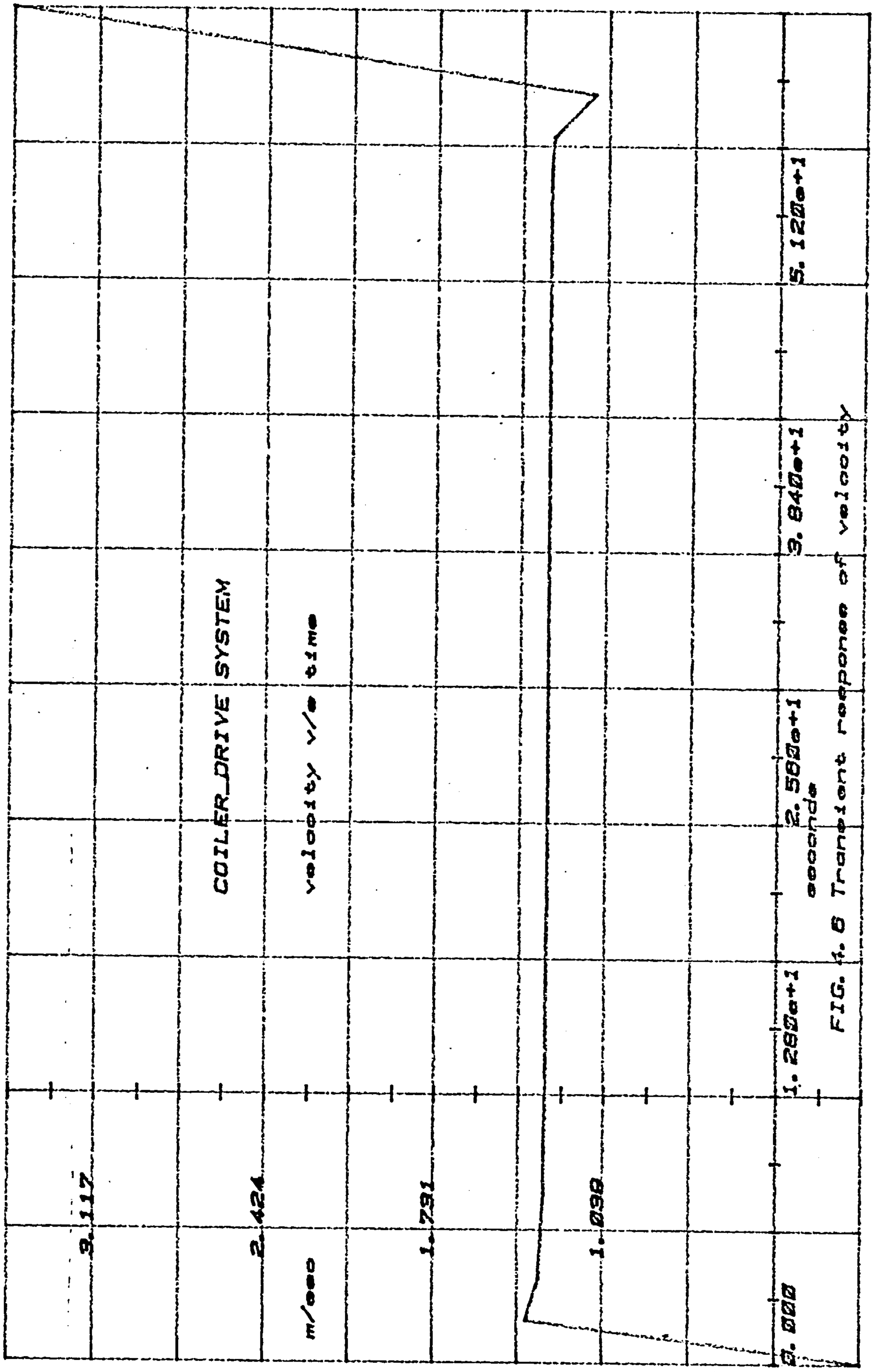

FIG. 4.6 Transient response of velocity

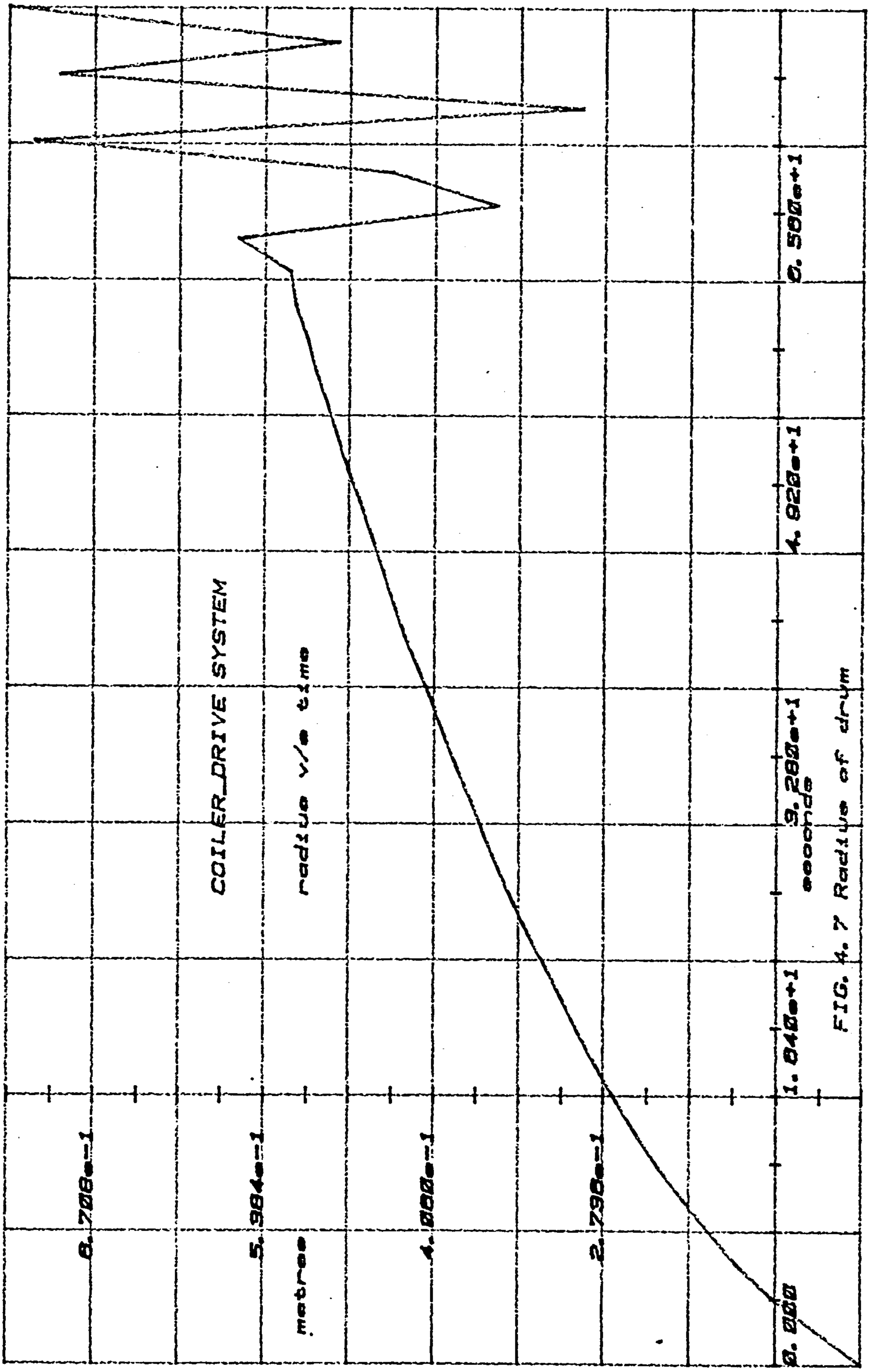

FIG. 4.7 Radius of drum

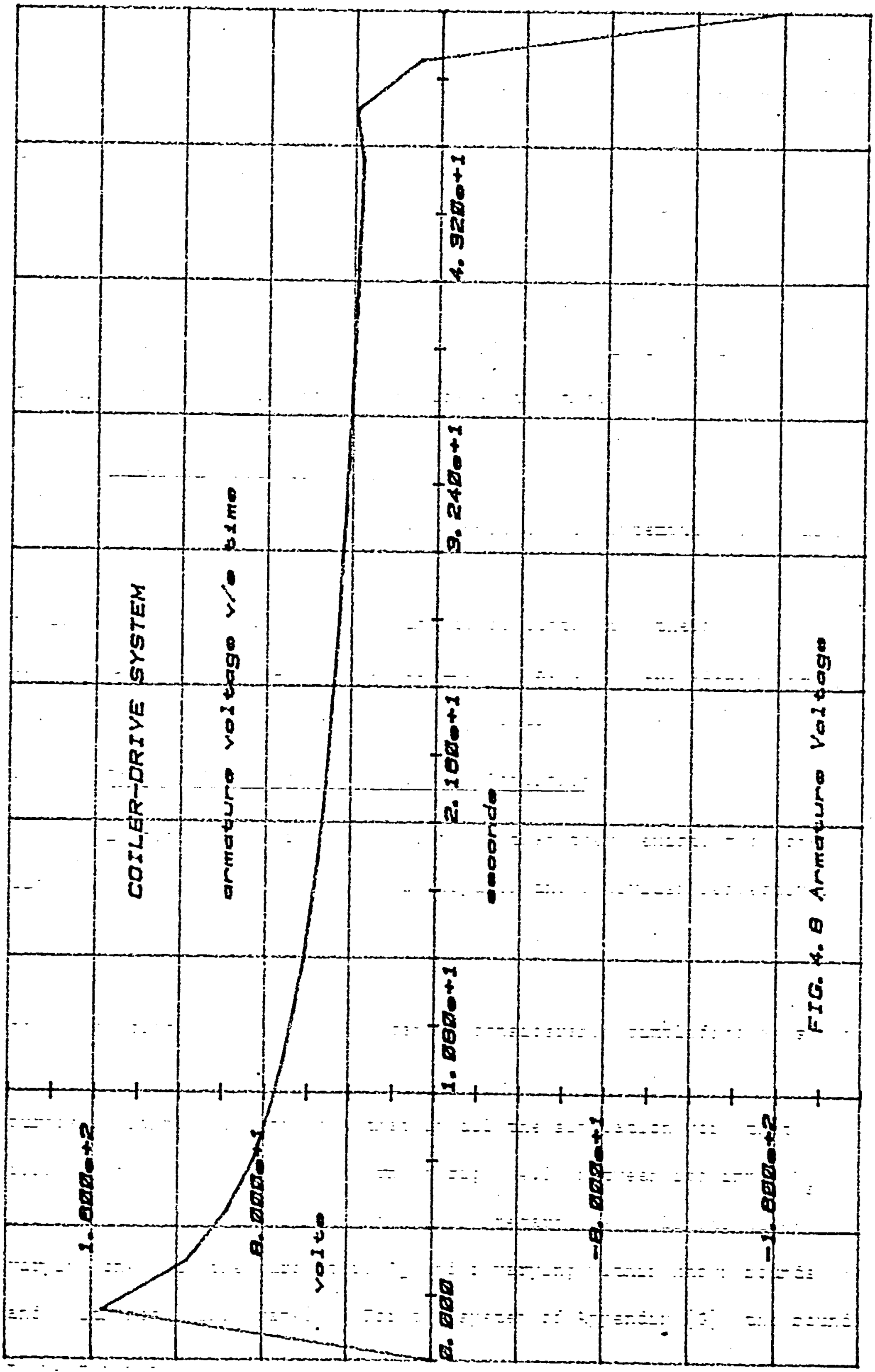

FIG. 4.8 Armature Voltage

(i.e. the armature voltage V_a) has been included for comparison later.

An attempt to solve the above problem using a variable structure approach is made in the next section. The VS design is not being advocated as the only solution to this particular system. A linear controller incorporating a phase advance network could provide a reasonable performance; other solutions are discussed in [3.10] based on optimal control theory and in [4.2] based on stability supervision. The purpose here is essentially to assess the theory.

4.3 Variable Structure Design

The first problem that presents itself in attempting a VS design for the coiler-drive is that the equations describing the plant are nonlinear (eqns. (4.1) - (4.13)) and consequently the theory of chapter three is not directly applicable. However, the problem can be reformulated and made amenable to a VS solution.

4.3.1 Problem Formulation and Sliding Conditions

Examination of fig. (4.4) reveals that there exists two non-linear loops which incorporate a multiplier and a divider respectively and which involve the two critical time-varying parameters, the radius r(t) and the inertia J(t). Assuming that these parameters are constants, the block diagram of fig. (4.4) can be considerably simplified as shown in fig. (4.9). Although this simplification is made for design purposes, it must be stressed that in all the simulation work that follows, the plant takes the form of fig. (4.3) between its input V_a and output v(t). The system can now be regarded as a linear time-varying one with the parameters J_t and r varying within known bounds and with negligible rates. For the system of Appendix [G], the bounds on J_t and r are,

$$\left.\begin{aligned} 0.54 \leq J_t \ (kg - m^2) \leq 1.6 \\ 0.075 \leq r(m) \leq 0.575 \end{aligned}\right\} \qquad (4.14)$$

Using the block-diagram of fig. (4.9), the instability which resulted in the linear design can be understood by noting the pole locations. The coiler drive system can be regarded as a time-varying second-order system consisting of an open-loop pair of complex poles in the left-half plane, which slowly migrate into the right-half plane when the loop is closed with an integral controller.

In fig. (4.9), if $u = V_a$, $x_2 = T_m$ and $x_1 = \int T_m \, dt$, then the state equations for the plant can be written as,

$$\left.\begin{aligned} v(t) &= \frac{r}{J_t N} \, x_1 \\ \dot{x}_1 &= x_2 \\ \dot{x}_2 &= -\frac{DEF}{J_t} x_1 - Dx_2 + DEu \end{aligned}\right\} \qquad (4.15)$$

The error signal is given as the difference between the reference and the measured velocity, i.e.,

$$e_1 = V_R - v(t) = V_R - \frac{r}{J_t N} x_1 \qquad (4.16)$$

Inspection of equation (4.15) indicates that an invariant sliding motion can be realised using the state variables x_1 and x_2, since the rank conditions of (3.46) are met. However, the vector $\underline{x}$ cannot be measured directly, and the time-varying parameter 'r' and 'J_t' also influence the output v(t), hence the sliding hyperplane must be chosen differently. The objective is to reduce e_1 in equation (4.16) to zero; a suitable hyperplane is defined by,

$$\sigma = c_1 e_1 + e_2 \qquad (4.17)$$

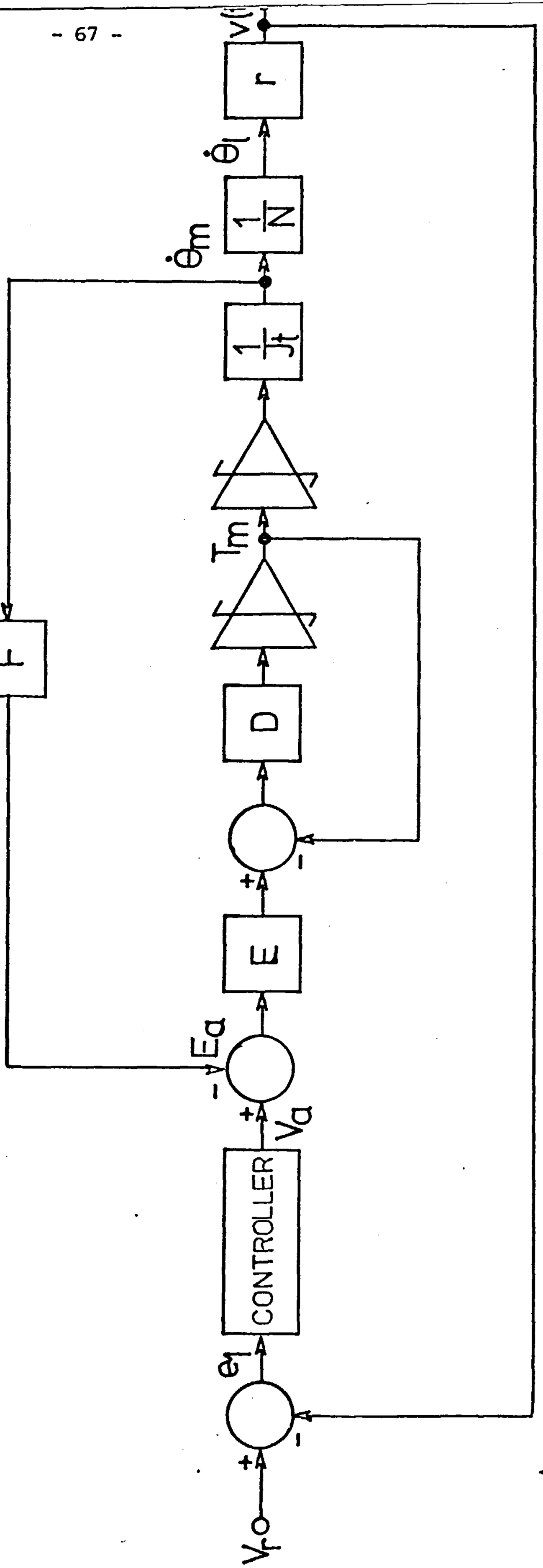

Figure 4.9 Coiler Drive - Simplified Block Diagram

where e_2 is obtained by differentiating e_1. For a constant velocity demand V_R and using equations (4.15) and (4.16), the following expression is obtained for e_2,

$$\dot{e}_1 = e_2 \doteq - \frac{r}{J_t N} \dot{x}_1 = - \frac{r}{J_t N} x_2 \qquad (4.18)$$

where the rates of change in r and J_t are assumed to be small.

From (4.16) and (4.18), the vector $\underline{x}$ can be written as a function of the error vector $\underline{e}$, i.e.

$$\left.\begin{aligned} x_1 &= (V_R - e_1) \frac{J_t N}{r} \\ \text{and} \quad x_2 &= - \frac{J_t N}{r} e_2 \end{aligned}\right\} \qquad (4.19)$$

From (4.15) and (4.18)

$$\dot{e}_2 = - \frac{r}{J_t N} \dot{x}_2$$

$$= - \frac{r}{J_t N} \left[- \frac{DEF}{J_t} x_1 - Dx_2 + DEu \right] \qquad (4.20)$$

Equation (4.19) is used to replace $\underline{x}$ in the last equation, the following equations of the system in the error space can now be written,

$$\left.\begin{aligned} \dot{e}_1 &= e_2 \\ \dot{e}_2 &= - \frac{DEF}{J_t} e_1 - De_2 + \frac{DEF}{J_t} V_R - \frac{DEr}{J_t N} u \end{aligned}\right\} \qquad (4.21)$$

The above system is similar to (3.21) except for the additional term containing the input reference V_R; the inequalities of the sliding conditions will thus be affected by V_R.

From (4.17),

$$\dot{\sigma} = c_1 \dot{e}_1 + \dot{e}_2$$

Replacing $\dot{e}_1$ and $\dot{e}_2$ gives,

$$\dot{\sigma} = c_1 e_2 + [-\frac{DEF}{J_t} e_1 - De_2 - \frac{DEr}{J_t N} u + \frac{DEF}{J_t} V_R] \tag{4.22}$$

Following the procedure of chapter three, $\sigma = 0$ in a sliding regime, hence $e_2 = -c_1 e_1$. Substituting for e_2 in (4.22) yields,

$$\dot{\sigma} = -c_1^2 e_1 - \frac{DEF}{J_t} e_1 + c_1 De_1 - \frac{DEr}{J_t N} u + \frac{DEF}{J_t} V_R$$
$$= [-c_1^2 - \frac{DEF}{J_t} + c_1 D] e_1 - \frac{DEr}{J_t N} u + \frac{DEF}{J_t} V_R \tag{4.23}$$

The reference V_R can be considered as an input disturbance and again since the rank conditions of (3.46) are satisfied, it will not affect the sliding motion. Further since V_R is a measurable disturbance it must be included in the control law as follows,

$$u = \psi_1 e_1 + \psi_R V_R \tag{4.24}$$

$$\text{where} \quad \psi_1 = \begin{cases} \alpha_1 & \text{if } e_1\sigma > 0 \\ \beta_1 & \text{if } e_1\sigma < 0 \end{cases}$$

$$\text{and} \quad \psi_R = \begin{cases} \alpha_R & \text{if } V_R\sigma > 0 \\ \beta_R & \text{if } V_R\sigma < 0 \end{cases} \tag{4.25}$$

Replacing u in equation (4.23) gives,

$$\dot{\sigma} = [-c_1^2 - \frac{DEF}{J_t} + c_1 D - \frac{DEr}{J_t N} \psi_1] e_1$$
$$+ [\frac{DEF}{J_t} - \frac{DEr}{J_t N} \psi_R] V_R \tag{4.26}$$

Applying the sliding conditions of chapter 3,

$$\left.\begin{array}{ll} \text{if } e_1\sigma > 0 & \alpha_1 \geq \sup \dfrac{J_t N}{DEr}\left[-c_1^2 - \dfrac{DEF}{J_t} + c_1 D\right] \\ \text{if } e_1\sigma < 0 & \beta_1 \leq \inf \dfrac{J_t N}{DEr}\left[-c_1^2 - \dfrac{DEF}{J_t} + c_1 D\right] \end{array}\right\} \qquad (4.27)$$

and,

$$\left.\begin{array}{ll} \text{if } V_R\sigma > 0 & \alpha_R \geq \sup \dfrac{NF}{r} \\ \text{if } V_R\sigma < 0 & \beta_R \leq \inf \dfrac{NF}{r} \end{array}\right\} \qquad (4.28)$$

The limits on the time-varying parameters of inequalities (4.27) and (4.28) can be shown to be,

$$\left.\begin{array}{l} 0.110 \leq \dfrac{J_t N}{DEr} \leq 0.283 \\ 202.0 \leq \dfrac{DEF}{J_t} \leq 600.0 \\ 22.0 \leq \dfrac{NF}{r} \leq 170.0 \end{array}\right\} \qquad (4.29)$$

The control design problem now rests in assigning values to α_1, β_1, α_R, β_R and c_1. The value of c_1 can be selected from stability conditions. For stability in the sliding hyperplane, c_1 must be greater than zero (para. 3.12) to satisfy the Routh-Hurwitz condition. Further, since the system has a sliding regime on the straight line $c_1 e_1 + e_2 = 0$, its motion in that mode is described by the equation,

$$e_1(t) = e_1(t_0)\ \exp[-c_1(t - t_0)] \qquad (4.30)$$

where $e_1(t_0)$ is the value of $e_1(t)$ at the initial instant t_0 of the

sliding regime. A large value of c_1 implies a fast sliding transient, but c_1 cannot be made indefinitely large on account of the possibility of the breakdown of the sliding motion, i.e. inequalities of (4.27) are not met.

Finally, hitting must take place for the successful realisation of a VSS. Theorem (3.5) does not take into account the effect of switching an external disturbance in the control law, hence the hitting conditions expressed in that theorem are not strictly applicable to the forced motion of the coiler-drive system. However, through the use of phase-plane techniques and simulation, sufficient conditions can be imposed on the gains to ensure that hitting will take place whilst the sliding inequalities of (4.27) - (4.29) are maintained.

4.3.2 Selection of Controller Parameters

To understand the hitting mechanism in the coiler-drive system, a phase plane approach will be used. Returning to the set of equations of (4.21) and substituting the values of the constant and known parameters result in the following equations,

$$\left.\begin{aligned} \dot{e}_1 &= e_2 \\ J_t\dot{e}_2 &= -324.0e_1 - 10J_te_2 + 324.0V_R - 25.46ru \\ u &= \psi_1 e_1 + \psi_r V_R \end{aligned}\right\} \qquad (4.31)$$

where J_t and r are the time-varying parameters. Equations (4.31) can be written more compactly as

$$J_t\ddot{e}_1 + 10J_t\dot{e}_1 + 324e_1 = 324V_R - 25.46r[\psi_1 e_1 + \psi_r V_R]$$

or

$$J_t\ddot{e}_1 + 10J_t\dot{e}_1 + (324 + 25.46r\psi_1)e_1 = (324 - 25.46r\psi_r)V_R \qquad (4.32)$$

For hitting to occur, the gain values in equation (4.32) must be chosen such that the phase trajectories will intercept the switching plane. Theorem 3.5 provides some insight in the choice of ψ_1 but the switching term on the RHS of (4.32) ψ_r, requires further examination. This can be done through a combination of algebra and guesswork.

At time t=0, J_t, r, V_R and $e_1(0)$ are constants and the Laplace transform of eqn. (4.32) gives the following expression for $e_1(s)$,

$$e_1(s) = \frac{1.27(324 - 1.91\psi_r)}{324 + 1.91\psi_1}\left[\frac{1}{s} - \frac{0.54s + 5.4}{0.54s^2 + 5.4s + 324 + 1.91\psi_1}\right]$$

$$+ \frac{0.686(s + 10.0)}{0.54s^2 + 5.4s + 324 + 1.91\psi_1} \qquad (4.33)$$

where $r(0) = 0.075m$, $J_t(0) = 0.54$ kg-m^2, $V_R = 1.27$ m/sec, $e_1(0) = 1.27$ m/sec and $\dot{e}_2(0) = 0.0$. To investigate whether the phase point crosses the switching plane $\sigma = c_1e_1 + e_2$ in an analytical way requires some complex algebraic manipulations which involves the elimination of the time variable in the solution for $\underline{e}(t)$. Instead some useful guidelines can be developed for the choice of the gain values in the following way.

If at $t = 0$, $\psi_1 = \alpha_1 > 0$ for $e_1\sigma > 0$, then the second term in eqn. (4.33) is of the form,

$$\frac{(s + 10.0)}{s^2 + 10s + 600 + 3.54\alpha_1}$$

and in the time domain, it has the following form,

$$e^{-at}\cos\omega t$$

where 'a' and 'ω' are related to the parameters of the frequency domain representation. The third term has a similar form in the time domain and given that the numerator $(324 - 1.91\ \psi_r)$ is negative, then the complete solution for $e_1(t)$ can be expressed as,

$$e_1(t) = -|M| + [e^{-a_1 t}\cos\omega_1 t]N_1 + [e^{-a_2 t}\cos\omega_2 t]N_2 \qquad (4.34)$$

where M, N_1 and N_2 are positive constants.

It is reasonable to assume now that with the sinusoidal terms in (4.34), $e_1(t)$ is set to become negative at some time $t > 0$; hence hitting will occur subject to the conditions

$$\dot{e}_1(0) > 0 \qquad \alpha_1 > 0 \quad \text{and} \quad \alpha_r > \frac{324}{1.91} = 170.0 \qquad (4.35)$$

Using a similar argument, the hitting constraints on the gains can be derived for different starting conditions. These are summarised in fig. (4.10). As the transient progresses, the time-varying parameters 'J_t' and 'r' will influence the hitting trajectory. It is therefore vital that these hitting guidelines be verified by simulation for the above conditions for all $\underline{e}(0)$ and V_R.

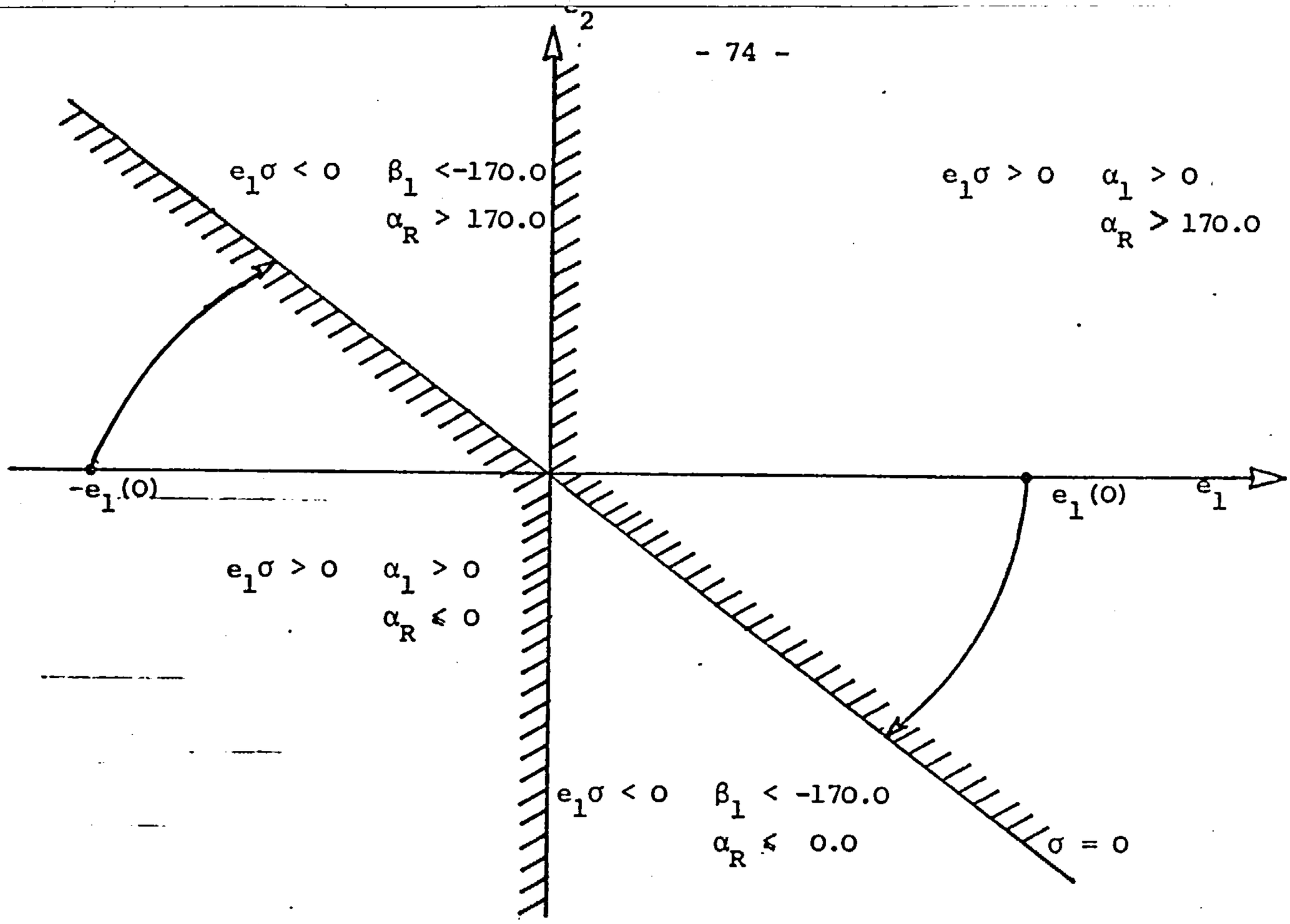

Fig. 4.10 Gain Contraints for Hitting in Coiler-Drive

4.3.3 Simulation Results

The final design task is to assign numerical values to the gains such that the hitting, sliding and stability conditions are met simultaneously. The following values of gains were selected after a number of simulation runs,

$$\left.\begin{array}{lll} \alpha_1 = 100.0 & \alpha_R = 200.0 & c_1 = 40.0 \\ \beta_1 = -600.0 & \beta_R = 0.0 & \end{array}\right\} \qquad (4.36)$$

Using CSMP, the coiler-drive system of fig. (4.3) was simulated using the VS controller. A functional block diagram of plant and controller is shown in fig. (4.11); the internal structure of the coiler-drive was left intact in the simulation even though the simplified structure of fig. (4.9) was utilised in the design. The simulation program is shown in fig. (4.12). Macro functions such as INTGRL, INSW are

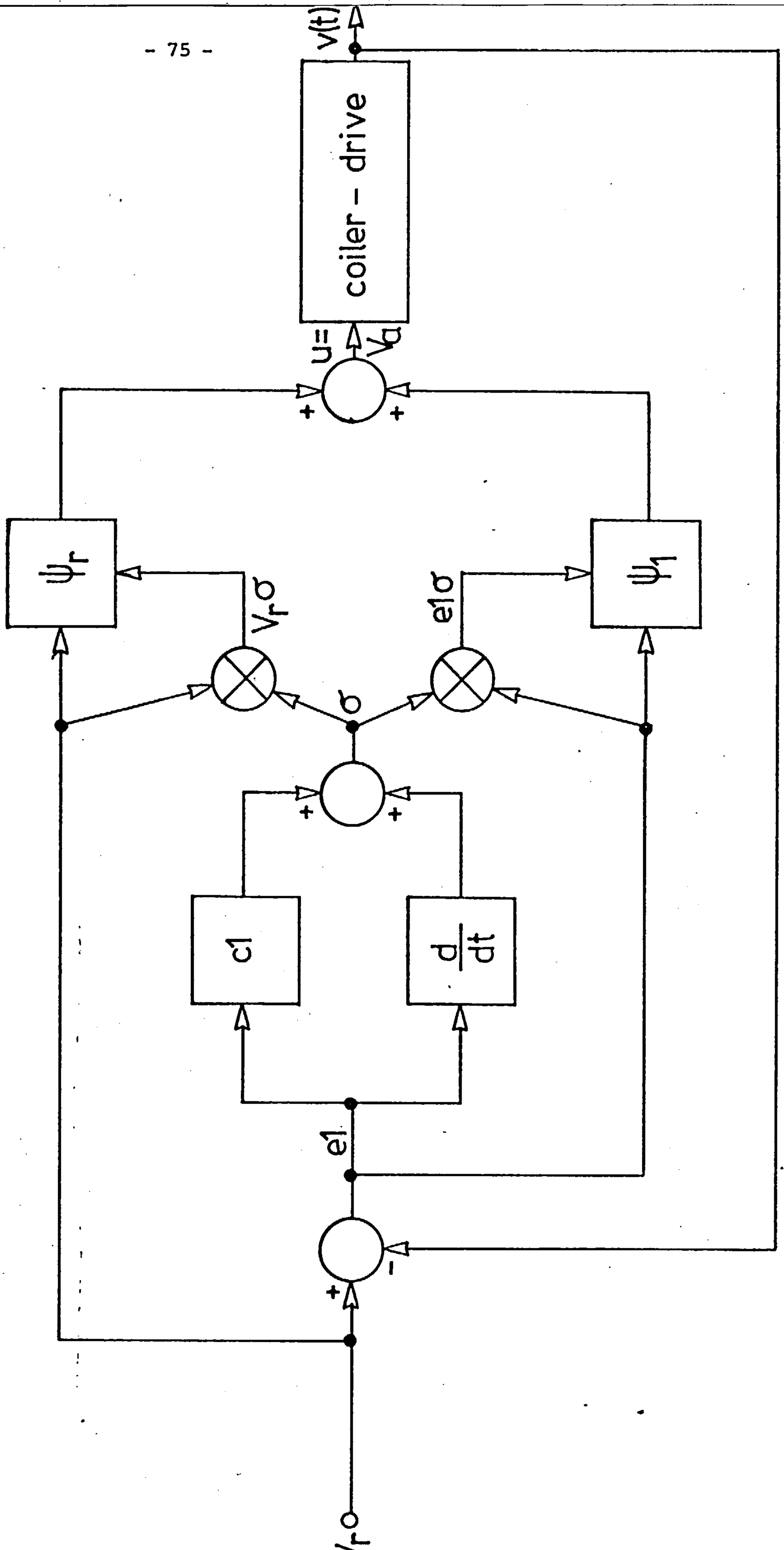

Figure 4.11 Coiler Drive - VS Controller

```
TITLE    COILER DRIVE SYSTEM
PARAMETER VREF =1. 27, KA=350. 0, K2=0. 3183, IF=4. 0, RA=0. 05, LA=0. 005, . . .
K1=0. 3183, JM=0. 5, N=10. 0, R=0. 075, RAU1=7840. 0, RAU2=1120. 0, . . .
THICK=0. 01, LENGTH=1. 0
PARAMETER C1=40. 0, ALPHA1=0. 0, BETA1=-500. 0, ALPHAR=200. 0, BETAR=0. 0
DYNAMIC
*
*    VSS CONTROLLER
*
E1=VREF-VELO
E2=DERIV(0. 0, E1)
SIGMA=C1*E1+E2
E1S=E1*SIGMA
VREFS=VREF*SIGMA
ES1=E1*ALPHA1
ES2=E1*BETA1
VS1=VREF*ALPHAR
VS2=VREF*BETAR
VX=INSW(E1S, ES2, ES1)
VY=INSW(VREFS, VS2, VS1)
VXVY=VX+VY
VA=LIMIT(-220. 0, 220. 0, VXVY)
*
*    MOTOR SUBSYSTEM
*
E=(K2*IF)/RA
D=RA/LA
I=K1*II
TL=0. 0
TMDOT=(E*(VA-EA)-TM)*D
TM=INTGRL(TMO, TMDOT)
ACTORQ=TM-TL
TEMP1=INTGRL(ACO, ACTORQ)
MOTVEL=TEMP1/JT
EA=MOTVEL*F
*
*     LOAD SUBSYSTEM
*
JT=JM+JL
LDAVEL=MOTVEL/N
C=THICK/(2. 0*3. 141592)
RADOT=C*LDAVEL
RAD=INTGRL(RO, RADOT)
TOTRAD=R+RAD
VELO=LDAVEL*TOTRAD
TEMP2=(RAU1-RAU2)*(R**4)
TEMP3=RAU2*(TOTRAD**4)
TEMP4=TEMP2+TEMP3
TEMP5=(LENGTH*3. 141592)/(2. 0*N*N)
JL=TEMP4*TEMP5
METHOD TRAPZ
TIMER FINTIM=200. 0, DELT=0. 002, OUTDEL=4. 0
PRTPLOT VREF, E1, E2, SIGMA, VELO, VA
PRTPLOT MOTVEL, LDAVEL, TOTRAD, JL, JT
PRTPLOT EA, VX, VY, VXVY
END
STOP
```

FIG. 4. 12 CSMP PROGRAM - VS CONTROL OF COILER DRIVE SYSTEM

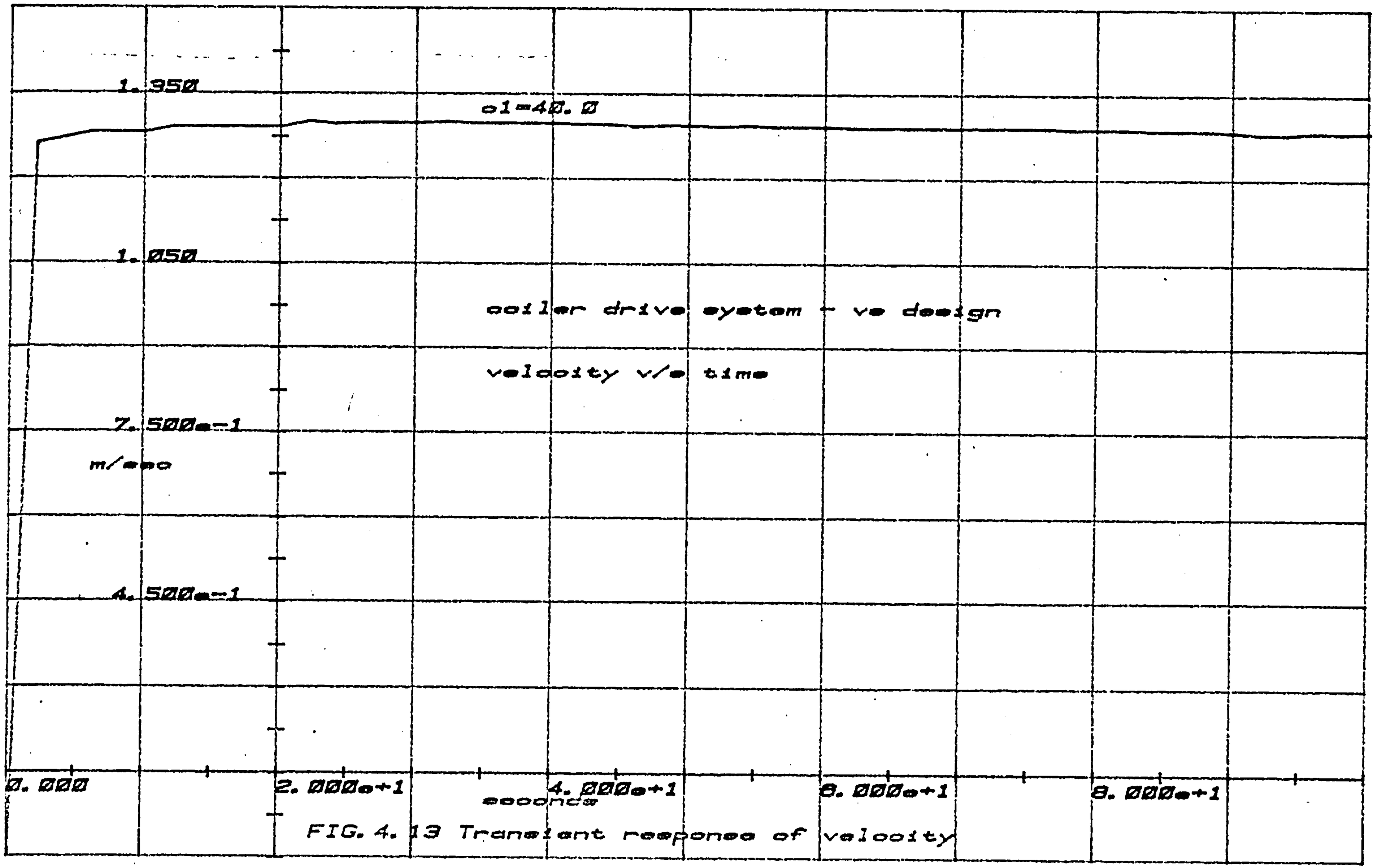

FIG. 4.13 Tranoiant rooponoo of vooooity

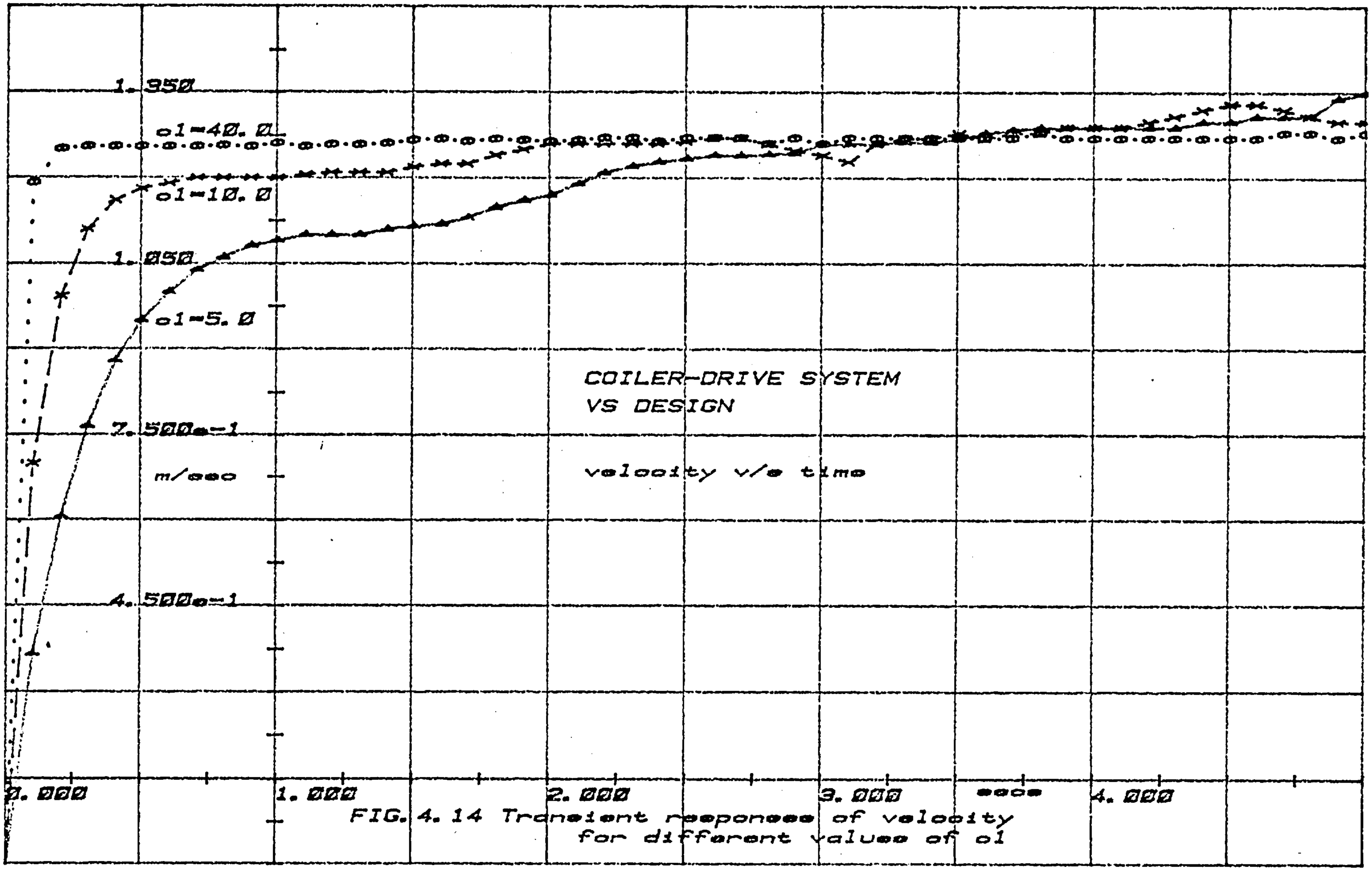

FIG. 4.14 Transient responses of velocity for different values of σ1

invaluable for integration and switching functions respectively. A comprehensive guide to using CSMP can be found in [4.4].

Fig.(4.13) shows the transient response of the velocity output for a reference input demand of 1.25 m/sec. The output settles to within 1% of the demanded value and stability is seen to be maintained for well over 200 seconds, corresponding to a radius of 0.9 m which exceeds favourably the design value of 0.575 m.

Fig. (4.14) also shows the transient response of the velocity output for the same reference input over a period of five seconds. The responses corresponding to lower values of c_1 are also shown and can be seen to be more sluggish; this is to be expected as the sliding motion is slowed down (refer to eqn. (4.30)).

Fig. (4.15) shows the formation of sliding in the coiler-drive system from different initial conditions. The dotted trajectory illustrates the breakdown of sliding when the reference V_R is excluded from the control law. The origin is the unique equilibrium point for the range of values which can be assumed by V_R and the time-varying parameters. The global uniqueness of the stable point cannot be guaranteed outside the design range but this is of little interest from a practical point of view.

Fig. (4.16) is the response of the input drive V_a or armature voltage over 500 milliseconds with saturation limits of ±250 volts. The waveform is modulated in width and amplitude; the width is a function of the penetration of the hyperplane by the phase point which in the simulation is caused by the finite integration step size and the amplitude is a function of e_1 and V_R. The lower half of the trace is enveloped in an exponential and is due to the switching

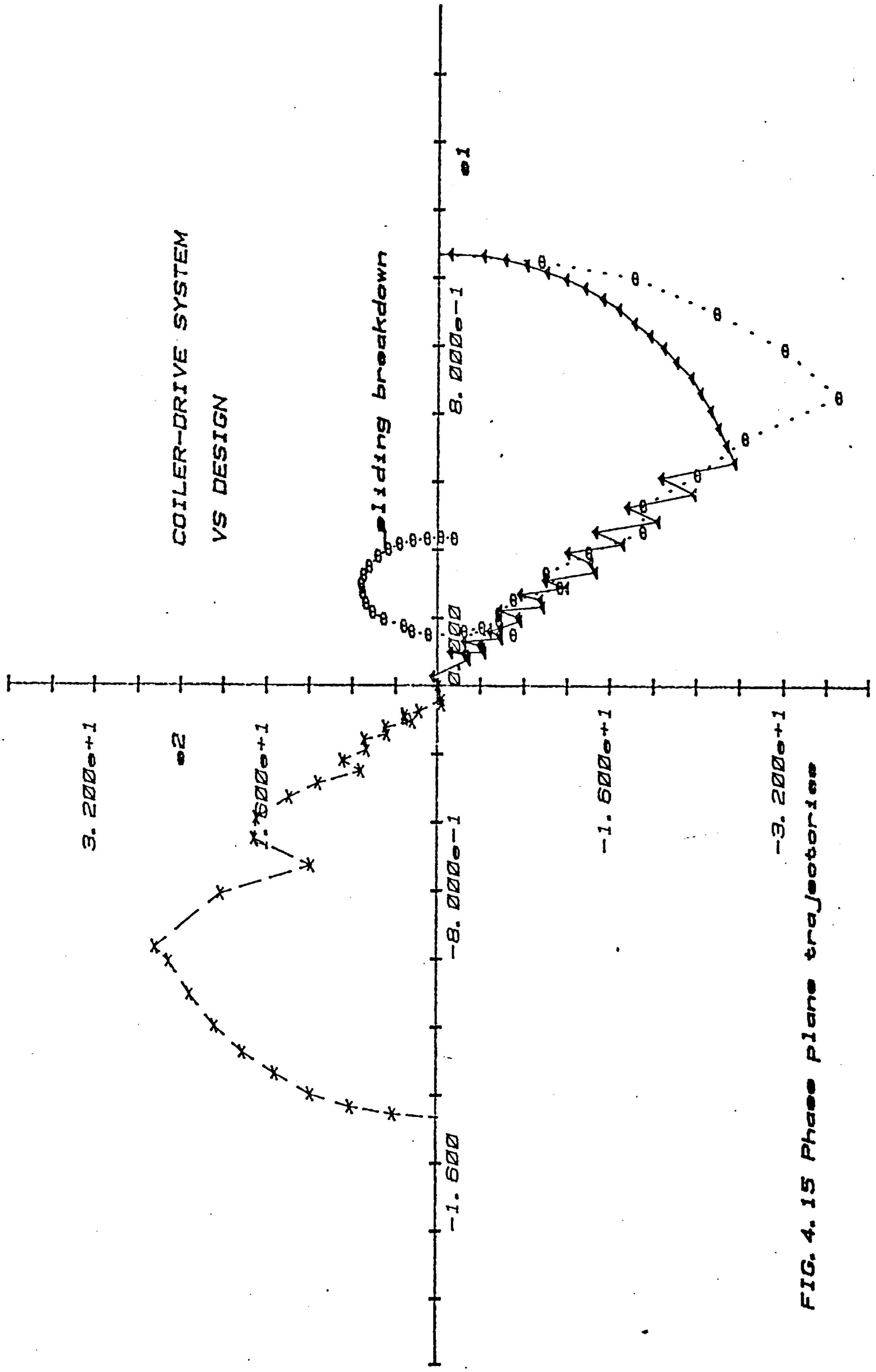

FIG. 4.15 Phase P

action of e_1 alone (since $\beta_r = 0.0$). The upper half of the trace is dominated by the contribution of V_R. The input drive V_a is effectively derived from the closed-loop system via e_1 and from V_R in an open loop fashion. Initially when e_1 is large both loops contribute equally in reducing e_1 to zero. But as $\underline{e}$ decreases to zero, the system is controlled in an open loop fashion through the switching of the reference V_R. The driving function V_a does not tend to zero in the limit as discussed in chapter three but contains a relay component due to V_R; as time increases, the relay stays off for longer periods (not shown in fig. (4.16)), and the average value of the signal is the correct one for maintaining a zero steady-state error in the plant's output.

Finally, it is interesting to note that the switching function σ ('sigma' in the simulation) can never quite settle to zero. Fig. (4.15) shows that the phase point is bouncing back and forth across the boundary in a non-ideal sliding regime and is constrained to within a small region around the hyperplane. In the literature this more realistic type of motion is known as a quasi-sliding regime.

4.4 General Comments

In this chapter, it has been shown that a slowly time-varying type 0 system can be successfully controlled and regulated by means of a VS controller. The control strategy has led to the synthesis of an input drive signal which differs radically from the normal exponential signals obtained with a PI controller in that it is modulated both in width and amplitude. The replacement of integration by a switching process has also lead to the inclusion of the input reference in the switching control law with a resulting

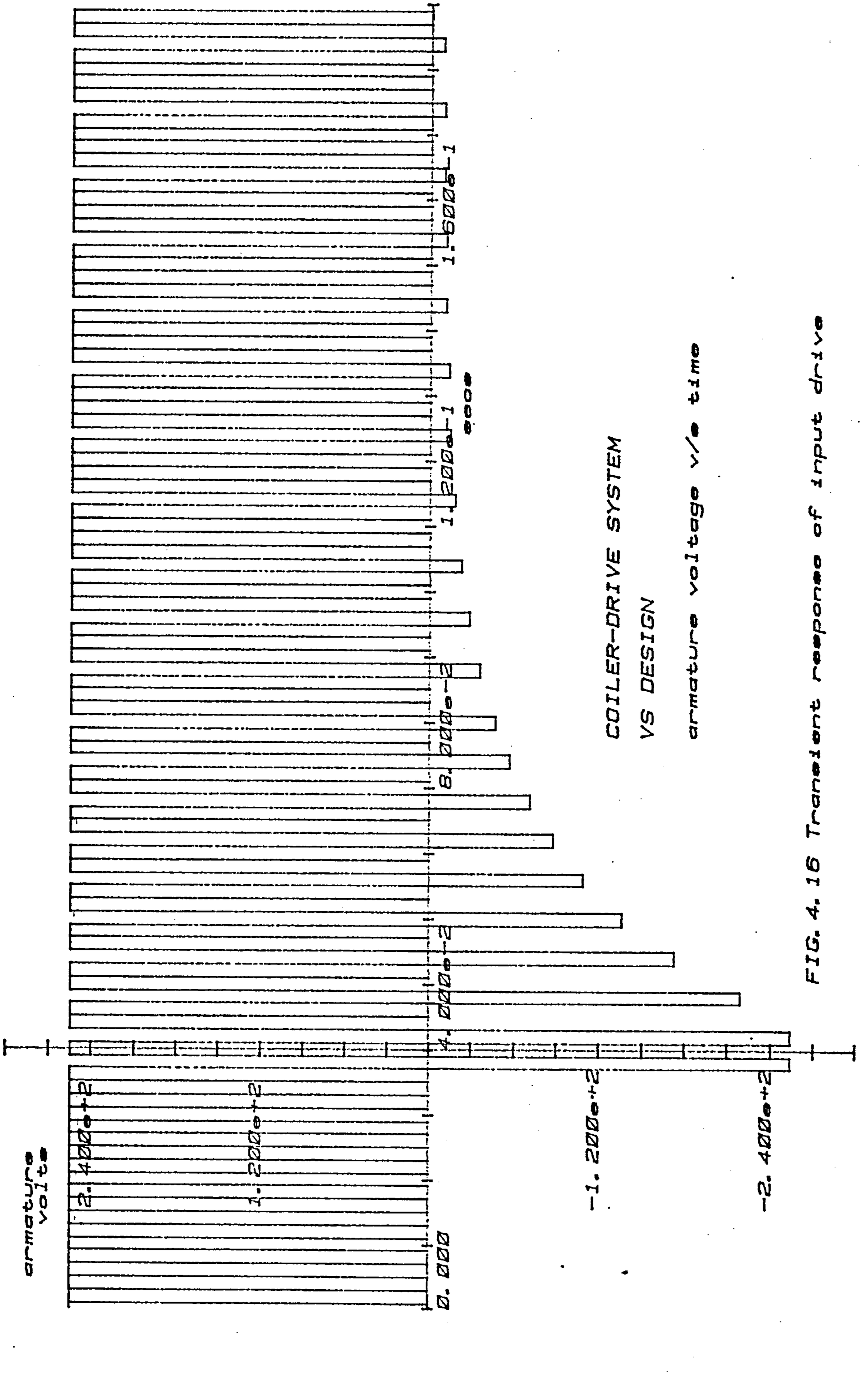

FIG. 4.16 Transient response of input drive coil-drive system vs design

relay action in the input drive. Consideration of type 0 system in general seems to indicate a similar result. The plant is consequently being controlled through a combination of open and closed loop actions.

The switching of the input reference V_R is inevitable as the sliding conditions of (4.23) and (4.26) indicate. But if it were possible to measure the radius, it is interesting to observe that this condition is lifted and that a VS adaptive solution is obtained. From (4.26), the second term disappears from the sliding equations if,

$$\psi_R = \frac{NF}{r} \tag{4.37}$$

The parameters N and F are known and by introducing a time-varying gain K_R in the feedback such that $K_R = \psi_R$ then a sliding motion can be formed without switching V_R. This adaptive solution is not considered any further since the radius has been assumed to be unmeasurable.

Some design difficulties were encountered in the choice of gains to ensure hitting but were satisfactorily overcome. A good and stable transient response has been obtained in a noise free coiler-drive system; it remains to assess the performance of the system with random noise added to the measurements. This is done in Chapter six.

CHAPTER FIVE

ANALYSIS AND DESIGN OF A VSS FOR A TYPE 1 PLANT SUBJECT TO DISTURBANCES

This Chapter continues the investigation of VS theory with the analysis and design of a VSS for a type 1 plant which is subjected to external disturbances. It is shown that a type 1 plant can be regulated with zero steady-state error in the presence of a step input demand and a constant disturbance in one of the state variables. The control objective is fulfilled through the switching of a local feedback around an integrator within the controller which results in an input drive to the plant composed of a mean level with a superimposed pulse amplitude and pulse width modulated signal. The mean level in effect balances the external disturbances acting on the plant while the switching takes place to enforce a sliding regime.

The particular example under study is that of designing an autopilot for a ship model. The ship is a type 1 system subject to external disturbances and with parameters that can change in a sudden and random fashion. Several autopilot designs can be found in the literature which have good overall performances but suffer from a common disadvantage in being rather poor at minimising the effects of external disturbances. The control objective in applying VS theory to the design of an autopilot is consequently directed at improving the rejection properties of the ship to external disturbances whilst maintaining the existing performance.

5.1 Introduction

Autopilots for ships have been designed for the ship on a constant course. The mathematical model of the ship can, therefore be a relatively simple, linear, time-invariant model. The linearisation is justified for course-keeping autopilots for small deviations from a set course and the resulting autopilot is only useful for correcting for small disturbances from that set course.

There is, however, a need for autopilots which can also give a desired response to course changes. The design of these autopilots requires a more detailed model of the ship's dynamics as the assumptions of linearity and time-invariance can no longer represent the behaviour of the ship over the desired range of maneouvres. The dynamic behaviour of the ship and therefore the parameters of the model are very dependent upon the ship's environment and the applied thrust power. When a ship is steered by an autopilot it becomes necessary to adjust the parameters of the controller in accordance with the change in the steering characteristics of the ship. For small variations in the steering characteristics, the feedback system corrects automatically the overall behaviour. For large parameter variations, the controller must be adapted, especially for large ships, e.g. supertankers where the variations can be large and sudden, for instance when the depth of water changes.

Firstly a description is given of an autopilot synthesised according to state feedback principles. Simulation results indicate that this controller configuration gives a very satisfactory performance with respect to all the design specifications except for the minimisation of disturbances. In the second part of the chapter, a VS autopilot is designed and is shown to improve the disturbance rejection properties of the overall control system. Other designs based on series compensation principles [5.1] and model reference adaptive systems [5.2] have been described in the literature. The series compensator design has some unsolved difficulties regarding the time-varying parameters, and the filtering of disturbances. The adaptive method requires a model of the ship to be stored in the controlling computer and is complex to implement. The filtering of sea disturbances is still a problem area with that particular technique.

5.2 Ship Model

The accurate control of ships in straight sailing and course alterations is an important area of applied research. With the present era of supertankers operating very often in crowded and narrow waterways, the design requirements placed on the autopilot are very demanding. The main specifications for the autopilot are that it should perform well at course-keeping and course-changing in the presence of (i) sudden and large parameter variations, (ii) sea disturbances on the system's variables and (iii) nonlinear effects.

Generally a ship can be described as a system with two inputs, rudder angle and the thrust power, and two outputs, course angle and speed. Ship's maneouvres are usually carried out using constant thrust power and consequently for the purpose of designing an auto-pilot, a linear differential equation relating the rudder-angle to the heading is often used to describe the motion of a ship moving in a horizontal plane, in deep unrestricted waters and at a constant speed. The equation is given by,

$$T_1T_2\dddot{\theta} + (T_1 + T_2)\ddot{\theta} + \dot{\theta} = k(T_3\dot{\delta} + \delta - \delta_x) \qquad (5.1)$$

where k, T_1, T_2 and T_3 are parameters related to the mass, speed of the ship and, the forces and turning moment acting upon it. The above equation is derived from the complicated nonlinear models that are used in shipbuilding technology [5.3]. The variable $\dot{\theta}$ is the angular velocity and δ_x is the rudder angle corresponding to $\dddot{\theta} = \ddot{\theta} = \dot{\theta} = \dot{\delta} = 0$.

Equation (5.1) is only accurate in a small range of $\dot{\theta}$ and δ, typically $\delta < 5^{\circ}$. For any significant range of maneouvres, rudder angles greater than 5.0° are necessary. When cruising on the ocean, a typical course change is 10° to 20° and much larger angles are involved when avoiding ships. Large rudder angles are also used when entering or leaving a port. The effect of large rudder changes is to cause the relationship between rudder angle and heading to be nonlinear. This nonlinear behaviour results mainly from the hydrodynamic damping. When the yaw rate $\dot{\theta}$ is small, the damping is also small. The extreme case being directional instability when the coefficient of the yaw rate becomes negative. The more intense the yaw rate, the larger the damping coefficient becomes. This nonlinear behaviour can be represented by

modifying equation (5.1) to include a nonlinearity $H(\dot{\theta})$ as proposed by Bech [5.4].

The coefficient of the yaw rate is obtained by dividing equation 5.1 by T_1T_2,

$$\dddot{\theta} + (\frac{1}{T_1} + \frac{1}{T_2})\ddot{\theta} + \frac{1}{T_1T_2}\dot{\theta} + \frac{k}{T_1T_2}\delta_x = \frac{k}{T_1T_2}(T_3\dot{\delta} + \delta) \qquad (5.2)$$

Bech [5.4] has shown that the terms $\frac{k}{T_1T_2}$, $(\frac{1}{T_1} + \frac{1}{T_2})$ and T_3 remain approximately constant during course changing maneouvres for a given ship whereas the δ_x changes considerably. The substitution,

$$\frac{1}{k}\dot{\theta} + \delta_x = H(\dot{\theta}) \qquad (5.3)$$

in equation (5.2) results in,

$$\dddot{\theta} + (\frac{1}{T_1} + \frac{1}{T_2})\ddot{\theta} + \frac{k}{T_1T_2}H(\dot{\theta}) = \frac{k}{T_1T_2}(T_3\dot{\delta} + \delta) \qquad (5.4)$$

The main nonlinearities of equation (5.2) have been lumped into $H(\dot{\theta})$. This nonlinearity is known as the steering characteristic of the ship and it defines the rudder angle required to outbalance the forces and moments acting upon the hull in a steady turn with rate $\dot{\theta}$, i.e. with $\dddot{\theta} = \ddot{\theta} = \dot{\delta} = 0$. $H(\dot{\theta})$ can be determined directly from ship trials using the Dieudonné spiral test [5.2]. Typical steering characteristics are shown in fig. (5.1). As seen from these characteristics, a normal ship will become increasingly stable as the rate of turn increases. The possibility exists, however, at least in theory, that a ship may be dynamically unstable in straight sailing. These abnormalities in the steering characteristic may be reflected in abrupt and seemingly random variations in steering performances.

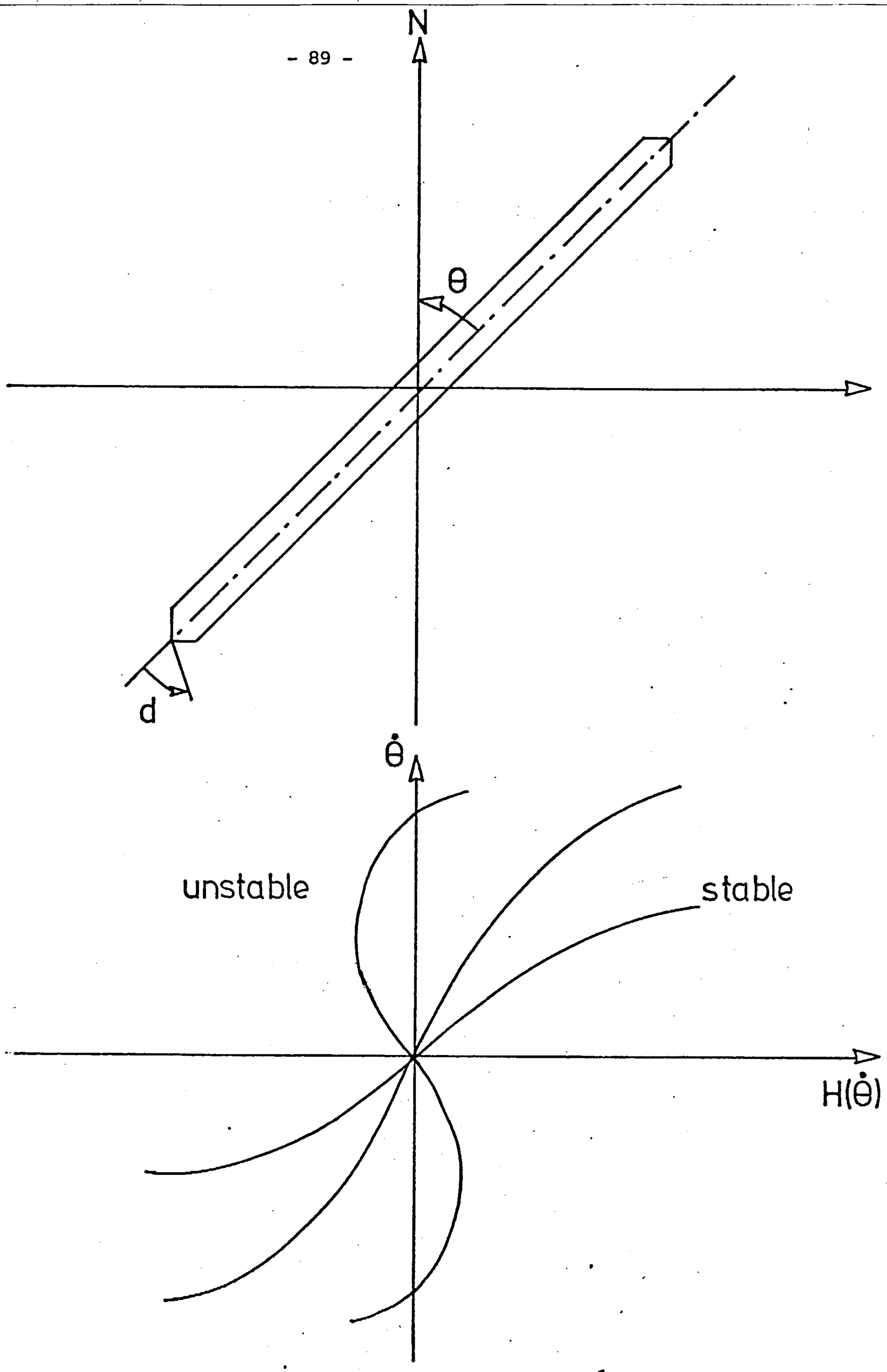

Figure 5.1 Steering Characteristics

Results from spiral tests indicate that $H(\dot{\theta})$ can be approximated by a cubic polynomial, [5.2],

$$H(\dot{\theta}) = a(\dot{\theta})^3 + b(\dot{\theta}) \tag{5.5}$$

where parameter 'a' is always positive in value but 'b' can be either positive or negative. When 'b' is negative, the open-loop ship can become course unstable.

Fig. (5.2) shows the block diagram representation of the ship's dynamics and of the steering gear. The available input for the control of the ship's heading is, in general, the control input of the steering gear. A typical steering gear consists of a hydraulic actuator with controlled delivery pumps which for small signal analysis can be represented by the transfer function between the rudder input demand (δ_i) and the rudder angle (δ),

$$\frac{\delta}{\delta_i}(s) = \frac{1}{sT_r + 1} \tag{5.6}$$

The measurement loop around the steering gear can be removed, giving rise to a true integrator, i.e.

$$\frac{\delta}{\delta_i}(s) = \frac{1}{sT_r} \tag{5.7}$$

If the nonlinear effect of δ_x is ignored in equation (5.3), and if the parameters are assumed constant, then the transfer function between θ and δ is linear and is given by,

$$\frac{\theta(s)}{\delta_i(s)} = \frac{kT_3}{T_1T_2T_r} \frac{(s + 1/T_3)}{s^2\{s^2 + (\frac{1}{T_1} + \frac{1}{T_2})s + \frac{1}{T_1T_2}\}} \tag{5.8}$$

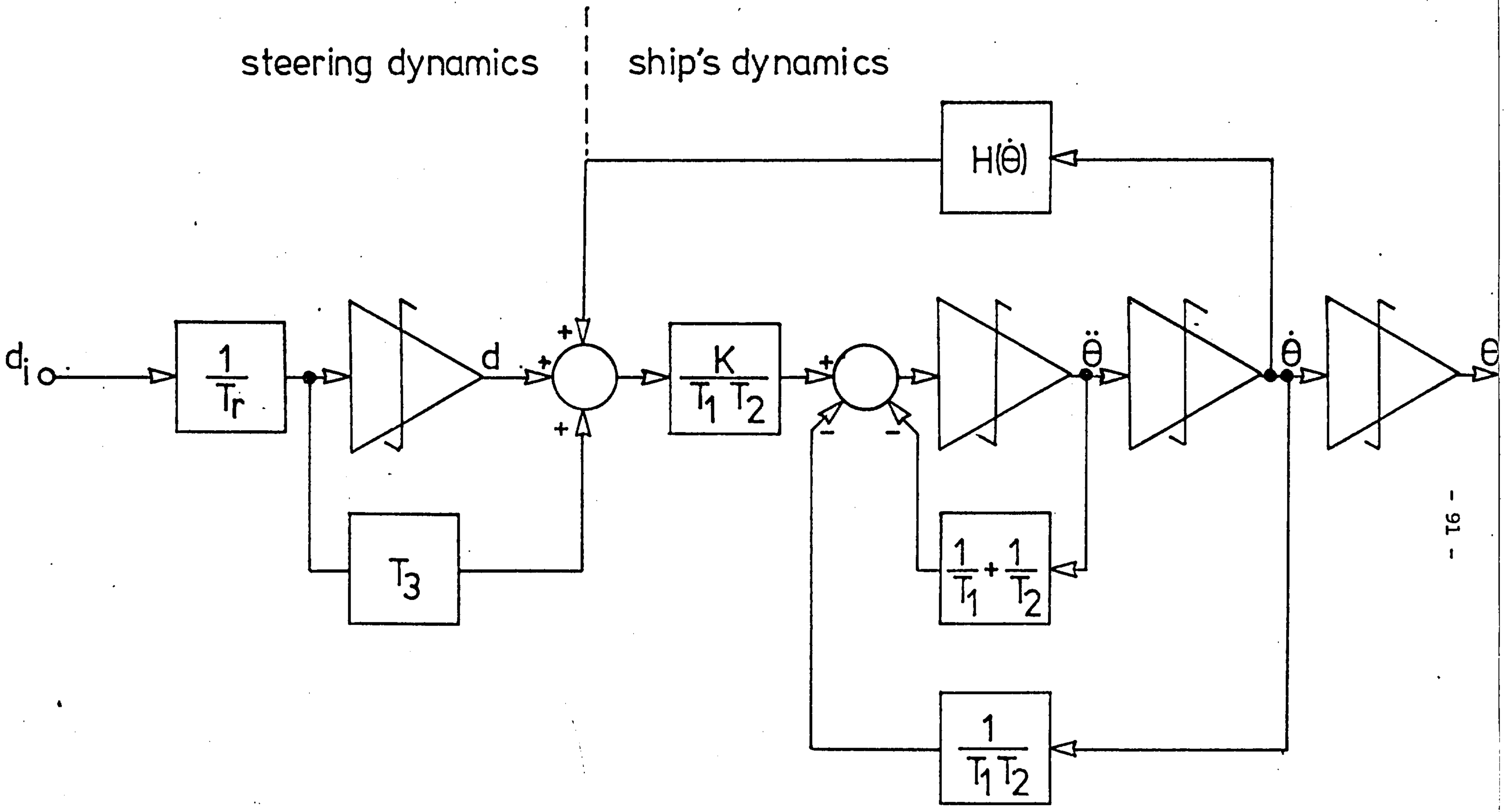

Figure 5.2 Ship and Steering Dynamics

Spiral tests carried on the 50,000-ton deadweight tanker 'British Bombardier' for the parameter identification of equation (5.8) gave the following nominal values, [5.4],

$$\left.\begin{aligned} \frac{1}{T_1 T_2} &= 0.001 \qquad \frac{1}{T_1} + \frac{1}{T_2} = 0.039 \\ \frac{1}{T_3} &= 0.083 \qquad \frac{1}{T_r} = 4.6 \\ \frac{kT_3}{T_1 T_2 T_r} &= 0.012 \qquad \frac{k}{T_1 T_2} = 0.0002165 \end{aligned}\right\} \qquad (5.9)$$

5.3 State-Feedback Design

The state-space formulation of the ship and steering gear dynamics is obtained in the usual notation by letting $\theta = x_1$, $\dot{\theta} = x_2$, $\ddot{\theta} = x_3$, $\delta = x_4$ and $\delta_i = u$. The state equations of fig. (5.2) are,

$$\left.\begin{aligned} \dot{x}_1 &= x_2 \\ \dot{x}_2 &= x_3 \\ \dot{x}_3 &= -\frac{1}{T_1 T_2} x_2 - \left(\frac{1}{T_1} + \frac{1}{T_2}\right) x_3 + \frac{k}{T_1 T_2} x_4 + \frac{kT_3}{T_1 T_2} \dot{x}_4 \\ \dot{x}_4 &= \frac{u}{T_r} \end{aligned}\right\} \qquad (5.10)$$

Substituting for $\dot{x}_4$ in the third equation of (5.10) gives,

$$\dot{\underline{x}} = \begin{bmatrix} 0.0 & 1.0 & 0.0 & 0.0 \\ 0.0 & 0.0 & 1.0 & 0.0 \\ 0.0 & -\frac{1}{T_1T_2} & -(\frac{1}{T_1}+\frac{1}{T_2}) & \frac{k}{T_1T_2} \\ 0.0 & 0.0 & 0.0 & 0.0 \end{bmatrix} \underline{x} + \begin{bmatrix} 0.0 \\ 0.0 \\ \frac{kT_3}{T_1T_2T_r} \\ \frac{1}{T_r} \end{bmatrix} u \quad (5.11)$$

And for the particular ship parameters of (5.9), (5.11) becomes

$$\dot{\underline{x}} = \begin{bmatrix} 0.0 & 1.0 & 0.0 & 0.0 \\ 0.0 & 0.0 & 1.0 & 0.0 \\ 0.0 & -0.001 & -0.039 & 0.0002165 \\ 0.0 & 0.0 & 0.0 & 0.0 \end{bmatrix} \underline{x} + \begin{bmatrix} 0.0 \\ 0.0 \\ 0.012 \\ 4.6 \end{bmatrix} u$$

$$= \underline{A}\,\underline{x} + \underline{b}\,u \quad (5.12)$$

The open-loop poles can be shown to be located at s = 0.0, 0.0, -0.0195 + j0.025,-0.0195 - j0.025 with an open-loop zero at s = -0.083. For reasons which will become apparent later, the feedback around the steering integrator has been removed hence the double poles at the origin.

Using the mathematical model of equation (5.12), a state-feedback autopilot was developed. The heading (θ) is obtained directly from the ship's compass whereas the yaw rate ($\dot{\theta}$) can be obtained from a gyro-compass. The yaw acceleration ($\ddot{\theta}$) can be derived either by differentiation within the controller or obtained directly by using an accelerometer. Since the system is type two, zero steady state error will automatically result to a demand step change in x_1. The following control law has been proposed by Russell [5.5] for the position control of this particular ship.

$$\left.\begin{aligned} u &= k_1(u_c - x_1) - k_2x_2 - k_3x_3 \\ &= k_1u_c - \underline{k}^T\underline{x} \end{aligned}\right\} \qquad (5.13)$$

where k_4 is assumed to be zero and u_c is the reference input.

Substituting for 'u' in equation (5.12) gives,

$$\dot{\underline{x}} = [\underline{A} - \underline{b}\,\underline{K}^T]\underline{x} + \underline{b}\,k_1u_c \qquad (5.14)$$

The following values for the $\underline{k}^T$ vector were found to give an acceptable time response,

$$\left.\begin{aligned} k_1 &= 0.4 \\ k_2 &= 30.0 \\ k_3 &= 357.0 \end{aligned}\right\} \qquad (5.15)$$

With these selected values of feedback gains, the closed-loop poles of the system are located at,

$$s = -0.017,\ -0.067,\ -0.085 \text{ and } -4.5 \qquad (5.16)$$

hence the system is completely stable. With the absence of feedback around the steering integrator, the system's type is two, the system is able to compensate for a step disturbance on the angular velocity due for example to a constant current, which is reflected as a ramp disturbance on the angular position.

The closed-loop system can now be represented by the diagram of fig. (5.3) and the closed-loop state-space equations are as follows,

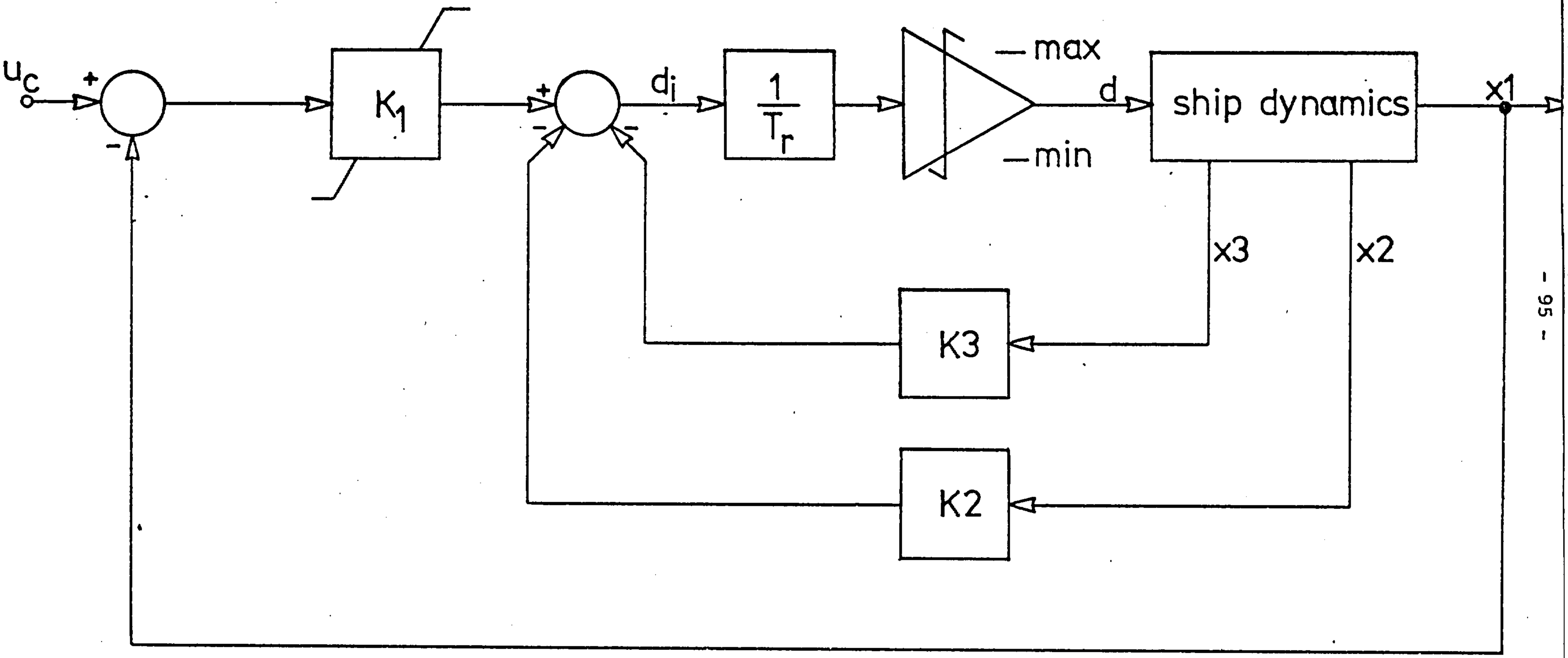

Figure 5.3 Ship Autopilot - State Feedback Controller

$$\dot{\underline{x}} = \begin{bmatrix} 0.0 & 1.0 & 0.0 & 0.0 \\ 0.0 & 0.0 & 1.0 & 0.0 \\ -0.0048 & -0.361 & -4.32 & 0.0002165 \\ -1.84 & -138.0 & -1642.2 & 0.0 \end{bmatrix} \underline{x} + \begin{bmatrix} 0.0 \\ 0.0 \\ 0.0048 \\ 1.84 \end{bmatrix} u_c \qquad (5.17)$$

Comparing equations (5.16) and (5.12), it can be observed that the effect of the selected feedback gains has been to swamp the variations in certain parameters, hence resulting in an insensitive closed-loop system.

Besides insensitivity to parametric variations and stability, other factors were taken into account in the choice of the state feedback gains. The output of amplifier k_1 (fig. (5.3) normally saturates under a large course change and consequently the transfer function between x_2, the angular velocity, and the output of amplifier k_1 is independent of the position loop during the saturation period. The saturation level of k_1 is selected under these conditions to give a constant rate of change of position, k_2 and k_3 are such that this inner loop is also stable.

Another nonlinearity is incorporated in the system by allowing the steering integrator to saturate. The steering integrator represents a hydraulic system between the rudder δ and its input point δ_i which is a floating lever. The effect of introducing saturation across the steering gear is to limit the amplitude of the low frequency sinusoidal signals which appear on the rudder as a result of the feedback of wave disturbances on the angular velocity. The level of saturation in this case is determined on an individual basis as the nonlinear function $H(\dot{\theta})$ must be taken into consideration; this is to ensure a stable response between x_1 and

δ under saturation conditions.

5.3.1 Simulation Results of State Feedback Autopilot

Fig. (5.4) shows the CSMP program used in the simulation of the ship and the state feedback autopilot and fig. (5.5) shows the step response of the system to a unit change in the reference position u_c. The transient is over in about 200 seconds and the steady state error in the heading is zero. The saturation limits on the output of amplifier k_1 were set at (-2.0, 2.0) (fig. 5.3) and at (-10.0, 10.0) for the steering integrator. However, with $u_c = 1.0$, the ship and autopilot operated entirely within a linear region.

Fig. (5.6) shows the effect of a step disturbance on the yaw rate; the variable DIST in the CSMP program was set to one after 200 seconds had elapsed. This relatively high disturbance causes a sharp change in the heading position but zero error is restored after an approximate time interval of 300 seconds. The system was forced in this instance, to operate temporarily in a nonlinear region, fig. (5.7). The output of amplifier k_1 (denoted by the variable ERROR in fig. (5.4) saturates thus preventing a large change in δ_i (DELTA in fig. (5.4)). The system eventually moves back into a linear region and the correct heading is established. Fig. (5.8) shows that the rudder angle (x_4) has settled to a value of -4.6 to compensate for the constant disturbance on the angular velocity. The effects of a sinusoidal disturbance in the yaw rate are shown in figs. (5.9) and (5.10); the amplitude and frequency of the disturbance were defined by DIST = 0.1 sine(t) to provide a representative disturbance. The angular position x_1 can be observed to maintain on average the correct heading, which from

```
TITLE  SHIP AUTOPILOT  -   STATE FEEDBACK CONTROLLER
PARAMETER A=0.0002165,B=0.039,C=0.001,...
D=0.0,E=0.0,F=4.6,K1=0.4,K2=30.0,K3=357.0,T3=12.048,...
LEVEL1=10.0,LEVEL2=-10.0,UC=1.0
DYNAMIC
*
*    SHIP DYNAMICS
*
* X1 = ANGULAR POSITION
* X2 = ANGULAR VELOCITY
* X3 = ANGULAR ACCELERATION
* X4 = RUDDER ANGLE
* DIST = DISTURBANCE ON ANGULAR VELOCITY
* NONLIN = NONLINEARITY RELATING ANGULAR VELOCITY TO RUDDER ANGLE
*
X1=INTGRL(X10,Y2)
Y2=X2+DIST
DIST=0.0
X2=INTGRL(X20,X3)
X3=INTGRL(X30,X3DOT)
X3DOT=A*Z1-B*X3-C*X2
X4DOT=DERIV(0.0,X4)
Z1=X4+T3*X4DOT+NONLIN
NONLIN=D*(Y2**3)+E*Y2
*
*    STEERING GEAR DYNAMICS
*
NOSORT
X4DOTE=DELTA*F
X4=INTGRL(0.0,X4DOTE)
       IF(X4.GT.LEVEL1) X4=LEVEL1
       IF(X4.LT.LEVEL2) X4=LEVEL2
SORT
*
*     STATE FEEDBACK CONTROLLER
*
TEMP1=K1*(UC-X1)
ERROR=LIMIT(-2.0,2.0,TEMP1)
DELTA=ERROR-K2*Y2-K3*X3
METHOD TRAPZ
TIMER FINTIM=1000.0,DELT=0.01,OUTDEL=20.0
PRTPLOT UC,X1,X2,X3,Z1,X4,X4DOT,X4DOTE
PRTPLOT TEMP1,ERROR,DELTA
END
STOP
```

FIG. 5.4 CSMP PROGRAM - STATE FEEDBACK AUTOPILOT

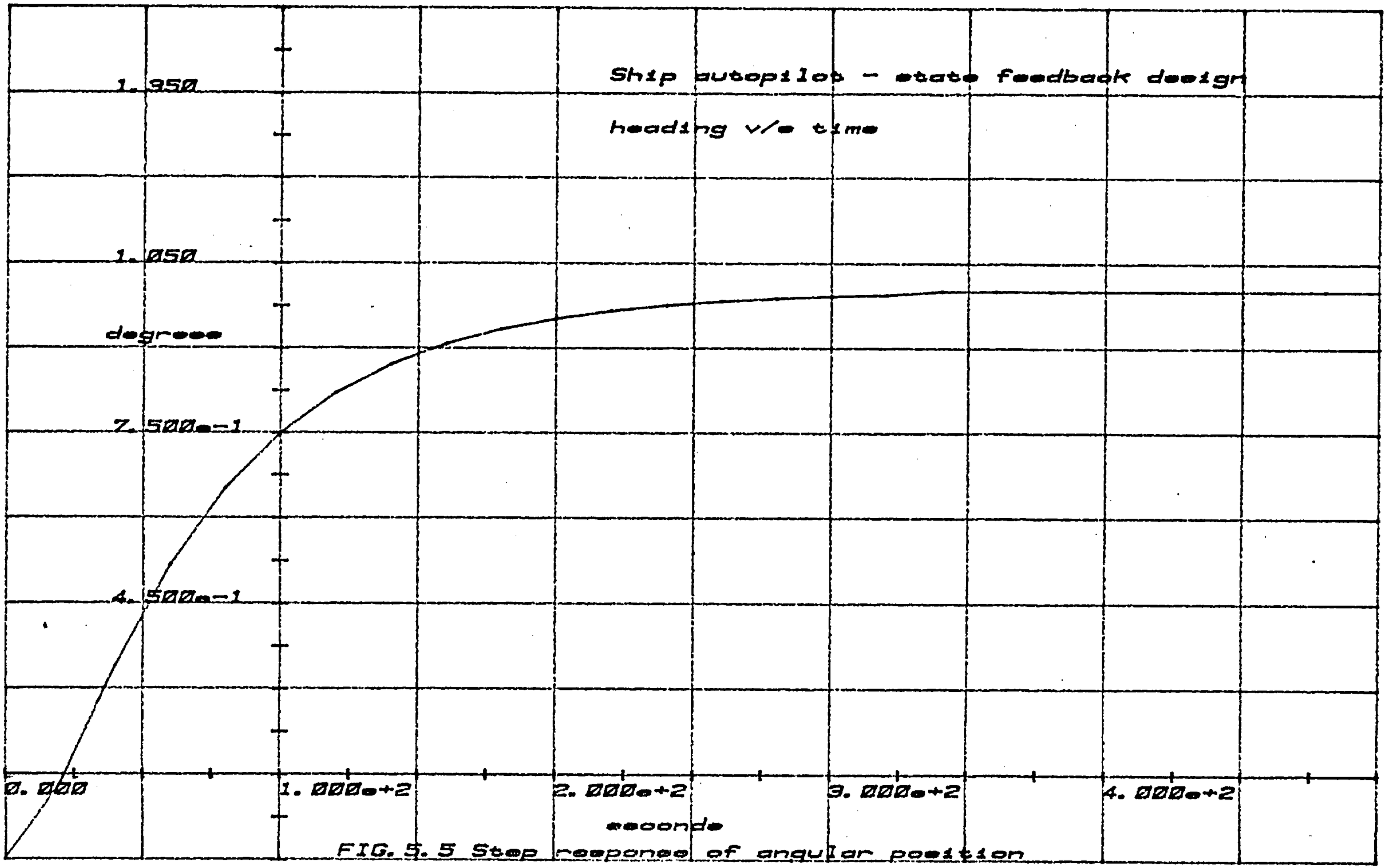

FIG. 5.5 Step response of angular position

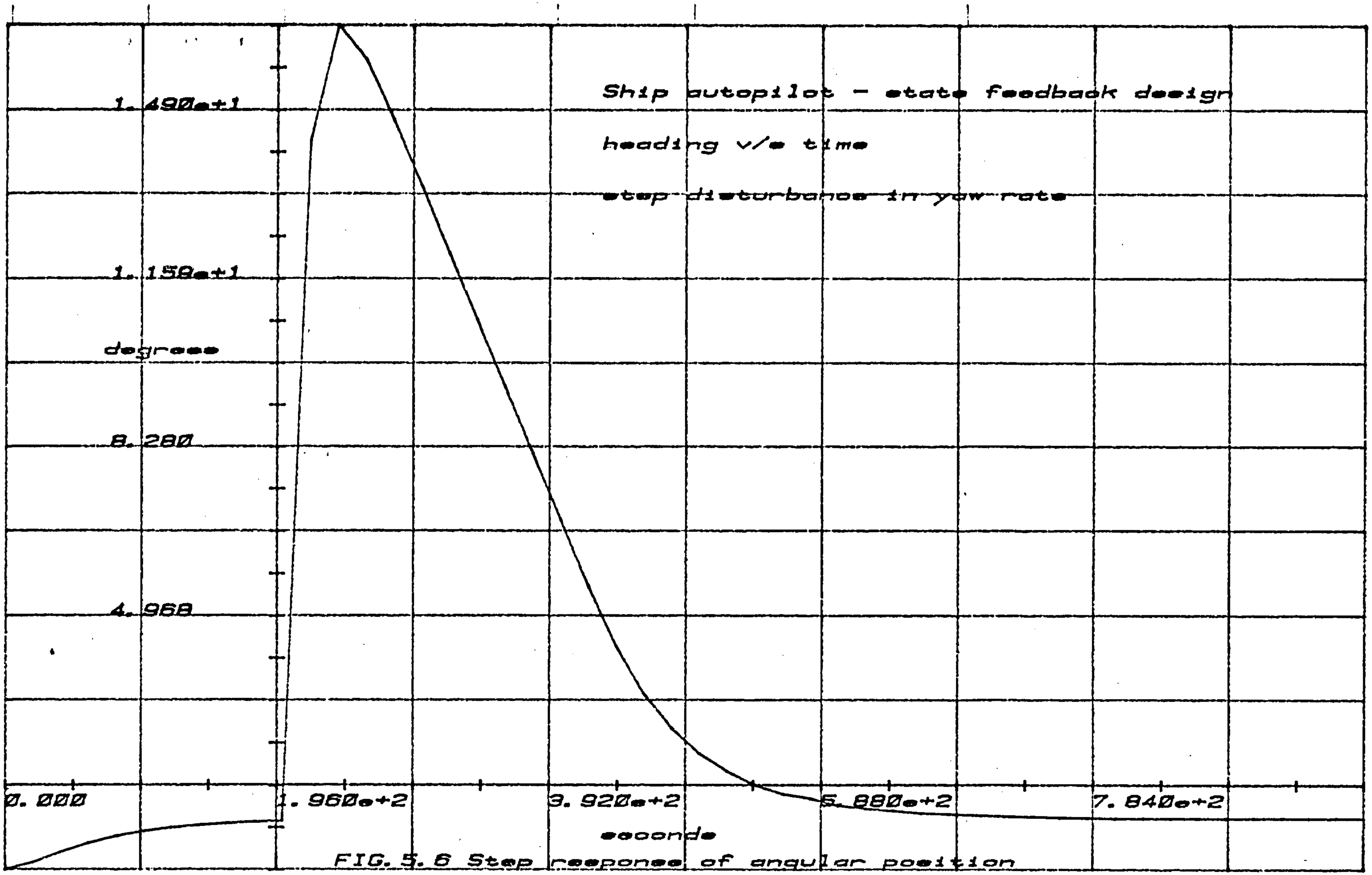

FIG. 5.6 Step response of angular position

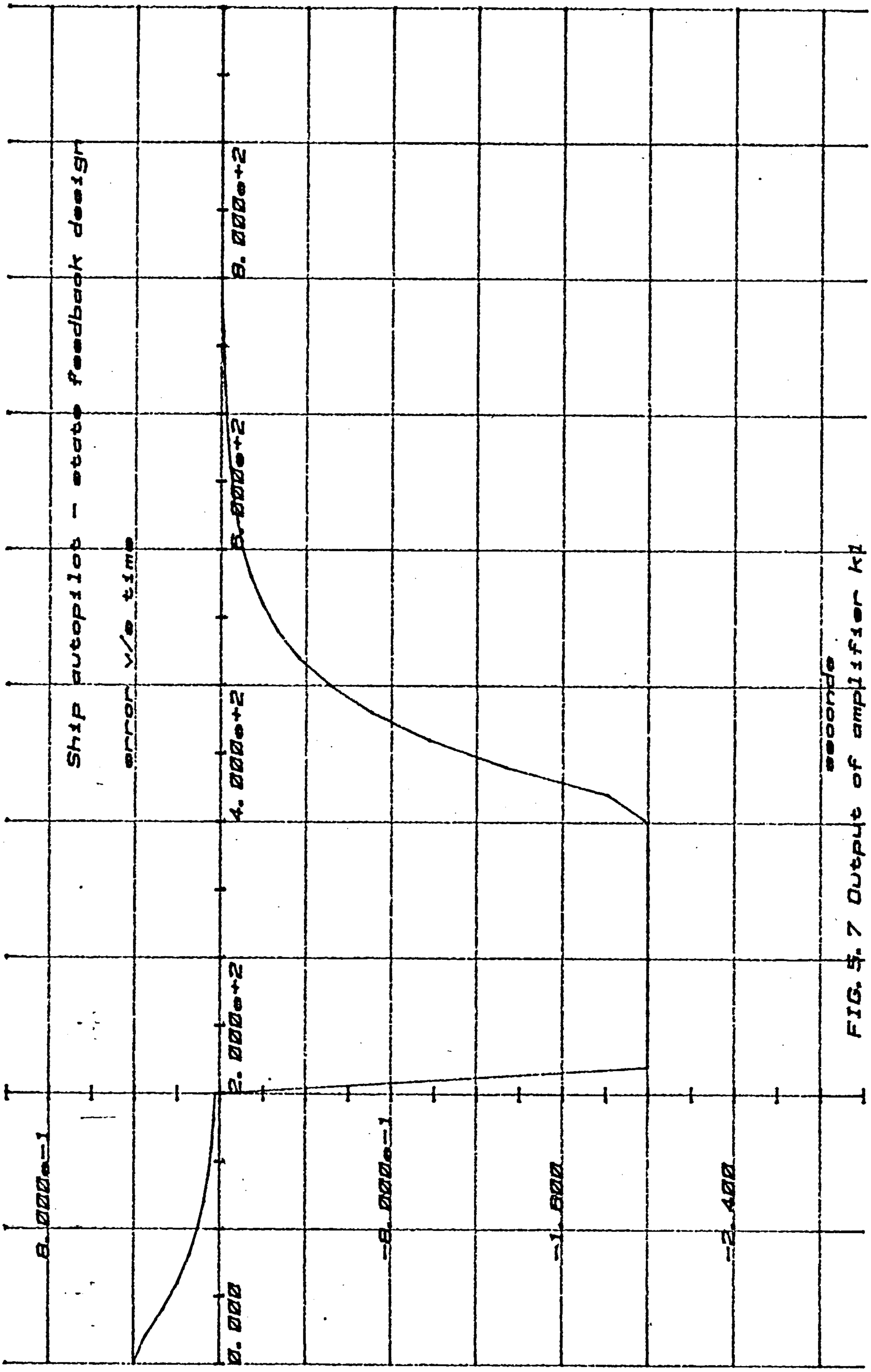

FIG. 5.7 Output of amplifier

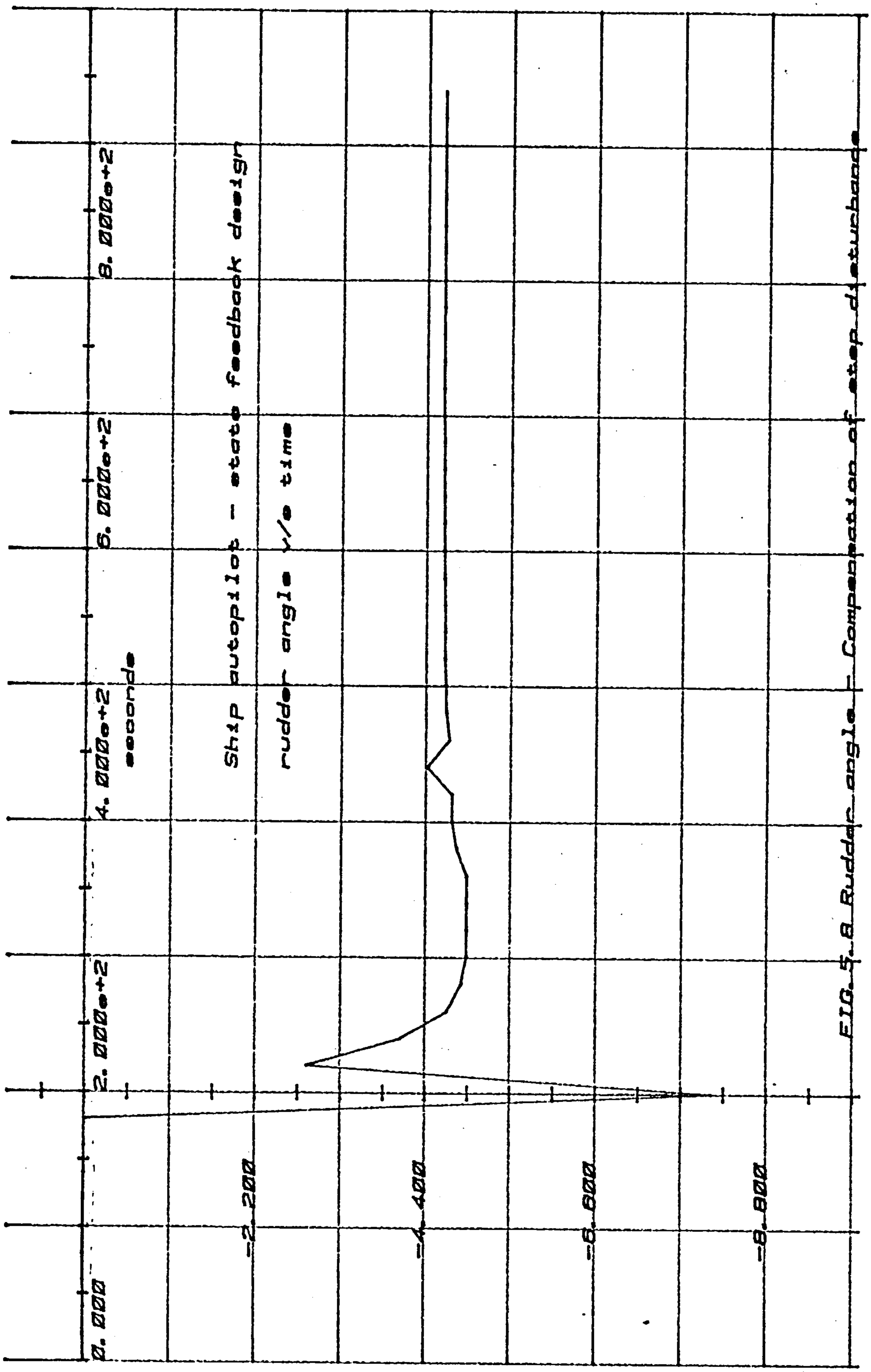
8.000e+2
6.000e+2
4.000e+2
2.000e+2
0.000
-2.000
-4.000
-6.000
-8.000
Ship autopilot - state feedback design
rudder angle v/s time
Compensation of step d
FIG.5.8 Rudder angle

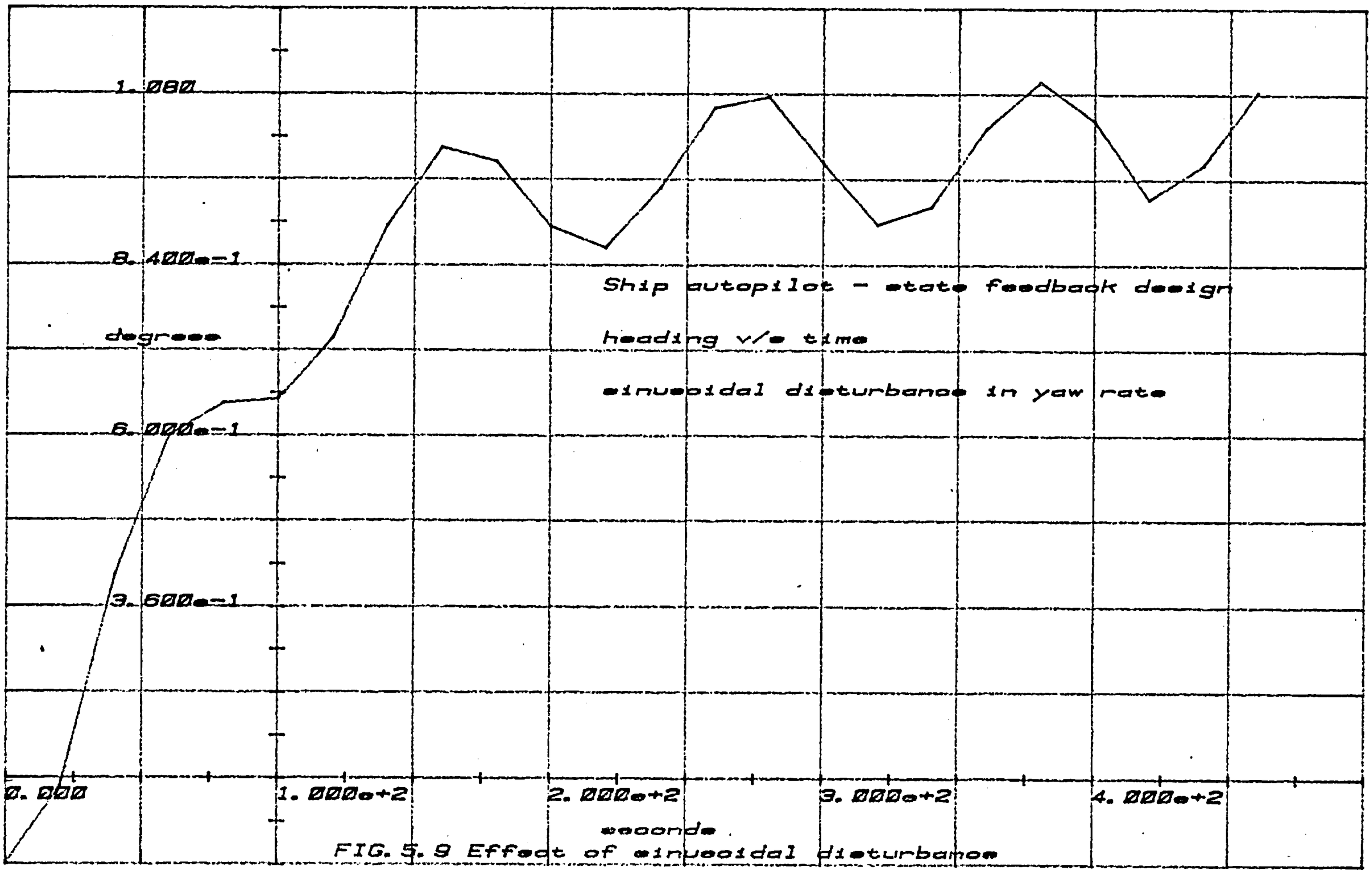

FIG. 5.9 Effect of sinusoidal disturbance

a navigational viewpoint is quite acceptable. The sinusoidal variations of the rudder angle, fig. (5.10), are however undesirable. They result in propulsion losses and increase the mechanical wear [5.1]. Under manual control and similar circumstances, the rudder position would normally be clamped at a fixed position by the helmsman and the heading would be correct on average. The minimisation of rudder activity is consequently an important design criterion in an autopilot system and the possibility of achieving this objective through the use of a variable structure controller is studied in the next section.

Fig. (5.11) illustrates the combined effect on the heading angle of the nonlinear function $H(\dot{\theta})$ and a step disturbance in yaw rate. For the simulation, the parameters D and E of the nonlinearity (NONLIN in fig. (5.4) were set at the typical values of -5.0 and 10.0 respectively; this is equivalent to setting 'a' and 'b' in equation (5.5) at 5.0 and -10.0. The response is slower but stability and zero steady error in the heading are maintained.

5.3.2 Assessment of the State-Feedback Autopilot

Two conflicting objectives arise in the design of a state-feedback autopilot. The cancellation of a constant disturbance on the angular velocity requires that the system be of type two. The application of the feedback law prescribed by equation (5.13) causes one of the poles to move deeper into the left-half of the complex plane. With the gains assigned, this pole lies at $s = -4.5$, if this pole is assigned closer to the $j\omega$ axis, it is found that the sinusoidal disturbances on the rudder angle can be minimised. However, the arbitrary position of this pole along the real axis

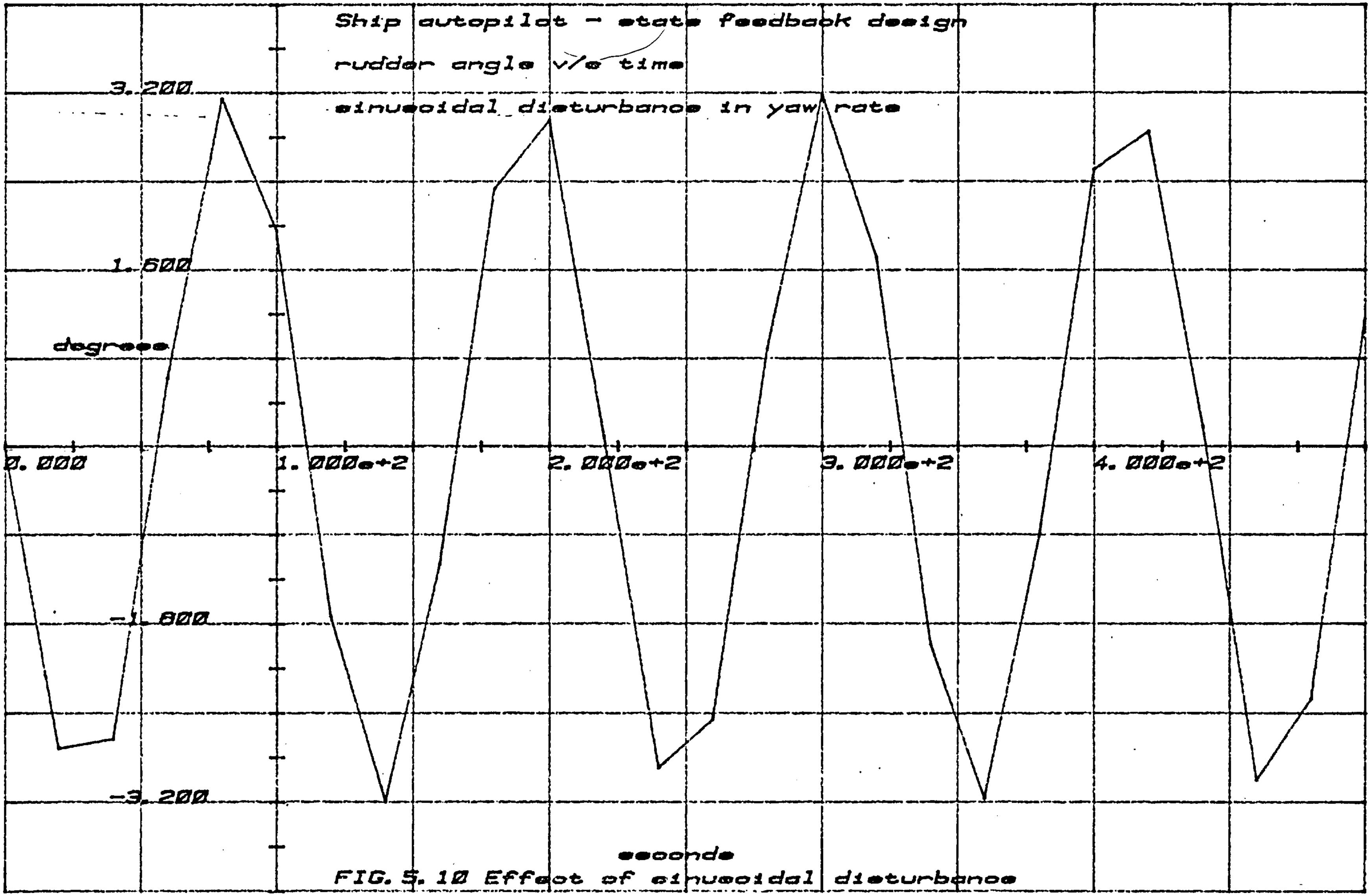

FIG. 5.10 Effect of sinusoidal disturbance

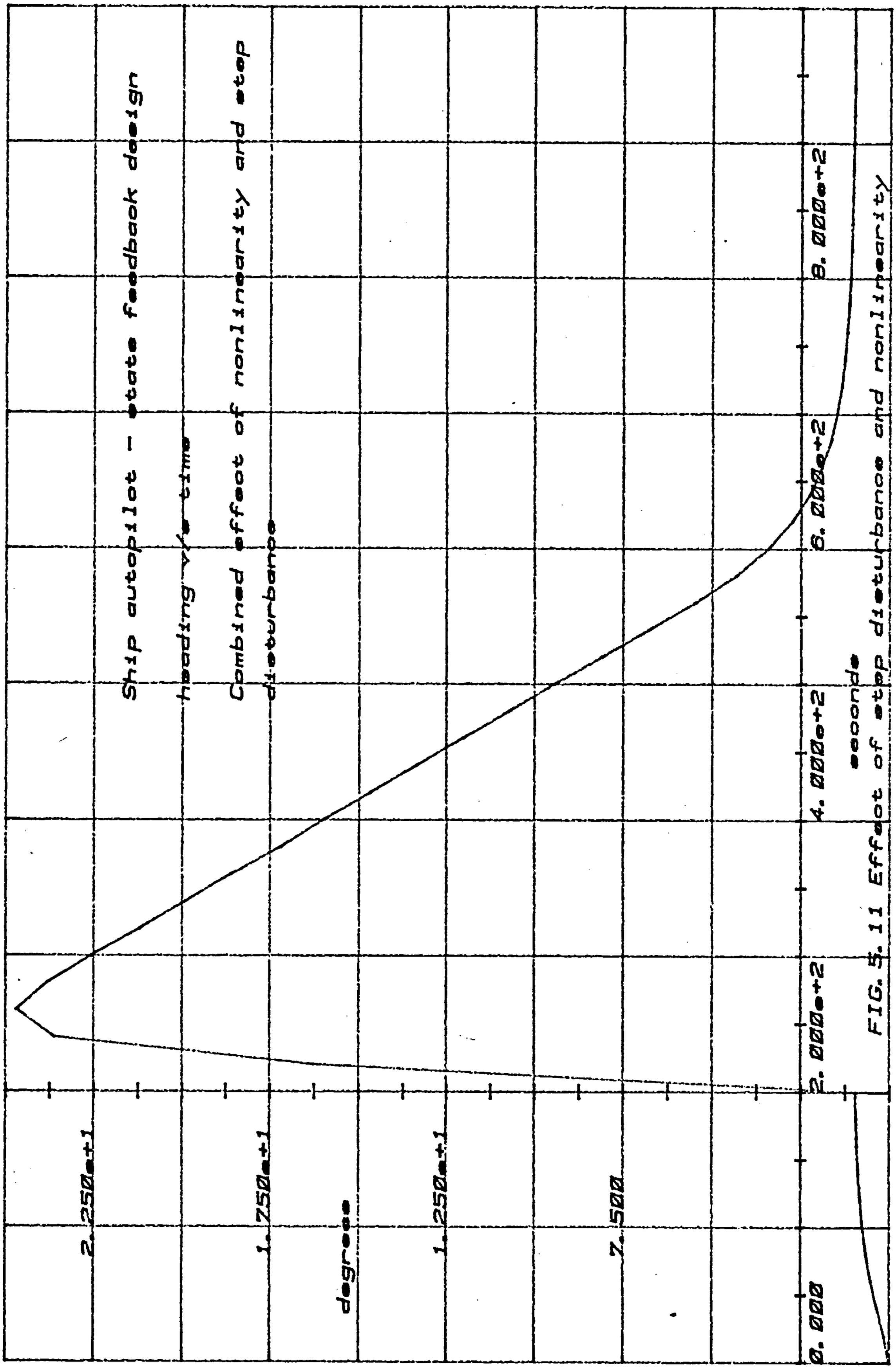

FIG. 5.11 Effect of nonlinearity and step disturbance

implies the application of feedback around the steering integrator, i.e. the rudder angle x_4 must appear in the control law with the consequent reduction in the system's type number to one. The system would thus be unable to track changes in heading angles with zero steady state error.

The above argument is illustrated by using the following feedback controller,

$$u = k_1(u_c - x_1) - k_2x_2 - k_3x_3 - k_4x_4 \qquad (5.18)$$

The values of k_1, k_2, k_3 and k_4 were chosen to keep three of the poles in their original positions at s=-0.017, -0.067 and -0.085. The fourth pole was assigned at s = -0.5. The feedback vector required to achieve these closed loop pole positions is given by,

$$k^T = [0.048 \quad 3.65 \quad 46.0 \quad 0.017] \qquad (5.19)$$

The transient response of the heading angle can be shown to be almost unchanged with the new feedback gains. The effect on x_4 of an identical sinusoidal disturbance in yaw rate is shown in fig. (5.12). The rudder activity can be observed to have decreased on average by approximately 50% in comparison with fig. (5.10), but the penalty for this is a constant heading error, fig. (5.13) following a step disturbance in the angular velocity.

The next section examines the possibility of reconciliating these design objectives through a variable structure controller.

5.4 A VS Autopilot

The design of an autopilot for the model described by equation (5.12) is considered in this section and is based on the VS theory developed in chapter three for the formation of sliding

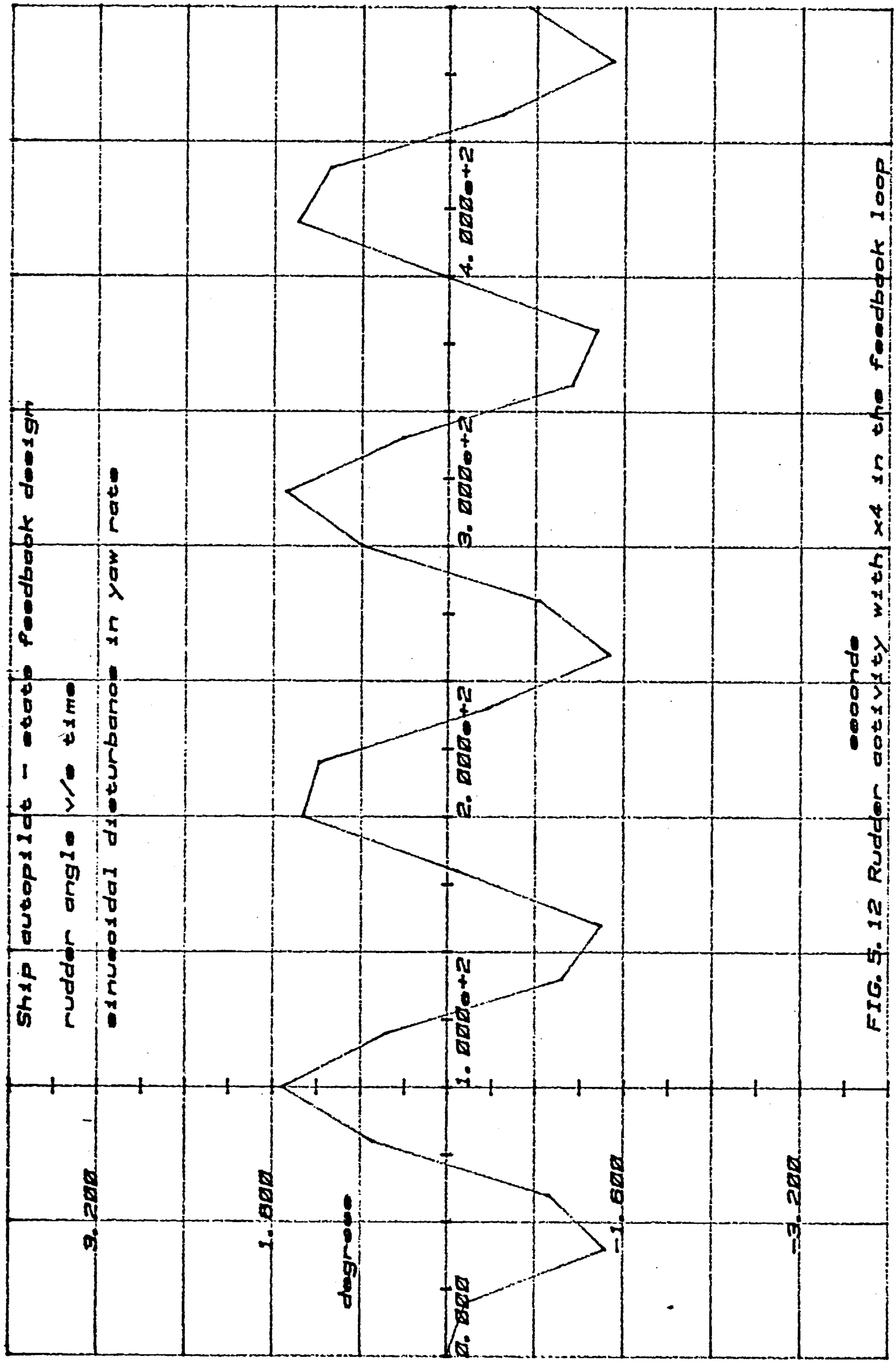

FIG. 5.12 Rudder activity with x4 in the f

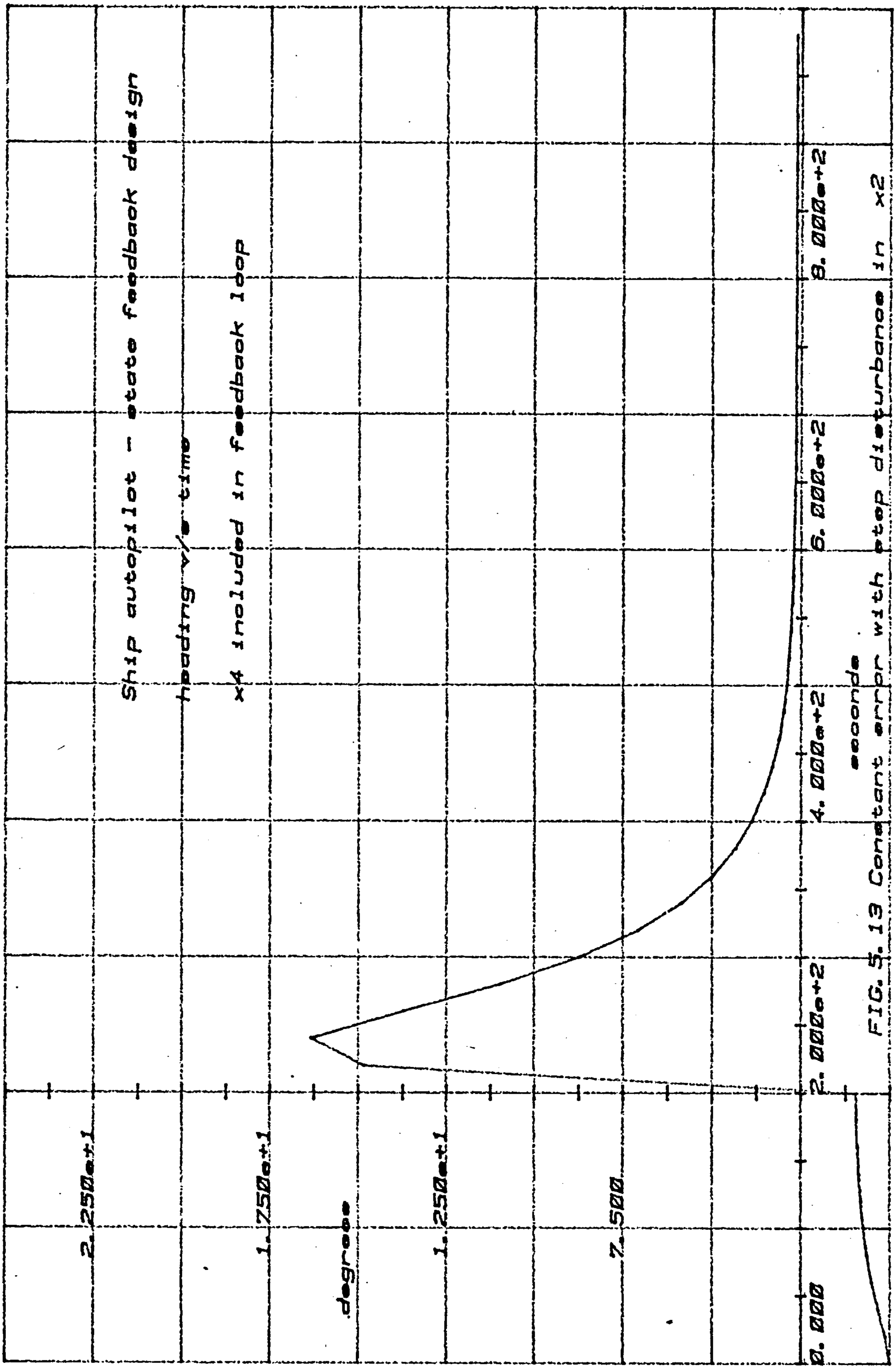

FIG. 5.13 Constant error

regimes.

5.4.1 Selection of a Sliding Plane for the Ship Model

The selection of a suitable sliding plane presents some problems. The purpose of the VS controller is to reduce the switching function σ to zero. If the system is to be regulated around the origin as the equilibrium point, then a switching function which is a linear combination of the state vector $\underline{x}$ is appropriate. In the state-feedback design it was observed that x_4 could attain arbitrary values, hence its inclusion in the switching function is not possible.

Referring back to fig. (5.2), the variables x_1, x_2, and x_3 (corresponding to θ, $\dot{\theta}$ and $\ddot{\theta}$) form part of a subsystem of the ship which is described by a set of differential equations in phase-variable form with $\dot{x}_4$ as a control input point. It seems feasible then to organise a sliding regime in that subspace of the ship based on an error vector $\underline{e}$ as suggested in chapter three on the tracking of inputs. The components of the vector $\underline{e}$ in this instance are simply related to the state vector $\underline{x}$ as follows,

$$\left.\begin{aligned} e_1 &= x_1 - u_c \\ e_2 &= x_2 = \dot{x}_1 \\ e_3 &= x_3 = \dot{x}_2 \end{aligned}\right\} \qquad (5.20)$$

Hence a suitable sliding plane is formed using e_1, e_2 and e_3, i.e.

$$\sigma = c_1 e_1 + e_2 + e_3 \qquad (5.21)$$

where by equation (5.20) e_2 and e_3 are the second and third derivatives of e_1 respectively for a constant input reference u_c.

The linearised equations of the ship are given in matrix form by (5.12) which can be expanded to the following,

$$\left.\begin{aligned} \dot{x}_1 &= x_2 \\ \dot{x}_2 &= x_3 \\ \dot{x}_3 &= -0.001\ x_2 - 0.039\ x_3 + 0.0002165\ x_4 + 0.012\ u \\ \dot{x}_4 &= 4.6\ u \end{aligned}\right\} \quad (5.22)$$

Equation (5.22) can be shown to be equivalent to,

$$\left.\begin{aligned} \dot{e}_1 &= e_2 \\ \dot{e}_2 &= e_3 \\ \dot{e}_3 &= -0.001\ e_2 - 0.039\ e_3 + 0.0002165\ x_4 + 0.012\ u \\ \dot{x}_4 &= 4.6\ u \end{aligned}\right\} \quad (5.23)$$

in the error space defined by (5.20). Taking the disturbance DIST acting on the yaw rate into account and noting that $u = \dot{x}_4/4.6$, equation (5.23) can be re-written as,

$$\left.\begin{aligned} \dot{e}_1 &= e_2 + DIST \\ \dot{e}_2 &= e_3 \\ \dot{e}_3 &= -0.001\ e_2 - 0.039\ e_3 + 0.0002165\ x_4 + 0.012\ u \\ \dot{x}_4 &= 4.6\ u \end{aligned}\right\} \quad (5.24)$$

In chapter three, it was shown that the sliding motion is invariant to disturbances and parameter changes provided that the control entered into the system at the same point as the disturbance. This condition however, is not fulfilled in the case of the ship and therefore sinusoidal disturbances on the angular velocity will influence the sliding motion. On the other hand a constant

disturbance on the yaw rate is equivalent to a new set of initial conditions in the state space and provided that the sliding motion is globally asymptotically stable, then

$$\lim_{t \to \infty} \underline{e}(t) = 0$$

The design philosophy is aimed firstly at reducing the effects of sinusoidal disturbances by re-assigning the closed-loop poles and secondly to superimpose a VS controller which takes care of the time-varying parameters, the nonlinear effects of the steering characteristics and the disturbances on the yaw rate. The V.S. controller can therefore be regarded as a second layer of control; fig. (5.14) illustrates the structure of the controller for the ship model.

5.4.2 Selection of Gain Values for the VS Autopilot

The control law under consideration is of the form,

$$\begin{aligned} u = &-k_1 e_1 - k_2 e_2 - k_3 e_3 - k_4 x_4 \\ &-\psi_1 e_1 - \psi_2 e_2 - \psi_4 x_4 \end{aligned} \tag{5.25}$$

where $\underline{k}^T$ is the feedback vector, and ψ_1, ψ_2, and ψ_4 are switchable gains defined by,

$$\psi_i = \begin{cases} \alpha_i & \text{if } e_i\sigma > 0 \\ \beta_i & \text{if } e_i\sigma < 0 \end{cases} \qquad i = 1, 2, 4 \tag{5.26}$$

The control law allows the arbitrary positioning of the closed-loop poles using the $\underline{k}^T$ vector while ψ_1, ψ_2 and ψ_4 enforce the sliding motion. Differentiating equation (5.21) and applying the procedure of chapter three for the formation of a sliding regime results in,

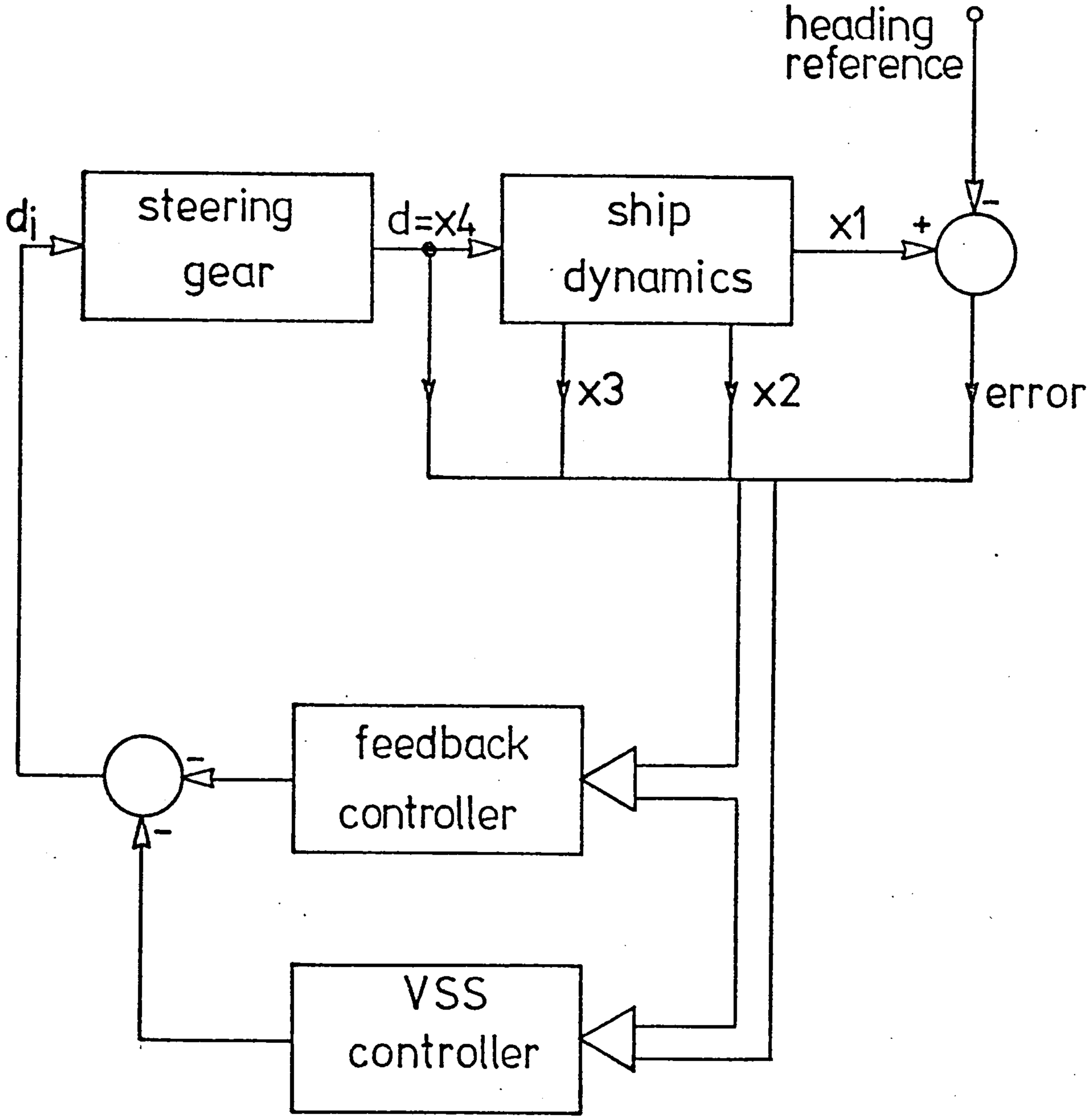

Figure 5.14 Two Level Control of Ship

$$\left.\begin{aligned}
\alpha_1 &> \frac{1}{0.012}\{-c_1c_2 + 0.039\ c_1 + 0.012\ k_3c_1 - 0.012\ k_1\} \quad \text{if } e_1\sigma > 0 \\
\alpha_2 &> \frac{1}{0.012}\{-c_2^2 + 0.039\ c_2 + 0.012\ k_3c_2 + c_1 - 0.001 - 0.012\ k_2\} \quad \text{if } e_2\sigma > 0 \\
\alpha_4 &> \frac{1}{0.012}\{0.0002165 - 0.012\ k_4\} \quad \text{if } x_4\sigma > 0
\end{aligned}\right\} \tag{5.27}$$

with corresponding inequalities for β_1, β_2 and β_4.

Inequalities of (5.27) are simplified by assigning the values of the $\underline{k}^T$ vector using the state-feedback procedure outlined in Appendix [C]. If the elements of the $\underline{k}^T$ vector are given by,

$$\underline{k}^T = [0.0096 \quad 0.73 \quad 15.0 \quad 0.018] \tag{5.28}$$

then the closed-loop poles are located at,

$$s = -0.0197, -0.05, -0.08, -0.16 \tag{5.29}$$

Three of the roots are approximately in the same locations as in the state feedback autopilot (equation 5.16). The fourth root which was located at $s = -4.5$ is now at $s = -0.16$.

Substituting (5.28) into (5.27) yields,

$$\left.\begin{aligned}
\alpha_1 &> \frac{1}{0.012}\{-c_1c_2 + 0.219\ c_1 - 0.0001152\} \\
\alpha_2 &> \frac{1}{0.012}\{-c_1c_2 + 0.219\ c_2 + c_1 - 0.00976\} \\
\alpha_4 &> \frac{1}{0.012}\{0.0002165 - 0.012\ k_4\} = 0.0
\end{aligned}\right\} \tag{5.30}$$

If the average gains of ψ_1 and ψ_2 are zero, (note that the average gain of ψ_4 is zero), then the inequalities of (5.30) result in,

$$\left.\begin{aligned} & c_1(0.219 - c_2) - 0.0001152 = 0 \\ \text{and} \\ & c_2(0.219 - c_2) + c_1 - 0.00976 = 0 \end{aligned}\right\} \qquad (5.31)$$

An exact solution for c_1 and c_2 involves solving a cubic equation in either c_1 or c_2; such expressions invariably occur when selecting coefficients for the switching hyperplane and are an undesirable feature of the design procedure. An approximate solution is obtained with the following values,

$$\left.\begin{aligned} c_1 &= 0.00976 \\ c_2 &= 0.219 \end{aligned}\right\} \qquad (5.32)$$

In general solutions for the c^T vector could lead to imaginary values with no significance. It appears that if the $\underline{k}^T$ vector is selected so as to position the closed-loop poles on the negative real axis, then the solutions obtained for $\underline{c}^T$ are real.

Since $e_3 = -c_1e_1 - c_2e_2$ in a sliding mode, the order of the equation (5.23) is reduced by one. The sliding equations are described by,

$$\left.\begin{aligned} \dot{e}_1 &= e_2 \\ \dot{e}_2 &= e_3 = -c_1e_1 - c_2e_2 \end{aligned}\right\} \qquad (5.33)$$

and stability is assured with positive values of c_1 and c_2. The stability of the sliding motion is also predictable through Theorem 3.1.

```
TITLE SHIP-AUTOPILOT  VARIABLE STRUCTURE CONTROLLER
PARAMETER A=0.0002165,B=0.039,C=0.001,...
D=0.0,E=0.0,F=4.6,K1=0.0096,K2=0.73,K3=15.0,T3=12.048,...
LEVEL1=10.0,LEVEL2=-10.0,UC=1.0,...
KV1=0.0,KV2=0.0,KV3=0.0,KV4=0.1,..
C1=0.00976,C2=0.219,C3=1.0,C4=0.0
DYNAMIC
*
* SHIP DYNAMICS
*
* X1= ANGULAR POSITION
* X2= ANGULAR VELOCITY
* X3= ANGULAR ACCELERATION
* X4= RUDDER ANGLE
* DIST= DISTURBANCE ON ANGULAR VELOCITY
* NONLIN= NONLINEARITY RELATING ANGULAR VELOCITY TO RUDDER ANGLE
*
X1=INTGRL(X10,Y2)
Y2=X2+DIST
DIST=0.0
X2=INTGRL(X20,X3)
X3=INTGRL(X30,X3DOT)
X3DOT=A*Z1-B*X3-C*X2
X4DOT=DERIV(0.0,X4)
Z1=X4+T3*X4DOT+NONLIN
NONLIN=D*(Y2**3)+E*Y2
*
* STEERING GEAR DYNAMICS
*
X4DOTE=(DELTA-UVSS-TR*X4)*F
X4=INTGRL(0.0,X4DOTE)
*
* STATE FEEDBACK CONTROLLER
*
TEMP1=K1*(UC-X1)
ERROR=LIMIT(-2.0,2.0,TEMP1)
DELTA=ERROR-K2*Y2-K3*X3
*
* VARIABLE STRUCTURE CONTROLLER
*
E1=X1-UC
SIGMA=C1*E1+C2*Y2+C3*X3+C4*X4
UVSS=(KV1*ABS(E1)+KV2*ABS(Y2)+KV3*ABS(X3)+KV4*ABS(X4))*SIGN(1.0,SIGMA)
METHOD TRAPZ
TIMER FINTIM=1000.0,DELT=0.01,OUTDEL=20.0
PRTPLOT UC,X1,X2,X3,Z1,X4,X4DOT,X4DOTE
PRTPLOT TEMP1,ERROR,DELTA
PRTPLOT SIGMA,UVSS
END
STOP
```

FIG.5.15 CSMP PROGRAM - VS AUTOPILOT

Substituting e_1 and e_2 in (5.30) gives the following,

$$\left.\begin{aligned} \alpha_1 &> 0.01 \div 0.0 \quad \text{if } e_1\sigma > 0 \\ \alpha_2 &> 0.0 \qquad\quad \text{if } e_2\sigma > 0 \\ \alpha_4 &> 0.0 \qquad\quad \text{if } x_4\sigma > 0 \end{aligned}\right\} \tag{5.34}$$

Since

$$\alpha_1, \alpha_2, \alpha_4 > 0 \quad \text{and} \quad \beta_1, \beta_2, \beta_4 < 0 \tag{5.35}$$

and the average values of the gains is zero, then equivalent control expressions for ψ_1, ψ_2 and ψ_4 in equation (5.25) are,

$$\left.\begin{aligned} \psi_1 e_1 &= \alpha_1 |e_1| \text{sign } (\sigma) \\ \psi_2 e_2 &= \alpha_2 |e_2| \text{sign } (\sigma) \\ \psi_4 x_4 &= \alpha_4 |x_4| \text{sign } (\sigma) \end{aligned}\right\} \tag{5.36}$$

provided that,

$$\left.\begin{aligned} |\alpha_1| &= |\beta_1| \\ |\alpha_2| &= |\beta_2| \\ |\alpha_4| &= |\beta_4| \end{aligned}\right\} \tag{5.37}$$

The validity of equation (5.36) can be checked by noting that,

$$|z| = z \text{ sign}(\sigma)$$

5.4.3 Simulation Results

The simulation program for the ship dynamics, steering gear, state-feedback and variable structure controllers is shown in fig. (5.15). The following values of gains were used to enforce

a sliding regime,

$$\left.\begin{aligned} |\alpha_1| &= KV1 = 0.0 \\ |\alpha_2| &= KV2 = 0.0 \\ |\alpha_4| &= KV4 = 0.1 \end{aligned}\right\} \qquad (5.38)$$

where KV1, KV2 and KV4 are the equivalent variables used in the simulation program. There are essentially two reasons for setting $|\alpha_1|$ and $|\alpha_2|$ to zero and for using $|\alpha_4|$ alone in the switching,

(i) Inspection of eqn. (5.36) shows that the switchable gains change sign simultaneously according to σ, hence switching one variable is equivalent to switching all the variables. This is a direct result of using pole-assignment in (5.27) - (5.30).

(i) e_1 and e_2 are considerably influenced by the sea state and it is therefore unwise to include them in the switching.

Two constraints must be imposed on the actual value of KV4 to ensure that sliding takes place,

(ii) it must be greater than the local feedback value,

i.e. $KV4 \geq K_4 = 0.018$ (from eqn. (5.28)).

(ii) it must be large enough to take into account parametric variations and the effects of the nonlinearity $H(\dot{\theta})$ on the rudder.

The response of the ship to a step change in heading reference and a disturbance in yaw rate applied after 150 seconds is shown in fig. (5.16). The heading settles at the desired value and when disturbed again returns to the correct steady state value. With $KV4 \gg K_4$, the initial response is faster than in the

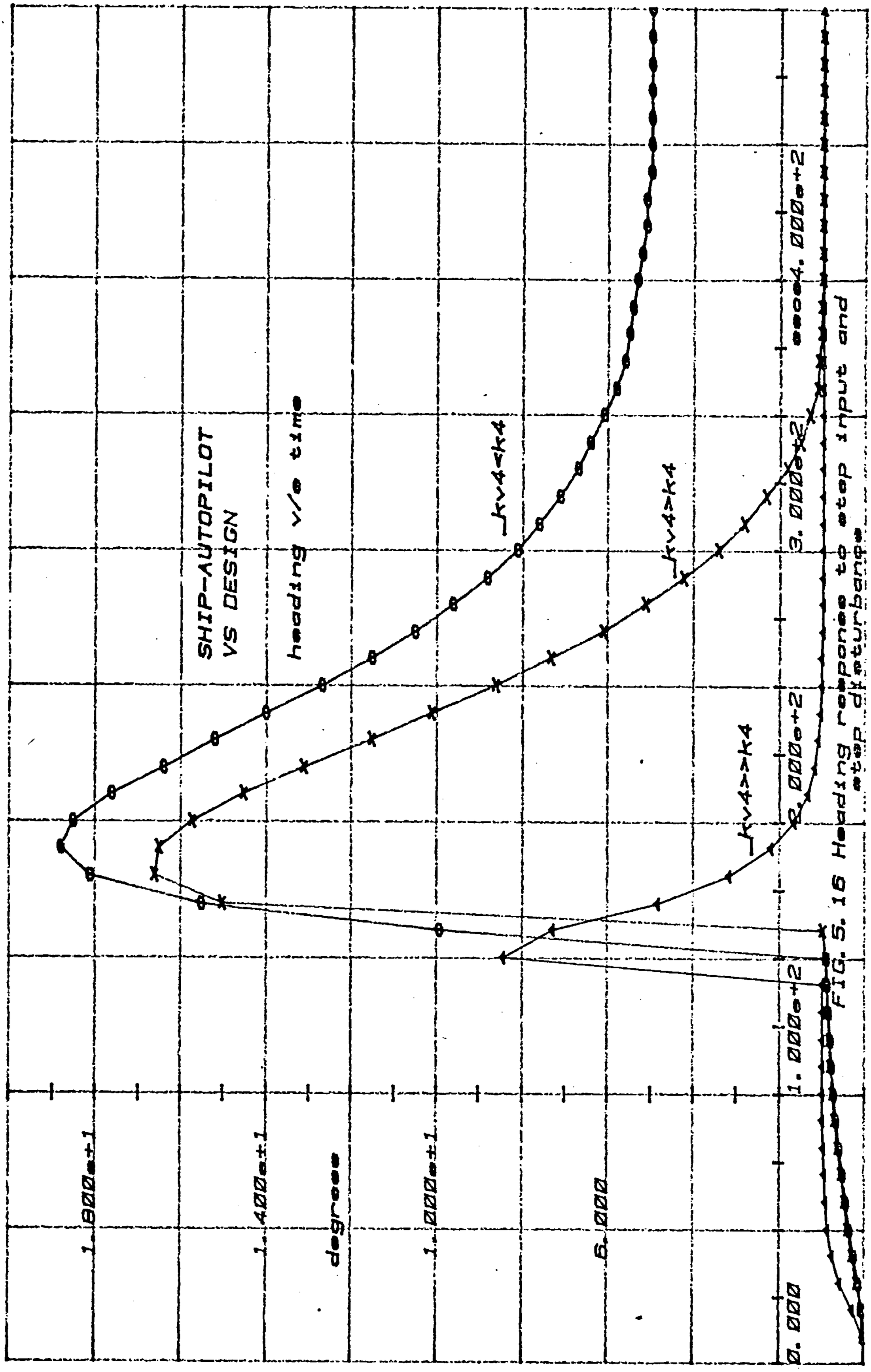

FIG. 5.16 Heading response to step input and step disturbance.

state-feedback case and the transient is over in approximately 90 seconds compared with about 200 seconds. The transient can, however, be slowed if desired by reducing the value of KV4 at the expense of a larger overshoot. Reducing KV4 below K_4 results in a steady-state error in the heading. Under this condition the system operates entirely in a linear region and is unable to enter in a sliding regime for t > 150 secs. It is worth noting that the feedback loop around the integrator can either be positive or negative depending on the sign of σ. The imposition of normal saturation limits on the rudder angle (x4) of $\pm 10^{o}$ did not affect the responses and have been omitted. The faster compensation rate of the heading error is attributed to the fact that the driving input is derived from the rudder angle and its rate of change. Deviations from the switching plane are detected by a change of sign in σ and lead to an instantaneous and significant change in the rate of change of the rudder angle. The rudder angle itself remains relatively unchanged at around an average value due to the integration. In a simulation duration of 500 seconds with an output every 10 seconds, the switching component of $\dot{x}_4$ is imperceptible in the plots and $\dot{x}_4$ appears as a constant. However, if the time scale is considerably expanded, the signal $\dot{x}_4$ is as shown in fig. (5.17). The sum $T_3\dot{x}_4 + x_4$ has the same response but is dc shifted.

Fig. (5.18) illustrates the effects of a sinusoidal disturbance in the yaw rate of the same magnitude and frequency as in section 5.3.1 on the rudder angle x_4, when applied after 150 seconds. The rudder activity is contained within $\pm 0.5^{o}$ and is approximately a 6 to 1 improvement on the state-space design,

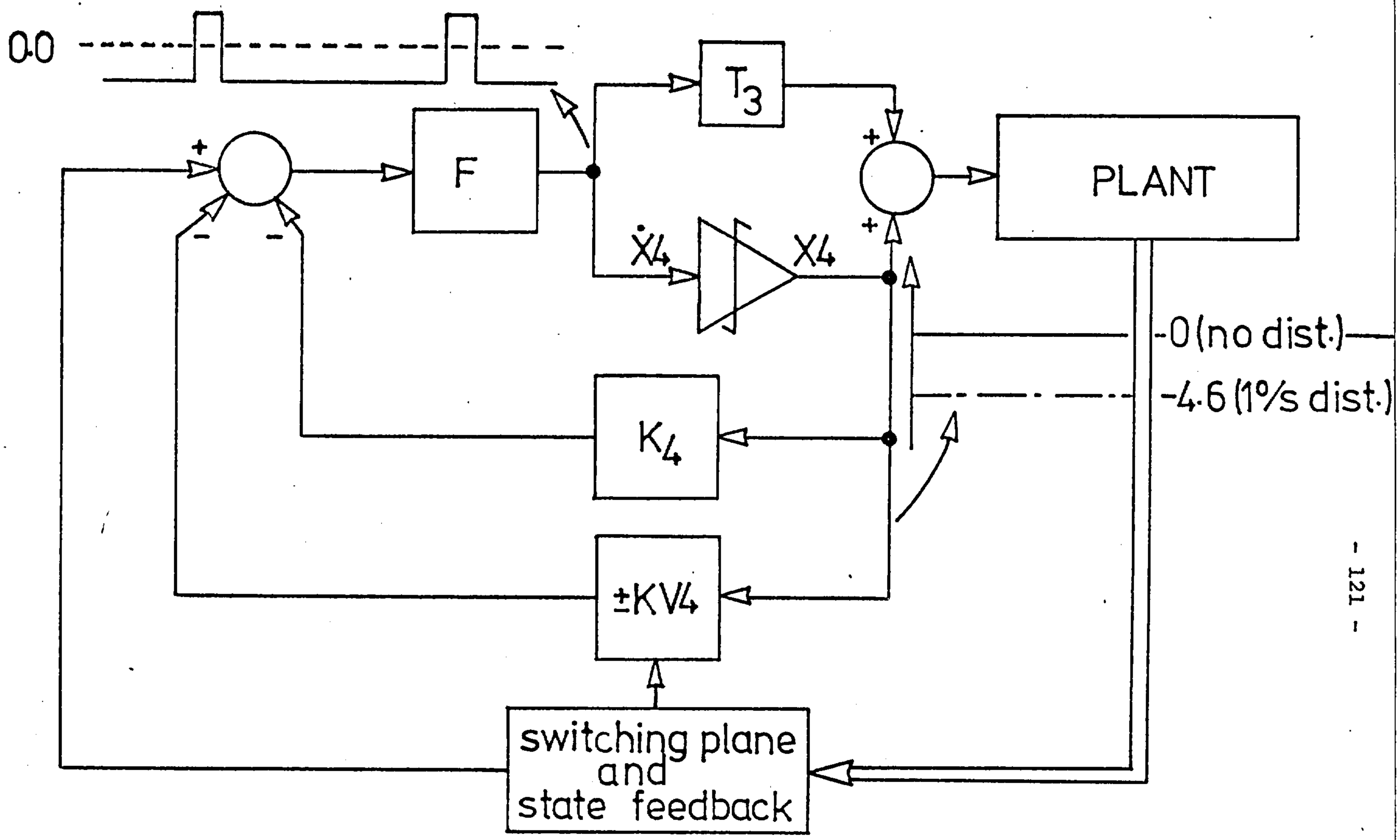

Figure 5.17 Structure of VS Autopilot

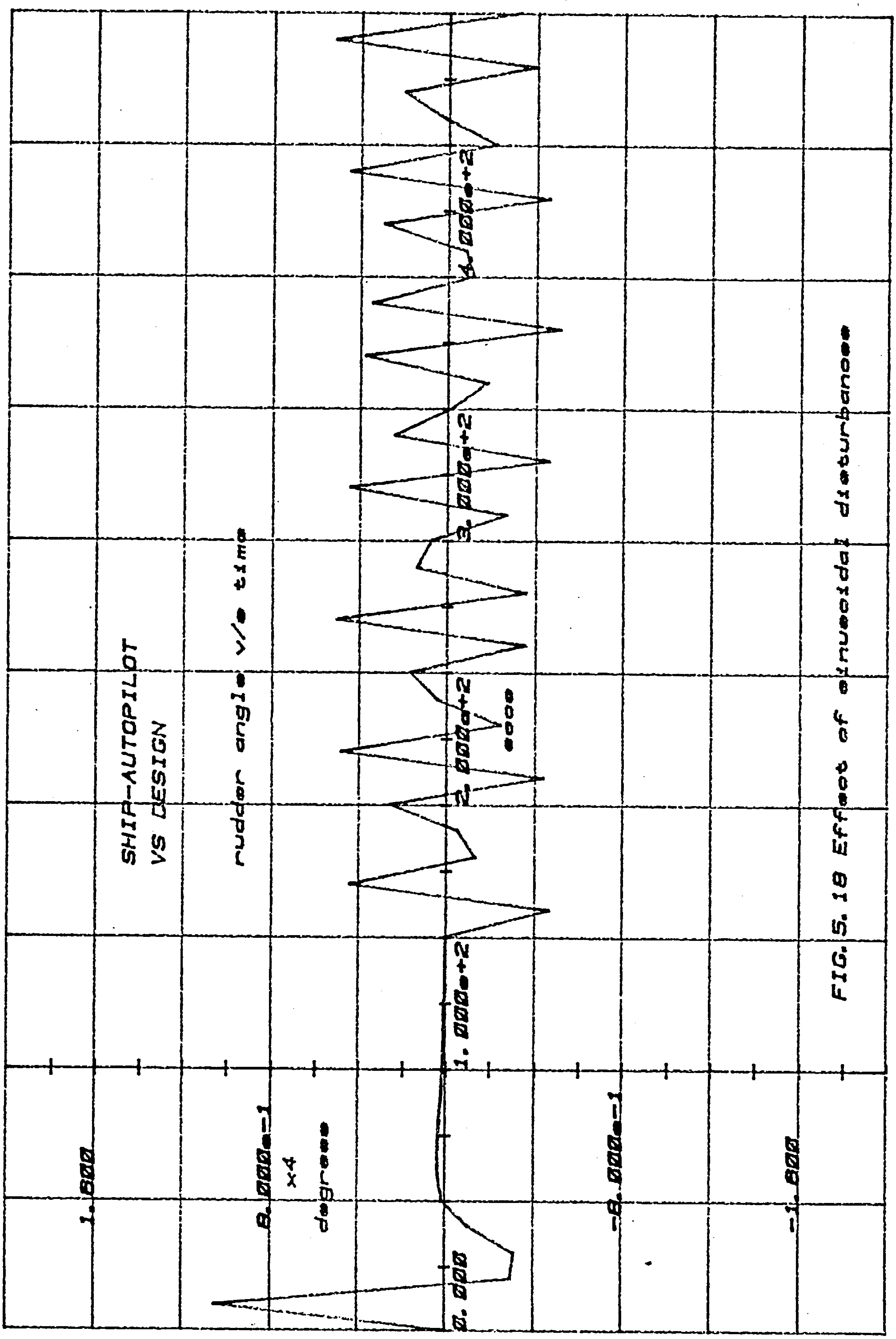

FIG. 5.18 Effect of sinusoidal disturbances

Fig.(5.10). It is difficult to analyse the effects of sinusoidal disturbances with a switching controller but the improvement has essentially been achieved by reducing the low frequency gain provided by the free steering integrator of the state-space design using a full-state feedback law.

The simulation results also indicate that the system is highly insensitive to large parameter variations and to the nonlinear effects of the steering characteristics.

5.5 General Comments

In this chapter, the designs of a state-feedback autopilot and of a VS one have been considered. In the state-feedback design, the performance was satisfactory except for the effect of the disturbances on the rudder angle. In the VS design, it was shown that a step change in the input reference or in the angular velocity due to a constant current could be compensated with zero steady-state error given that the plant is only of type one. In the design, the rate of change of the rudder angle is switched to enforce a sliding motion in a sub-space of the plant whilst the rudder angle assumes a mean level which balances the disturbance present in the yaw rate.

The main difference between the type 0 system of chapter three and the type 1 system of this chapter lies in the formation of the control law required to enforce a sliding regime. In the type 0 system, the switching of the input reference signal was essential but is not required in the type 1 loop. This situation can be explained by comparing equations (4.15) and (5.22). In (4.15), $\dot{x}_2$ is a $f(x_1,x_2,u)$ and in (5.22), $\dot{x}_3$ is a $f(x_2,x_3,x_4,u)$,

i.e. it is independent of x_1. The transformation of the state equations to the error equations involves the substitution of x_1 by $V_R - e_1$ and consequently V_R will appear in the error space equations of the type 0 system but not in those of the type 1 system. A similar observation can be made in the sliding inequalities.

A noteworthy difference exists between the two VS controllers in that integration is used in one controller but not in the other. In the ship the integrator is a mechanical one as it forms part of the steering assembly and is thus an inseparable part of the controller. It has the property of extracting and storing the necessary mean level required to balance the disturbances acting on the ship, this mean level being zero when disturbances are absent. Thus whereas the input signal is a $f(V_R, \sigma)$ in the memoryless controller, it is a $f(x_4, \sigma)$ in the VS autopilot.

The design-study of a variable structure autopilot has opened up some new possibilities in the position control of ships. It has been shown that its performance is satisfactory in the presence of parameter variations, nonlinear effects due to the steering and well-defined disturbances. Further the pulse-amplitude and pulse-width modulated nature of the input drive is compatible with the existing mechanical and electrical hardware which operate by the opening and closing of the control valves to the hydraulic system of the rudder, and does not present any great difficulty in the implementation.

Some further work is however required to meet another control objective. In the state-feedback design, a deliberate nonlinearity was introduced in the shape of saturation limits on the amplified

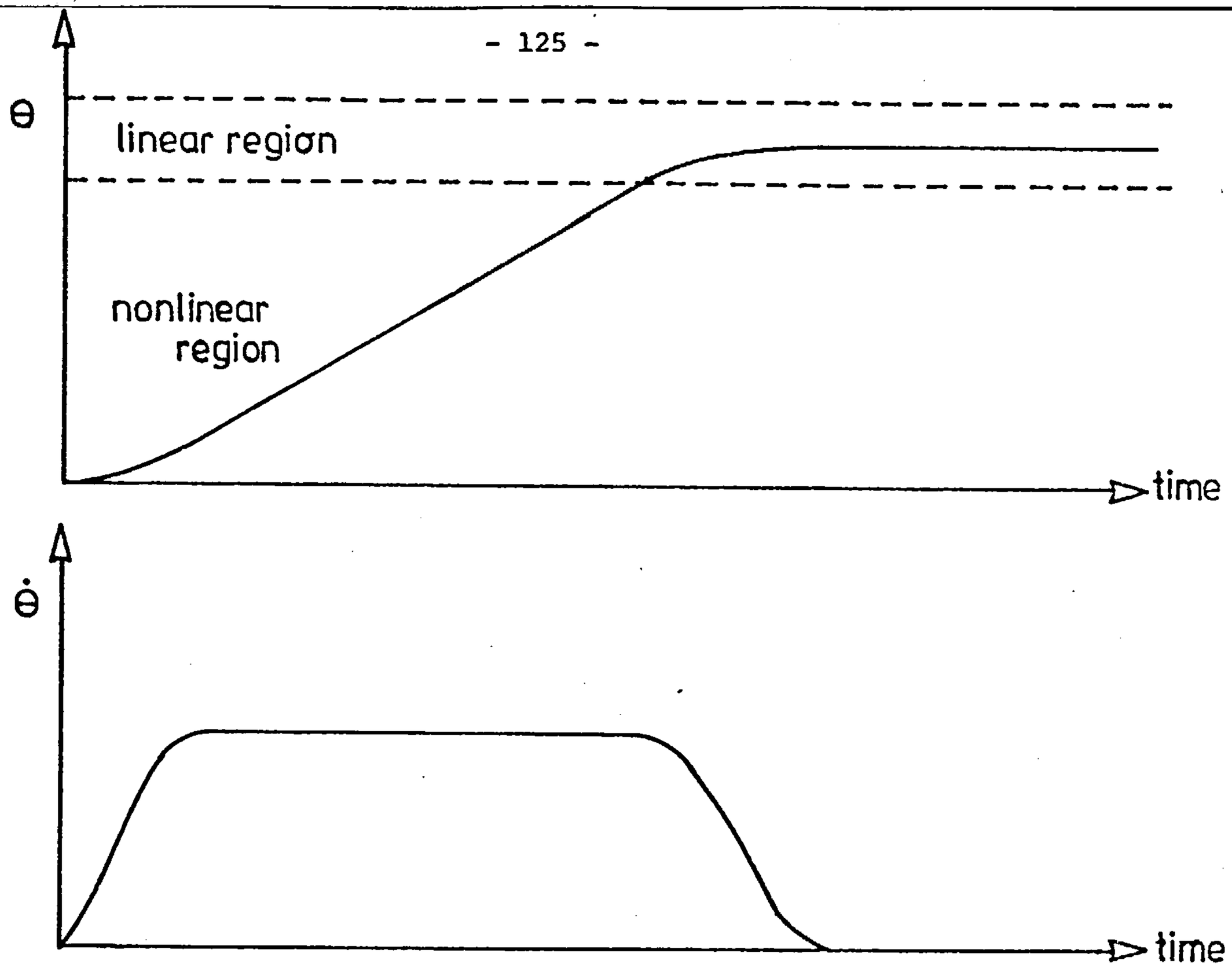

a/ Constant rate of turn

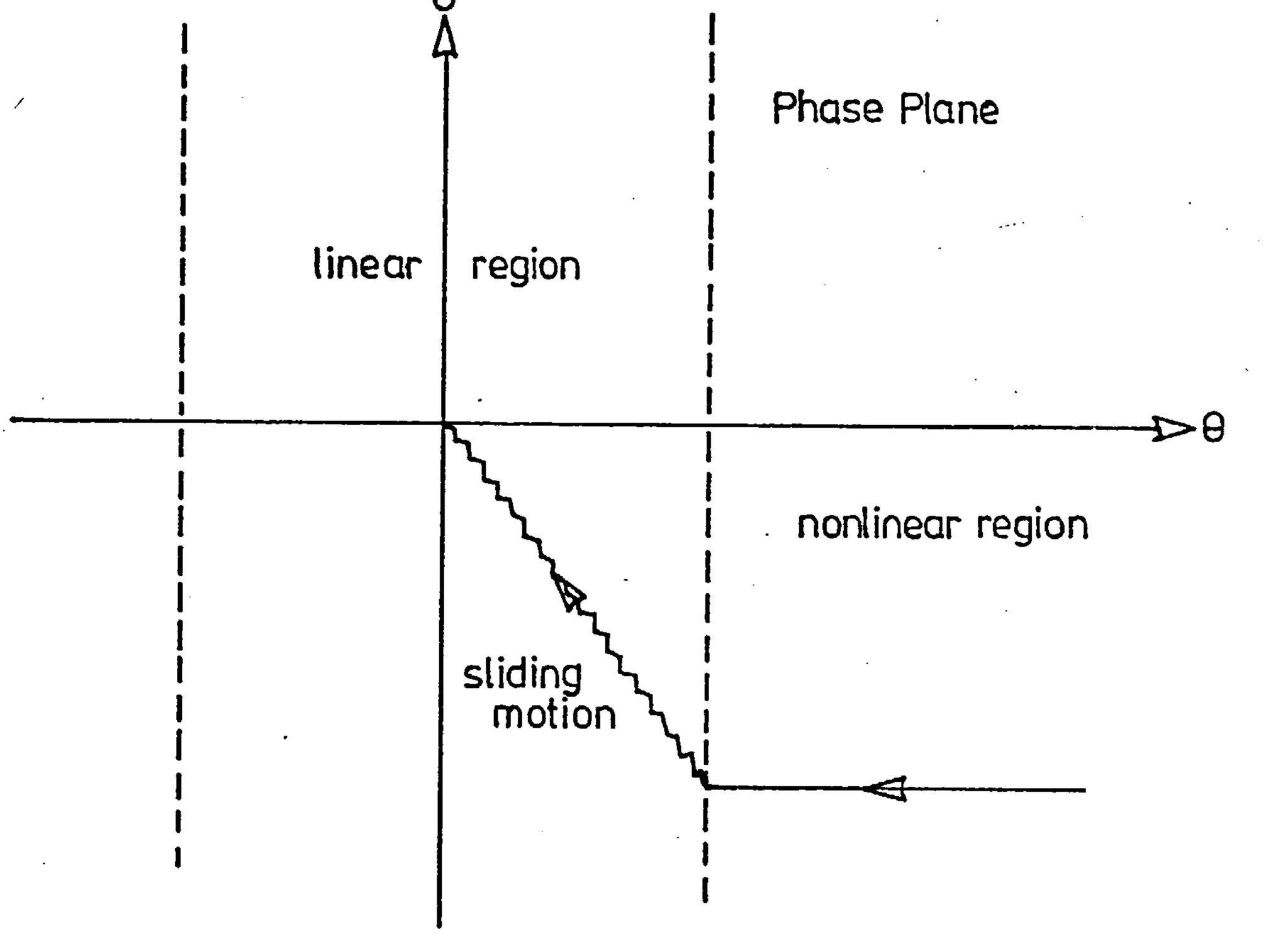

b/ Constant rate of turn and sliding motion

Figure 5.19 Control Objectives in Autopilot Design

heading error. The purpose of this nonlinearity is to produce a reference for the angular velocity control loop, fig. (5.3) such that a constant rate of turn can be achieved for large heading changes. Fig. (5.19a) illustrates the desired transient behaviour in θ and $\dot{\theta}$. The constant rate of change in θ is a desirable characteristic which should be preserved in a VS design. Fig. (5.19b) illustrates how a VSS based on a sliding regime could be combined with a nonlinearity due to saturation to meet the control objectives.

This possibility should be explored in any future design. In the following chapter, the robustness of the VS autopilot when noise is present in the measurements is assessed.

CHAPTER SIX

EFFECTS OF NOISY MEASUREMENTS ON THE VS DESIGNS

The case-studies of the two previous chapters have illustrated the application of VS theory in the control of plants with variable parameters and subject to defined external disturbances. Given that the first design step of selecting the parameters of the VS controller has been satisfactorily accomplished, it is necessary to gauge the performance of the overall system when some uncertainty is introduced in the loop. The objective of this chapter is to assess the robustness of the VS designs when this uncertainty takes the form of noise in the measurement of the plant's variables.

In the simulation studies of VSS carried out so far, the controller and plant have been assumed ideal with the measurements uncorrupted by noise. As a result, the structure of the system switched instantaneously and at the exact instant when the state crossed the switching hyperplane, at least as close as the simulation accuracy would allow. In practice, however, these assumptions can only be satisfied approximately owing to the effects of backlash, small time delays and noise. These effects can, however, be built into the simulation and the extent to which the performance of the VS controller is degraded by these factors can be assessed.

It has been suggested that for the formation of a sliding regime, it is necessary to obtain the instantaneous

values of the error and its higher derivatives. If the plant exists in phase-variable form as in the case of the ship, it is possible to measure the derivatives directly, provided that they are accessible. In other cases such as the coiler-drive system where only the output is available, a differentiator is an essential part of the VS controller. In practice, differentiation is a noisy process which is further enhanced by the presence of measurement noise.

Two techniques were investigated for reducing the effects of noise in VSS. In the first, a sliding zone is defined around the hyperplane $\sigma=0$ and is a measure of the uncertainty in the system arising from the noisy measurements. No switching takes place within that region on account of the indeterminacy in the sign of σ. In the second method, lead-lag networks are used for filtering the noise and estimating σ. Of the two, the latter is the more promising method but can lead to an error in the output.

Before presenting the results, the effects of non-ideal switching due to noise are discussed.

6.1 Quasi-Sliding Regimes

In the simulation results of the previous chapters, it was observed that the switching function σ ('sigma' in the simulations) never actually vanished. Instead the state point moved in an oscillatory fashion along the hyperplane in a non-ideal sliding regime known as a quasi-sliding regime.

The effect of noise, small delays, hysteresis etc., is similar and the system structure is switched not at the instant when the phase point crosses the hyperplane, but when it is at a distance from it. A measure of the nonlinearities within the system is obtained by introducing an error vector $\underline{\varepsilon}$ into the measurement of the state vector $\underline{x}$. The measured values are thus given by,

$$\bar{\underline{x}} = \underline{x} + \underline{\varepsilon} \tag{6.1}$$

The error is reflected in the switching function,

$$\bar{\sigma} = \underline{c}^T\bar{\underline{x}} = \sigma + \Delta\sigma = \underline{c}^T\underline{x} + \underline{c}^T\underline{\varepsilon} \tag{6.2}$$

where $\Delta\sigma$ is a measure of the error introduced in the switching function. Itkis [1.1], has given a geometrical interpretation of the effect.of the nonlinearities on the switching plane. He has shown that it is convenient to regard the real switching point as belonging to a certain nonstationary hyperplane passing through the origin and which is constrained to move in some neighbourhood of the ideal switching hyperplane. Given that $\underline{\varepsilon}$ is bounded, Itkis has shown that this sliding region is also bounded and is defined by,

$$\left.\begin{aligned} \sigma^k &= x_n + \sum_{i=1}^{n-1} m_i^k x_i = 0 \quad k = 1, \ldots, 2^{n-1} \\ \text{where} \quad & \\ m_i^k &= c_i \pm b_i \qquad \begin{matrix} i = 1, \ldots, n-1 \\ k = 1, \ldots, 2^{n-1} \end{matrix} \end{aligned}\right\} \tag{6.3}$$

and b_i is the maximum deviation in the coefficients c_i of the hyperplane due to the error $\underline{\varepsilon}$. In equation (6.3) if, for example, n = 3, then the following four hyperplanes define the sliding region,

$$\left.\begin{aligned} \sigma_1 &= (c_1 + b_1)x_1 + (c_2 + b_2)x_2 + x_3 = 0 \\ \sigma_2 &= (c_1 - b_1)x_1 + (c_2 + b_2)x_2 + x_3 = 0 \\ \sigma_3 &= (c_1 + b_1)x_1 + (c_2 - b_2)x_2 + x_3 = 0 \\ \sigma_4 &= (c_1 - b_1)x_1 + (c_2 - b_2)x_2 + x_3 = 0 \end{aligned}\right\} \tag{6.4}$$

For a second-order system, the sliding region takes the form of a sector bounded by the two straight lines $\sigma_1 = x_2 + (c_1 + b_1)x_1 = 0$ and $\sigma_2 = x_2 + (c_1 - b_1)x_1 = 0$ as shown in fig. (6.1). An undefined region also exists around the origin.

When the phase point is outside the region defined by H and Q then,

$$\text{sign } \bar{\sigma} = \text{sign } \sigma \tag{6.5}$$

and the controller correctly determines the structure of the system. But if $\underline{x} \in HUQ$, then the correct structure cannot be guaranteed.

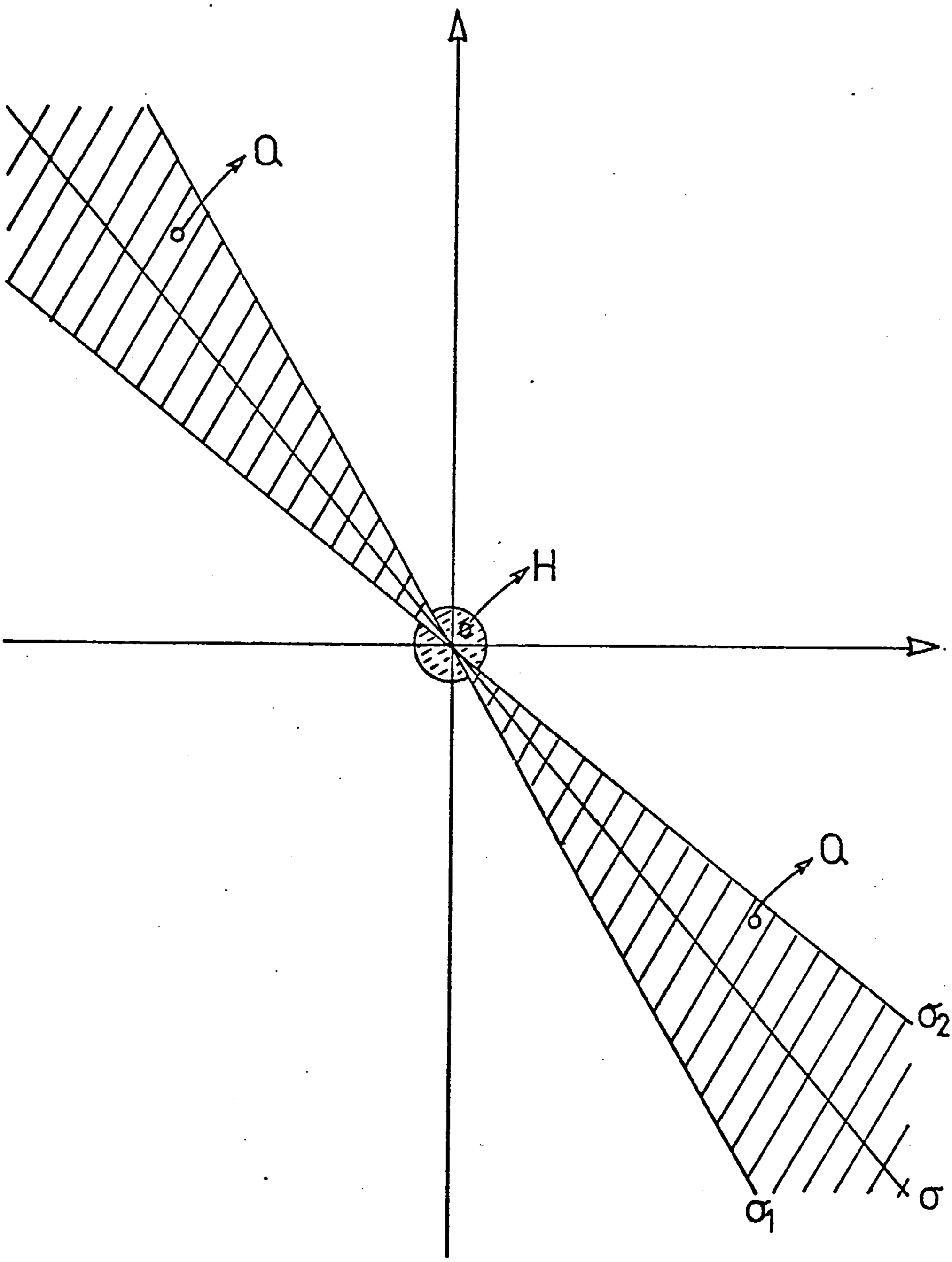

Figure 6.1 Sliding Region in VSS

Fig. (6.1) is helpful in the selection of the feedback gains. When $\underline{x} \notin$ HUQ, high values of gains in the feedback are desirable for a fast transition into the sliding region. When $\underline{x} \in$ HUQ, it is desirable to have a feedback system which is robust to noise and nonlinearities, hence the sliding equations should be synthesised on the basis that its eigenvalues are placed in positions associated with a damped transient response. This two time scale property of VSS can be exploited by separately placing the fast and slow eigenvalues through a state-feedback design. An analogy between VSS and high gain feedback systems has been drawn up recently by Kokotovic [6.1].

The definition of the H and Q regions is not an easy task from a mathematical analysis of the nonlinearities. Besides nonlinearities, errors introduced as a result of the inaccuracies and drift in the instrumentation must be taken into account, and such problems are often more formidable than the actual control one. H and Q are consequently best defined through experimentation and using the data specifications on the instrumentation.

6.2 Effect of Noise in the VS Autopilot

The effect of noisy measurements on the performance of the VS autopilot has been investigated and the results obtained are reported below.

In the ship model, noise was added to the states x_2 and x_3 (corresponding to the angular velocity and the angular acceleration respectively) which in practice are the states most likely to be influenced by noise. The noise source was provided by the function RNDGEN from the CSMP library and which represents a uniform random

number distribution between 0 and 1.0. The macro call in the program is initiated by,

$$x = (A)*RNDGEN(N)$$

where A is a scaling factor, N is a seed value.

The lack of data about the noise level in the variables prevented a true assessment of the autopilot. Instead an arbitrary level was first assigned to the angular velocity in the following manner,

$$x2 = (RNDGEN(5) - 0.5)*(0.5) + INTGRL(x20, x3) \qquad (6.7)$$

with the first term on the RHS representing a zero mean stochastic process which can assume values in the range -0.25 and 0.25. Typically x2 without noise can vary in the range of $-1.0^{o}/_{s}$ and $+1.0^{o}/_{s}$ depending on the input demand and the saturation levels imposed on the rudder angle x_4, and settles at zero in the steady state when no external disturbance is present. The state feedback and VS autopilots were both simulated under these conditions. In both instances, the transient performance of the angular position was unaffected and the results are therefore omitted. The system was further disturbed by the addition of random noise to the angular acceleration such that,

$$x3 = (RNDGEN(7) - 0.5)*(0.01) + INTGRL(x30, x3DOT) \qquad (6.8)$$

i.e. the angular acceleration is corrupted by a zero mean stochastic process with values in the range -0.05 and 0.05. Typically x3 without noise can vary in the range $-0.1^{o}/sec^{2}$ and $0.1^{o}/sec^{2}$. Again both autopilots were simulated and the only noticeable change

was a small random variation in the heading around its reference value.

The simultaneous effect of noise and of a step disturbance in the angular velocity on the heading output was then investigated. The noise sources in the velocity and acceleration were activated at t = 100 seconds and the step disturbance applied at t = 300.0 secs. Fig. (6.2) shows the heading response for different noise intensities in the angular velocity. The response up to t = 300.0 secs is relatively unchanged except for a small oscillation around the reference. However, the step disturbance in angular velocity has now introduced a steady state error in the heading, which increases with an increased noise intensity. The state-feedback autopilot on the other hand displays a random oscillation with the reference heading as mean level; this is to be expected since the noise sources are zero mean processes. The steady state error which arises in the VS autopilot is not properly understood. Recalling that the input drive can be written in the following way, (from eqns. (5.25) and (5.38)),

$$u = -k_1 e_1 - k_2 e_2 - k_3 e_3 - k_4 x_4 - KV4|x_4|\text{sign}(\sigma) \qquad (6.9)$$

where $\sigma = c_1 e_1 + c_2 e_2 + e_3$

then, since $\underline{e}$ is a zero mean stochastic vector, the probability of σ being positive or negative is equal. In the steady state $\underline{e} \to 0$, hence

$$u_{st} = -k_4 x_{4st} - KV4|x_{4st}|\text{sign}(\sigma) \qquad (6.10)$$

i.e. the 'steady state value' of u, u_{st}, is a constant level

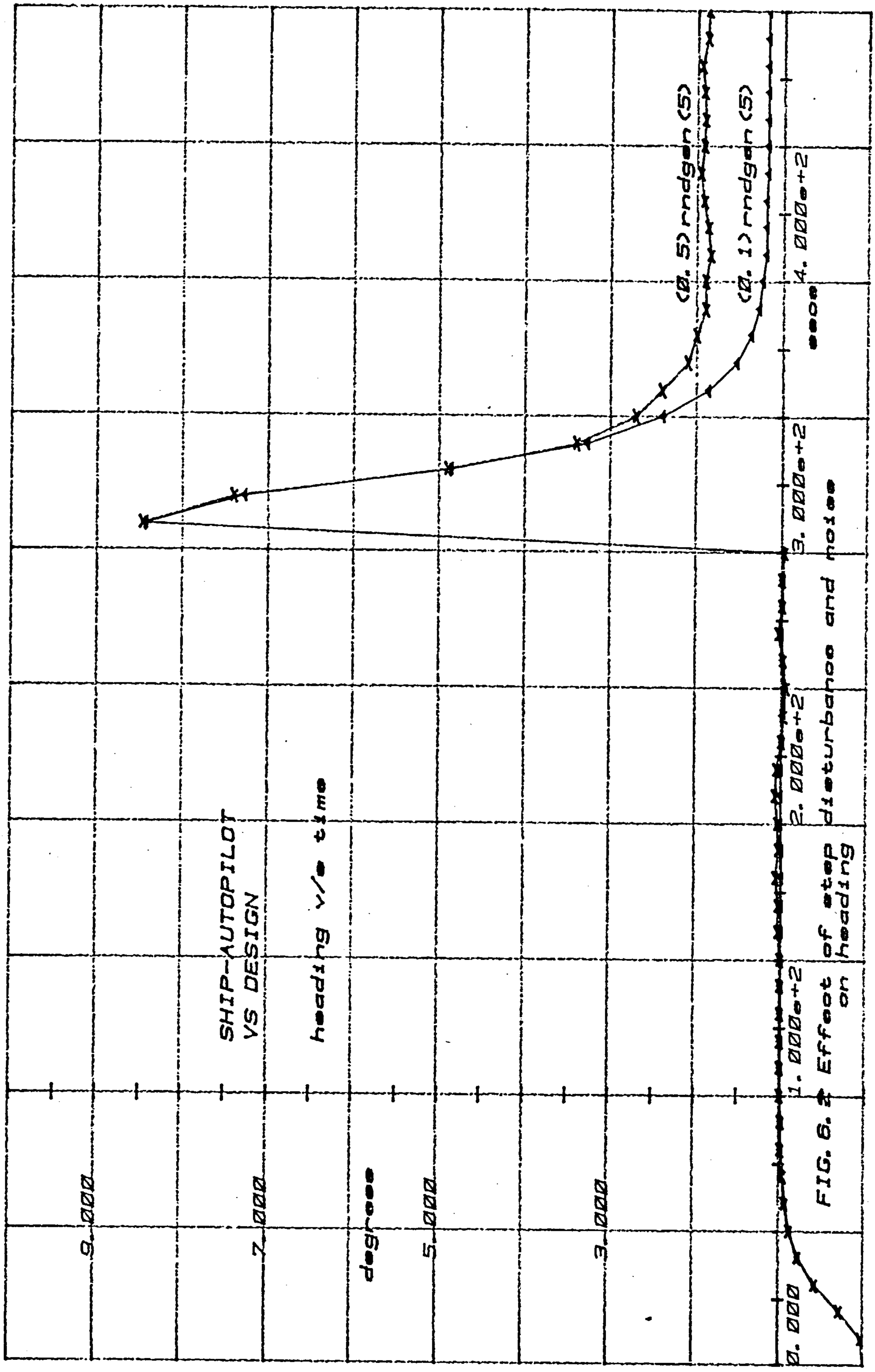
SHIP-AUTOPILOT
VS DESIGN
heading v/s time
degrees
9.000
7.000
5.000
3.000
1.000e+2
2.000e+2
3.000e+2
4.000e+2
time and noise
(a. 1) rndgen (5)
(a. 5) rndgen (5)
1. Effect of step disturbance on heading
2. Effect of step disturbance on heading
FIG. 6.

superimposed with a switching function which switches positively or negatively with equal amplitudes and with equal probability. The average value of u_{st} should therefore be the correct one to produce a zero mean variation in the heading error. The above simulation results indicate otherwise and suggest that the mean level of u_{st} drifts in the presence of noise. No clear explanation can be given for this occurence and further work is required to clarify the effects of random variations on the mean level of a switching signal.

Efforts to reduce the steady state error were made through

(i) the definition of a sliding region

(ii) the smoothing of the noisy measurements.

6.2.1 Definition of a Sliding Region

The definition of a sliding region was done by enclosing the plane $\sigma = 0$ within the planes $\sigma + \Delta\sigma = 0$ and $\sigma - \Delta\sigma = 0$. This is realised within the CSMP simulation program by the following few lines of FORTRAN,

```
NOSORT
        IF (ABS(SIGMA).LE.DELSIG) GO TO 2000
        UVSS = KV4*ABS(x4)*SIGN(1.0, SIGMA)
        GO TO 3000
2000    UVSS = 0.0
3000    CONTINUE
SORT
```

CSMP and FORTRAN statements can be mixed freely. The NOSORT section forces the execution of the program in the order that the statements are presented for every integration step. In the program, the absolute value of σ is compared to a defined value of $\Delta\sigma$ (DELSIG); if $|\sigma| \leq \Delta\sigma$, then the variable structure component of the control, UVSS, is bypassed and set to zero for that particular integration cycle. Several simulations were performed for different values of DELSIG such that

$$|\Delta\sigma| \geq c_1|\Delta e_1| + c_2|\Delta e_2| + \Delta e_3 \qquad (6.11)$$

where Δe_1, Δe_2 and Δe_3 represent the maximum noise amplitude levels. A steady state error was always present under these test conditions, and were typically of the same magnitude as in fig. (6.2). As this particular technique did not promise any improvement in the steady state performance of the VS autopilot when subjected to the combined effect of an external disturbance and measurement noise, it was not pursued further. But the experience gained has highlighted a problem in the choice of the weighting coefficients c_1, c_2 and c_3 of the hyperplane σ; the design values for c_1, c_2 and c_3 are respectively 0.0096, 0.219 and 1.0. In practice, the uncertainty in e_3 is more significant than the undertainty in e_1, hence for a reliable measure of σ the coefficients should be selected such that $c_1 > c_2 > c_3$ and not the other way. However, the choice of c_1, c_2 and c_3 is linked to the state-feedback design procedure used for placing the closed-loop poles and unfortunately no design rules exist which allow the pole positions to be related to the coefficients. The design procedure becomes an iterative one at this stage where values of c_1, c_2 and c_3 are computed for different pole locations until an acceptable solution is reached.

6.2.2 Smoothing of Noisy States

The second method investigated for reducing the steady state error was through the smoothing of the measured variables. First order lags of the form $1/(s\tau + 1)$ were used as the smoothing networks with the measured states as inputs. The filtered outputs were then fed to the controller. Using this technique, the steady state error was reduced to a fraction of a degree, with noise sources in the angular velocity and angular acceleration. With τ set to 0.5 seconds for all three channels, the heading error was contained within a fraction of the reference. The error could be increased by either reducing the smoothing or increasing the noise intensity. Figs. (6.3) and (6.4) illustrate the responses under these test conditions. Clearly before a final choice can be made for the values of τ, some more field information concerning the noise is required.

6.3 Effect of Noise in the VS Coiler-drive System

The assessment of the noise performance of the variable structure coiler-drive system is an interesting and informative study as the system possesses characteristics which are not strictly compatible with a good noise performance. Firstly, in the VS control of the system, it was necessary to obtain the derivative of the output error; differentiation is basically a noisy process which is worsened by any additive noise present in the input signal. Secondly, a switching plane based on e_1 and e_2 is synthesised and is used in deciding whether a large signal $\psi_r V_R$ is to be added to the input drive or not, to enforce a sliding motion. Thus the uncertainty within the loop.is enchanced

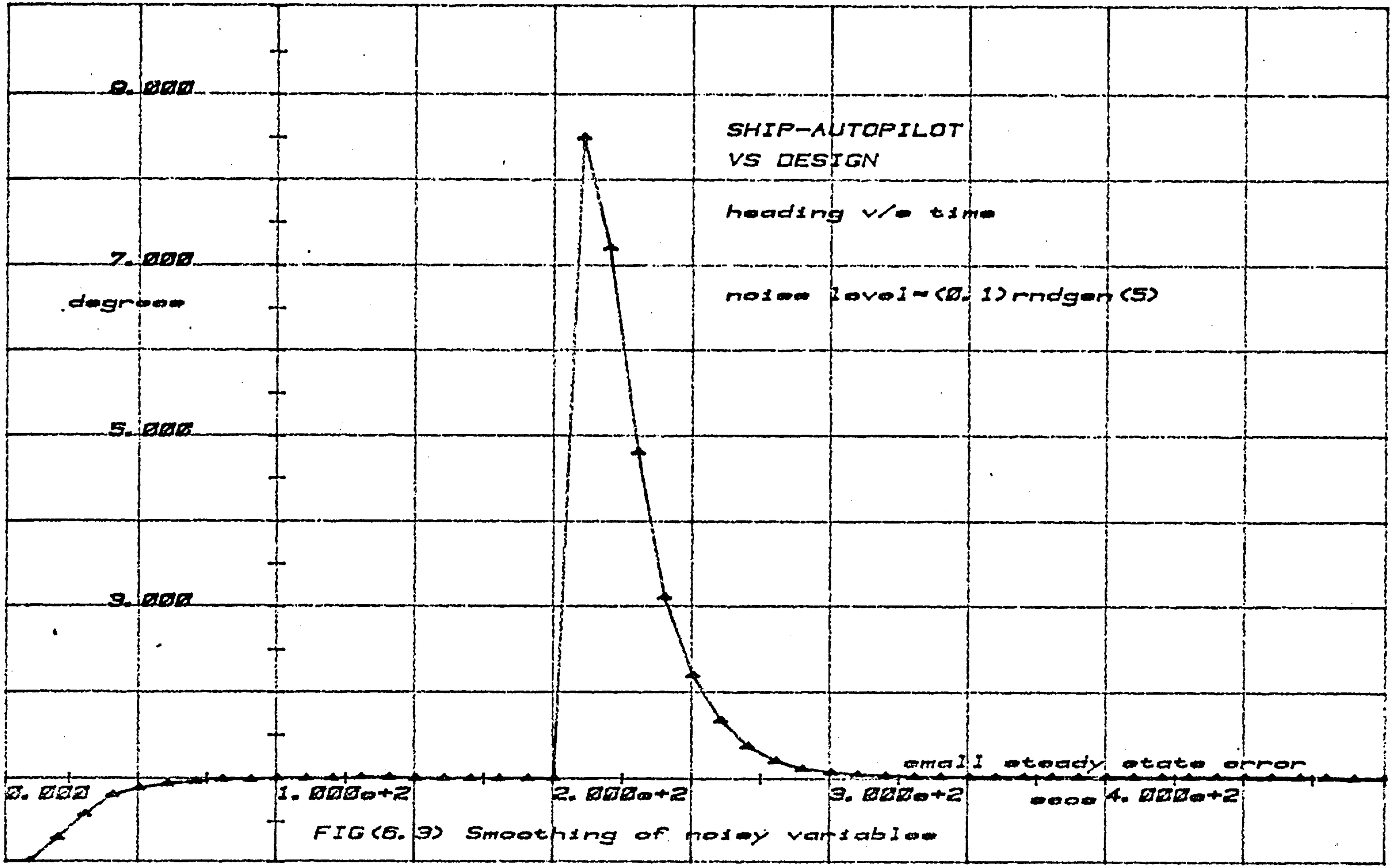

FIG(6.3) Smoothing of noisy variables

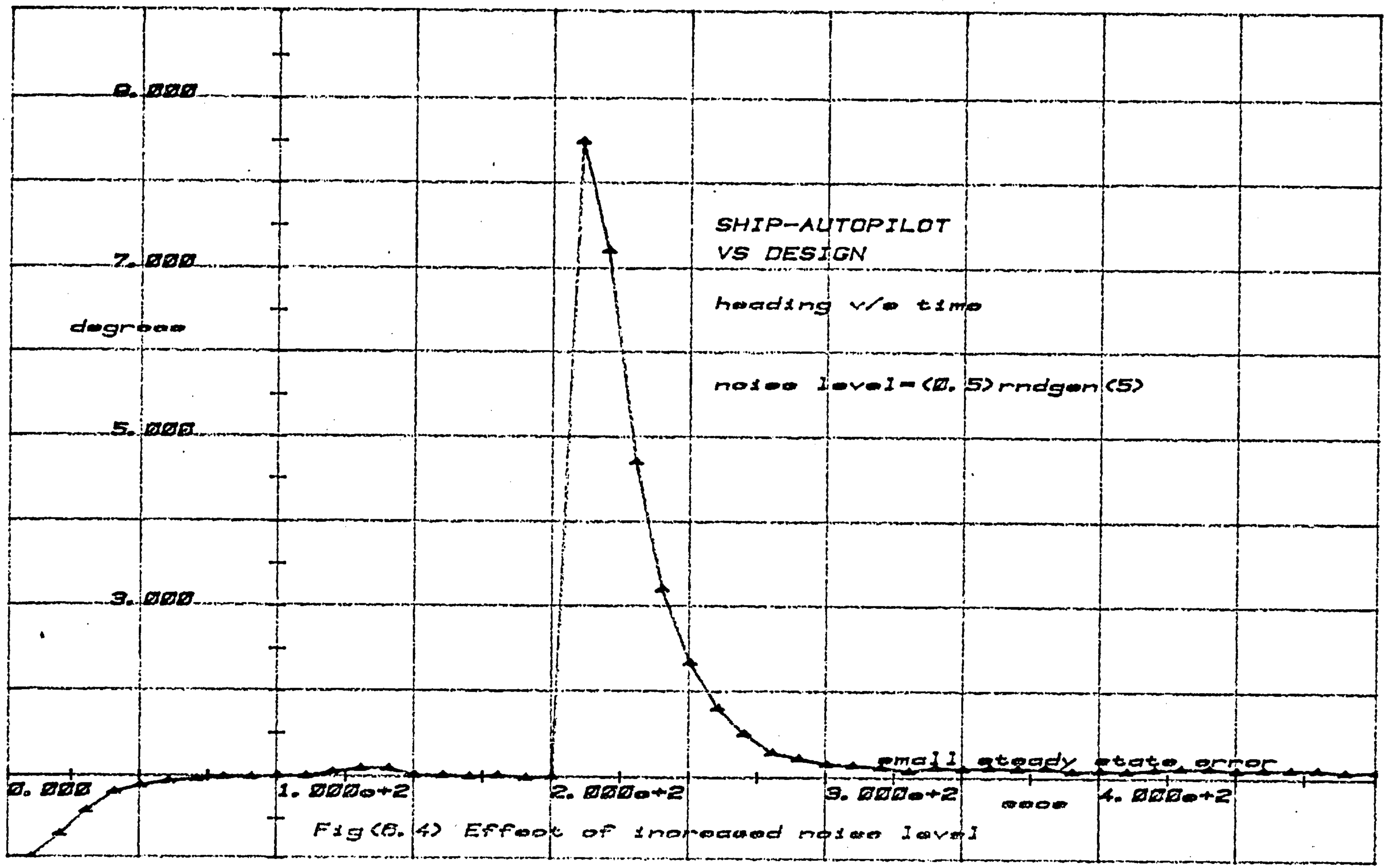

Fig(6.4) Effect of increased noise level

and the performance of the overall system could become unpredictable.

Fig. (6.5) shows the effects of noise on the output velocity for different noise levels. A noise source was added to the radius variable (referred to as TOTRAD in fig.(4.5)) which bears a direct influence on the output velocity. The noise level was assigned an arbitrary value and could assume random values between (i) ± 0.01 m and (ii) ± 0.05 m. Initially when the radius is small (0.075 m), the signal to noise ratio is poor but improves as it increases to its final value of 0.575 m. With a noise level defined by (0.01)rndgen(5), some degree of stability is preserved but the output cannot be maintained at the desired level. Increasing the noise level to (0.05)rndgen(5) produced a steady upward drift in the velocity. In both instances the performance did not improve with the increase in radius.

Intuitively, the performance should improve either by reducing the amplitude of the input reference V_R and/or obtaining a more reliable estimate of σ. As discussed previously, switching V_R is an essential component of the control law and cannot be avoided without resorting to an adaptive system. The alternative therefore rests in methods of estimating the derivatives in a more reliable way; two methods were investigated (i) the use of Luenberger observers and (ii) Lead-lag networks.

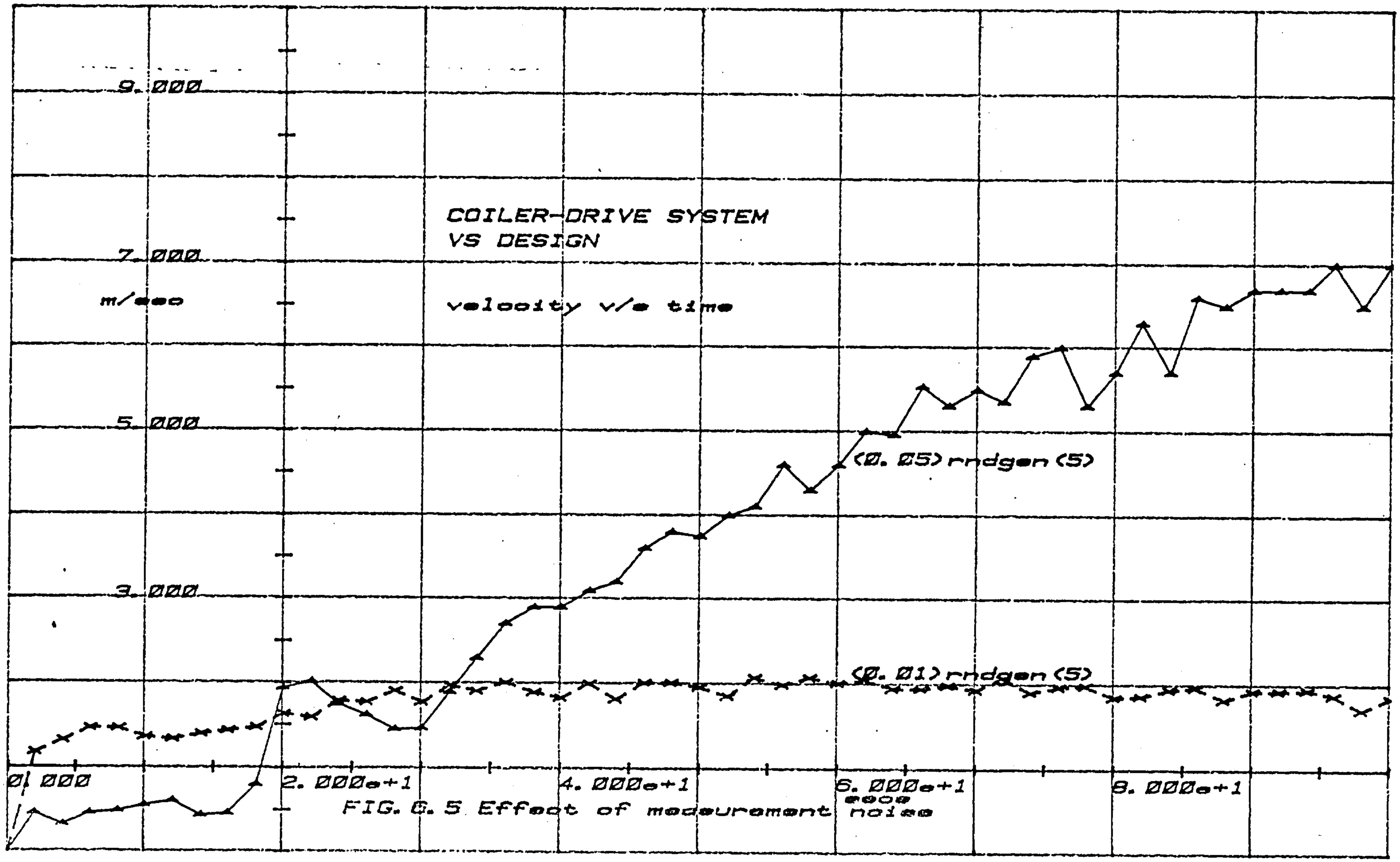

FIG. 6.5 Effect of measurement noise

6.3.1 Luenberger Observers [6.2, 6.3]

Luenberger has shown that it is possible to estimate the state of a linear time-invariant plant by constructing a model of the given plant and driving it, with the same input as the real plant and the observation error, i.e. the error between the true output and the estimated output. Such a system is referred to as a Luenberger observer. The possibility of utilising Luenberger observers in a VS context has been investigated.

Given that a single-input single-output plant is described by the following set of differential equations,

$$\left.\begin{aligned} \dot{\underline{x}}(t) &= \underline{A}\,\underline{x}(t) + \underline{b}\,u(t) \\ y(t) &= \underline{c}^T\,\underline{x}(t) \end{aligned}\right\} \qquad (6.12)$$

Then an estimate of the state $\underline{x}$ (denoted by $\hat{\underline{x}}$) can be obtained using the following observer,

$$\dot{\hat{\underline{x}}}(t) = \underline{A}\,\hat{\underline{x}}(t) + \underline{b}\,u(t) + \underline{k}[y(t) - \underline{c}^T\,\underline{x}(t)]$$

which simplifies to,

$$\dot{\hat{\underline{x}}}(t) = [\underline{A} - \underline{k}\underline{c}^T]\hat{\underline{x}}(t) + \underline{b}\,u(t) + \underline{k}\,y(t) \qquad (6.13)$$

The last equation indicates that the stability of the observer is determined by the matrix $[\underline{A} - \underline{k}\underline{c}^T]$ and whose characteristic values are referred to as the observer poles. In addition, the reconstruction error defined by,

$$\underline{e}(t) = \underline{x}(t) - \hat{\underline{x}}(t)$$

has the property that,

$$\lim_{t\to\infty} \underline{e}(t) = 0$$

for all $\underline{e}(t_o)$, if and only if the observer is asymptotically stable. In selecting the observer gain vector $\underline{k}$, it is desirable that the dynamics of the observer be faster than the system it observes but not so fast as to possess the undesirable characteristics of differentiators (which correspond to poles at $S=-\infty$).

The interesting feature of observers from a VSS viewpoint is that the observer dynamics can be represented in a canonical form. Thus if a phase-variable form is used, then the output and its n derivatives are available to the VS controller. Several experiments were conducted in state estimation based on Luenberger observers using an analogue computer to represent low order models and a microcomputer as a controller and/or estimator; further details of the hybrid computer system are included in a later chapter. The experience acquired using that form of computation indicates that the states of a linear plant can be readily estimated in a phase-variable form and fed into a linear controller such as a PID one whilst maintaining closed-loop stability. The parameters of the plant can also be varied over a defined and significant range, with the output of the plant being tracked with almost zero steady state error. Stability problems were however encountered when the loop was closed with a VS controller which made use of an estimate of $\underline{e}$. The reason for the instabilities was thought to be due to the fact that in the plant-observer-VS controller configuration, the input is constantly switching, hence the observer estimates are unable to catch up with the true states and a large uncertainty develops in the observed estimates.

A similar approach is discussed in [6.4] based on a Kalman filter but it is felt that a great deal of further work is required in that area before realising such a scheme.

6.3.2 Lead-Lag Networks

The other alternative for the estimation of the derivatives is to approximate the differentiation process by a lead-lag network. The method has already been advocated in VS literature [6.5, 6.6] and is applied here to the coiler-drive system. The lead-lag network approximates the switching function $\sigma = c_1 e_1 + e_2$ by $\hat{\sigma}$ where

$$\hat{\sigma}(s) = \frac{(s + c_1)}{s\tau + 1} e_1(s) \qquad (6.14)$$

and τ is the time-constant of the filter. When $\tau=0$, the above filter is reduced to a pure differentiator. A similar filtering process can be applied to an nth order system where $\sigma = \sum_{i=1}^{n} c_i x_i$. In this case σ can be approximated by a filter with transfer function,

$$\hat{\sigma}(s) = \frac{\sum_{i=1}^{n} c_i s^{i-1}}{\prod_{i=1}^{n-1} (\tau_i s+1)} \qquad (6.15)$$

6.3.3 VS Coiler-Drive System with Lead-Lag Network

Using the technique suggested above, the performance of the VS coiler-drive system was assessed when a lead-lag network was used to estimate σ. Several forms can be used to realise equation (6.14); the chosen one for the coiler-drive example is shown in fig. (6.6). It can be easily verified that $\hat{\sigma}(s)$ is given by,

$$\hat{\sigma}(s) = \frac{s + c_1}{s\tau + 1} e_1(s) \qquad (6.16)$$

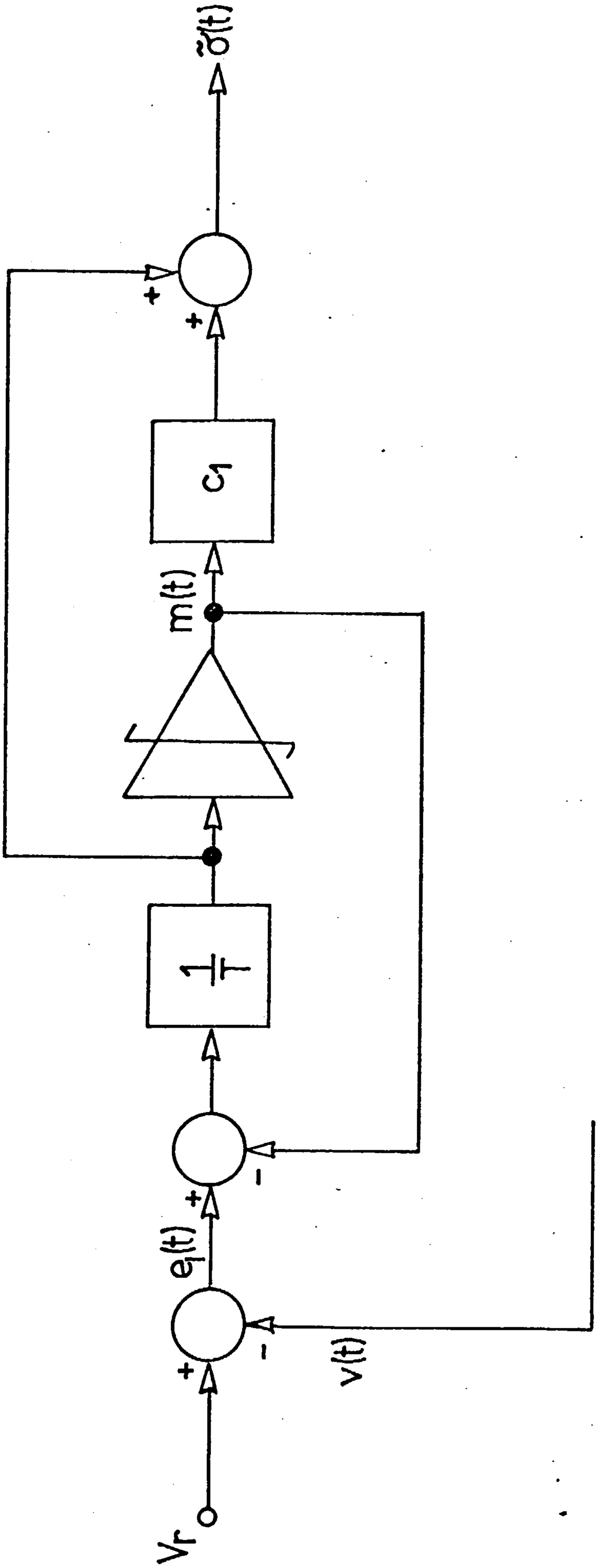

Figure 6.6 Approximation of Switching Function

The value of c_1 was left unchanged at 40.0; the time constant τ of the filter was selected somewhat arbitrarily as a multiple of the integration step size. With an integration step size of 0.001, τ was set at 0.02 and 0.04. In the absence of noise, the response of the velocity output is shown in fig. (6.7). With τ = 0.02, the velocity transient is unaffected, but with τ = 0.04 the transient is very oscillatory initially and settles down subsequently. This is due to the fact that the time constant of the filter is becoming comparable to the time constants of the motor and cannot be ignored in the design.

Fig. (6.8) shows the velocity response for two different noise levels present in the radius and with τ = 0.01. The random variations are due to the noise source near the output. As the noise level increases, the mean level of the output drifts upwards. Comparing figs. (6.5) and (6.8), it can be seen that the response is improved by the lead-lag network and that the output is bounded for a higher noise level.

The drift in the output from its reference value can only be attributed to the uncertainty in σ combined with the switching of a large input drive. The results again indicate that information concerning the noise levels is a necessary specification in order to determine whether a lead-lag network is needed and if so, whether it is able to smooth the noisy signals enough to hold the output within an acceptable error margin.

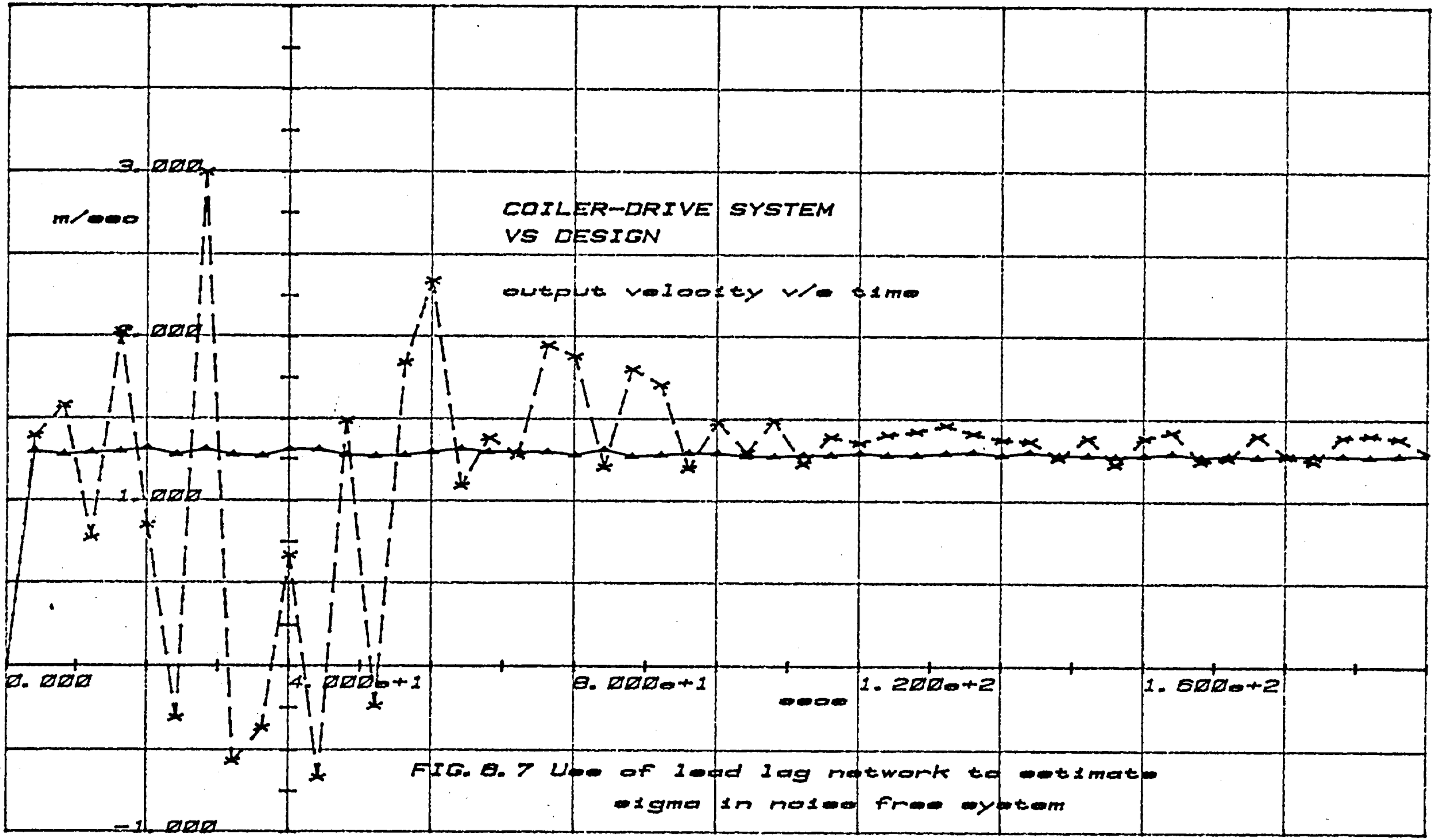

FIG. 8.7 Use of lead lag network to estimate sigma in noise free system

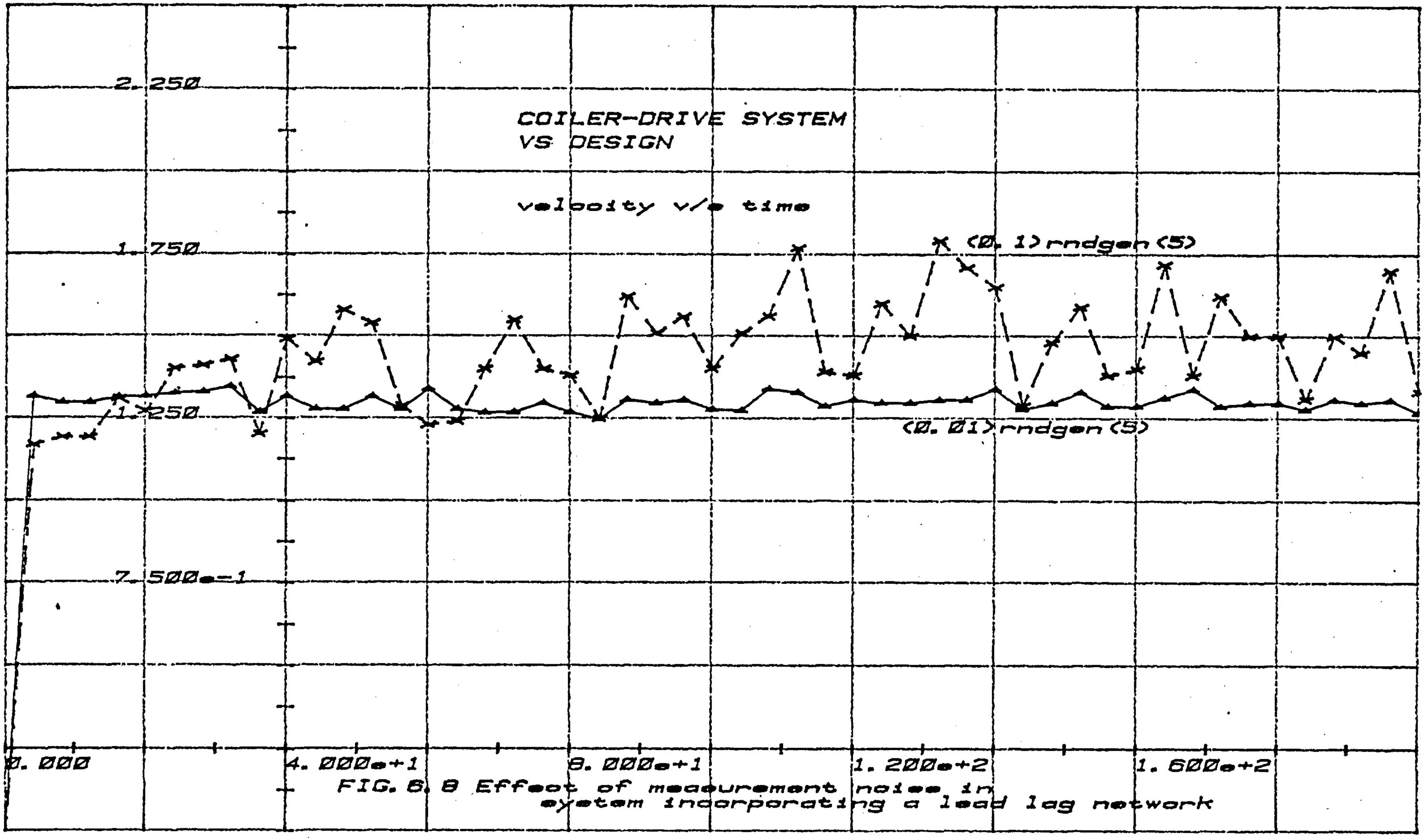

FIG. 6. 8 Effect of measurement noise in system incorporating a lead lag network

6.4 General Comments

This chapter has concentrated on the performance of the VS designs when noisy measurements were fed to the controller.

In both examples, smoothing is the most effective way of improving the performance but a steady state error is possible. In the case of the VS autopilot, the noise had little influence on the output when the switched variable x_4 assumed a zero steady state value. With an external disturbance on the angular velocity, x_4 is non-zero in the steady-state and leads to a small and variable output error when switched randomly. A similar observation was made in the coiler-drive system where the input reference V_R is constantly switched.

To summarise, the drift in the output appear to be caused by:

(i) uncertainty in σ and usage of σ in deciding to switch a constant level positively or negatively, and

(ii) high noise levels or insufficient smoothing.

The general comment is that the benefits gained by adopting a variable structure approach are partly offset by a reduced but acceptable performance compared to a linear controller under noisy conditions, and that further work is required to clarify the effects of random switching of the input drive in VSS.

CHAPTER SEVEN

IMPLEMENTATION AND APPLICATION OF VSS

In this chapter, experimental work in VSS using hybrid computation is reported. The plant is simulated on an analogue computer while the controller program is resident within the memory of a microcomputer system. This form of laboratory experiment was chosen because the analogue computer with its inherent problems of drift, noise and subjection to external disturbances is a good approximation to real life plants and gives a better feel for practical systems than the exact digital simulation. It is shown that under these test conditions, the VSS is able to cope with different inputs, a variety of disturbances, and an unstable plant.

The computer system is first described; the design and implementation of a VS controller for a third order plant is outlined and the results are presented.

7.1 The Real Time Computer Implementation System

A real time microcomputer implementation system has been developed at Heriot-Watt University by J.T. Herd [7.1] and J. McKie. The facility allows the user to specify the control algorithm in a high level language on a host machine. An interactive utility program is then used to provide a simple method for creating and building load modules suitable for real time execution on the microcomputer.

The hardware facility consists of a DEC PDP-11/45 mini-computer with a medium speed serial data link to a DEC LSI-11 micro-computer. The PDP-11 series of computer provides a good basis for this work due to the good instruction set, comprehensive group of addressing modes and easy interfacing. Program preparation is accomplished on the multi-user PDP 11/45 with 144 k bytes of main

memory, 86 M bytes of on-line storage and six terminals. The PDP 11/45 computer runs under the 'UNIX' operating system developed by Bell Telephone Company [7.2] in the USA which uses the high level language 'C' [7.3]. The operating system provides excellent editing and program preparation facilities which allow quick and easy software implementation of the control algorithm.

Once the 'C' program is written, it is then used in conjunction with an interactive utility program to produce efficient machine code which runs in real time on the LSI-11 computer. The code is transferred to the LSI-11 via a medium speed serial data link. The real time software is run on the LSI-11 computer system which contains 16 K bytes of main memory, a teletype, 16 analogue-to-digital channels and 2 digital-to-analogue channels. The LSI-11 micro-computer, although small, executes the instruction set of the PDP 11/40 computer including integer multiply/divide and floating point add/subtract/multiply and divide. It is interesting to note that for large programs, 'C' generated code is better than that produced by an average assembly language program [7.4].

As part of the control system design facility established within the Department of Electrical Engineering, Heriot-Watt University, two suites of control system design programs have been implemented on the PDP 11/45 computer. These are:

(i) The MELSA C.A.D. suite and, [7.5]

(ii) The UMIST C.A.D. suite [7.6]

Both suites are written in Fortran. The Melsa suite is designed for batch operation, using punch card input, whereas the UMIST suite is intended for interactive use with graphics facilities.

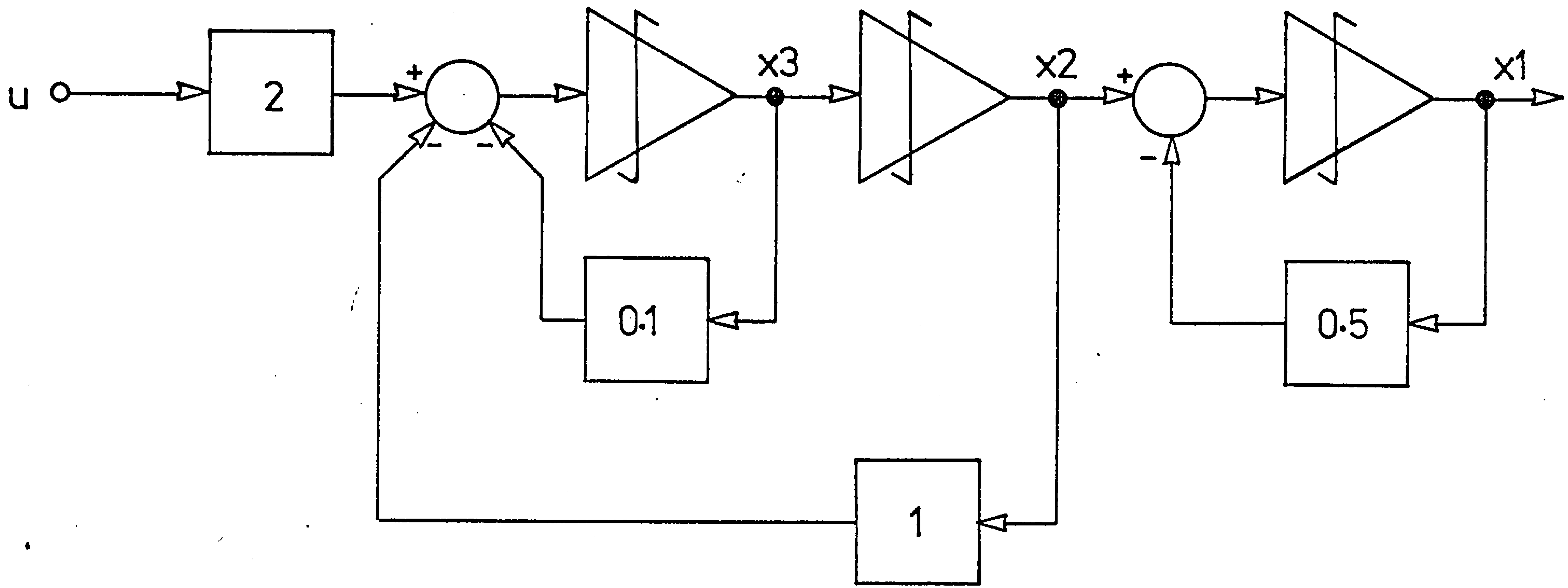

Figure 7.1 Third Order Example

Both suites have been amended to run on the PDP 11/45 in a pseudo interactive mode.

The Melsa programs are concerned basically with the design of single-input single-output systems and includes classical transfer function techniques, e.g. frequency response, root-locus, etc. as well as modern state-space techniques e.g. Kalman Filter, Luenberger Observer, etc. A complete list of the programs and a list of the coding are given in [7.5].

The UMIST package is oriented towards multivariable systems and contains the recently developed Characteristic Locus and Inverse Nyquist Array. It also has a useful data conversion program which can convert a state-space description to a transfer function representation and conversely can produce a minimal state space realisation from a given transfer function.

Extensive use was made of the Melsa package throughout this thesis as the systems studied were in state-space form with controller designs based on state-feedback principles.

7.2 Third Order Example

The CSMP simulations have shown that in synthesising VSS controllers, the full state vector must be available for a reliable design. Hence it will be assumed here that $\underline{x}$ can be measured. The plant under consideration is described by the following set of differential equations,

$$\dot{\underline{x}} = \begin{bmatrix} -0.5 & 1.0 & 0.0 \\ 0.0 & 0.0 & 1.0 \\ 0.0 & -1.0 & -0.1 \end{bmatrix} \underline{x} + \begin{bmatrix} 0.0 \\ 0.0 \\ 2.0 \end{bmatrix} u \qquad (7.1)$$

The control problem is to design a controller which will force the output x_1 to track a reference step with zero steady state error.

Assuming that the plant is time-invariant, the open-loop poles can be shown to be located at

$$s = -0.5,\ -0.05 + j\ 1.0,\ -0.05 - j\ 1.0 \qquad (7.2)$$

The complex pair is highly underdamped and gives rise to an oscillatory open-loop response with a large steady state error. Output feedback is not an appropriate solution in this case; a root locus plot reveals that closing the loop around the output alone has a de-stabilising effect as a result of the real pole moving right whilst the complex pair moves left; reversal of the feedback sign has a similar de-stabilising effect with the complex pair moving closer to the RHP.

A good control solution for the example is obtained using the full state vector in a state feedback design. Using the theory of Appendix C, a set of feedback gains can be selected such that zero steady state error is obtained. However, any parameter variation will influence this condition.

A more robust solution is reached by including an integrator in the controller as shown in fig. (7.2), zero steady state error can now be maintained for a wider range of plant parameter variations. This controller configuration is a well-used one in practice and is discussed by P.C. Young and J.C. Willems in [3.11].

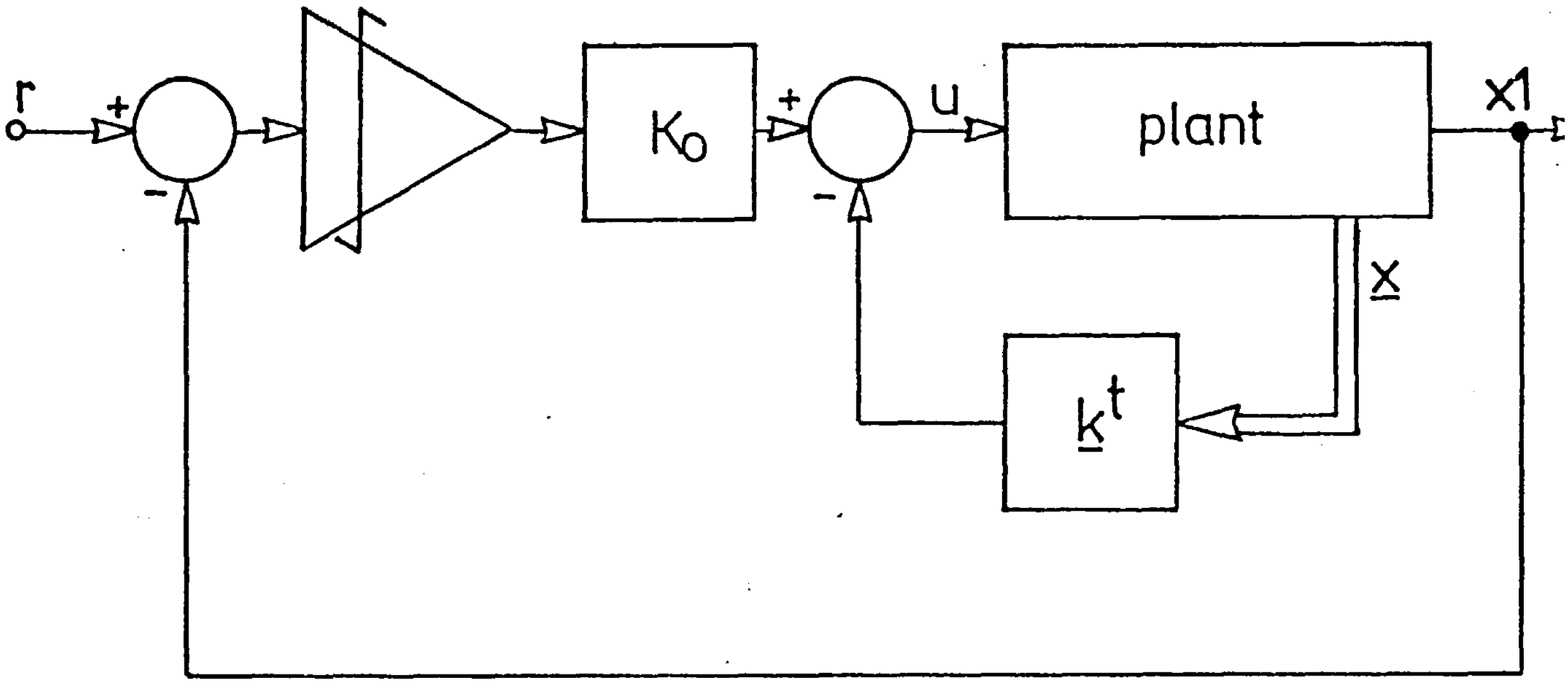

Figure 7.2 A Single-Input Type One Servomechanism

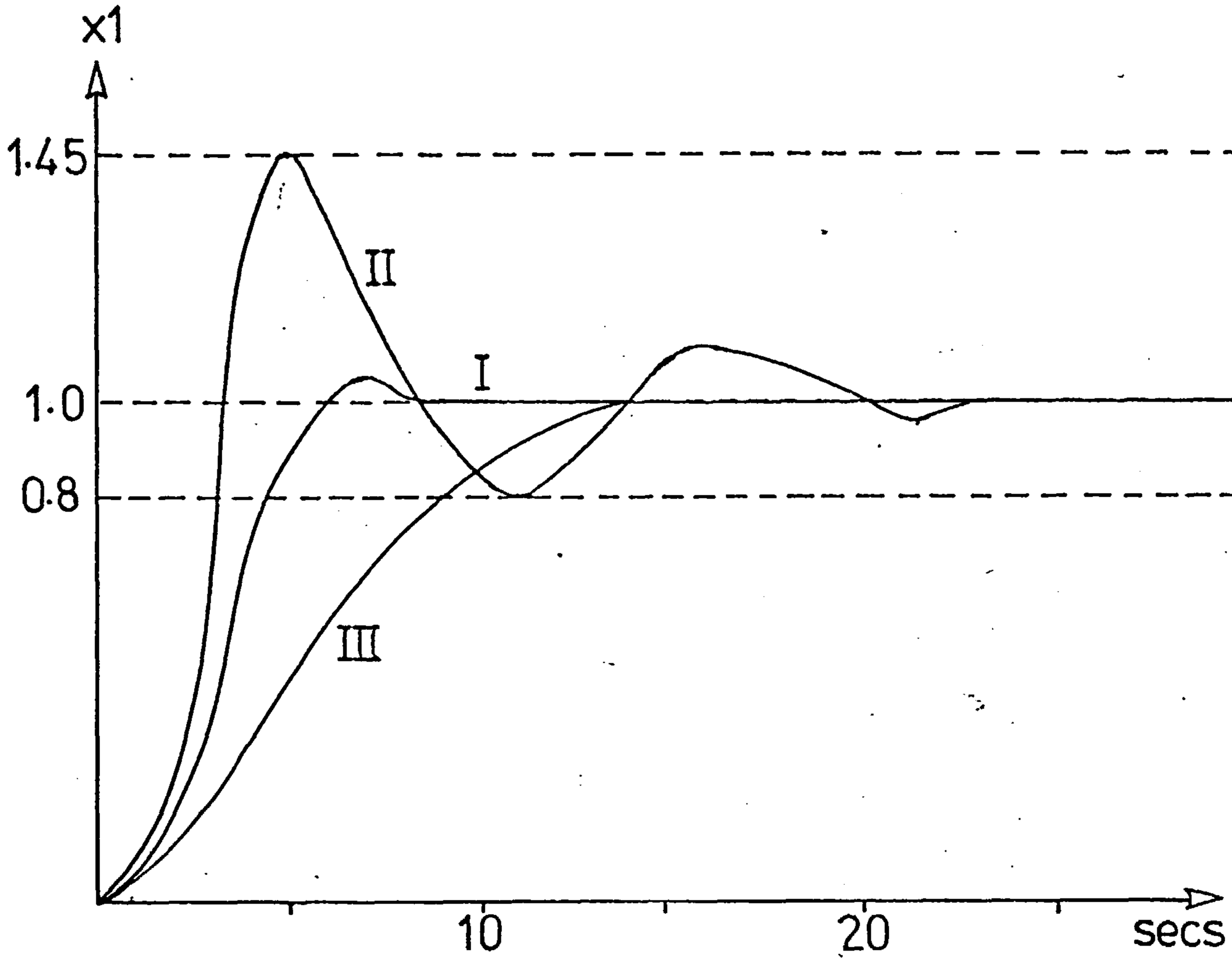

Figure 7.3 Transient Response to a Step Input

For the system of fig. (7.2), the following values of gains

$$k_o = 3.0 \qquad \underline{k}^T = [3.8125 \quad 7.373 \quad 3.7] \tag{7.3}$$

assign the closed-loop poles at,

$$s = -3.0,\ -4.0,\ -0.5 + j0.5,\ -0.5 - j0.5 \tag{7.4}$$

Fig. (9.3) shows the transient response of the closed-loop system to a step input. Graph I is the nominal response, graph II corresponds to the case when the leading parameter ['0.5' in fig. (7.1)] is set to zero. The controller is unchanged and the response is now oscillatory. Graph III represents the response with the same parameter set to one and can be observed to be sluggish. Further, the system can only tolerate a small negative excursion of the leading parameter before the onset of instability. Stability could of course be restored by moving the closed-loop poles deeper into the LHP at the expense of higher feedback gains.

A VS design for the example is discussed next and its performance is assessed using the real time hybrid computer system.

7.2.1 VS Solution

The first problem which is encountered in the VS design is the selection of a suitable switching plane. A hyperplane comprising the variables x_1, x_2 and x_3 and given by,

$$\sigma = c_1x_1 + c_2x_2 + x_3 \tag{7.3}$$

is only suitable if the equilibrium point is the origin. If the set-point for x_1 is a constant, then x_2 must settle at $x_1/2$ in the

steady state according to fig. (7.1). Since c_1 and c_2 are normally positive, then for a positive set-point, the steady state value of σ will be greater than zero and will vary according to the magnitude of the set-point. The theory of chapter three unfortunately does not give an answer to that type of problem and only deals with the case $\sigma \to 0$. However, the problem can be reformulated using the error space equations and the switching plane defined as,

$$\left.\begin{aligned} \sigma &= c_1 e_1 + c_2 e_2 + e_3 \\ \text{where} \quad e_1 &= x_1 - R \qquad R = \text{input reference} \\ e_2 &= \dot{e}_1 \\ e_3 &= \dot{e}_2 \end{aligned}\right\} \qquad (7.4)$$

assuming that e_2 and e_3 can be obtained in a satisfactory way, for example, x_1, x_2 and x_3 can be suitably combined to give e_2 and e_3 in a time-invariant system.

Since only (n-1) roots are relevant in a sliding regime, then the first step in the design is to assign two of the three roots. Using the following feedback gains,

$$\left.\begin{aligned} & k_1 = -0.4375 \qquad k_2 = -0.6375 \\ \text{and} \quad & u = \dot{u}_c - k_1 x_1 - k_2 x_2 \end{aligned}\right\} \qquad (7.5)$$

where 'u' is defined in equation (7.1), the closed-loop poles are located at,

$$s = -0.75 + j0.75,\ -0.75 - j0.75,\ 0.9 \qquad (7.6)$$

The complex pair is well positioned for a good transient response; the unstable pole at s = 0.9 does not present difficulties in the VS design. The new closed-loop unstable system becomes,

$$\left.\begin{aligned} \dot{x}_1 &= -0.5x_1 + x_2 \\ \dot{x}_2 &= x_3 \\ \dot{x}_3 &= 0.875x_1 + 0.275x_2 - 0.1x_3 + 2u_c \end{aligned}\right\} \qquad (7.7)$$

and using equation (7.4), (7.7) can be re-written as,

$$\left.\begin{aligned} \dot{e}_1 &= e_2 \\ \dot{e}_2 &= e_3 \\ \dot{e}_3 &= 1.0125e_1 + 0.225e_2 - 0.6e_2 + 1.0125R + \\ &\qquad \dot{0.225R} - \ddot{0.6R} + 2.0u_c \end{aligned}\right\} \qquad (7.8)$$

Using equations (7.4) and (7.8), it can be shown that,

$$\left.\begin{aligned} \sigma\dot{\sigma} = {} & [1.0125 - c_1c_2 + 0.6c_1 - 2\psi_1]e_1\sigma + \\ & [c_1 + 0.225 - c_2^2 + 0.6c_2 - 2\psi_2]e_2\sigma + \\ & [1.0125R + \dot{0.225R} - \ddot{0.6R} - 2\psi_r]\sigma \end{aligned}\right\} \qquad (7.9)$$

where,

$$u_c = -\psi_1 e_1 - \psi_2 e_2 - \psi_r R \qquad (7.10)$$

ψ_1, ψ_2 and ψ_r are defined in the usual way. Applying the sliding conditions,

$$\left.\begin{aligned} \alpha_1 &> \tfrac{1}{2}[1.0125 - c_1c_2 + 0.6c_1] && \text{if } e_1\sigma > 0 \\ \alpha_2 &> \tfrac{1}{2}[c_1 + 0.225 - c_2^2 + 0.6c_2] && \text{if } e_2\sigma > 0 \\ \text{and} \quad \alpha_r &> \tfrac{1}{2}[1.0125R + 0.225\dot{R} - 0.6\ddot{R}] && \text{if } R\sigma > 0 \end{aligned}\right\} \qquad (7.11)$$

with the inequality sign reversed for β_1, β_2 and β_r. Since the poles of the sliding motion have already been positioned, the values of c_1 and c_2 are determined by,

$$\left.\begin{aligned} &\tfrac{1}{2}[1.0125 - c_1c_2 + 0.6c_1] = 0.0 \\ \text{and} \quad &\tfrac{1}{2}[c_1 + 0.225 - c_2^2 + 0.6c_2] = 0.0 \end{aligned}\right\} \qquad (7.12)$$

Eliminating c_1 from one of the equations of (7.12) results in a cubic in c_2,

$$c_2^3 - 1.2c_2^2 + 0.135c_2 - 0.8775 = 0.0 \qquad (7.13)$$

A solution for c_2 is 1.5 giving a value 1.125 for c_1.

$$c_1 = 1.125 \qquad c_2 = 1.5 \qquad (7.14)$$

For a constant set-point, $\dot{R} = \ddot{R} = 0$ and the third inequality of (7.11) becomes,

$$\alpha_r > \frac{1}{2} \times 1.0125 \doteqdot 0.5 \qquad \text{if } R\sigma > 0 \qquad (7.15)$$

7.2.2 Results of Hybrid Computation

A software program was written in the high level language 'C' to run in real time for the VS controller of the previous section. The program is listed in fig. (7.4) and is almost self-explanatory. The program statements,

```
x1 = rd - ad(0);

x2 = rd - ad(1);
```

are calls to the system's subroutines for reading channels 0 and 1 respectively of the A/D converter. Similarly, the statement

```
Wrt - da (0, u);
```

instructs the system to output the variable 'u' on channel 0. The sampling time is set by,

```
cycle (tsamp);
```

where 'tsamp' is related at present to the mains frequency; a value of one for 'tsamp' is equivalent to a sampling time of 20 milliseconds, hence

$$\text{sampling time} = \frac{1000}{50} \times \text{tsamp} \quad \text{ms}$$

The program execution time must be within the set sampling time and it can be estimated experimentally by setting and resetting a flag at the beginning and the end of the program respectively [7.1]. In the example considered, a sampling time of forty milliseconds was found to be adequate for performing all the calculations. With the dominant time constants of the loop being in the range of seconds, the overall system is essentially operating on a continuous basis.

In the results shown in figures (7.5) to (7.10), the set-point was one and the switchable gains were as follows,

$$\left.\begin{array}{ll} |\alpha_1| = |\alpha_2| = 5.0 & |\beta_1| = |\beta_2| = 5.0 \\ \alpha_r = 1.5 & \beta_r = -0.5 \end{array}\right\} \qquad (7.16)$$

```
vss1(){
/* VSS CONTROLLER FOR THIRD ORDER EXAMPLE */
register int tsamp;
register int xyz;  /* dummy declaration to force compiler not to use r3 */
register int fpu;  /* dummy declaration to force compiler not to use r2 */
float rd_ad();uc;zero;e1n;e2n;e3n;sigma;x1;x2;x3;
float es1;es2;esr;ps1;ps2;psr;uf;uv;u;y1;r;
tsamp=1;zero=0.00;r=1.0;
printf("start of vss program\r\n");
cycle(tsamp);
loop:
x1=rd_ad(0);       /* input value of a/d channel 1 */
x2= -rd_ad(1);     /* input value of a/d channel 2*/
x3=rd_ad(2);      /* input value of a/d channel 3 */
/* calculate error vector */
e1n=x1-r;
e2n= -0.5*x1+x2;
e3n=0.25*x1-0.5*x2+x3;
/* VSS Controller Implementation */
sigma=1.125*e1n+1.5*e2n+e3n;
es1=e1n*sigma;
es2=e2n*sigma;
esr=r*sigma;
if((es1)>zero)
        ps1=5.0*e1n;
if((es1)< -zero)
        ps1= -5.0*e1n;
if((es2)>zero)
        ps2=5.0*e2n;
if((es2)< -zero)
        ps2= -5.0*e2n;
if((esr)>zero)
        psr=1.5*r;
if((esr)< -zero)
        psr= -0.5*r;
uv=ps1+ps2+psr;
/* Pole Assignment Equation */
uf= -0.4375*x1-0.6375*x2;
u= -uf-uv;
/* Limiter */
if(u>10.0)
    u=10.0;
if(u< -10.0
    u= -10.0;
uc= -u;
/* Trigger for oscilloscope */
y1=rd_ad(3);
if((y1)>5.0){
       uc=0.0;e1n=0.0;e2n=0.0;e3n=0.0;es1=0.0;es2=0.0;esr=0.0;
}
wrt_da(0,uc);
wait();
goto loop;
}
```

FIG.7.4 'C' Program _ VS Controller for third order example.

The derivatives of e_1, i.e. e_2 and e_3 were estimated using the following expressions,

$$\left.\begin{aligned} e_1 &= x_1 - R \\ e_2 &= -0.5x_1 + x_2 \\ e_3 &= 0.25x_1 - 0.5x_2 + x_3 \end{aligned}\right\} \qquad (7.17)$$

The error vector $\underline{e}$ is thus obtained from the measurement of the full state vector $\underline{x}$.

Fig. 7.5a) illustrates the response of the output x_1 due to a step change of 1.0 volt in the reference R. The upper trace is the driving function u (scale: 10 V/div), the middle trace is the output x_1, (scale: 1 V/div) and the lower trace is the switching function sigma, (scale: 2 V/div). The horizontal scale is 0.5 secs/div. The output x_1 settles at the desired value after approximately three seconds. The input u is very active and is continuously switching with the envelope of the switching waveform decaying exponentially. In the steady state, i.e. with x_1 equal to the reference, the input is still switching. Recalling from equations (7.5) and (7.10) that u is given by

$$u = -\psi_1 e_1 - \psi_2 e_2 - \psi_r R - k_1 x_1 - k_2 x_2 \qquad (7.18)$$

then in the steady state,

$$u_{st} = -\psi_r R - k_1 x_{1st} - k_2 x_{2st} \qquad (7.19)$$

since e_1 and e_2 both converge to zero, and, x_1 and x_2 converge to the steady-state values x_{1st} and x_{2st} respectively. Substituting for the variables in (7.19) results in,

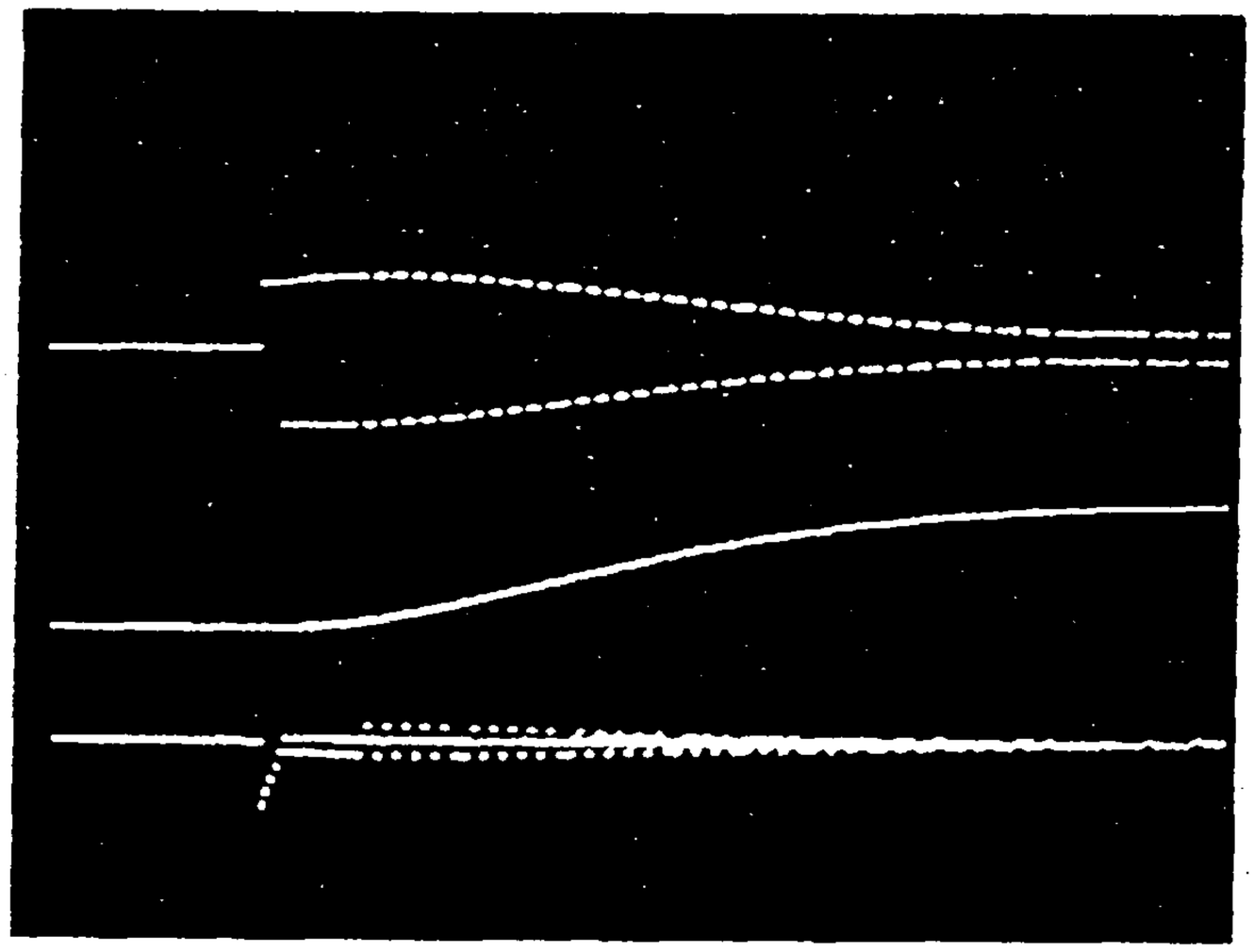

(a) Step Response of Third Order VSS

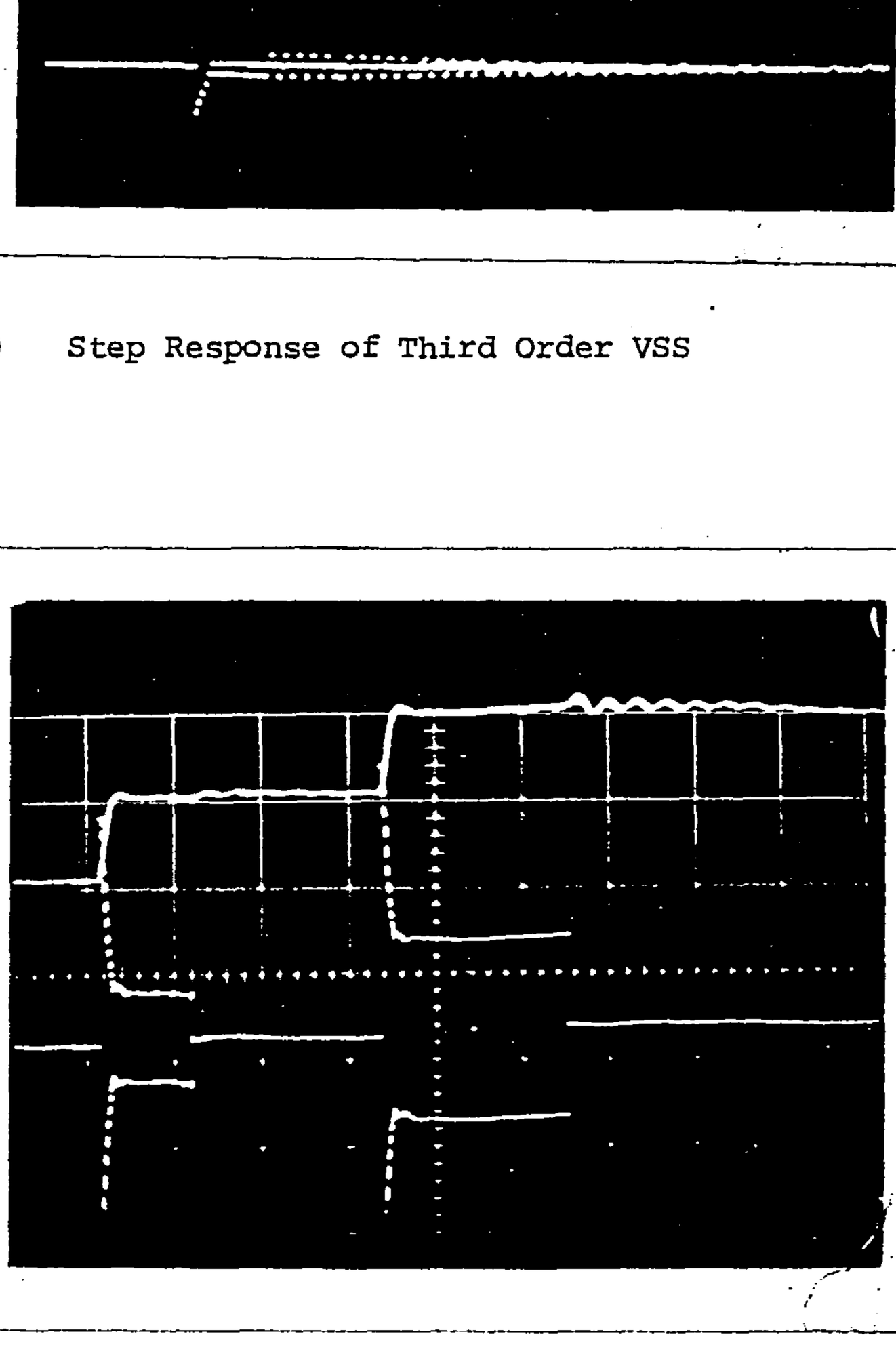

Time Scale Uncalibrated

(b) Effect of Averaging Input

Figure 7.5 Third Order VSS

$$u_{st} = -\begin{bmatrix} 1.5 \\ -0.5 \end{bmatrix}(1.0) - (-0.4375)(1.0) - (-0.6375)(0.5)$$

$$= \begin{bmatrix} -1.5 \\ 0.5 \end{bmatrix} + 0.756 = 1.256 \text{ or } -0.744 \qquad (7.20)$$

Hence in the steady-state, the input switches between 1.256 volts and -0.744 volts, and the total amplitude is 2.0 volts. This is approximately in line with the observed result which is slightly in excess of two volts. The frequency of switching in the steady state is such as to produce an average level sufficient to compensate for the steady state values of the variables within the plant. Referring back to Fig. (7.1), when x_1 is 1.0 volt, then u must be equal to 0.25 volt. Since the average value of u in this instance is close to zero and u switches between approximately ±1.0 volt, then it can be expected that u will be switching continuously. This fact can be observed from the results. The switching function 'sigma' indicates that a sliding regime is established after approximately 1.5 seconds when its value becomes close to zero.

The average value of the input in the steady-state has been shown experimentally, to be the correct level required to maintain the output at a desired set-point. The results are shown in Fig. (7.5b). The upper trace displays the output when the reference is equal to one and two volts respectively. The lower trace is the input to the plant. Its average value is computed over a large number of samples and is then substituted for the switching input to the plant. A slight oscillatory transient occurs as can be expected from the underdamped plant but the output is maintained at the current level. A higher average input level is obtained for

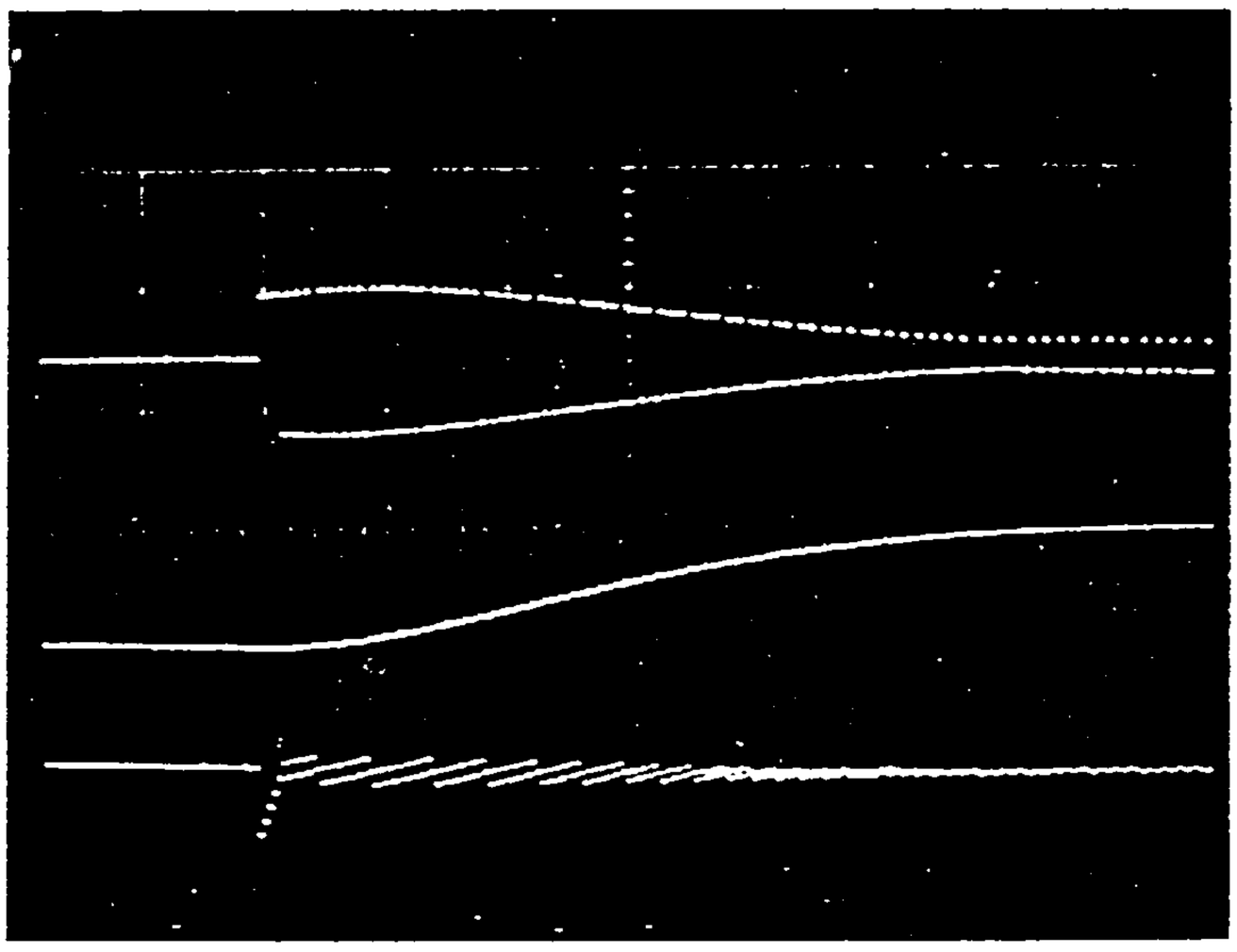

Figure 7.6 Third Order VSS with Constant Input Disturbance of +0.5 Volt

the higher set-point.

Fig. (7.6) shows the responses when a constant disturbance of 0.5 volt is added to the input. It can be seen that the driving input u remains negative for longer periods indicating that the average value of the input level has been lowered. This can be explained as follows; from the previous paragraph, the average input level to maintain the output at 1.0 volt is 0.25 volt. With a disturbance of +0.5 volt, the average input level must therefore drop to -0.25 volt to maintain the steady state conditions; hence the switching input drive must remain negative for longer periods to produce the appropriate average input.

If the input disturbance is increased, the driving input should remain negative for longer periods. This effect is shown in Fig. (7.7) where the average value of the input drive has been lowered by the switching to compensate for a disturbance of +1.0 volt. Correspondingly, if the input disturbance is negative, the driving function should stay positive for longer periods. This is illustrated in Fig. (7.8) where the input disturbance is -1.0 volt. In both instances the output x_1 is maintained at the correct level.

The responses of Figs. (7.7) and (7.8) are effectively combined when a sinusoidal input disturbance is added to the input. Fig. (7.9) shows the periodic variations in the input u as the disturbance becomes increasingly positive or negative. On the positive half cycles, the average value of the input is lowered and raised on the negative ones; the output remains unchanged at the desired level of one volt. A similar performance is unlikely to be obtained using a linear controller.

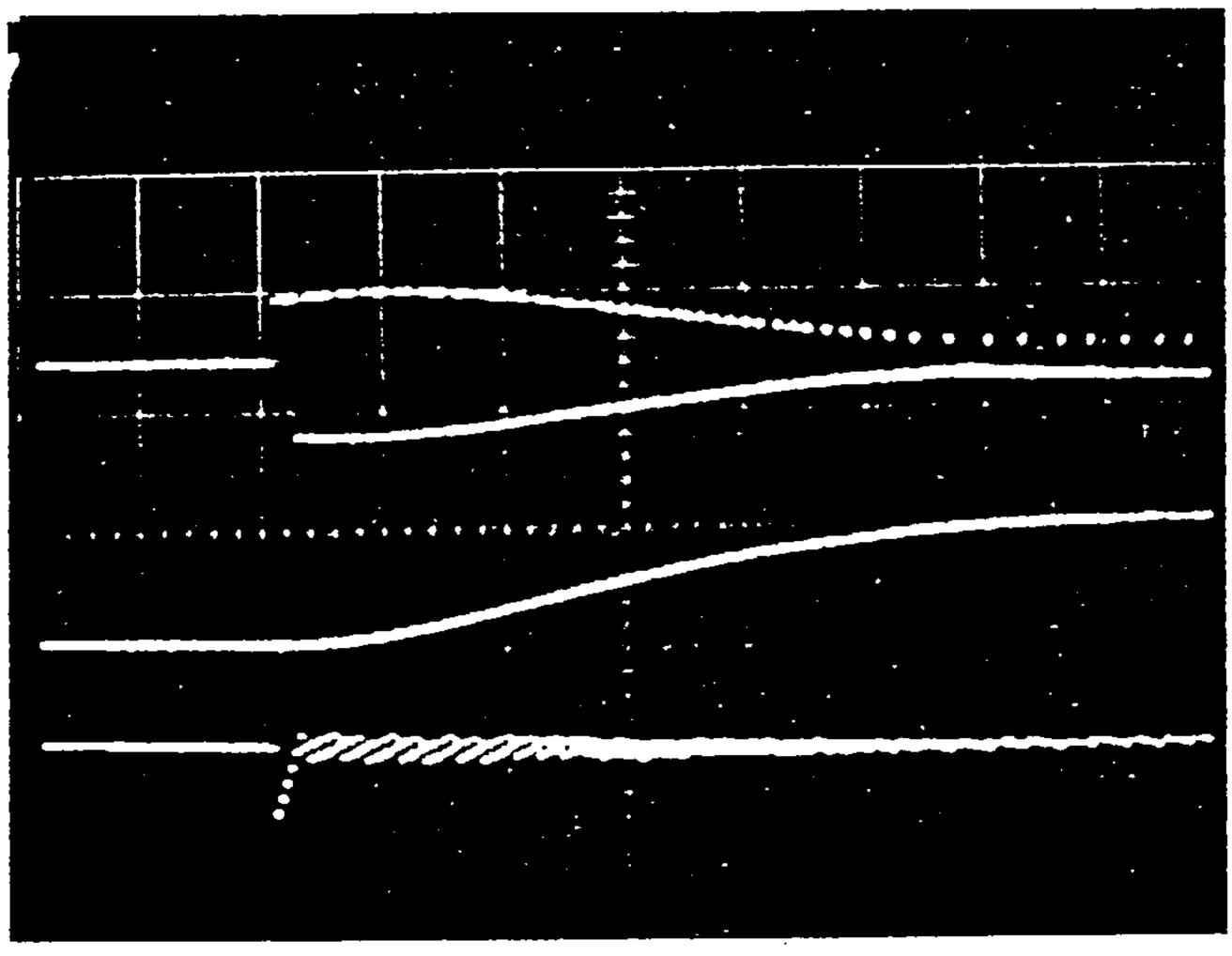

Figure 7.7 Constant Input Disturbance of +1.0 Volt

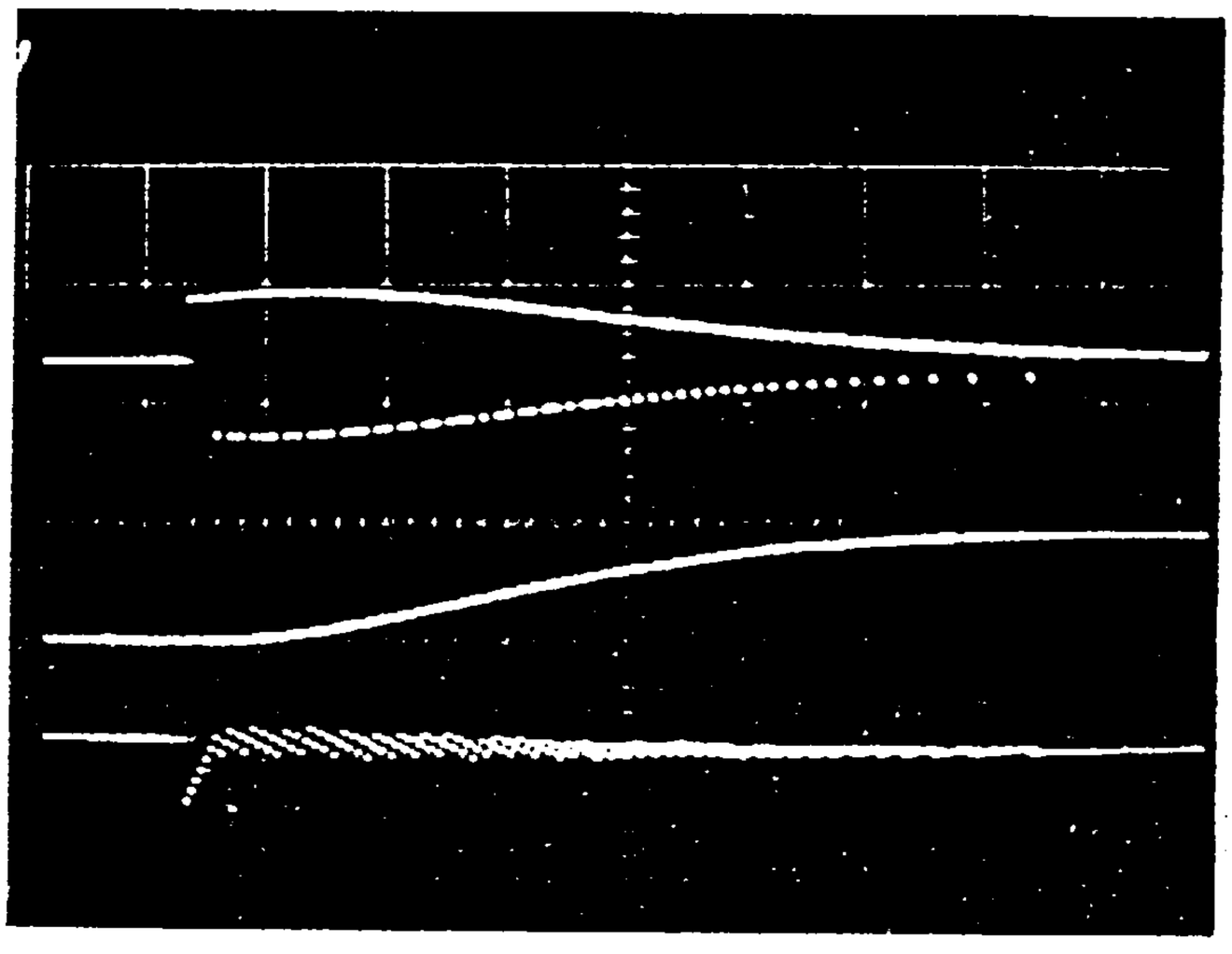

Figure 7.8 Constant Input Disturbance of -1.0 Volt

Fig. (7.10) shows the response of the system when the reference input is changed from a step to a ramp with no changes made to the controller. In this test the output can track the input with a very small steady-state error. For zero steady-state error, the rate of change of the input must be considered and included in the sliding inequalities.

It is worth noting at this stage that the results have been obtained without a detailed analysis of the hitting conditions; in practice it may only be sufficient to satisfy the sliding inequalities.

From the sliding inequalities of (7.11), it was necessary to switch the reference to force a sliding motion. If the reference is omitted from the switching law, sliding breaks down; this occurrence is shown in Fig. (7.11). Initially the system enters into a sliding regime indicated by sigma approaching zero. The error in the output then gradually builds up and leads to a further burst of switching which restores the sliding motion and reduces the error. The cycle then repeats itself. The test shows that switching the error can only maintain the sliding conditions for a short time and that the switching of the reference is an essential component of a VS controller. The same observation was made earlier in the coiler-drive example.

Fig. (7.12) shows the effect of improper plant identification on the VSS. A parasitic lag was introduced between the controller and the plant, defined by,

$$\frac{u_1(s)}{u(s)} = \frac{1}{0.10\,s + 1}. \qquad (7.21)$$

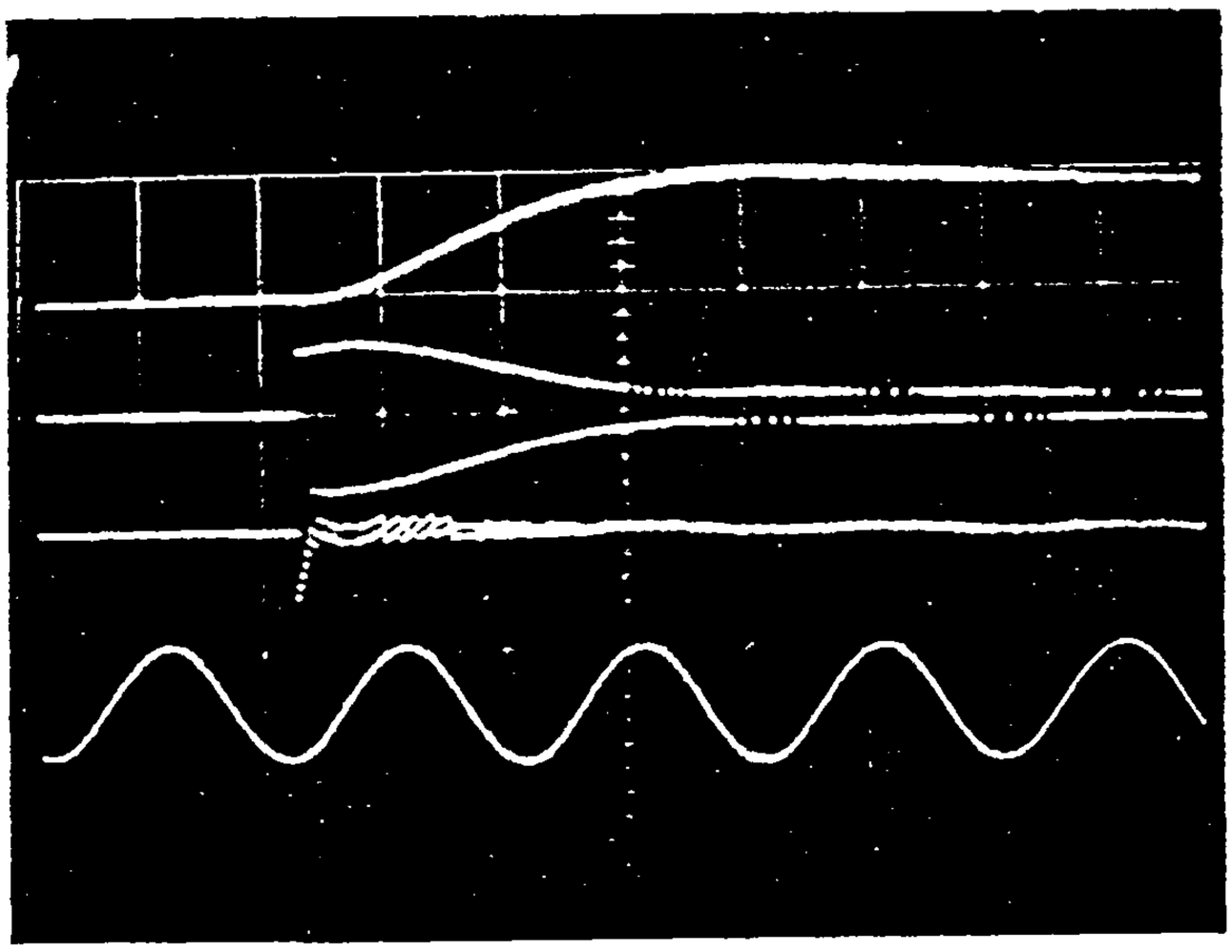

Figure 7.9 Sinusoidal Input Disturbance

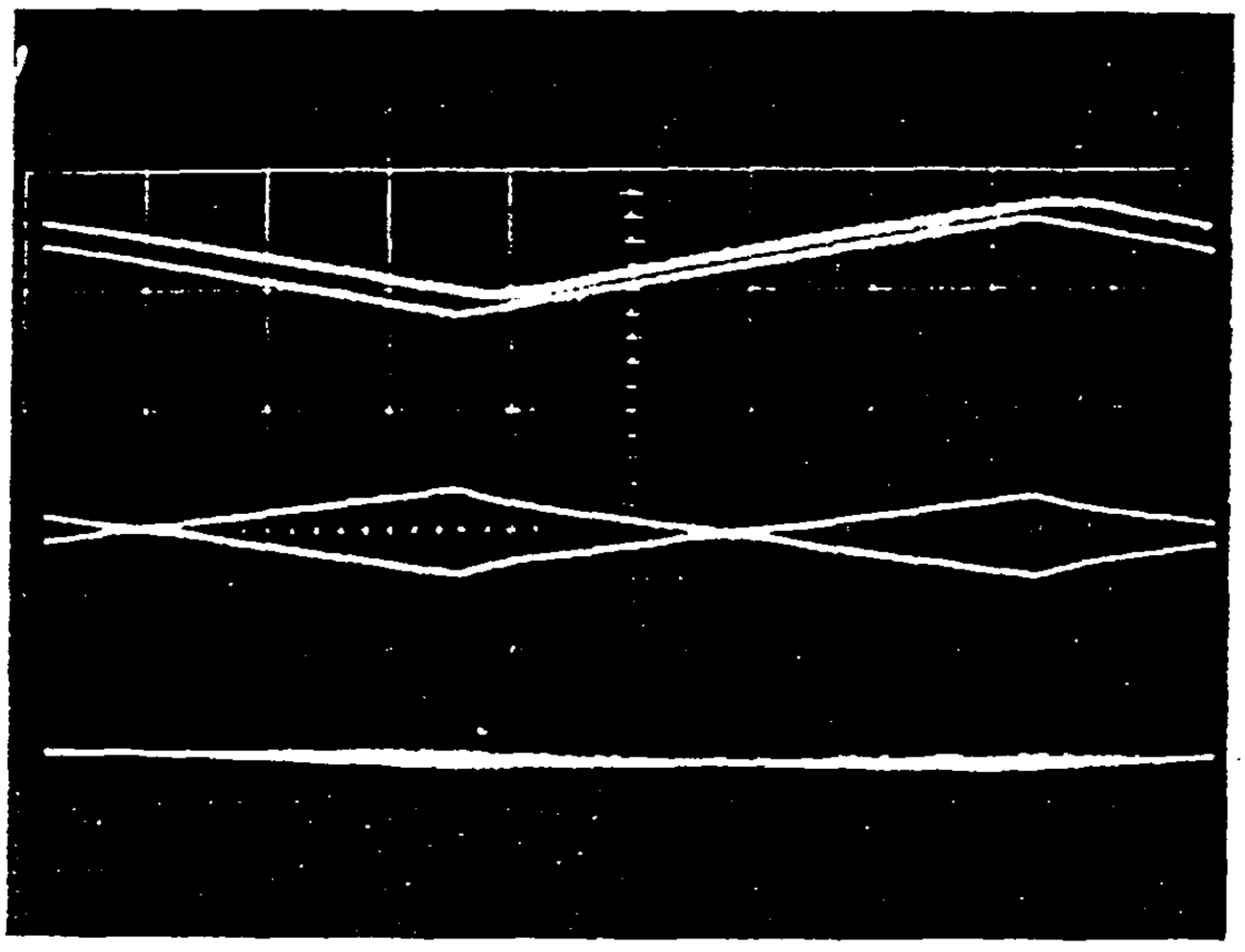

Figure 7.10 Ramp Input

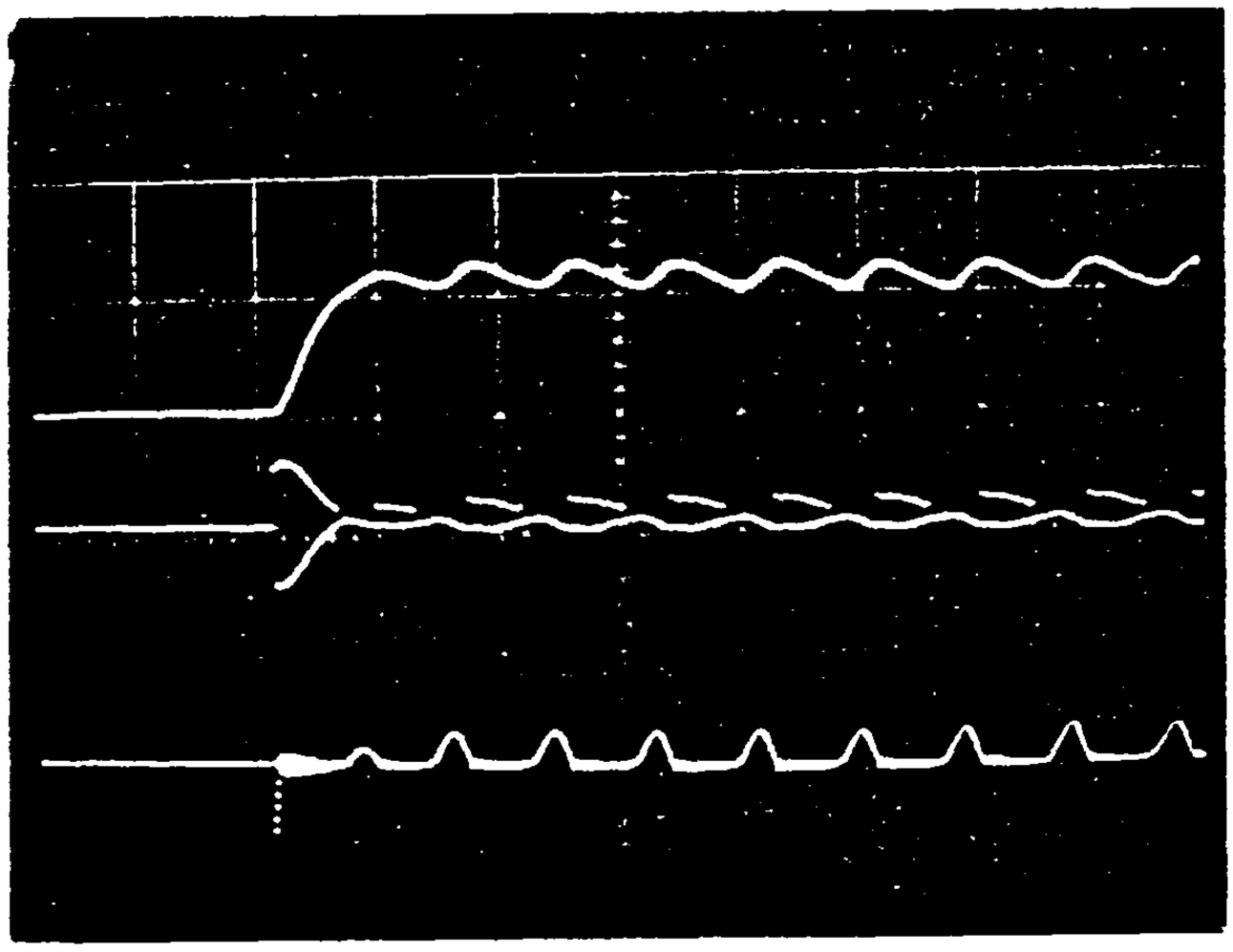

Figure 7.11 Sliding Breakdown

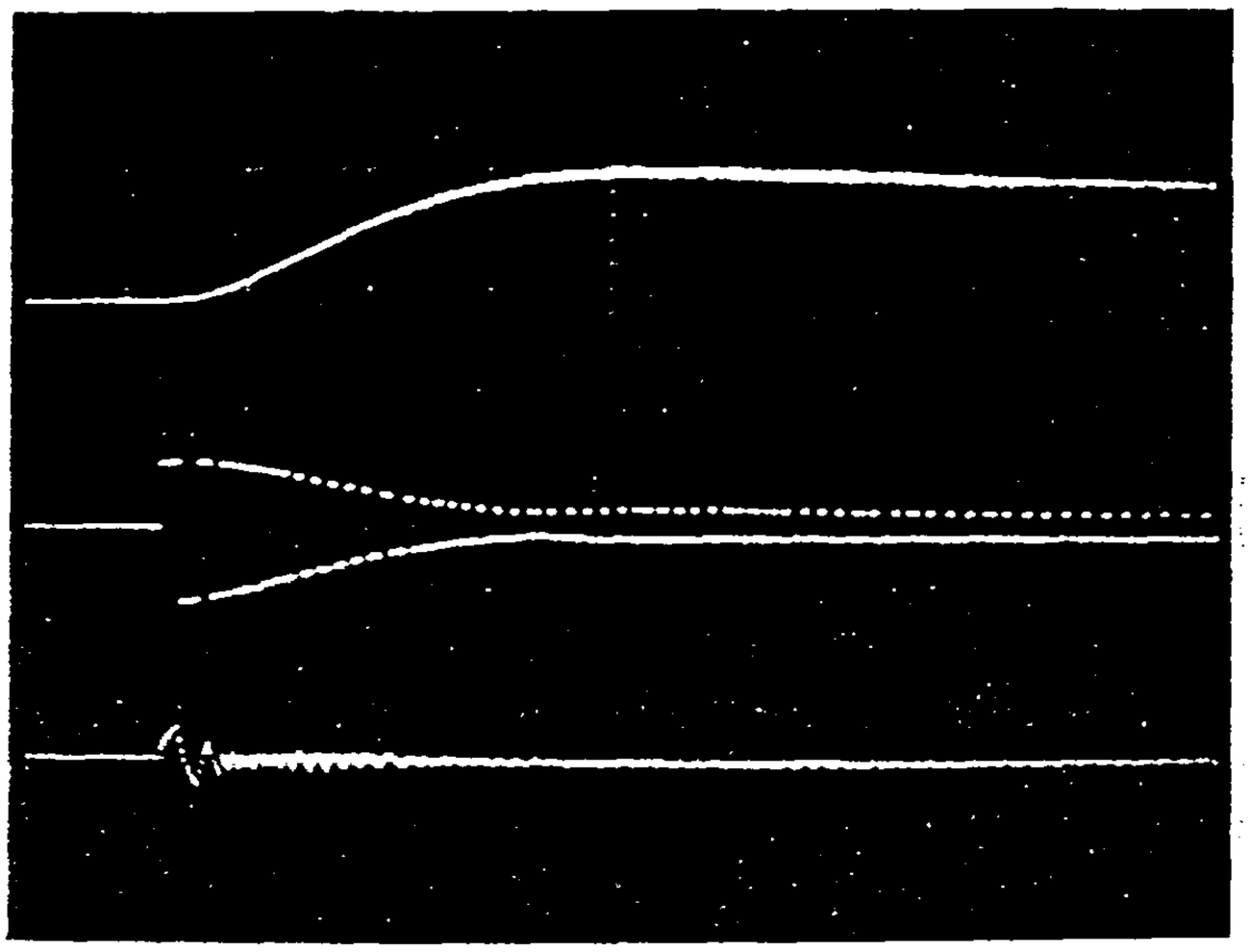

Figure 7.12 Effect of Unidentified Lag

The output is almost unchanged with perhaps a small steady-state error; the integration effect of the parasitic lag on the driving function is also shown. Changing the location of the pole from s = -10.0 to s = -1.0 led to an unstable system; it is necessary then that all the dominant poles are carefully identified before a VS controller can be designed and implemented.

The effects of moving the disturbance closer to the plant's output are shown in Fig. (7.13). A disturbance of one volt was added to the summing junction on the extreme right of Fig. (7.1). The output in this instance settled at 2.0 volts, i.e. with an error of one volt. Consequently, the input drive switches between wider amplitude levels and the switching function oscillates about zero. The reason for this large steady-state error occurs as a result of the method used to estimate the error vector (refer to eqn. 7.17). In this method, no information concerning the disturbance is actually transmitted to the controller as e_2 is derived from x_1 and x_2 alone. A similar situation was encountered in the design of the VS autopilot with the difference that the disturbance in the yaw rate was contained in the measurement and was successfully compensated. The error vector was then estimated by direct differentiation of e_1, the output error. This was achieved by storing past values of $\underline{e}$ and, $\dot{\underline{e}}$ was obtained by dividing the difference between present and past values of $\underline{e}$ by the clock interval. Fig. (7.14) illustrates the responses obtained by this method and with no disturbance present. The output is well-behaved and settles at the desired value, whereas the switching function is considerably noisier.

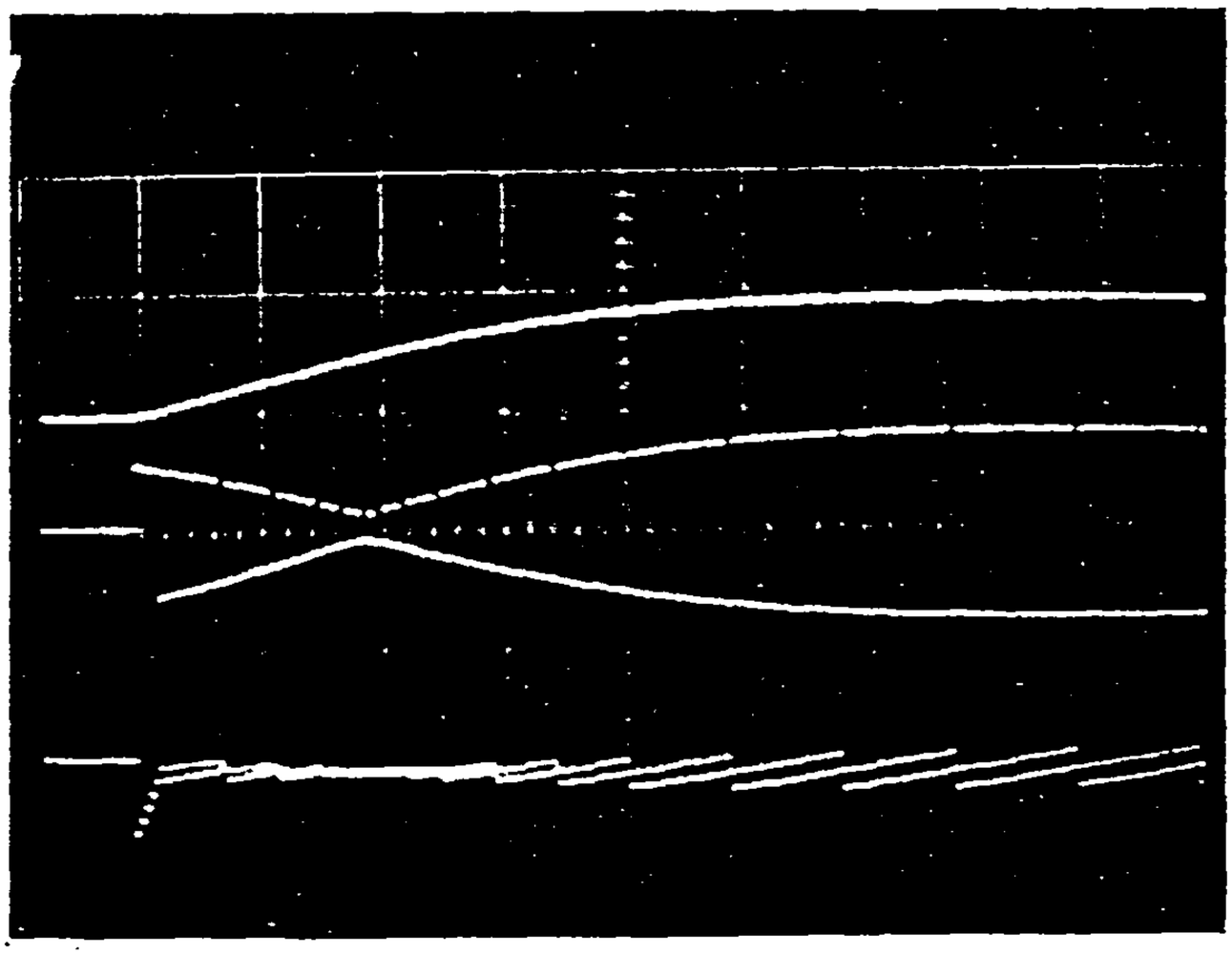

Figure 7.13 Disturbance in x_2

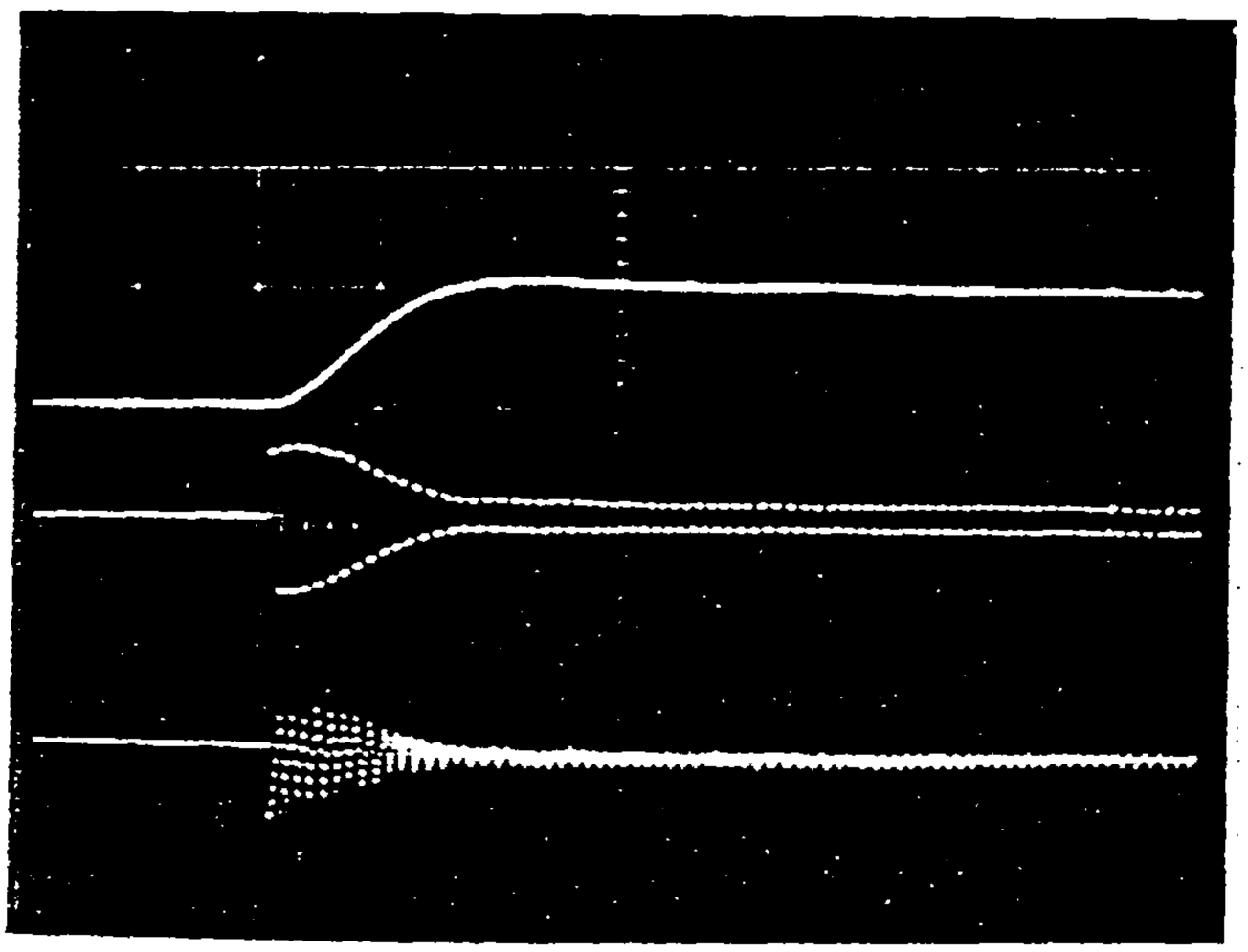

Figure 7.14 Error Vector Obtained by Differentiation

Fig. (7.15) shows the responses when a unit disturbance was added to x_2. The output has a small overshoot and settles at the reference value. The levels of the input u are now comparable to those in the previous tests. Fig. (7.16) illustrates the case for a disturbance of -2.0 volts. The output goes negative before recovering while the input operates temporarily under saturation conditions.

Those tests show that ideally the error vector should be obtained by differentiation for its greater information content. Differentiation is, however, not recommended in the form used in the above test because of the possibility of noise in the variables. Figs. (7.17) and (7.18) compare the effects of noise when the error vector is (i) estimated using eqn. (7.17), Fig. (7.17), and by (ii) direct differentiation, Fig. (7.18). In both tests, a random noise source was added to the output as follows,

$$x_1 = x_1 + (\text{frand}(\ ) - 0.5)*(A); \qquad (7.22)$$

where frand ( ) generates random numbers between 0 and 1 and A is a scaling factor. The results of Fig. (7.17) were obtained with A set at 0.1 and those of Fig. (7.18) with A set at 0.001. It is clear from these figures that a very small level of noise is going to upset a VSS based on direct differentiation.

In order to enhance the noise rejection capability of the VSS, x_1 was smoothed using a first order lag defined by,

$$\frac{x_1'(s)}{x_1(s)} = \frac{1}{0.5s + 1} \qquad (7.23)$$

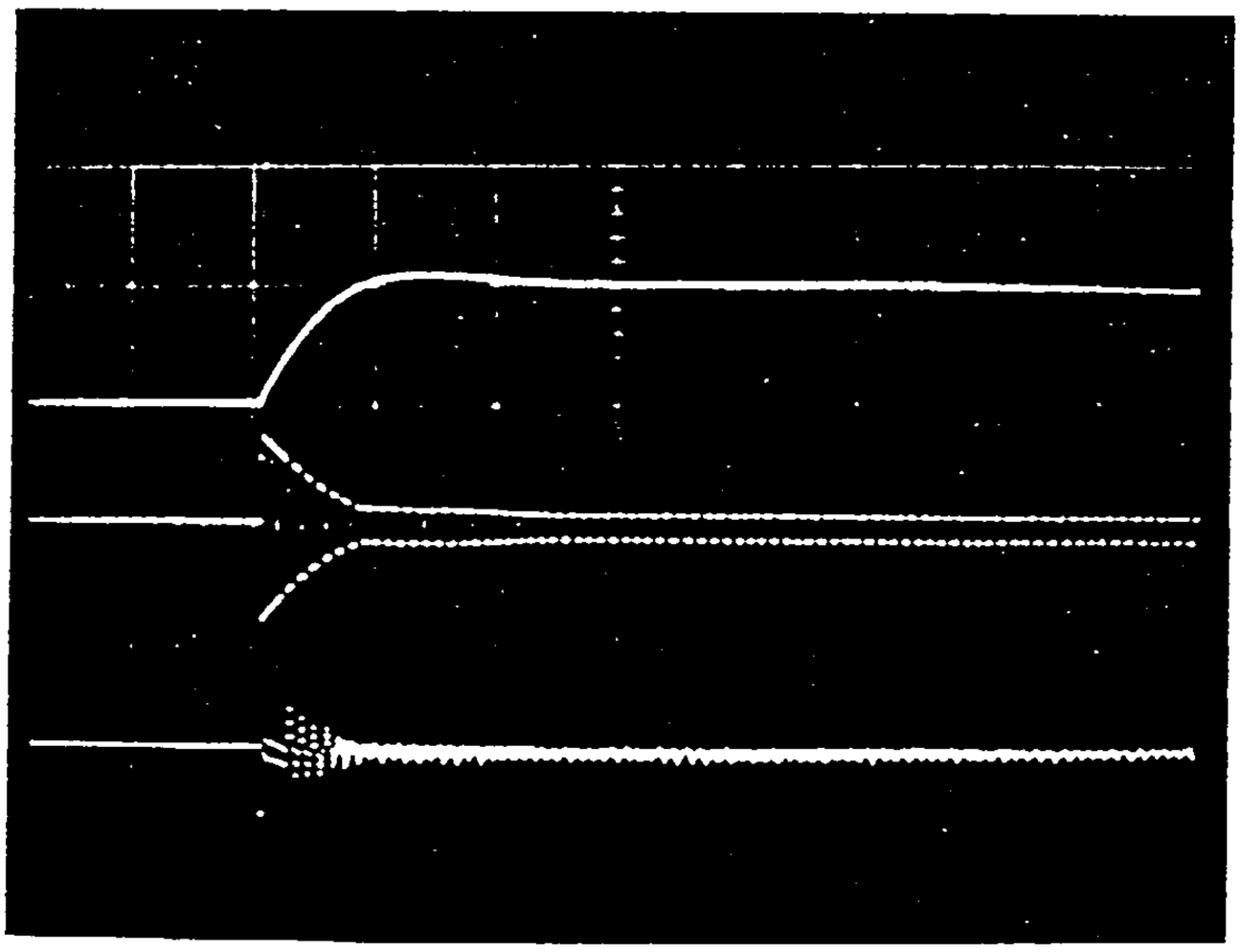

Figure 7.15 Disturbance in x_2 and Error Vector Obtained by Differentiation

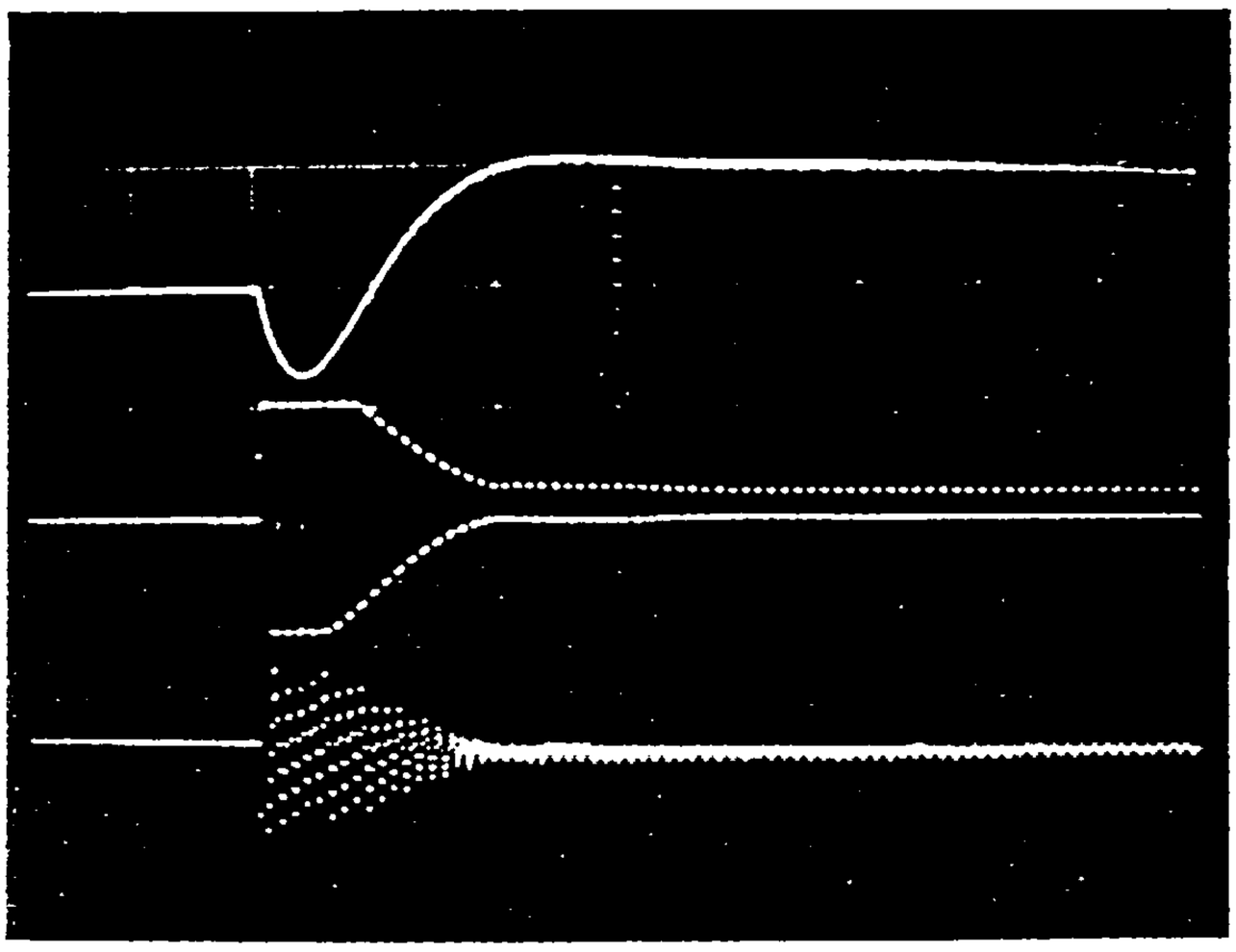

Figure 7.16 Disturbance in x_2 and Error Vector Obtained by Differentiation

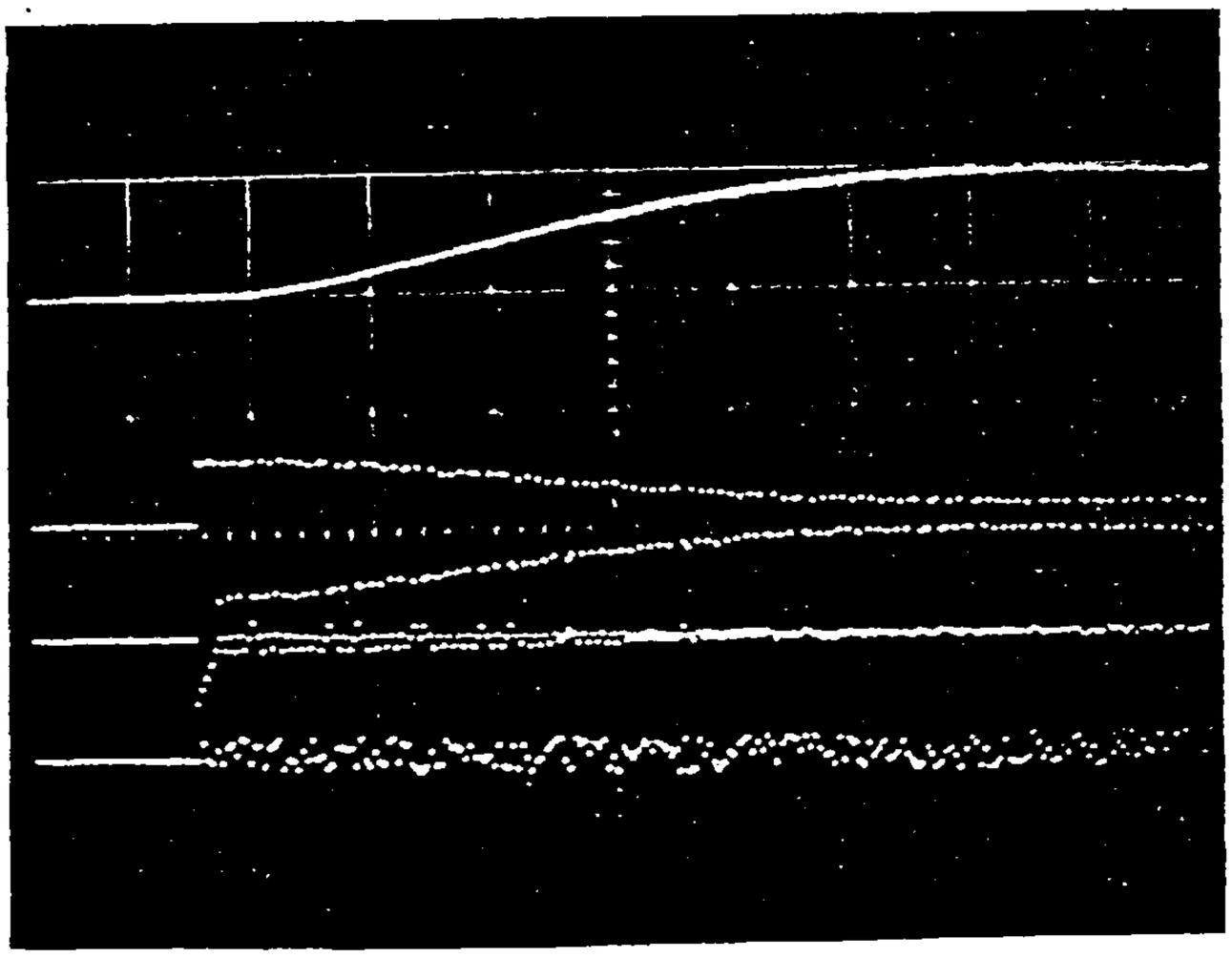

Figure 7.17 Effect of Noise-Error Vector Derived Indirectly

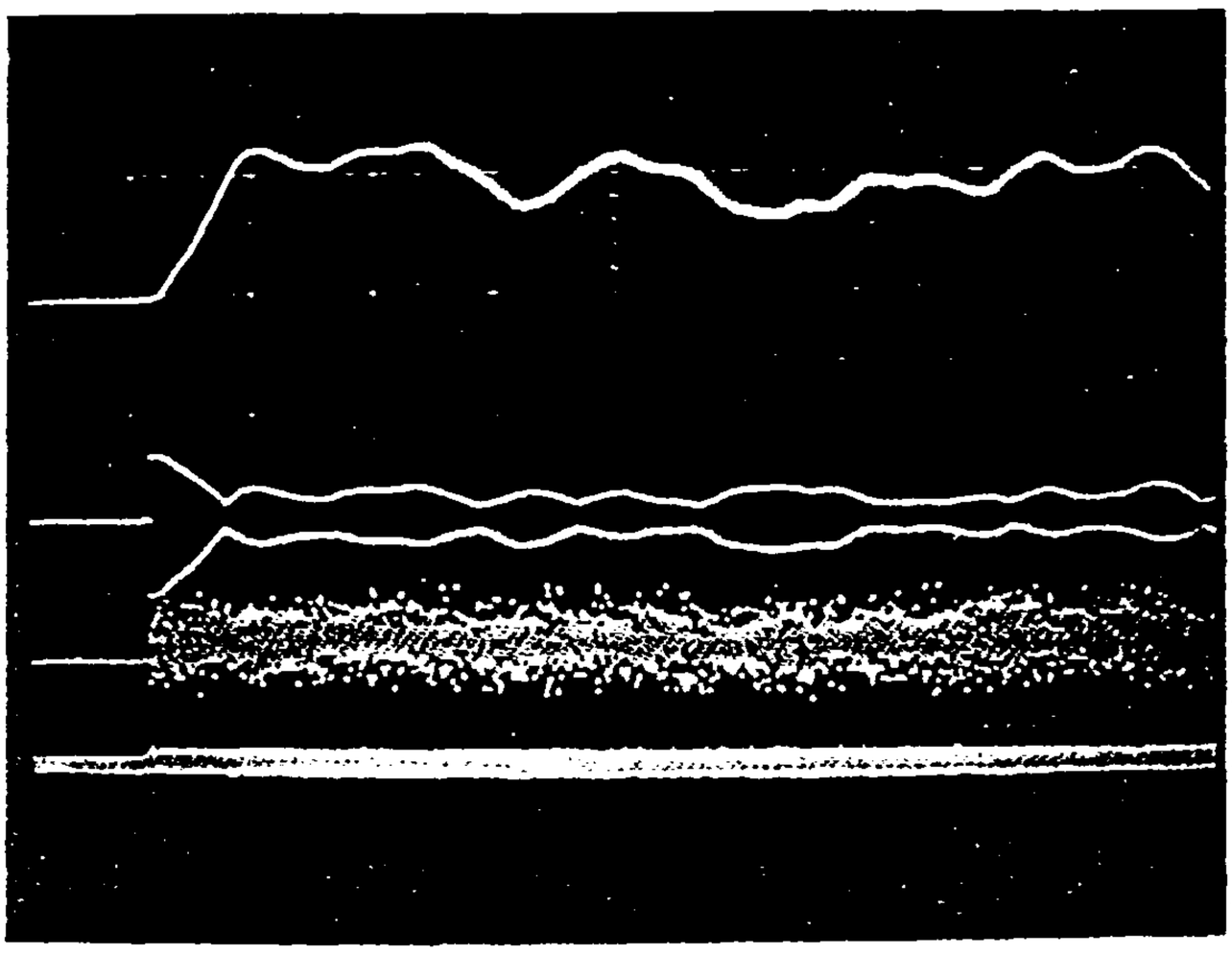

Figure 7.18 Effect of Noise-Error Vector Obtained by Differentiation

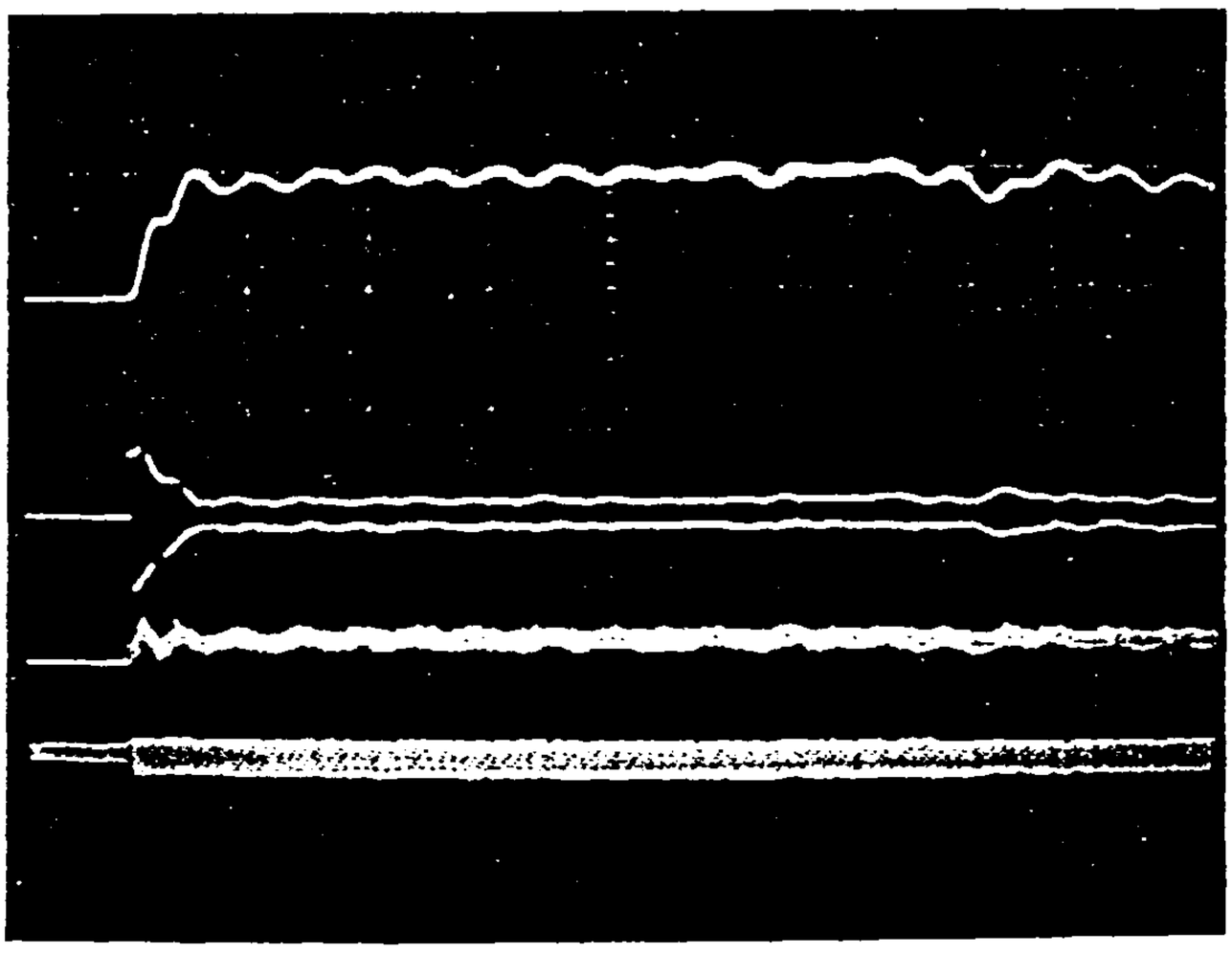

x_1 1 V/div

u 10 V/div

sigma 10 V/div

noise 0.05 V/div

5 secs/div

Figure 7.19 Smoothing of Noisy Signals

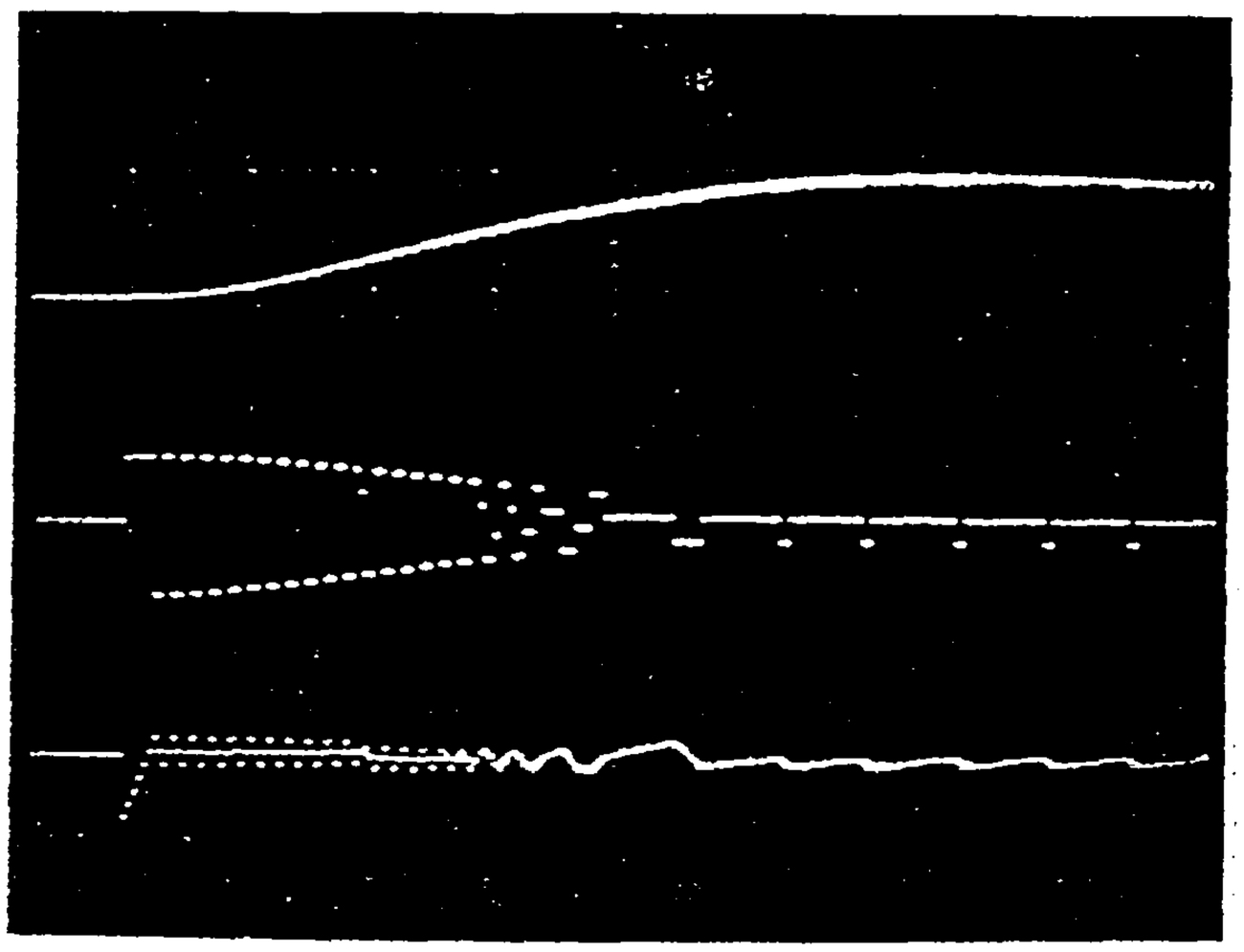

x_1 1 V/div

u 10 V/div

sigma 2 V/div

Figure 7.20 Effect of a Switching Zone

which has a pole at $\sigma = -2.0$. Fig. (7.19) shows the responses with A set at 0.01. The output performance is better and tracks the reference input more closely. The smoothing, however, cannot be increased without upsetting the stability of the system.

Further experiments were conducted in which the derivatives were estimated using an observer in phase-variable form. This particular estimation configuration was found to be unsuitable owing to stability problems. The instability was thought to arise as a result of the discontinuous nature of the input waveform to the observer which prevented the estimates to catch up and track the plant variables.

Fig. (7.20) illustrates the case when the inequalities $e_1\sigma$, $e_2\sigma$ and $R\sigma$ are compared not to zero as indicated by (7.11) but to small positive and negative values as defined by the variable 'zero' in the program listing of Fig. (7.4), thereby creating a switching zone. By adjusting the magnitude of 'zero', some control is exerted on the frequency of switching. With 'zero' set at 0.05, the switching has decreased considerably in the steady state. This result can be used in applications where excessive switching could be detrimental, for example in mechanical systems.

7.3 General Comments

The experiments reported in this chapter have shown that VS theory can be made to operate in practice. The digital simulations performed in the previous designs were reproduced in the more real situation of a computer control analogue system. The real-time VS controller coped with (i) step and ramp inputs, (ii) constant and sinusoidal disturbances at different points in the plant, and

(iii) some uncertainty due to model inaccuracy. In the example, a sliding motion was realised only when the reference was included in the switching law. With the error vector derived indirectly, the system is insensitive to noise and other unquantified disturbances such as mains interference, quantisation and finite word length in the converters and micro-computer system. The VS controller has also stabilised the system since the plant and state feedback controller together form an unstable loop.

The control problem in the implementation of VSS is the reliable determination of the error vector. In well-defined systems where access to the plant's states is possible, the error vector can be estimated accurately. If the full state-vector is not accessible to measurement, observers or differentiators are the only alternatives. Observers are not promising at the moment and the preferred solution as pointed out in the tests is to use a combination of smoothing and differentiation.

CHAPTER EIGHT

REAL TIME VS CONTROL OF A DC MOTOR

The digital and hybrid simulation studies of the previous chapters have provided greater insight in the control mechanism of VSS. The switching of the input drive to the plant was seen to be equivalent to an integral action and to be able to compensate for plant parameter variations and for certain external disturbances. The successful application of the method was found to be dependent on the reliability of the information concerning the plant's variables. It remains now to verify whether the control waveforms are reproducible in a real situation where the plant is uncertain in terms of its parameters, order, noise levels and non-linearities.

In this Chapter, the applicability of VSS is assessed by considering a specific engineering problem, namely the speed control of a DC motor. The experimental hardware is identical to the hybrid computation system of Chapter Seven with the analogue computer replaced by a DC motor. [8.1]

8.1 Description of System

The system configuration is shown in fig. 8.1. It consists of an electric motor with associated power supplies and amplifier stages to control the power input to the motor in response to the control signal. The armature is connected in the emitter circuit and the field coil forms part of the collector circuit. Thus the back emf appears between the emitter and ground, hence the control voltage is increased or decreased to speed up the motor or to slow it down. When the motor is loaded, the speed drops and the armature current increases provided that the input control voltage is held

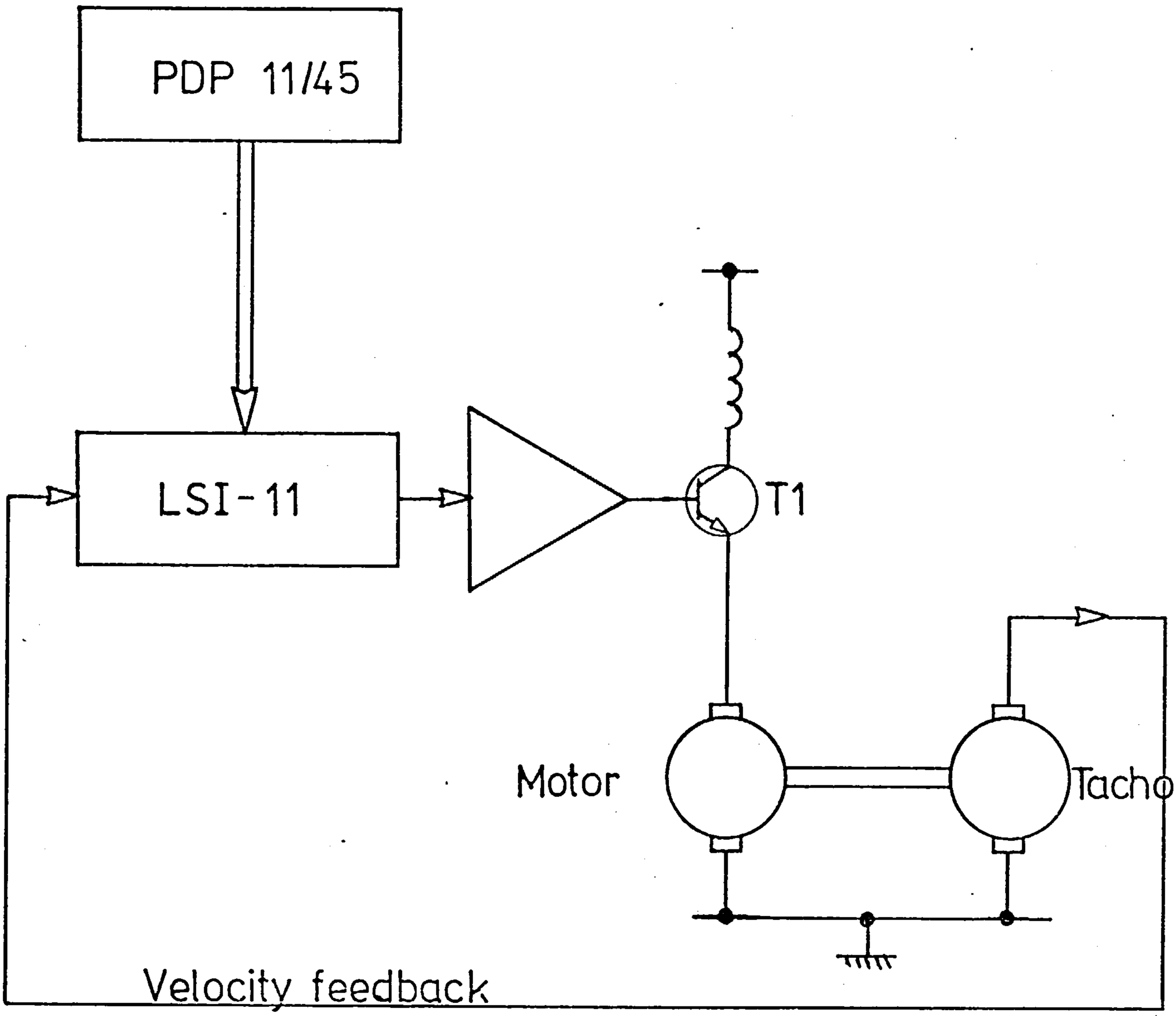

Fig. 8.1: VS Control of a DC Motor using a Microcomputer System

constant. Hence the torque can rise to keep the load moving.

The motor speed is measured by a tachogenerator which has a constant of 2.5 - 3.0 volts/rpm. The tachogenerator output is fed to one of the A/D channels and the drive to the motor is accessed through the D/A converter.

8.1.1 Model of the DC Motor

The starting point in the design is the derivation of a model for the motor which relates its speed to its input voltage. Modelling and/or identification are difficult operations to perform and usually result only in approximate models [8.2]; a simpler method was used instead to obtain a model of the motor.

The DC gain between the motor speed and the input voltage was measured in the steady state for different speeds. Its value was found to vary between 0.5 and 10.0, the steady-state speed was itself very dependent on the amount of friction in the bearings; a value of 5.0 was selected for the VS design. The order of the system was chosen as two; this is in line with the literature on DC motor models (see Chapter Four). The model can thus be described by

$$\frac{x_1(s)}{u(s)} = \frac{5.0}{as^2 + bs + 1} \qquad (8.1)$$

where x_1 is the speed, u is the input, and the parameters 'a' and 'b' are related to the transient response of the motor. Since the response varies from a few hundred milliseconds to a few seconds depending on the loading conditions, 'a' and 'b' can change quite significantly. Load changes are made by attaching discs of different weights to the motor shaft. The parameters 'a' and 'b' were chosen

somewhat arbitrarily as follows:

$$\left.\begin{aligned} a &= T^2 \\ b &= 2T \end{aligned}\right\} \qquad (8.2)$$

where T = 0.5 seconds. These values give rise to a characteristic response of the motor. The complete model is given by:

$$G(s) = \frac{x_1(s)}{u(s)} = \frac{5.0}{0.25\ s^2 + 0.5\ s + 1} \qquad (8.3)$$

The above transfer function is an approximate description of the motor dynamics. No account is taken of the parameter variations and nonlinearities in the system due for example to the product of field current and armature current.

Under the assumption of linearity, equation 8.3 can be represented in phase variable form by:

$$\left.\begin{aligned} \dot{x}_1 &= x_2 \\ 0.25\ \dot{x}_2 &= -x_1 - x_2 + 5u \end{aligned}\right\} \qquad (8.4)$$

The above differential equations are used to design a VS speed controller.

8.1.2 Design of a VS Speed Controller

The control objective is to design a VS controller which forces the tachogenerator output to follow a reference input with zero steady-state error given that only the speed is directly measurable. The speed error is given by,

$$e_1 = x_1 - R \qquad (8.5)$$

where 'R' is the speed reference.

Following VS principles, a switching function is defined, let

$$\sigma = c_1 e_1 + e_2 \tag{8.6}$$

where e_2 is the first derivative of e_1 and $\sigma = 0$ in an ideal sliding regime. It is shown in Appendix H that the sliding inequality is given by,

$$\left.\begin{aligned} 0.25\ \sigma\dot{\sigma} = e_1\sigma\ (-\ 0.25\ c_1^2 + c_1 - 1.0 - 5\psi_1) \\ + R\sigma\ (-\ 1.0 - 5\psi_r) \lesssim 0 \end{aligned}\right\} \tag{8.7}$$

where

$$u = -\psi_1 e_1 - \psi_r R \tag{8.8}$$

When $e_1\sigma > 0$, $\psi_1 = \alpha_1$ and when $e_1\sigma < 0$, $\psi_1 = \beta_1$; hence

$$\left.\begin{aligned} \alpha_1 &> \tfrac{1}{5}\ (0.25\ c_1^2 - c_1 + 1.0) \\ \text{and} \quad \beta_1 &< \tfrac{1}{5}\ (0.25\ c_1^2 - c_1 + 1.0) \end{aligned}\right\} \tag{8.9}$$

Similarly when $R\sigma > 0$, $\psi_r = \alpha_r$ and when $R\sigma < 0$ $\psi_r = \beta_r$, thus

$$\left.\begin{aligned} \alpha_r &> -0.2 \\ \beta_r &< -0.2 \end{aligned}\right\} \tag{8.10}$$

The parameter c_1 was chosen by setting the RHS of inequality (8.9) to zero, yielding a value of $c_1 = 2.0$. This value can be altered by introducing a state-feedback controller. The switching gains ψ_1 and ψ_r were selected after a number of experiments as,

$$\left.\begin{aligned} |\alpha_1| = |\beta_1| &= 5.0 \\ |\alpha_r| &= 0.3 \\ |\beta_r| &= -0.3 \end{aligned}\right\} \tag{8.11}$$

```
vssmot1(){
/* VSS CONTROLLER FOR DC MOTOR */
register int tsamp;
register int xyz;  /* dummy declaration to force compiler not to use r3 */
register int fpu;  /* dummy declaration to force compiler not to use r2 */
int i;
float rd_ad(),x1,x1p,x2,r;
float x1n,x1dot,zero;
float x2n,x2dot,es1,esr,ps1,psr;
float ref,e1,e2,sigma,u;
tsamp=1;
i=0;
x1n=0.0;x2=0.0;x1p=0.0;x1=0.0;x1dot=0.0;
r=0.0;zero=0.00;
x2n=0.0;x2dot=0.0;
ref=5.0;e1=0.0;e2=0.0;sigma=0.0;
es1=0.0;u=0.0;esr=0.0;
ps1=0.0;psr=0.0;
printf("start of vss program\r\n");
cycle(tsamp);
loop:
i=i+1;
if(i==1000){
ref=3.0;
}
if(i==2000){
ref=5.0;
i=0;
}
x1=rd_ad(8);
x1dot=(x1-x1n)*(10.0);
x1n=x1n+x1dot*(0.02);
x2=(x1n-x1p)/(0.02);
x2dot=(x2-x2n)*(10.0);
x2n=x2n+x2dot*(0.02);
e1=x1n-ref;
e2=x2n;
sigma=(2.0)*e1+(1.0)*e2;
/* vss controller */
es1=e1*sigma;
esr=ref*sigma;
if(es1>zero){
   ps1=(5.0)*e1;
}
if(es1<zero){
   ps1= -(5.0)*e1;
}
if(esr>zero){
   psr=0.3*ref;
}
if(esr<zero){
   psr= -0.3*ref;
}
x1p=x1n;
u=ps1+psr-5.0;
wrt_da(0,u);

wrt_da(1,e1);
wrt_da(-2,e2);
wait();
goto loop;
}
```

8.1.3 Performance of the VS Controller

The program which implements the control law described by the relationships (8.8) → (8.10) is reproduced in fig. (8.2). The program was set to cycle at the rate of twenty milliseconds thus adding a finite delay in the loop. The delay is however negligible compared to the motor time constants which are sufficiently high to ensure that the controller appears relatively continuous.

The reference input was switched alternately between five and three volts which correspond approximately to 1700 rpm and 1000 rpm respectively. A constant disturbance of one volt was also added to the input (eqn. 8.8).

Fig. (8.3) shows the responses obtained under the above conditions. The upper trace is the input drive as observed at the base of transistor T_1 in fig. (8.1). The middle trace is the switching function and the lower trace is the tachogenerator output. The lower two traces indicate that the system is stable and that the output is forced to follow the reference speed very closely. The upper trace is a characteristic waveform of the input drive in a VSS. The initial switching transient is contained within a decaying exponential envelope which settles down in the steady-state to the switching of the input reference. The transient shows that the system operates temporarily in the presence of two types of nonlinearities when the reference is five volts. The input signal saturates at just over 10 volts on the positive swings and transistor T_1 (fig. 8.1) is reverse biased on the negative ones. A satisfactory performance is achieved in spite of those nonlinear effects. Two points are to be noted, firstly no

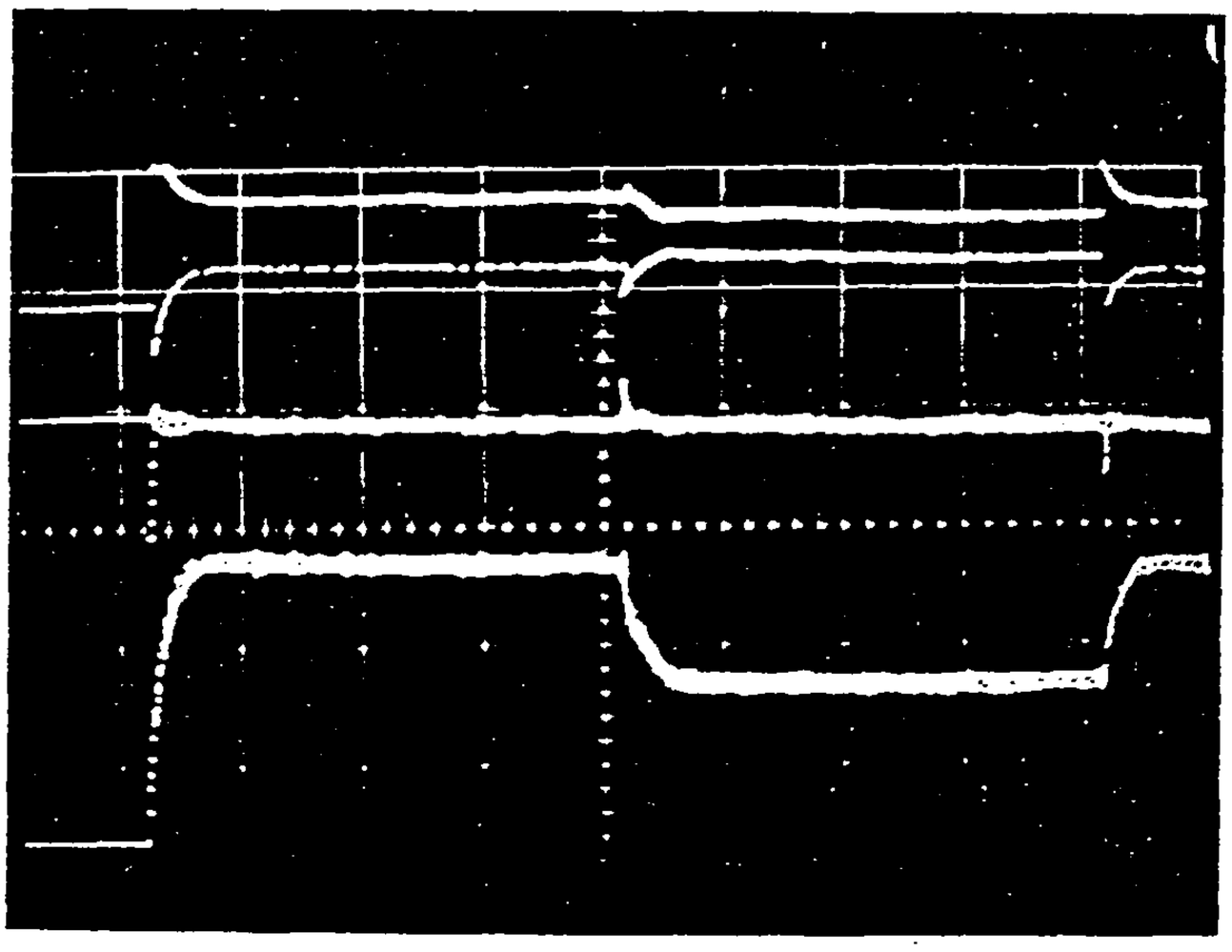

Fig. 8.3 - Step Responses of DC Motor

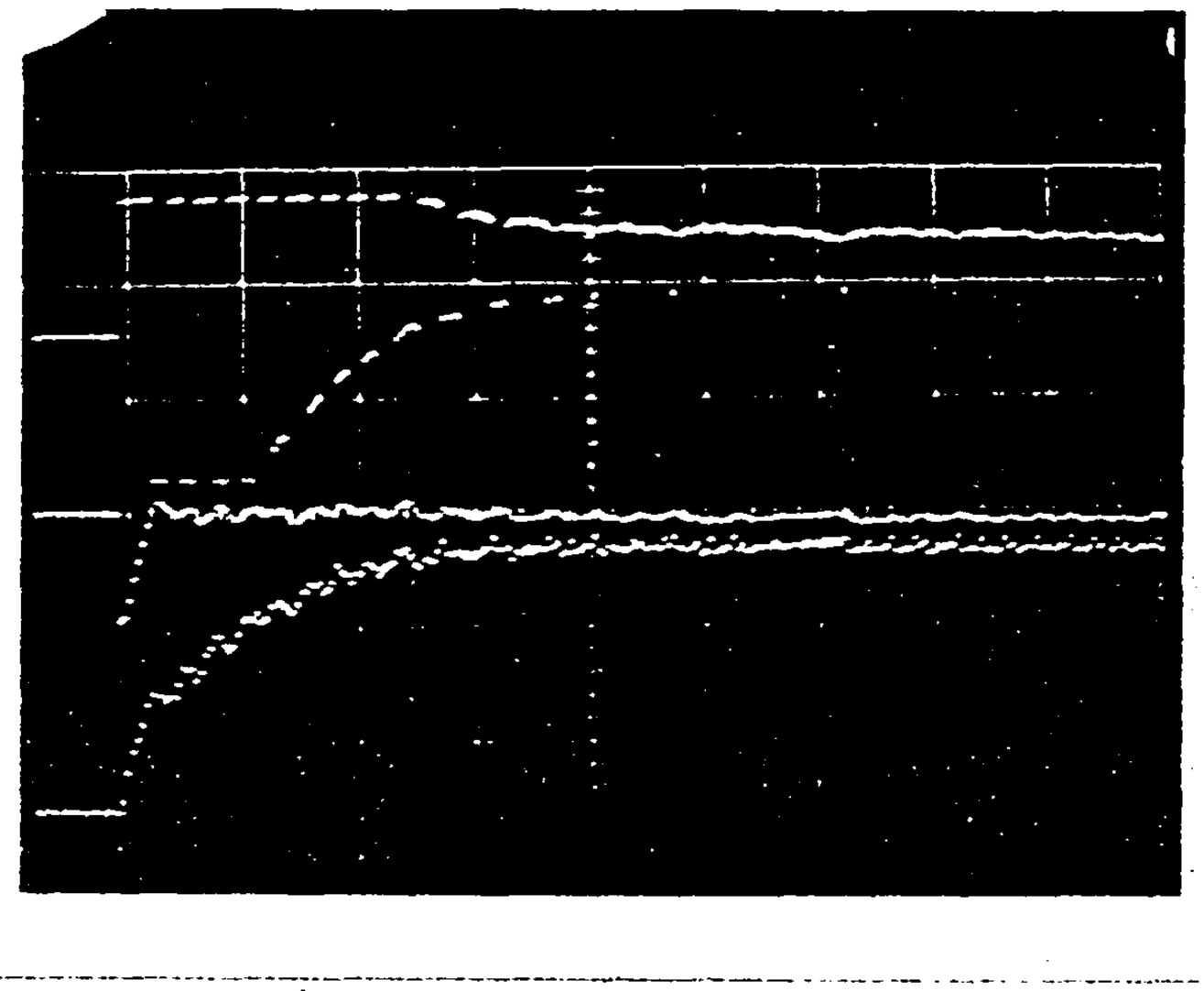

Fig. 8.4 - Step Responses on Faster Time Base

detailed analysis of the hitting conditions was required. Secondly, the derivative of the error signal was calculated to a first approximation by dividing the difference between the present and past values of the error by the clock interval of 0.02 seconds. The velocity variable x_1 (fig. 8.2) was smoothed prior to differentiation. This was accomplished by simulating a first order lag defined by,

$$H(s) = \frac{1}{sT_a + 1} \qquad (8.12)$$

The integration within the lag was performed by multiplying current values of the derivative by the clock interval and accumulating the results.

Two main differences are observed in the input drives for the two reference levels. Firstly, as can be expected, the amplitude of the switched signal when the output has settled at the desired level, is greater when the speed is 1700 rpm, and secondly the input drive in that instance has a higher average value indicated by long periods at the maximum drive level; this again is to be expected as a higher drive is required for a higher speed.

Fig. (8.4) shows the same results on an expanded time scale. The transition from the initial conditions into the sliding plane is very fast and a quasi-sliding regime is then established. The output is slightly noisy, hence the requirement for a smoothing algorithm in the program. The noise arises as a result of the motor's bandwidth which is wide enough to respond to the narrow step changes in the input drive produced by the VS controller.

Figs. (8.5) and (8.6) illustrate the effects of loading on the speed output and the input drive. In fig. (8.5), the loading was effected by the braking action of a magnet on a light thin disc attached to the shaft of the motor. Comparing figs. (8.3) and (8.5), the main difference is in the input drive; when the motor is loaded, the average level of the input drive increases to maintain the speed at the demanded level. No obvious difference is to be observed in the input drive when the speed reference is 1000 rpm. In fig. (8.6), the loading was in the form of a heavy disc attached to the motor. Again the average value of the input drive has risen to compensate for the loading disturbance. With a speed reference of 1700 rpm, the average value of the input drive required to produce zero steady-state error is outside the dynamic range of the switched reference and switching has stopped altogether leaving a steady-state error. Under these conditions, the system behaves like a closed-loop system with a pure gain in the controller and the input drive becomes a function of the error signal. When the speed reference is dropped from 1700 rpm to 1000 rpm, transistor T_1 is reverse biased and no control is exerted on the motor, hence the fall-time is entirely dependent on the motor dynamics during that phase. Control is restored when T_1 is forward biased once more.

The effect of introducing an "unidentified lag" between the controller and the motor is shown in fig. (8.7). The lag has a time constant of 0.1 seconds compared to the motor time constant of the order of 0.5 seconds. The integrating effect on the input drive is clear and the system is still controllable. In the steady state, the switching input has been completely smoothed to a d.c. level and a small error exists in the output.

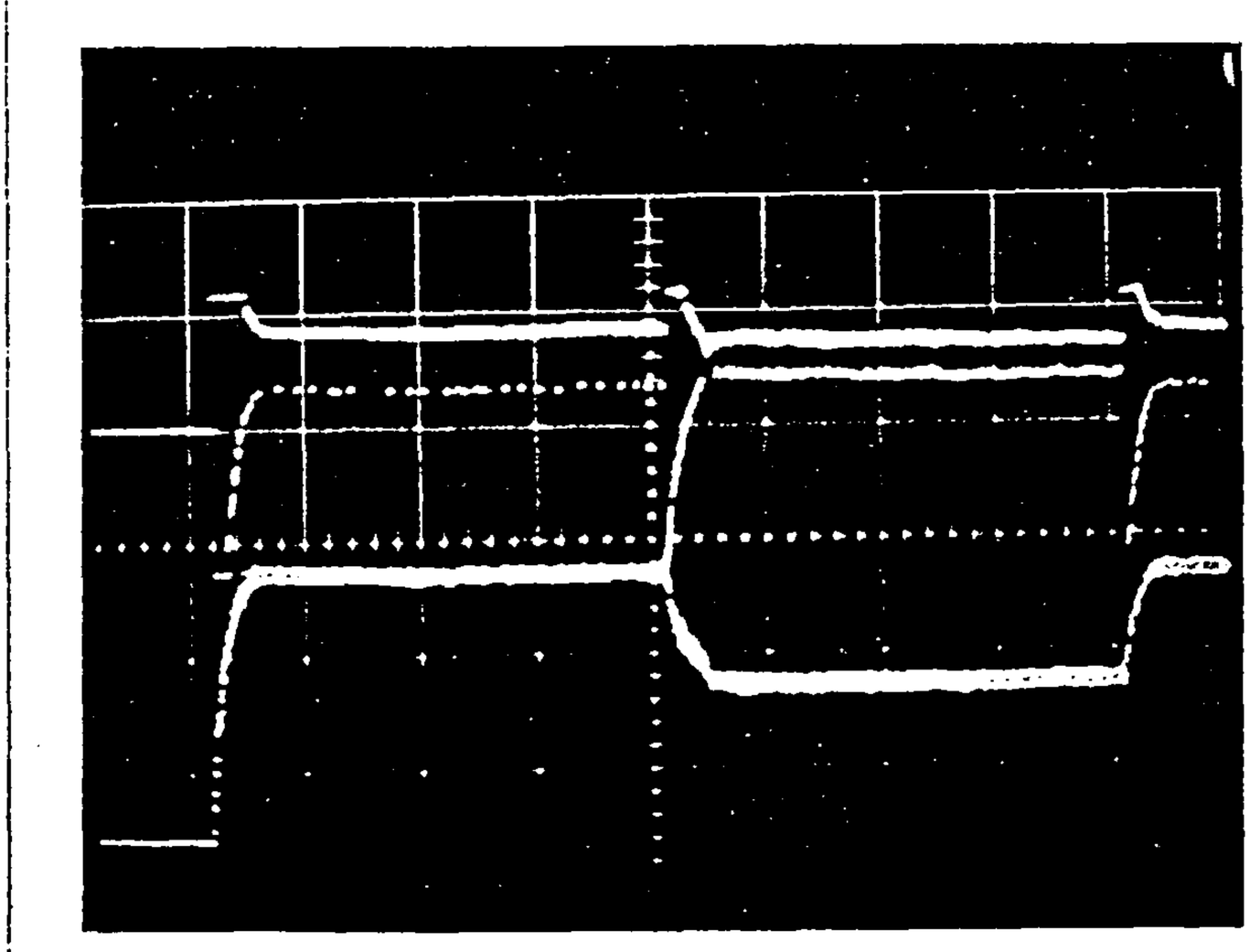

Input drive 10 V/div

Output 2 V/div

5 secs/div

Fig. 8.5 - Step Response with Load

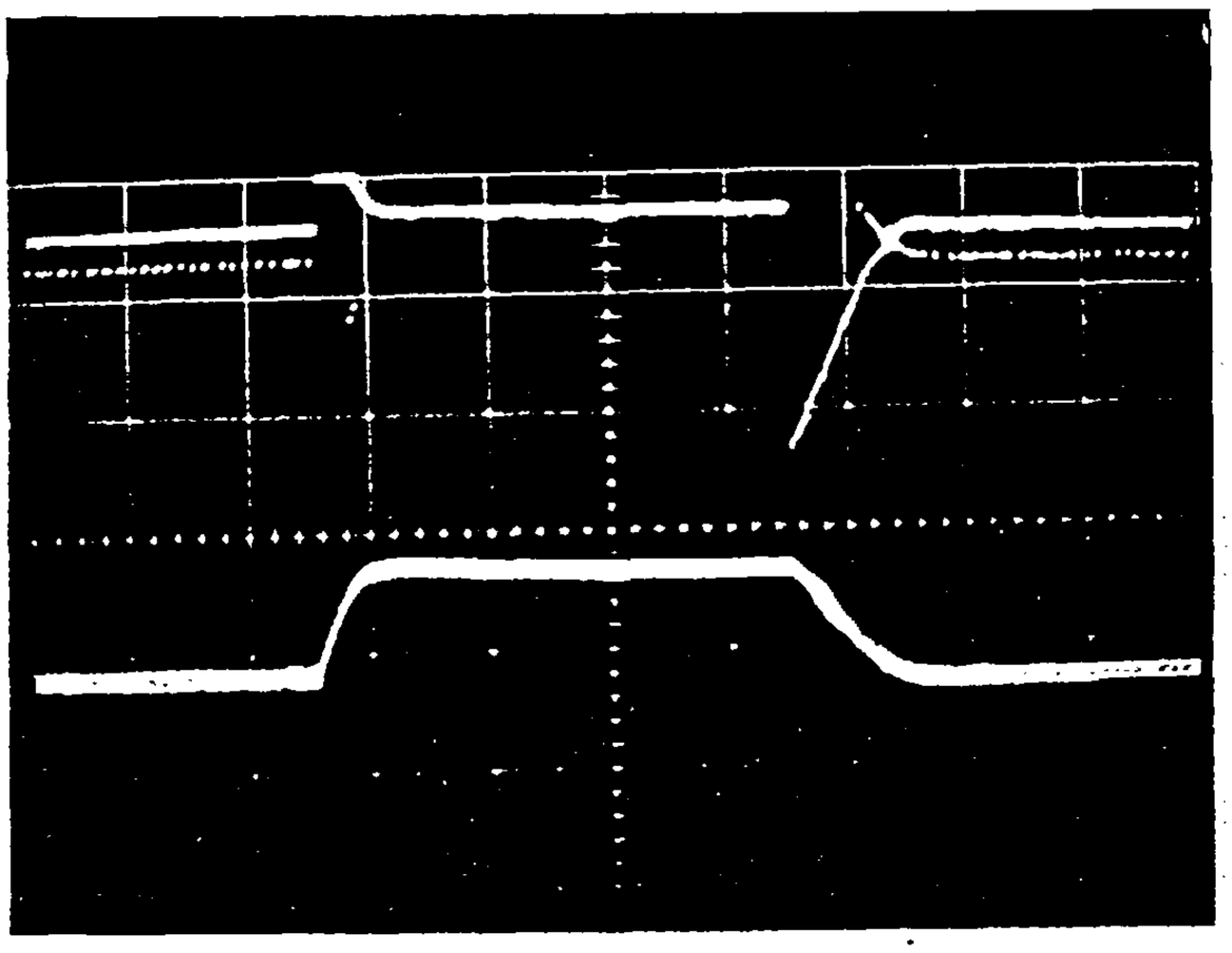

Input drive 10 V/div

Output 2 V/div

5 secs/div

Fig. 8.6 Step Response with Increased Load

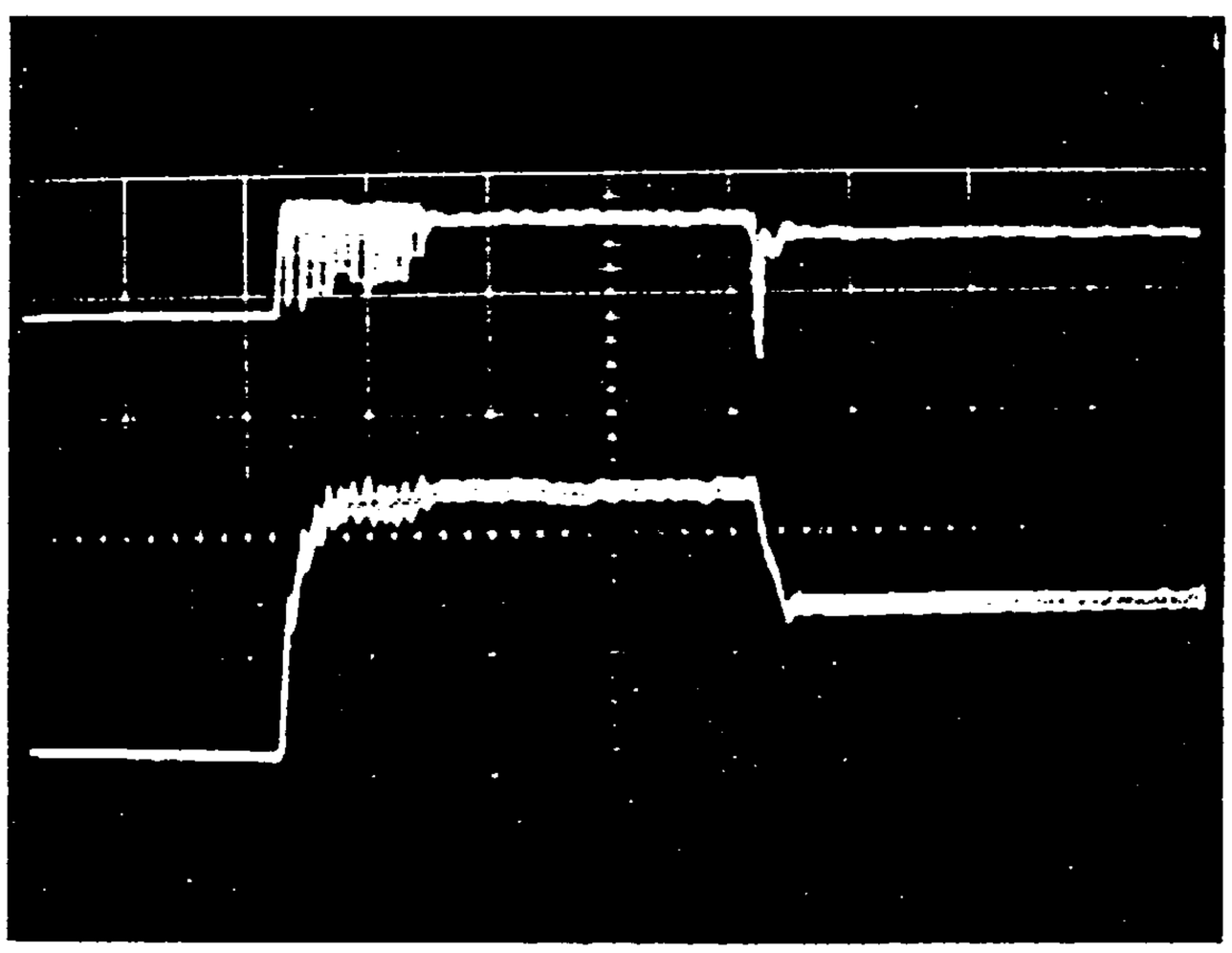

Fig. 8.7 - Effect of First Order Lag in Control Path

8.2 General Comments

The experimental work reported in this chapter has shown that it is possible to control a small DC motor from a microcomputer using a VS program. Starting from an imprecise model of the motor in terms of its parameters, order, noise levels and nonlinearities, a satisfactory speed control performance has been obtained in the presence of internal and external disturbances. The performance could undoubtedly be optimised for example with respect to risetime but the purpose of the experiment was to demonstrate the realisability of VSS and its tolerance to uncertainties normally present in most engineering systems. Further the differentiation method used within the software control program did not pose any serious noise problem. The switching of the reference based on an uncertain value of the switching function did not affect the performance.

The control waveforms observed in the simulated VS systems studied in earlier chapters have been reproduced in the real-time control of a DC motor. The experiment has contributed to enhance the credibility of VS techniques as a practical solution to control problems.

CHAPTER NINE

CONCLUSION AND FURTHER WORK

9.1 Conclusion

In this research, an attempt has been made to find an engineering solution to the control of plants which are characterised by time-varying parameters, nonlinearities, modelling errors and which are influenced by external disturbances. Of the different theories put forward in the literature to the solution of those problems, VS theory was selected as the basis of the investigation principally for its invariancy properties to parametric changes and to external disturbances. The theory, like any other, has advantages and disadvantanges which can only be properly gauged in a detailed investigation.

The main objective of this thesis was to elaborate on those aspects through a detailed study of test cases in order that the theoretical and practical problems which arise in using VS principles could be appreciated and assessed. The motivation behind the research was the simplicity of the control algorithms which would lead to a relatively straightforward software implementation and real-time operation within a microcomputer system.

Chapters two and three were concerned with the fundamentals of the theory. In chapter two, the sliding regime of VSS was explained and the invariancy property to parameter changes and disturbances of this type of motion became apparent. The necessary conditions required to enforce a sliding motion in plants described in phase-variable form were reviewed in chapter three for

time-invariant and time-varying plants. The control mechanism was further clarified. The input drive was shown to be a switching signal consisting of a linear combination of the error signal and its derivatives during the transient stage and which converges to a mean level in the steady-state. The extension of the theory to more general state-space systems is not straightforward. In a time-invariant plant described by a set of ordinary differential equations, the sliding motion is in fact dependent on the plant's parameters. Complete invariancy is achieved if the controls and disturbances enter the plant at the same points.

Several problem areas arise in the theory for which mathematical solutions are extremely difficult, if not impossible, to find. This is the case in the tracking problem. Some solutions proposed are unacceptable from an engineering viewpoint, for example, the control of plants described by a transfer function with zeros. Such problems are however not unique to VSS; the regulation of an arbitrary state around an operating point is an equally difficult problem in linear systems theory.

From a mathematical standpoint, the subject has reached a point where progress is now very slow. Further evolution in the field lies more in applying the principles to engineering problems and to ascertain their performance. In this way, the method can gain wider acceptance as a design procedure. With this theme in mind, chapters four to eight have dealt specifically with VS designs and the assessment of their performances using digital simulation, hybrid simulation and a real system.

In chapter four, the VS design of a type 0 time-varying system was investigated. It was shown that a time-varying coiler-

drive system could be stabilised and successfully controlled over a certain operating range. The main result of the coiler-drive study showed that the system cannot be controlled using a switching law based solely on the error vector; the reference input must be included in the switching control law, otherwise sliding breaks down and can result in limit cycles. In general, this relay action is an essential component of the input drive in the regulation of type 0 systems.

In chapter five, the VS design of an autopilot was considered. A state-feedback autopilot was first studied and was found satisfactory with respect to all the control objectives except for the effects of sea disturbances on the rudder position. The rudder activity was considerably diminished by lowering the feedback gains and using a VS controller to ensure zero steady-state error in the heading. An important difference was found between the coiler-drive and the ship. In the latter, the system is type one and as a result the reference did not appear in the switching control law. This is a characteristic of position control systems in which the output variable is related to the angular velocity by an integrator and is not generally true for type one systems. A property of the steering integrator was its ability to extract from the switching input drive the average level required to balance the forces acting on the ship. In the steady-state and with no external forces acting on the vessel, the rudder position would settle at zero. But as external forces build up on the ship, the rudder is displaced from its zero position and a switching component gradually appears in the input drive, proportional to the rudder displacement. In that respect, the

control mechanism is similar as in the coiler-drive case except that the input switches equally about its mean level in the steady-state. In the coiler-drive, the switching must be uneven to provide a mean level which changes slowly to compensate for the time-varying effect of the coiled material. A further property of the VS autopilot was the almost direct effect of the local feedback gain around the steering integrator on the transient response of the heading.

From an engineering viewpoint, it was important to investigate the robustness of the VS solutions when noise is present. In chapter six, the effects of noise in the measurements of the variables of the coiler-drive and ship with VS controllers were studied via simulation. The two test cases were shown to be adversely affected by noise in the form of steady-state errors and drift. Of the two cases, the coiler-drive is the most susceptible to random disturbances; the differentiation of the error signal followed by the switching of the input reference together with the greater bandwidth of the motor were contributory factors to the reduced performance. In both cases, smoothing of the noisy signals using lead-lag networks is the most effective way of improving the performance. The amount of smoothing that is tolerable can only be determined in practice and is dependent on the noise characteristics, i.e. on its intensity and spectral distribution and on the extent to which the plant's dynamics are modified by the additional networks.

The investigation of VSS has been confined to that point to the carefully controlled conditions of digital simulation. In chapters seven and eight, the study was extended to test the performance of practical VSS. In chapter seven, the hybrid

simulation of a third order plant controlled by a VSS has been shown to work successfully in spite of the unstable loop formed by the plant and the state-feedback controller. The overall system behaved in accordance to the studies of the previous chapters and was able to handle a variety of disturbances and nonlinearities. The most striking example of disturbance rejection was evidenced when the plant was disturbed by a sinusoidal signal of arbitrary frequency added to the input drive. The overall system then behaved as an adaptive notch filter removing the sinusoidal component completely from the output.

The VS coiler-drive system was shown to be the worst performer of the design examples studied. It was appropriate, therefore, to undertake the real test on motor system and, in which the controller switches the reference input and uses differentiation. In chapter eight, it was shown that VS principles could be readily applied to the speed control of a DC motor using an ill-defined model in the design. It was also shown that the effect of modelling due to an "unidentified lag" could be tolerated; hence in general, a satisfactory performance should be obtained if only the dominant time constants of the plant are used in the model.

The main contribution of this thesis has been to study and clarify the control mechanism in VSS through simulation and experimentation, and, to show how such systems can be designed, implemented and made to operate satisfactorily. The VS controller behaves in a similar way to an integral controller and has the ability of shifting its average level over a certain dynamic range defined by the control law to compensate for disturbances on the plant. In the case of an input disturbance, the compensation is almost instantaneous and is much faster than an equivalent linear

control system. An essential part of the controller was shown to be the switching of the input reference. Uncertainty in the form of random noise can be sufficiently reduced by smoothing to maintain performance. The real-time operation of VSS has been demonstrated using a microcomputer system to implement the control algorithms.

9.2 Further Work

The successful application of control theory depends largely upon the reliability and accuracy of the information which is fed to the controller. VS controllers are no exception to that rule and depend on the reliable estimation of the error vector from state measurements. In most control applications, this amounts to estimating the error vector by differentiating the output to the required order. In the VS controllers considered, this was accomplished very crudely by dividing the difference between present and past values of the signal by the clock interval followed by a smoothing network. Signal processing and digital filtering theory offer new ways of designing band-limited differentiators which could be readily implemented within a microcomputer system [9.1]. Such techniques should be investigated with a view to applying VS methods to plants of order higher than three or four.

It is very hard to visualise VSS in the frequency domain. It is speculated that if theory of variable structures could be evolved from a frequency approach, then the filtering of say an input sinusoidal disturbance could be better understood and lead possibly to the design of VS networks with specific frequency responses.

APPENDIX A

Proof of Theorem 3.1

To prove theorem 3.1, the following nonsingular transformation is made.

Let,

$$\left.\begin{aligned} y_i &= x_i \qquad (i = 1, \ldots, n-1) \\ y_n &= \sum_{i=1}^{n} c_i x_i \end{aligned}\right\} \tag{A.1}$$

The system of (3.8) becomes,

$$\left.\begin{aligned} \dot{y}_i &= y_{i+1} \qquad (i = 1, \ldots, n-2) \\ \dot{y}_{n-1} &= y_n - \sum_{i=1}^{n-1} c_i y_i \end{aligned}\right\} \tag{A.2}$$

$$\dot{y}_n = -(a_n - c_{n-1})y_n + \sum_{i=2}^{n-1} (c_{i-1} - a_i - c_i c_{n-1} + c_i a_n)y_i + (-a_1 - c_1 c_{n-1} + c_1 a_n - b\psi_1)y_1$$

The last equation in (A.2) is derived in a similar way as equation (3.12). Using conditions (3.13), the system (A.2) can be simplified as follows:

$$\left.\begin{aligned} \dot{y}_i &= y_{i+1} \qquad (i = 1, \ldots, n-2) \\ \dot{y}_{n-1} &= y_n - \sum_{i=1}^{n-1} c_i y_i \\ \dot{y}_n &= -(a_n - c_{n-1})y_n + (-a_1 + c_1 a_n - c_1 c_{n-1} - b\psi_1)y_1 \end{aligned}\right\} \tag{A.3}$$

The transformation is equivalent to replacing the coordinate x_n by $y_n = \sigma$.

Replacing ψ_1 in (A.2) by $\theta_1 = \frac{1}{b}(c_1 a_n - c_1 c_{n-1} - a_1)$, (equation 3.15), gives,

$$\left.\begin{aligned} \dot{y}_i &= y_{i+1} \qquad (i = 1, \ldots, n-2) \\ \dot{y}_{n-1} &= y_n - \sum_{i=1}^{n-1} c_i y_i \\ \dot{y}_n &= -(a_n - c_{n-1}) y_n \end{aligned}\right\} \qquad (A.4)$$

It follows from (A.4) that the $\lambda_n = c_{n-1} - a_n$ is a characteristic root. Consequently the characteristic equation of the original system (3.8) with $\psi_1 = \theta_1$,

$$s^n + a_n s^{n-1} + \ldots + a_2 s + (a_1 + b\theta_1) = 0 \qquad (A.5)$$

also has the root $\lambda_n = c_{n-1} = a_n$. The general solution of (A.4) is given by,

$$y_1(t) = \sum_{i=1}^{n-1} A_i e^{\lambda_i t} + A_n e^{\lambda_n t} \qquad (A.6)$$

where A_i are the initial conditions. In the sliding regime $\sigma=0$, hence $y_n = A_n = 0$, (by eqn. A.1). Then the coordinate $y_1(t)$ and all its derivatives $y_i(t)$ $(i = 2, \ldots, n-1)$ do not depend on the root λ_n and the system (A.4) reduces to,

$$\left.\begin{aligned} \dot{y}_i &= y_{i+1} \\ \dot{y}_{n-1} &= -\sum_{i=1}^{n-1} c_i y_i \end{aligned}\right\} \qquad (A.5)$$

All the characteristic roots of system (A.5) must have negative real parts for stability. But since the system (A.5) is equivalent to (3.11), it follows that the latter is also stable. This completes the proof of Theorem 3.1.

APPENDIX B

Proof of Theorem 3.2

Assume on the contrary that the RP can reach the sliding surfaces from any initial condition and that the characteristic equation with $\psi_1 = \alpha_1$,

$$s_n + a_n s^{n-1} + \ldots + a_2 s + (a_1 + b\alpha_1) = 0 \qquad (B.1)$$

has at least one root $\lambda_1 \geq 0$. The theorem shall be proved by exhibiting the initial conditions under which hitting cannot occur. The solution of equation (3.8) has the general form,

$$x_1(t) = A_1 e^{\lambda_1 t} + A_2 e^{\lambda_2 t} + \ldots + A_n e^{\lambda_n t} \qquad (B.2)$$

where $\lambda_2, \ldots, \lambda_n$ are the remaining (n-1) roots, A_1, A_2 to A_n are coefficients determined by the initial conditions. If the initial conditions are chosen such that $A_2 = A_3 = \ldots = A_n = 0$, then

$$x_1(t) = A_1 e^{\lambda_1 t} \qquad (B.3)$$

The switching surface defined in equation (3.7) becomes,

$$\sigma(t) = c_1 x_1 + c_2 x_2 \ldots . + x_n$$

$$= A_1 (c_1 + c_2\lambda_1 + \ldots + \lambda_1^{n-1}) e^{\lambda_1 t} \qquad (B.4)$$

hence for any $t \geq 0$,

$$x_1\sigma(t) = A_1^2 (c_1 + c_2\lambda_1 + \ldots + \lambda_1^n) e^{2\lambda_1 t} > 0 \qquad (B.5)$$

Consequently the structure of the system cannot change for any t and so $\sigma(t) \neq 0$ for any $t \geq 0$ as required and the sliding surface σ cannot be reached. Using the above arguement, it can be

shown that $\sigma(t)$ is a periodic function, i.e. its sign is variable, when the roots are complex with either positive or real parts; the structure changes implying that hitting must occur. If the roots are real and negative, asymptotic hitting takes place,

$$\lim_{t \to \infty} x_1(t) = \lim_{t \to \infty} x_2(t) \ldots = \lim_{t \to \infty} x_n(t) = \lim_{t \to \infty} s(t) = 0 \qquad \text{(B.6)}$$

When $\psi_1 = \beta_1$, the plant is part of a positive feedback loop and the characteristic equation is,

$$s_n + a_n s^{n-1} + \ldots + a_2 s + (a_1 + b\beta_1) = 0 \qquad \text{(B.7)}$$

If the roots are negative or complex, then the behaviour of the phase trajectories is as above and hitting will occur. If equation (B.7) has positive roots and if the initial conditions are such that the RP is in the region defined by $x_1\sigma(t) < 0$, then from (3.7) and (B.2)

$$\left.\begin{aligned} \sigma(t) = {} & A_1(c_1 + c_2\lambda_1 + c_3\lambda_1^2 + \ldots + \lambda_1^{n-1})e^{\lambda_1 t} \\ & + A_2(c_1 + c_2\lambda_2 + c_3\lambda_2^2 + \ldots + \lambda_2^{n-1})e^{\lambda_2 t} \\ & + A_n(c_1 + c_2\lambda_n + c_3\lambda_n^2 + \ldots + \lambda_n^{n-1})e^{\lambda_n t} \end{aligned}\right\} \qquad \text{(B.8)}$$

Hence by (B.8) and (B.2), there exists $t_0 > 0$ such that,

$$\text{sign}[x_1(t_0)] = \text{sign}[\sigma(t_0)] \qquad \text{(B.9)}$$

The RP enters the region $x_1\sigma(t) > 0$, the controller gain switches to α_1 and the case reduces to the preceding one. This completes the proof.

APPENDIX C

This appendix reviews briefly the principles of pole-assignment in single-input linear time-invariant systems using state-variable feedback techniques. As it is shown in some of the examples discussed in the thesis, state-feedback is useful in the determination of the coefficients of the switching hyperplane in a VSS.

C1.1 State-Feedback Systems [3.6]

State-feedback is an extension of the classical root-locus technique. The concept of feeding back the system states rather than a single output, allows greater freedom in the assignment of the closed-loop poles.

Consider a completely controllable and completely observable single-input system represented in the following state-space form,

$$\dot{\underline{x}} = \underline{A}\underline{x} + \underline{b}u \tag{C.1}$$

where $\underline{x}$ is the n-column state vector, $\underline{A}$ is the constant nxn plant matrix, $\underline{b}$ is nxl vector which couples the scalar input u to the rest of the plant. The transfer function is thus given by,

$$\left.\begin{aligned} \underline{x}(s) &= \frac{\underline{g}(s)}{d(s)}\, u(s) \\ \text{where,} \quad \frac{\underline{g}(s)}{d(s)} &= [s\underline{I} - \underline{A}]^{-1}\, \underline{b} \end{aligned}\right\} \tag{C.2}$$

The following conclusions can be drawn from equations (C.2), (C.6) and (C.9):

(i) the numerators of the transfer functions are identical, hence the zeros of the system are invariant under feedback.

(ii) the closed-loop characteristic polynomial $d_c(s)$ is given by

$$d_c(s) = d(s) + \underline{k}^T \underline{g}(s) \qquad (C.10)$$

which is known as the pole-assignment equation and relates the closed-loop poles to the open-loop system and the feedback vector. It can be inferred from (C.10) that if the full state-vector is not available, then there is a restriction in the attainable closed-loop poles.

APPENDIX D

Sliding Conditions in Linear Time-Varying Systems

From (3.22),

$$\sigma = \sum_{i=1}^{n-1} c_i x_i + x_n \qquad (D.1)$$

Differentiating (D.1) gives,

$$\dot{\sigma} = \sum_{i=1}^{n-1} c_i \dot{x}_i + \dot{x}_n$$

$$= \sum_{i=1}^{n-1} c_i x_{i+1} + \{- \sum_{i=1}^{n} a_i(t) x_i - b(t) \sum_{i=1}^{k} \psi_i x_i\} \quad \text{from (3.21)}$$

$$= \sum_{i=1}^{n-1} c_{i-1} x_i + c_{n-1} x_n + \{- \sum_{i=k+1}^{n-1} a_i(t) x_i - \sum_{i=1}^{k} a_i(t) x_i - a_n(t) x_n$$

$$- b(t) \sum_{i=1}^{k} \psi_i x_i\}$$

But from (D.1), $x_n = \sigma - \sum_{i=1}^{n-1} c_i x_i = \sigma - \sum_{i=k+1}^{n-1} c_i x_i - \sum_{i=1}^{k} c_i x_i$

Therefore, $\dot{\sigma} = -\{a_n(t) - c_{n-1}\}\sigma + \sum_{i=k+1}^{n-1} \{c_{i-1} - a_i(t) + c_i a_n(t) - c_i c_{n-1}\} x_i$

$$+ \sum_{i-1}^{k} \{c_{i-1} - a_i(t) + c_i a_n(t) - c_i c_{n-1} - b(t)\ \psi_i\} x_i$$

Multiplying throughout by σ and applying conditions (3.16),

$$\sigma\dot{\sigma} = -\{a_n(t) - c_{n-1}\}\sigma^2 + \sum_{i=k+1}^{n-1} \{c_{i-1} - a_i(t) + c_i a_n(t) - c_i c_{n-1}\} x_i$$

$$+ \sum_{i=1}^{k} \{c_{i-1} - a_i(t) + c_i a_n(t) - c_i c_{n-1} - b(t)\psi_i\} x_i \sigma \leq 0$$

The numerator of the transfer function vector is given by the n-column vector $\underline{g}(s)$, $d(s)$ is the open-loop characteristic polynomial whose roots are the open-loop poles, given by,

$$d(s) = |s\underline{I} - \underline{A}| \tag{C.3}$$

where $\underline{I}$ is the unit matrix. If a constant state-feedback controller is now introduced such that,

$$u = u_c - \underline{k}^T\underline{x} \tag{C.4}$$

where $\underline{k}^T$ is a constant n-row feedback vector and u_c is the reference input signal, the closed-loop system b is described by,

$$\dot{\underline{x}} = [\underline{A} - \underline{b}\underline{k}^T]\underline{x} + \underline{b}u_c \tag{C.5}$$

or in the frequency domain by,

$$\underline{x}(s) = \frac{\underline{g}_c(s)}{d_c(s)}\, u_c(s) \tag{C.6}$$

where,

$$d_c(s) = |s\underline{I} - \underline{A} + \underline{b}\underline{k}^T| \tag{C.7}$$

is the closed-loop characteristic polynomial. The closed-loop transfer function which relates the output z to the reference u_c is given by,

$$\frac{z(s)}{u_c(s)} = \underline{k}^T \cdot \frac{\underline{g}(s)}{d(s) + \underline{k}^T\underline{g}(s)} \tag{C.8}$$

and consequently the transfer function relating u_c to $\underline{x}$ is,

$$\frac{\underline{x}(s)}{u_c(s)} = \frac{\underline{g}(s)}{d(s) + \underline{k}^T\underline{g}(s)} \tag{C.9}$$

For the above inequality to be fulfilled, each term on the LHS must be less or equal than zero, i.e.

$$\inf a_n(t) \geqslant c_{n-1}$$

$$\left.\begin{aligned} c_{i-1} - a_i(t) &= c_i\{c_{n-1} - a_n(t)\} \qquad i = k+1, \ldots, n-1 \\ \alpha_i &\geqslant \sup \frac{1}{b(t)}\{c_{i-1} - a_i(t) + c_i a_n(t) - c_i c_{n-1}\} \quad i=1,\ldots,k \\ \beta_i &\leqslant \inf \frac{1}{b(t)}\{c_{i-1} - a_i(t) + c_i a_n(t) - c_i c_{n-1}\} \end{aligned}\right\} \quad (D.2)$$

The restrictions imposed on parameters c_{i-1} for $i = k+1, \ldots, n-1$ are unrealistic in practice, since they must vary in such a way as to satisfy the equality in (D.2). The parameters $a_{k+1}, a_{k+2} \ldots a_n$ are therefore assumed to be constants.

APPENDIX E

Proof of Theorem 3.5

From Appendix D,

$$\dot{\sigma} = -\{a_n(t) - c_{n-1}\}\dot{\sigma} + \sum_{i=k+1}^{n-1} \{c_{i-1} - a_i(t) + c_i a_n(t) - c_i c_{n-1}\}x_i$$
$$+ \sum_{i=1}^{k} \{c_{i-1} - a_i(t) + c_i a_n(t) - c_i c_{n-1} - b(t)\psi_i\}x_i$$

Assuming that the conditions expressed in (D.2) are satisfied, then

$$\sigma \leq \sum_{i=1}^{k} \int_0^t \{c_{i-1} - a_i(t) + c_i a_n(t) - c_i c_{n-1} - b(t)\psi_i\}x_i \qquad \text{(E.1)}$$

Let $\sigma(t) > 0$, now if

$x_i > 0 \qquad \psi_i = \alpha_i$ and by (D.2) and (E.1) $\sigma(t) < 0$

and if $x_i < 0 \qquad \psi_i = \beta_i$ and by (D.2) and (E.1) $\sigma(t) < 0$

which contradict the initial assumption that $\sigma(t) > 0$, hence hitting must occur. The same arguement applies assuming that $\sigma(t) < 0$.

APPENDIX F

Invariance Condition to External Disturbance

Equation (3.45) can be re-written as,

$$\underline{df} = \underline{b}(\underline{c}^T \underline{b})^{-1} \underline{c}^T \underline{df} \qquad (F.1)$$

The necessary condition for the fulfilment of (F.1) is that the vector $\underline{df}$ can be written in the form,

$$\underline{df} = \underline{bm} \qquad (F.2)$$

which can be proved by replacing $\underline{df}$ on the RHS of (F.1) by $\underline{bm}$. Equation (F.2) can only be fulfilled for arbitrary values of f if,

$$\text{rank } [\underline{b}\ \underline{d}] = \text{rank } [\underline{b}] \qquad (F.3)$$

i.e. all the vector d is a linear combination of vector b.

APPENDIX G

PARAMETERS OF COILER DRIVE SYSTEM

The coiler drive system specifications are given below. The winding of a photograph film represents the load.

Coiler Drive System Specification

Load

Radius of drum (R)	= 0.075 m
Maximum radius of coil (r)	= 0.5 m
Density of steel (ρ_1)	= 7840.0 kg/m^3
Density of film (ρ_2)	= 1120.0 kg/m^3
Load inertia (J_L) maximum	= 111.3 kg-m^2
minimum	= 0.4 kg-m^2
Linear speed of film (V_R)	= 1.27 m/sec
Width of film (e)	= 1 m
Thickness of film (a)	= 0.01 m

Motor

Rated speed	= 1500 rpm
Rated back emf (E_a)	= 200 volts
Rated armature current (I_a)	= 100 amps
Power rating	= 25 HP
Field current (I_f)	= 4 amps
Rated torque	= 118.5 Nm
Motor inertia (J_m)	= 0.5 kg-m^2
Armature Resistance (R_a)	= 0.05 Ω
Armature Inductance (L_a)	= 0.005 H
Gearbox Ratio (N)	= 10:1

Using the specified rated values, the motor constants k_1 and k_2 can be calculated from equations (4.2) and (4.3),

$$k_1 = \frac{E_a}{I_f \dot{\theta}_m} = \frac{1}{\pi} \text{ volts/amps - rad/sec} \qquad \text{(G.1)}$$

and $$k_2 = \frac{T_m}{I_a I_f} \doteq \frac{1}{\pi} \text{ N-m/amp}^2 \qquad \text{(G.2)}$$

The system parameters A,B, ... , F of fig. (4.4) can be calculated from the specifications and eqns. (G.1) and (G.2).

$$A = \frac{e\pi}{2N^2} = \frac{\pi}{200} = 1.572 \times 10^{-2} \text{ m} \qquad \text{(G.3)}$$

$$B = \rho_2 = 1120 \text{ kg/m}^3 \qquad \text{(G.4)}$$

$$(\rho_1 - \rho_2)R^4 = 6720.0\ (0.075)^4 = 0.212 \text{ kg-m} \qquad \text{(G.5)}$$

$$C = \frac{a}{2\pi} = \frac{0.01}{2\pi} = 1.592 \times 10^{-3} \text{ m} \qquad \text{(G.6)}$$

$$D = \frac{1}{\tau_a} = \frac{R_a}{L_a} = 10.0 \text{ sec}^{-1} \qquad \text{(G.7)}$$

$$E = \frac{k_2 I_f}{R_a} = \frac{1.272}{0.05} = 25.44 \text{ N-m/volts} \qquad \text{(G.8)}$$

$$F = k_1 I_f = \frac{4}{\pi} = 1.272 \text{ Volts/rad/sec} \qquad \text{(G.9)}$$

$$J_m = 0.5 \text{ kg-m}^2 \qquad \text{(G.10)}$$

$$T_\ell = 0.0 \qquad \text{(G.11)}$$

REFERENCES

[1.1] ITKIS, U:
"Control systems of Variable Structure", Israel Universities Press, 1976.

[1.2] ERSCHLER, J., ROUBELLAT, F., and VERNHES, J:
"Automation of a hydroelectric power station using Variable Structure Control Systems", Automatics, Vol. 10, pp 31-36, 1974.

[1.3] SOBOTTA, W:
"Realisation and application of a new nonlinear attitude control and stabilisation system", Proc. 4th IFAC Symposium Control in Space.

[1.4] MELSA, J.L., and SCHULTZ, D.G:
"Linear Control Systems", McGraw-Hill, 1969.

[1.5] LAYTON, J.M:
"Multivariable Control Theory", IEE Control Engineering Series 1.

[1.6] HOROWITZ, I.M:
"Plant Adaptive Systems versus Ordinary Feedback Systems", IRE Transactions on Automatic Control, January 1962, pp 48-56.

[1.7] EVELEIGH, V.W:
"Adaptive Control and Optimisation Techniques", McGraw-Hill, 1967.

[1.8] WRIGHT, P:
"A Composite Control Strategy for the Attitude and Position Control of a Pilotless Helicopter", Ph.D. Thesis, Heriot-Watt University, 1978.

[1.9] DRAPER, C.S., and LI, Y.T:
"Principles of Optimising Control Systems and an Application to the Internal Combustion Engine", Amer. Soc. Mech. Eng., Sept. 1951.

[1.10] NARENDRA, K.S., and KUDVA, P:
"Stable Adaptive Schemes for System Identification and Control - Parts I and II", IEEE Transactions on Systems, Man and Cybernetics, Vol. SMC-4, No. 6, November 1974.

[1.11] CARROLL, R.L., and LINDORFF, D.P:
"An Adaptive Observer for Single-Input Single-Output Linear Systems", IEEE Transactions on Automatic Control, Vol. AC-18, No. 5, October 1973.

[1.12] NARENDRA, K.S., and VALVANI, L.S:
"Stable Adaptive Observers and Controllers", Proceedings of the IEEE, August 1976, Vol. 64, No. 8.

[1.13] SCOTT, D.A:
"Dynamic Performance of a Class of Digitally Controlled Processes", Research Memorandum, RM/74/9, Heriot-Watt University.

[2.1] BARBASHIN, E.A:
"Introduction to the Theory of Stability", Wolters Noordhoff Publishing, Groningen, The Netherlands, 1970.

[2.2] FLUGGE-LOTZ, I:
"Discontinuous Automatic Control", Princeton.

[3.1] UTKIN, V.I:
"Variable Structure Systems with Sliding Modes", IEEE, Transactions on Automatic Control, Vol. AC-22, No. 2, April 1977.

[3.2] SILVERMAN, L.M:
"Transformation of Time-Variable Systems to Canonical Form", IEEE Transactions on Automatic Control, April 1966.

[3.3] WONHAM, W:
"Optimal Bang-Bang Control with Quadratic Performance Index", 4th Joint Automatic Control Conference, Minneapolis 1962.

[3.4] HSU, J.C., and MEYER, A.U:
"Modern Control Principles and Applications", McGraw-Hill.

[3.5] UTKIN, V.I:
"Equations of Sliding Mode in Discontinuous Systems Vols. I and II", Automatic and Remote Control, No. 12, pp 1897-1907, No. 2, pp 211-219, 1972.

[3.6] FALLSIDE, F:
"Control System Design by Pole-Zero Assignment", Academic Press, 1977.

[3.7] BEZVODINSKAYA, T.A., and SABAEV, E.F:
"Stability Conditions in the Large for Variable Structure Systems", Automatic and Remote Control, No. 10, pp 1596-1599, 1974.

[3.8] DRAZENOVIC, B:
"The Invariance Conditions in Variable Structure Systems", Automatica, Vol. 5, pp 287-295, 1969.

[3.9] MELSA, J.L., and JONES, S.K:
"Computer Programs for the Computational Assistance in the Study of Linear Control Theory", McGraw-Hill, 1973.

[3.10] KWAKERNAAK, H., and SIVAN, R:
"Linear Optimal Control Systems", Wiley-Interscience, 1972.

[3.11] YOUNG, P.C., and WILLEMS, J.C:
"An Approach to the Linear Multivariable Servomechanism Problem", Int. J. Control, 1972, Vol. 15, No. 5, pp 961-979.

[3.12] EMELYANOV, S.V., and FEDOTOVA, A.I:
"Producing Astaticism in Servosystems with a Variable Structure", Automatic and Remote Control, Vol. 23, No. 10, pp 1298-1312, October 1962.

[3.13] EMELYANOV, S.V., and FEDOTOVA, A.I:
"Reproduction of the Controlling Action $g(t) = \alpha t^n$ by Astatic Servo Systems with Variable Structure", Automatic and Remote Control, Vol. 26, No. 1, pp 67-72, January 1965.

[3.14] EMELYANOV, S.V., and UTKIN, V.I:
"Invariant Solutions of Differential Equations with Dis-continuous Coefficients", Mathematical Theory of Control, New York, Academic, 1967.

[3.15] LINDORFF, D.P:
"Relay Control of Systems with Parameter Uncertainties and Disturbances", Automatica, Vol. 5, pp 755-762, 1969.

[3.16] LINDORFF, D.P:
"Control of Non-linear multivariable systems", IEEE Transactions on Automatic Control, Vol. AC-12, No. 5, October 1967.

[3.17] MONOPOLI, R.V:
"Control of Linear Plants with Zeros and Slowly Varying Parameters", IEEE Transactions on Automatic Control, February 1967.

[4.1] COLE, R.G:
"Stability Analysis of a Coiler Drive System", B.Sc., Thesis, Heriot-Watt University, 1970.

[4.2] MALCOLM, J.M:
"An Investigation of a Class of Forced Non-linear Systems Incorporating a Real Time Stability Supervisor", Ph.D. Thesis, Heriot-Watt University, 1975.

[4.3] BUDEK, J., et al:
"Semiconductor Circuit Design", Texas Instruments Limited, 1972.

[4.4] SPECKHART, D.:
"Guide to CSMP".

[5.1] BECH, M.I:
"Some Aspects of the Stability of Automatic Course Control of Ships", The Journal of Mechanical Engineering Science, Vol. 14, No. 7, Supplementary issue 1972.

[5.2] VAN AMERONGEN, J., and UDINK TEN CATE, A.J:
"Model Reference Adaptive Autopilots for Ships", Automatica, Vol. 11, pp 441-449, 1975.

[5.3] NOMOTO, K:
"Problems and Requirements of Directional Stability and Control of Surface Ships", The Journal of Mechanical Engineering Science, Vol. 14, No. 7, Supplementary issue 1972.

[5.4] CLARKE, D:
"Maneouvring Trials with the 50,000 ton Deadweight Tanker - 'British Bombardier'," The British Ship Research Association, Report No. 142, 1966.

[5.5] RUSSELL, G.T:
"Consultancy Work on Autopilot Design", Department of Electrical Engineering, Heriot-Watt University.

[6.1] KOKOTOVIC, P.V., YOUNG, K.K.D., and UTKIN, V.I:
"A Singular Perturbation Analysis of High Gain Feedback Systems", IEEE Trans., Automatic Control, Vol. AC-22, pp 931-938, 1977.

[6.2] LUENBERGER, D.G:
"An Introduction to Observers", IEEE Trans., Automatic Contol, AC-16, pp 596-602, 1971.

[6.3] SAGE, A.P:
"Optimum Systems Control", Second Edition, Prentice-Hall, 1977.

[6.4] MISHULINA, O.A:
"Design of a Non-Linear Stochastic Control System with given Phase Motion", Translated from Avtomatika: Telemekhanika, No. 11, pp. 22-29, November 1973.

[6.5] TARAN, V.A:
"The Control of a Linear Object by a Variable-Structure, Astatic Control without the use of Pure Derivatives in the Control Law, I", Automatic and Remote Control, pp 1278-1288, Vol. 24, Part 10, 1964.

[6.6] TARAN, V.A:
"Control of Linear Systems by means of Floating-Control Regulators with Variable Structure without using Pure Derivates in the Control Law, II", Automatic and Remote Control, Vol. 24, Part II, pp 1406-1412, 1964.

[7.1] HERD, J.T:
"Integrated Computer Aided Design System Users Manual", Department of Electrical Engineering, Heriot-Watt University, August 1978.

[7.2] RITCHIE, D.M, and THOMPSON, K.L:
"The UNIX Time-Sharing System", CACM, Vol. 7, No. 17, July 1974.

[7.3] RITCHIE, D.M, and THOMPSON, K.L:
"UNIX Programmers Manual", Bell Laboratories, 1973.

[7.4] RITCHIE, D:
"C Reference Manual", Bell Laboratories.

[7.5] MELSA, J.L:
"Computer Programs for Computational Assistance in the Study of Linear Control Theory", McGraw-Hill, 1970.

[7.6] "UMIST Manual", Department of Electrical Engineering, Heriot-Watt University.

[8.1] FEEDBACK LIMITED:
"DC Feedback Manual".

[9.1] RABINER, L, and GOLD, B:
"Theory and Application of Digital Signal Processing", Prentice-Hall.